SYNTHESIS AND PROPERTIES OF SOME NOVEL LIQUID CRYSTALLINE SYSTEMS INCLUDING METALLOMESOGENS

ASHLEY CHANDLER SCRIBBINS

A thesis submitted in partial fulfilment of the
requirements of The Nottingham Trent University
for the degree of Doctor of Philosophy

September 1997

Abstract

The synthesis of five novel homologous series of 4′-n-alkoxybiphenyl-4-yl cycloalkanecarboxylates **(7-11)** is described, along with their liquid crystalline behaviour which was characterised by thermal optical microscopy and differential scanning calorimetry. An unusual observed texture is obtained on cooling **(7-11)** from the isotropic liquid, which had not been recognisable as any known mesophase type, but exhibited many of the characteristics of a crystalline solid separating from the isotropic liquid. The nature of this mesophase type has been investigated by extensive miscibility studies and has been determined to be that of the smectic crystal G phase.

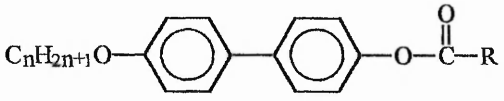

(7-11) Where R = cycloalkyl ring C3-C7

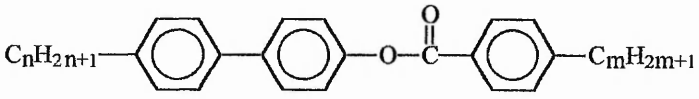

(17) Where n = 5-7,10 and m = 1-10

The synthesis of four series of 4′-n-alkylbiphenyl-4-yl 4-n-alkylbenzoates **(17)**, is also described. Compounds of this type had been previously cited in a patent granted to Steinsträsser *et al.*[44] although no attempt had been made by the authors to identify the smectic phases present. A discussion of the characterisation of the liquid crystalline behaviour of these homologous series by thermal optical microscopy and differential scanning calorimetry is given. These esters exhibit extensive smectic polymorphism and a comparison of their mesophase behaviour and thermal stability with that of the analogous 4′-n-alkylbiphenyl-4-yl 5-n-alkylthiophene-2-carboxylates **(20)** reported by Butcher *et al.*[45] is given.

In recent years, much attention has been drawn to the relatively new subject area of metallomesogens (metal -containing liquid crystals). A great deal of success has been reported utilising either ferrocene-1,1′- **(47)** or -1,3-dicarboxylic acid **(75)**. The preparation of several novel 1,1′-disubstituted ferrocene compounds is reported in an attempt to synthesise novel ferrocene metallomesogens, which were not derived from either of the afore mentioned systems. Although non of the compounds proved mesogenic, an indication as to the possible effect of the central linking group, **X**, on the thermotropic behaviour of some 1,1′-bis(4′-n-alkyl(oxy)biphenyl-4-yl)ferrocenes **(33)**, **(59)**, **(61)**, and **(67)** is given. The preparation of a novel mono-substituted ferrocene **(60)** and two other 1,1′-di-substituted ferrocenes **(70)**, **(72)** is also reported.

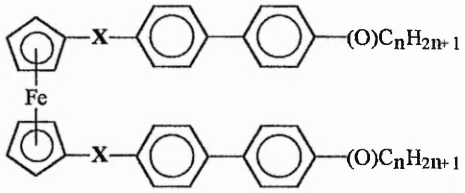

Acknowledgements

The author wishes to thank Dr K Moss, Dr A S Matharu and Dr R C Wilson for their invaluable help, guidance, and not least patience, throughout this project; Mrs P Flemming and Mr M Wood for advice and spectral analysis; and Professor D J Byron for consultation on miscibility studies and phase identification.

I would also like to express my thanks to The Nottingham Trent University for the award of the research studentship which enabled the undertaking of this project.

Abbreviations

DCC	Dicyclohexylcarbodiimide
DCM	Dichloromethane
DMAP	Dimethylaminopyridine
DSC	Differential Scanning Calorimetry
GAA	Glacial Acetic Acid
IMS	Industrial Methylated Spirits
TFAA	Trifluroacetic Anhydride
THF	Tetrahydrofuran
TMEDA	N,N,N′,N′-Tetramethylethylenediamine
TLC	Thin Layer Chromatography
$S_{A\text{-}E,F \text{ and } I}$	Smectic liquid crystal phases
G	Smectic crystal G phase
J	Smectic crystal J phase
H	Smectic crystal H phase
K	Smectic crystal K phase
N	Nematic phase
I	Isotropic liquid
C	Crystalline state

Contents

1. *An introduction to liquid crystals*

1 *An introduction to liquid crystals*

1.1 *Historical background*

Classically, physical science recognises the existence of three states of matter: solid, liquid and gas. The liquid crystal state, however, is a state of matter which is observed, in certain materials, between the crystalline solid and the isotropic liquid.

The discovery of this intermediate state is credited to two chemists: Reinitzer and Lehmann. In 1888, Reinitzer[1] observed that upon heating a pure sample of cholesteryl benzoate to 145.5 °C, a turbid melt was obtained which persisted until 178.5 °C whereupon the isotropic liquid formed. On cooling the clear liquid, he noticed the appearance of an unusual colour effect. Examination of other cholesterol derivatives provided similar results. Lehmann[2] confirmed Reinitzer's observations and employed a polarising microscope to aid the study of the transitions. Lehmann later showed that many other compounds (e.g. ammonium oleate and *p*-azoxyanisole) exhibited this unusual double melting behaviour, and introduced the term ***liquid crystal*** to describe this phenomenon.

Many new liquid crystalline materials were then synthesised, most notably by Gattermann[3] and Vorländer[4]. It soon became apparent that compounds which exhibited liquid crystalline behaviour shared certain structural characteristics, i.e. they all possessed an elongated, lath-like molecular geometry.

The first detailed classification of liquid crystals was proposed on a structural basis by Friedel[5] in 1922. He introduced the term ***mesophase*** derived from the Greek word *mesos*, meaning intermediate, which stressed the nature of the phase, i.e. belonging neither to the crystalline solid nor the isotropic liquid, but possessing properties

characteristic of both. Friedel divided the liquid crystalline compounds known to him at that time into three categories: ***nematic***, ***smectic***, and ***cholesteric***; each possessing characteristic textures when observed under a polarising microscope. Friedel's classification did not, however, take into account smectic polymorphism. The first compound to display this type of behaviour was later synthesised by Vorländer[6].

Theoretical investigations into the nature of the liquid crystalline state were also being pursued. Two hypotheses were proposed, namely the swarm hypothesis and the continuum or distortion hypothesis. The swarm theory was originally suggested by Bose[7] in 1909 and was subsequently supported by the work of Ornstein[8]. The theory assumes that the molecules in the mesomorphic state are not orientated in the same direction throughout the whole medium but rather that they are grouped in aggregates or swarms. The continuum hypothesis was initially proposed by Zocher[9] in 1922 and was based on the interpretation of the effects of a magnetic field on nematic structuring. This theory was later revised by Oseen[10] and Frank[11] and is now accepted as the principal theory of molecular structuring in the liquid crystalline state.

Further advances in liquid crystal chemistry were delayed until after the end of the second world war when some important publications revitalised the subject area. Work by Weygand[12] and Gray[13] took a systematic approach to liquid crystal development, looking at the relationships between molecular structure and behaviour of the mesomorphic state.

Sackmann and Demus[14] undertook extensive microscopic and X-ray investigations of some liquid crystalline systems which led to the classification of the smectic types A,B,C,D,E,F and G. In more recent years smectic types H,I,J and K have also been identified.

The development of low melting liquid crystalline materials, coupled with investigations into their electro-optical properties, culminated in the 1970's with the introduction of the Twisted Nematic Liquid Crystal Display (TN LCD). These low power, flat panelled systems revolutionised the world of optical displays and promoted liquid crystals as a major field of chemical research.

1.2 *Classification*

The liquid crystalline or mesomorphic state is often regarded as the fourth state of matter which exists between the crystalline solid and isotropic liquid. It displays one- or two-dimensional order dependant upon the phase type. The formation of the liquid crystalline state is characterised by the reduction or loss of positional order coupled with the retention of some orientational order, compared to that of the three-dimensional crystalline solid.

On heating a liquid crystalline solid at its melting point, the solid phase converts into a viscous turbid state, which appears birefringent when viewed between crossed polarisers. Further heating causes an increase in entropy giving rise to the isotropic liquid when the sample becomes optically clear, i.e. at the clearing point. These two temperatures define the range over which the mesophase is thermally stable. Both of these changes can be characterised by latent heat and density measurements.

Liquid crystals can be grouped into two broad categories :

(a) ***thermotropic liquid crystals*** - formed by ***calamitic*** (rod-shaped) or ***discotic*** (disc-shaped) molecules: they are compounds which display liquid crystalline properties through the action of heat alone;

(b) ***lyotropic liquid crystals*** - displayed by compounds which possess both lipophilic and hydrophilic characteristics: these liquid crystal phases are formed through the action of a solvent, usually water, upon a crystalline solid (the amount of solvent is the most important variable).

However, liquid crystals may display both thermotropic and lyotropic characteristics and hence this classification is not fundamentally justifiable, although it is still widely used as it represents a convenient sub-division. A better classification is that of ***amphiphiles*** and ***non-amphiphiles***.

Amphiphiles are molecules which contain both lipophilic and hydrophilic moieties within their structure. Certain compounds of this type are mesogenic:

(a) anionic, e.g. $Me(CH_2)_nCO_2^-Na^+$;

(b) cationic, e.g. $R(CH_2)_nN^+(CH_3)_3Cl^-$;

(c) non-ionic, e.g. $C_8H_{17}NH_2$.

Phase formation arises from different 'mutually ordered' micellular aggregations rather than an arrangement involving single molecules. Many of these compounds give rise to both thermotropic and lyotropic mesophases.

Non-amphiphiles are non-polar or moderately polar organic compounds, which are hydrophobic in character. The molecules consist entirely of covalently bound atoms with no ionised groups present, although they may contain strongly polar groups, e.g. CN. The formation of the mesophase is dependent upon the arrangement of individual molecules.

Many compounds with globular or spherical molecular units are also termed non-amphiphilic. These compounds were first recognised by Timmermanns[16] in 1935, who termed them ***Plastic Crystals***. Upon heating, these crystalline solids retain their position on a regular three-dimensional lattice but gain free orientational motion, causing a breakdown in long- range ordering. This provides a three-dimensional lattice which is less rigid and hence is referred to as a soft plastic crystal. Further heating gives rise to the isotropic liquid.

1.3 *A simplified view of mesophase classification*

As mentioned earlier, the liquid crystalline state may consist of several mesophase types, i.e. the nematic, smectic and cholesteric phases. A detailed discussion of these liquid crystal phases is given later in section **1.7**, but a brief outline of their general characteristics follows:

The Nematic Phase (N)

This is the most disordered of the phase types, where the molecules are said to align statistically parallel to one another. The phase possesses long range orientational order but zero positional order. The direction of alignment is given by the director, n (n = average orientation of long axes). A further discussion of the nematic phase appears in section **1.7.1**.

The Smectic Phase (S)

In the smectic phase the molecules occur in diffuse layers. Within these layers the molecules may either be tilted or orthogonal (i.e. at right angles) with respect to the layer

plane. A number of smectic phases exist which differ by the amount or degree of both positional and orientational order and hence this type of mesophase is said to be polymorphic. The different phases are differentiated by the use of a code letter, e.g. S_A, S_B, S_C, etc. Smectic polymorphism is discussed in more detail in sections **1.7.3** and **1.7.4**.

The Cholesteric Phase (Ch)

This phase was originally discovered in derivatives of cholesterol and may be visualised as a layered nematic state. It is now known to occur in molecules which contain chiral centres (i.e. optically active compounds give cholesteric rather than nematic mesophases). The director, n, has a natural twist superimposed upon it and is unidirectionally skewed clockwise or anticlockwise to the layer above or below it, dependent upon the chirality of the species. This provides the cholesteric phase with a helical configuration as the layers are transcended. A more detailed discussion of the cholesteric phase may be found in section **1.7.2**.

The Discotic Phase (D)

First recognised by Chandrasekhar,[17] the molecules in a discotic phase are disc-like in shape and have no rigid internal segments. In the discotic phase the molecules stack like coins (i.e. in a columnar manner). Examples of such molecules can be seen in the fully substituted benzenes - **Fig.1**.

Two different types of discotic phase exist :

(a) N_D-phase - this is a fluid phase with an optical texture similar to that of a nematic phase;

(b) D-phase - this is similar to a smectic phase as it exhibits polymorphism (i.e. ordered, disordered, tilted, hexagonal, rectangular, oblique).

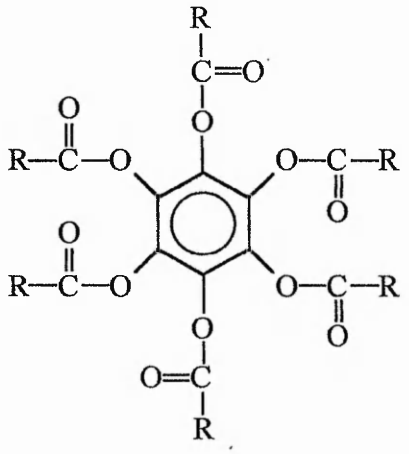

Fig.1 - Fully substituted benzene of the type giving rise to discotic phas

Re-entrant Phases

A re-entrant phase is one which reappears, on cooling, after it has already been present at a higher temperature in the phase-change pattern. Normally, the phenomenon only occurs in molecules with strong dipolar end groups. The re-entrant phase may be either nematic or smectic and may be temperature or pressure induced. For example, under normal conditions the melting behaviour of TBBA (Terephthalylidene-*bis*-4-n-butylaniline) **(1)** is I-N-S_A-S_C-G-H-S_{VII}, but at high pressure the phase-change pattern becomes I-N-S_A-N. In this example, the appearance of the re-entrant phase is due to competition in stability between the molecular ordering in the S_A layers at different temperatures.

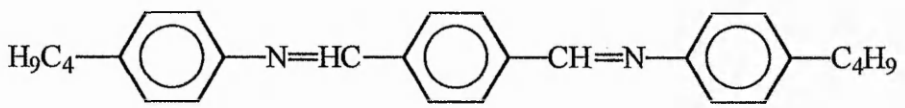

(1)

1.4 *Mesophase formation and crystal structure*

Most liquid crystal molecules are said to be geometrically anisotropic, e.g. rod or lath-shaped. Geometric anisotropy leads to anisotropy of molecular forces so that on heating, the forces which maintain order breakdown in stages. Lateral forces dominate over terminal forces which produces a stepwise breakdown of the crystal to create liquid crystal phases with intermediate degrees of order. Two types of molecular packing within the crystal, namely ***layer*** and ***non-layer lattices***, have been identified by X-ray crystallography of liquid crystalline compounds.[18]

Crystals With A ***Layer Lattice*** *Structure* - **Fig.2**

(a) If terminal forces are weak between the molecular planes compared to the lateral attractive forces between the molecules, then at temperature T_1 the layers may slide and rotate over each other to form a smectic mesophase.

(b) Upon heating this smectic phase two possibilities may arise:

(i) the intermolecular forces weaken so that at temperature T_2 the molecules slide out of the layers to form a nematic mesophase. A further increase in temperature to T_3 reduces the lateral and terminal attractions and the molecules lose parallel orientation to form the isotropic liquid.

(ii) the smectic mesophase may form the isotropic liquid directly, at temperature T_4, by the rapid breakdown of cohesive forces so that the nematic state with parallel order is not formed.

(c) It is also possible for the layer lattice to form the nematic mesophase directly, at temperature T_6.

Crystals With a ***Non-Layer/Interdigitated Lattice*** *Structure* - **Fig.2**

(a) This crystal type will give rise to a nematic mesophase at temperature T_5.

(b) It was originally thought that this lattice type could not form a smectic mesophase directly. However, this is not true as alkylcyanobiphenyls (which possess this interdigitated structure in the crystalline state) give rise to a smectic A (S_A) phase, which is strictly termed the S_Ad phase.

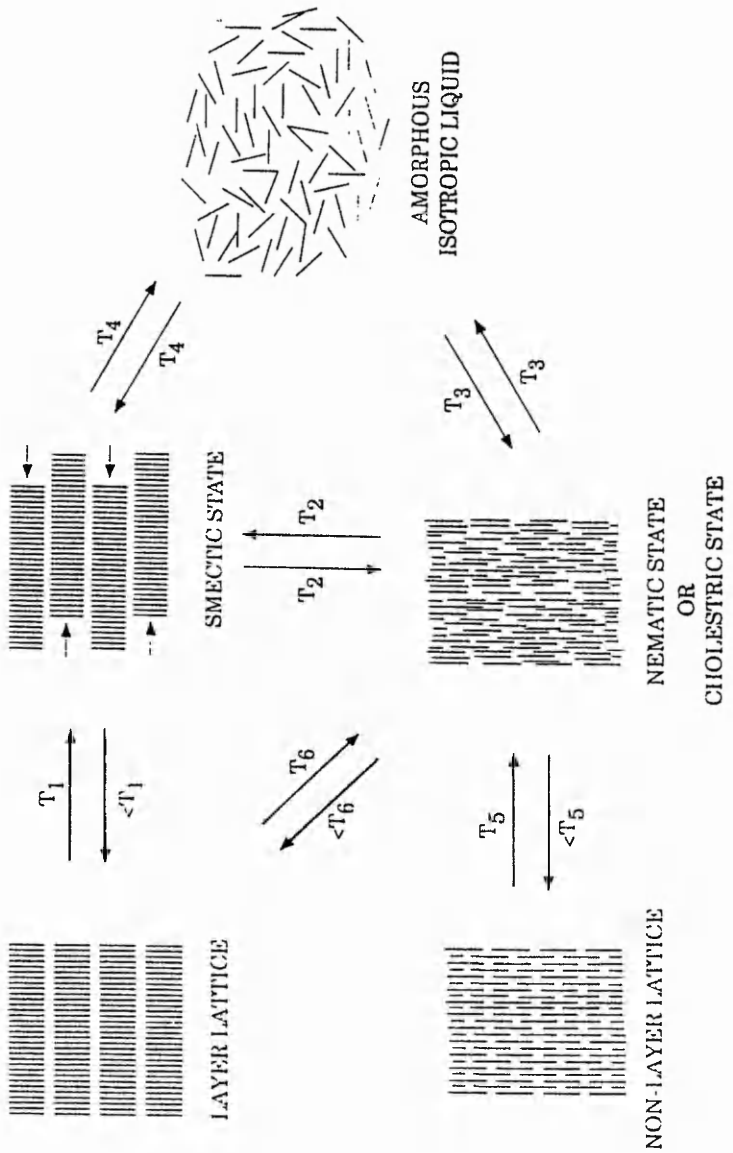

Fig.2 - Diagrammatic representation of molecular rearrangement of mesophases

1.5 *Determination of transition temperatures and mesophase type*

There are several methods for the determination of transition temperatures and mesophase type. The techniques are complementary and hence the results from each need to be analysed together for accurate mesophase identification. Listed below is a brief over-view of the techniques available.

Capillary Melting Point

This method is very limited and will only provide the melting point and some indication of liquid crystalline character. On the action of heat the crystal will form a viscous turbid liquid which may stick to the vessel walls before clearing and relaxing to give the isotropic liquid.

Optical Microscopy

A sample of the crystal under study is mounted between a microscope slide and a cover slip and then placed within a hot stage. The sample is then viewed through the microscope between crossed polarisers so that the optical textures can be identified as the temperature is raised or lowered. The phases appear as 'wave-fronts', due to the changing orientations of the molecules within the mesophases, passing across the slide on both heating and cooling. The result of viewing an anisotropic crystal between crossed polarisers may be explained using a simple diagram - **Fig.3**.

Light entering a Nicol prism from the polariser is resolved into two vibrations at right angles to each other, but parallel to the vibration directions of the prism. These rays then enter the analyser where they are broken into two vibrations parallel to the long diagonal of the prism, which are reflected out, and two vibrations parallel to the short

diagonal which emerge. The two emergent rays although in the same plane differ in phase and interfere with one another. The result of this is shown by the double arrow.

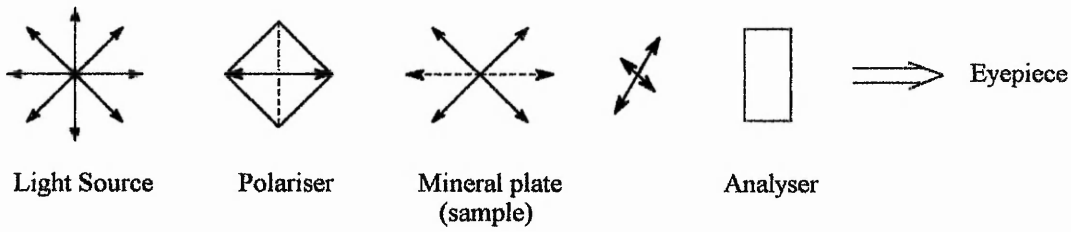

Fig.3 - An anisotropic crystal viewed between crossed polarisers.

In white light, for a given thickness of plate or crystal, the phase difference may be such that the destructive interference occurs for a particular wavelength and is hence subtracted from the transmitted light. Therefore the complementary colour is seen through the eyepiece. The colour produced is called the interference colour. For crystals of a given thickness the intensity of colour will depend upon the birefringence of the crystal concerned.

Differential Thermal Analysis (DTA)

This type of analysis measures the difference in latent heat between the sample and a reference material. Both samples are heated and cooled at the same rate and the absolute temperature and the differential temperature are recorded. These values are then plotted and the area under the curve is equated to energy (in calories) by calibration with a standard. Hence the enthalpy for each phase change may be recorded quantitatively.

Differential Scanning Calorimetry (DSC)

This is similar to DTA except the heat is added via two differential heaters. One heater heats the sample and the reference at a constant rate, whilst the other adds heat to the system. This system is very accurate and errors only occur if the transitions do not reach equilibrium quickly. The results are presented as a plot and the calorific energy may be calculated as for DTA.

1.6 *Textures of liquid crystals*

Distinctive optical textures are observed when a sample of a liquid crystalline material, mounted between a slide and cover slip, is viewed through a polarising microscope. These are caused by defects in the crystal structure which are characteristic of different liquid crystal phases.

Prior surface preparation of the glass support can achieve different molecular alignments of the sample which are an aid to phase identification. The most common alignments are the homeotropic and the homogeneous alignment - **Fig.4**.

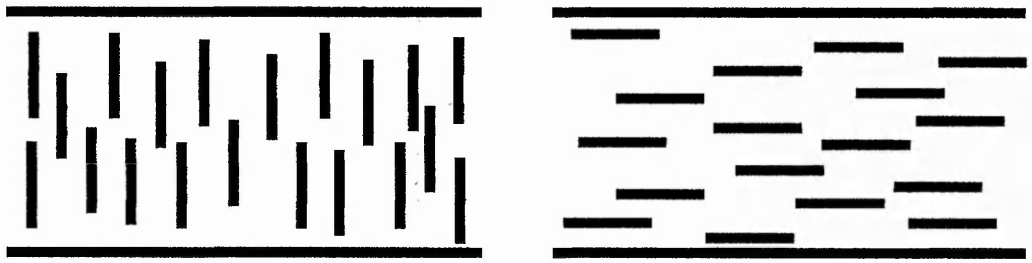

(a) the homeotropic alignment (b) the homogeneous alignment

Fig.4 - The homeotropic and homogeneous alignments

The Homeotropic Alignment (a)

Here the molecules are arranged with their optic axes parallel to the viewing direction, allowing light to pass through the sample readily. The simplest way to prepare this arrangement is to heat the material held between two glass supports to the isotropic liquid, letting the sample flow by capillary action. Treatment of the supports with surfactants will also provide the desired texture. These may either bond to the glass surface, e.g. trichloro-octadecylsilane, or show no interaction with the glass, e.g. lecithin.

The homeotropic alignment is useful in the identification of mesophase type, as a precursor for paramorphotic textures, in the construction of display devices, and the determination of optical rotation in chiral liquid crystals.

The Homogeneous Alignment (b)

Here the molecules lie parallel to the glass slide and perpendicular to the viewing direction. Hence, when a sample is viewed between crossed polarisers it will appear dark (black) when the optic axes of the molecules are parallel to either axes of the polarisers.

Preparation of this alignment may be achieved by either rubbing the glass surface in one direction, or by using surfactants and polymer solutions, e.g. PVA (polyvinyl alcohol).

The homogeneous alignment is useful for mesophase identification, pitch length determination in chiral smectics, the construction of display devices, and the determination of polarisation in ferroelectrics.

1.7 *Structure and optical textures of liquid crystals*

Friedel[5] classified the more common of the thermotropic mesophase types into three categories: nematic, smectic, and cholesteric. The following sections detail the structures of the various phase types and their optical characteristics when viewed through a polarising microscope with particular attention being paid to the various types of smectic polymorphic modifications.

1.7.1 *The nematic phase,* N

Derived from the Greek word *nematos*, meaning thread-like, the nematic phase is formed by many rod-like and disc-like molecules. The phase possesses the greatest entropy of any mesophase type and therefore is the most disordered system. The phase exhibits long range orientational order but zero positional order. The molecules within the nematic phase align statistically parallel to one another. The average direction of this orientational alignment is defined as the director, n, which is shown in **Fig.5**.

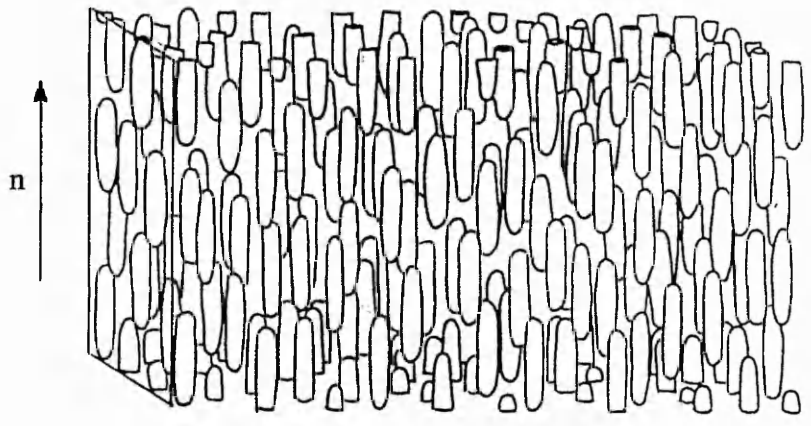

Fig.5 - Nematic ordering

This orientational ordering produces an optically isotropic material which is highly birefringent, i.e. $n_{\perp} \neq n_{\parallel}$, where n is the refractive index of light perpendicular or parallel to an external reference.

On cooling from the isotropic liquid the nematic phase separates out as droplets often characterised by the presence of extinction crosses when viewed between crossed polarisers. These droplets coalesce to form the observed textures.

The homogeneous texture of the nematic phase is referred to as the marbled texture, which exhibits sharp, straight bordered areas that impart the appearance of marble. A *schlieren* texture is also seen with characteristic *schlieren* brushes radiating from point singularities. These arise from strong distortions in the director field and exhibit either two or four brushes (the *schlieren* texture of the S_C phase only exhibits point singularities with four brushes). A threaded texture may also be observed which also arises from abrupt changes in the director field, creating the optical discontinuity. The nematic phase also exhibits a homeotropic texture which creates an optically isotropic (dark) field of view when viewed between crossed polarisers, due to the alignment of the molecules within the sample.

The nematic texture is also characterised by the observation of Brownian motion and, under mechanical stress, flashing when the optical appearance brightens.

1.7.2 *The cholesteric phase,* Ch

The cholesteric phase may be regarded as a layered nematic mesophase where the alignment of the director, n, has a twist superimposed upon it, giving rise to a helical arrangement of layers. Hence, from a structural point of view, the cholesteric phase is a chiral nematic phase. The distance required for the director to complete one revolution

(i.e. traverse 360°) is referred to as the pitch, P. The repetition period is defined as $^{P}/_{2}$. The pitch is much larger than the molecular dimensions and changes in the pitch length allow selective reflection of light which gives rise to an iridescent colour.

The cholesteric phase may exhibit three different textural types. On cooling the isotropic liquid the focal conic or undisturbed fan texture is obtained. The texture is birefringent but is optically inactive as the helices are perpendicular to the light path - **Fig.6**. Mechanical shear of the focal conic texture produces the Grandjean (planar or disturbed) texture, were the helices are aligned parallel to the light path. The cholesteric phase also exhibits the homeotropic texture.

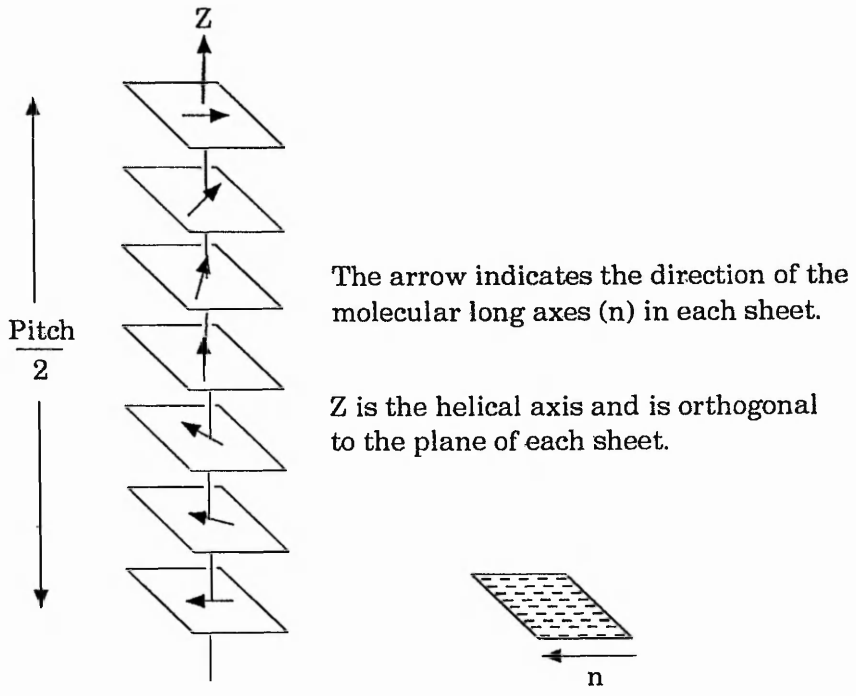

Fig. 6 - The cholesteric phase

The structural similarities between the nematic and cholesteric phases are confirmed by the following observations:

(a) transitions between nematic and cholesteric phases have never been observed

(b) the nematic and cholesteric phases are completely miscible.

(c) the mixture of (+) and (-) forms of a cholesteric compound give rise to a nematic phase.

(d) the same smectic phase will be shown by a (+), (-) or a racemic (±) form of a compound.

(e) X-ray studies show that similar Bragg reflections are observed for nematic and cholesteric phases.

Blue phases are observed for some cholesteric substances between the isotropic liquid and the formation of the cholesteric phase. They exist only over a narrow temperature range (generally less than 1°C) and are characterised by a bluish foggy texture.

Three types of blue phase have been identified. BPI and BPII have a cubic structure, whilst BPIII is still under investigation. A review on blue phases has been given by Crooker[19].

1.7.3 *Smectic mesophases,* S, *and polymorphism*[52]

The molecules within the smectic mesophase are arranged in stratified layers and possess differing degrees of positional and orientational order dependent upon the type of polymorphic modification. The molecular long axes of the molecules may either be tilted or orthogonal with respect to the layer planes.

Sackmann, Demus[20] and co-workers initially identified and coded polymorphs S_A-S_G on the basis of X-ray work and the ***Miscibility Rule*** which states '*all liquid crystalline modifications which exhibit an uninterrupted series of mixed crystals in binary systems without contradiction can be marked with the same symbol*'. Later work identified the smectic I phase and the smectic crystal phases of H, J and K.

There is a thermodynamic ordering to the formation of these modifications, which is listed below in order of decreasing entropy:

$$I - N - S_A - S_D - S_C - S_{Bh} - S_I - S_{Bc} - S_F - J - G - S_E - K - H - Crystal$$

Transitions between these phases may also be limited by the direction of tilt of the polymorphs.

As identification of different phase types plays a major part in later discussions, the structure and textures of each polymorph are discussed in greater detail below:

The smectic A phase, S_A

The S_A phase possesses the least order of any smectic phase, and will proceed any other polymorphic modification on cooling from the isotropic liquid or the nematic state.

X-Ray diffraction studies show that the molecules within the S_A phase are arranged with their molecular long axes perpendicular to the layer planes. The molecular distribution within the layer is random and hence the molecules are free to rotate about their long axes. For a lath-like mesogen, a simple representation of the S_A phase is as shown in **Fig.7**.

Nevertheless, X-ray investigations show that this model is inaccurate as the lamella spacings (*d*) do not necessarily correspond to the molecular length (*l*). In fact the *d*:*l* ratio can vary from 0.8-1.4 : 1. Proposed theories on shorter lamella spacings suggest that the molecules are randomly tilted within the layers, the angle of tilt being between 10-25°.

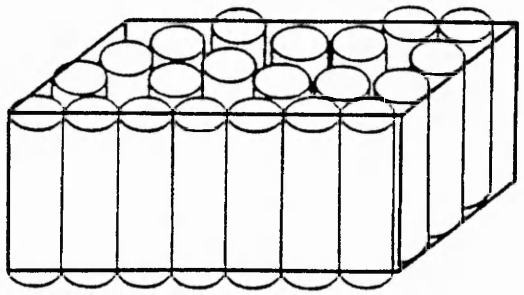

Fig.7 - A simple model for the S_A phase

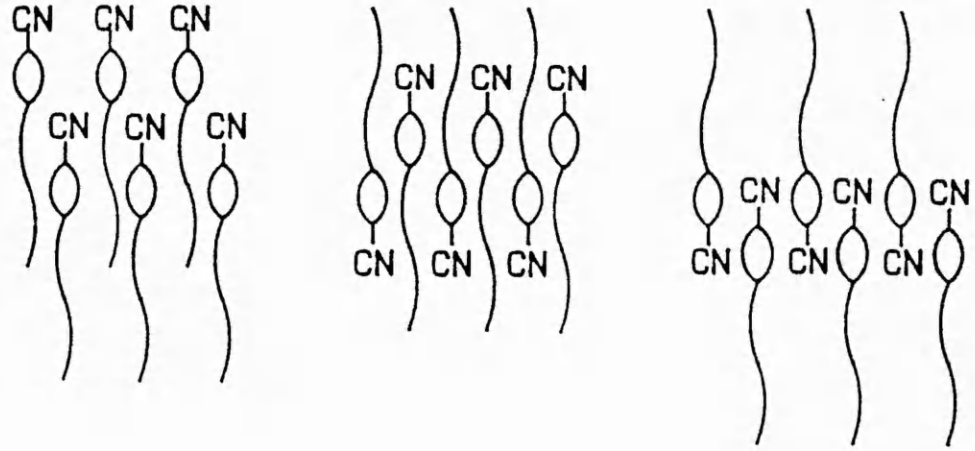

Fig.8 - Possible arrangements for the interdigitated bilayer of the S_A phase

This random tilt creates an averaging effect across the layers and produces an overall orthogonal arrangement of the molecular long axes. Longer lamella spacings are explained by the existence of a semi-bilayer or interdigitated arrangement of molecules. All known molecules which this type of structure contain terminal CN moieties, e.g. 4-*n*-alkyl- or 4-*n*-alkoxy-4′-cyanobiphenyls. Smectic phases with this molecular arrangement are commonly referred to as of the S_Ad type - **Fig.8**.

There are only two optical textures exhibited by the S_A phase: the homeotropic or pseudo-isotropic texture and the focal conic or fan texture. The homeotropic texture appears black when viewed between crossed polarisers, except near deformations, as the molecules are aligned with an average perpendicular arrangement to the layers which lie parallel to the surfaces of the slide. The focal conic texture is generally observed on cooling the isotropic liquid or the nematic phase and separates out as bâtonnets, which coalesce to form fans. The texture contains optical discontinuities in the form of ellipses and hyperbolae, which appear as dark lines arising as a consequence of arrangements of concentric and equidistant layers (a simplified picture of this arrangement using circles and straight lines is given in **Fig.9**).

More recently another variant of the S_A phase has been discovered, which is termed the ***Twist Grain Boundary*** A phase (TGBA phase).[26,52] The molecular arrangement within this phase is similar to that of the classical S_A phase except for the inclusion of a screw dislocation. Such a defect causes a section of the layers to adopt a helical arrangement. Optically, this texture is characterised by the appearance of threads or filaments in a predominantly homeotropic texture.

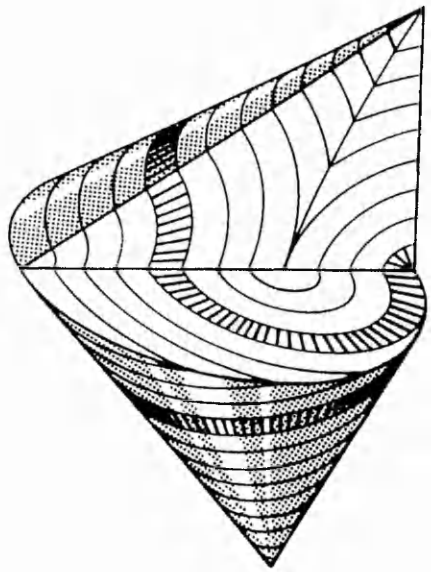

Fig.9 - Section through a focal conic domain in the special case of a circle and a straight line (rather than an ellipse and hyperbola)

The smectic B phase, S_B

Within this phase the molecules are arranged in layers with their molecular centres positioned in a hexagonally close-packed array. The molecular long axes are orthogonal with respect to the layer planes as shown in **Fig.10**.

The hexagonal packing within the phase may possess long range order with the hexagonal net extending over an extremely large number of layers, providing an S_B phase which is essentially crystalline, although its physical properties are mesogenic. Hence, the S_B phase is known to exist in either a three-dimensional (crystal) or two-dimensional hexatic (liquid crystalline) form.

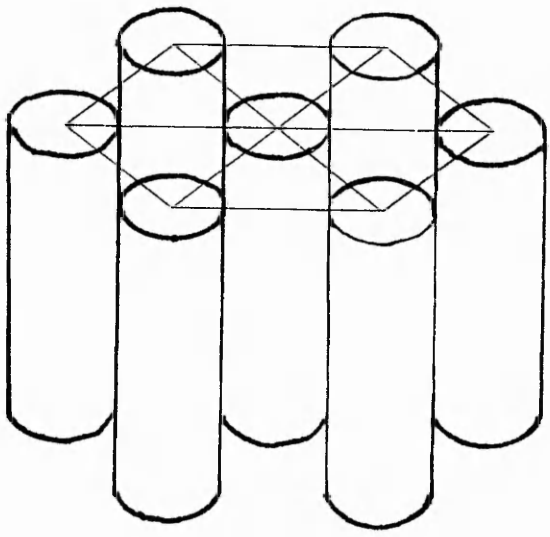

Fig.10 - Simplified model of the S_B phase showing the hexagonal net

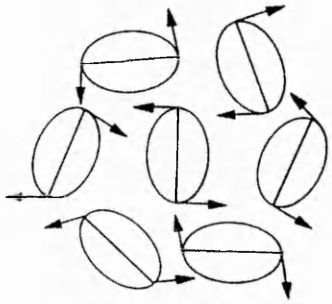

Fig.11 - Co-operative rotation viewed from above the unit cell

The molecules rotate rapidly about their long axes, although this rotation is not free. Molecular rotation must occur completely co-operatively and is controlled by the dimensions of the hexagonal net - **Fig.11**.

There are two naturally occurring textures of the S_B phase, these being the homeotropic and the mosaic textures. The homeotropic texture is similar to that of the S_A phase as the molecules are arranged perpendicular to the layer planes. If the S_B phase is formed by cooling the isotropic liquid then usually both textures are observed. However, if it is formed on cooling the nematic phase, then the texture observed is somewhat dependent upon that of the nematic, i.e. a homeotropic nematic will give rise to a homeotropic S_B texture and a homogeneous or *schlieren* nematic texture will produce an S_B mosaic.

The S_B phase does not naturally form a focal conic texture. This texture is said to be paramorphotic (i.e. a texture imposed by the texture and alignment of the molecules in

the previous phase) and is only observed on cooling an S_A or S_C phase which exhibits this texture. The fans may appear truncated with stepped edges. On cooling the S_A to the S_B phase transition bars may be observed. These are lines which may appear across the backs of the fans in concentric arcs due to the molecular reorganisation in the layers as the transition commences. As the transition reaches completion these lines disappear.

The smectic C phase, S_C

X-ray diffraction studies of the smectic C phase indicate that the molecules are arranged within layers and are randomly packed as in the S_A phase. However, the molecular long axes are tilted with respect to the layer normal - **Fig.12**, which is shown by the fact that $l>d$. The layers are free to slide over one another indicating that there is no long range correlation between layers except for the angle of tilt. The molecules within the layers are free to rotate around their long axes. The angle of tilt within the S_C phase has been shown to increase with decreasing temperature and hence there is no large change in tilt angle at the S_A-S_C transition.

The S_C phase exhibits a higher degree of disorder (i.e. a greater entropy) than the S_B phase. Therefore, on cooling it is possible to obtain a S_A-S_C-S_B transition where the molecules have adopted an orthogonal-tilted-orthogonal arrangement.

The occurrence of the S_C phase seems to be influenced by certain structural characteristics of the molecule. The phase is generally exhibited by compounds that possess two terminal alkyl or alkoxy chains, the length of which also appears to be influential. The introduction of branching or a dipole moment to these terminal chains also appears to increase the chance of S_C formation. Molecules which have some degree of symmetry appear to exhibit the S_C phase most readily.

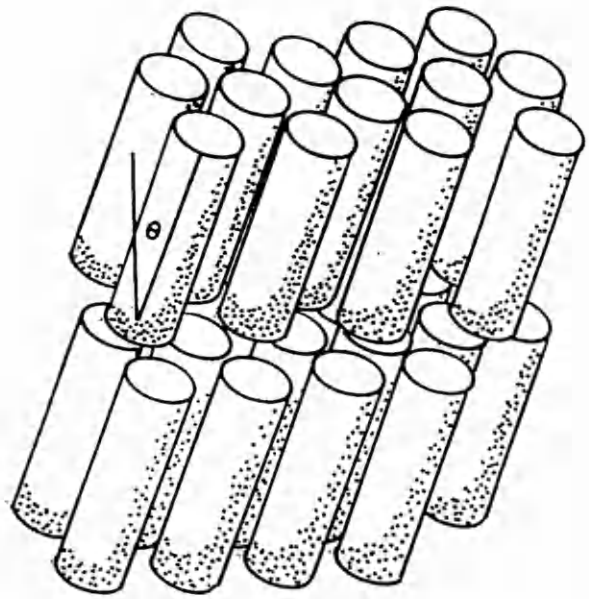

Fig.12 - Model of the S_C phase showing the tilt angle, θ

The smectic C phase can only be obtained on cooling the N, S_A or S_D phases and hence its optical textures are limited. The S_C phase exhibits a *schlieren* texture with *brushes* radiating out from point singularities. The *schlieren* texture of the N and the S_C phases may be distinguished by the number of brushes associated with each point singularity. For the N phase, point singularities with both two and four brushes are observed (see **Plate H**, **Appendix 1**), whereas for the S_C phase only four brush singularities are seen - **Fig.13**.

The S_C phase also exhibits two other types of *schlieren* texture, these being the sanded and the lined *schlieren* textures. The natural focal conic texture of the S_C is not as broken as that obtained paramorphotically from an S_A phase where shattered fans with a grainy appearance are formed.

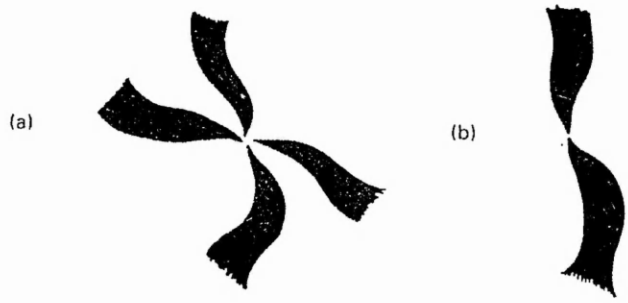

Fig.13 - Point singularities with (a) four brushes, and (b) two brushes

DSC studies indicate that the enthalpy change at the S_A-S_C transition is extremely small and is second order in nature, with approximate enthalpy values of <1 kJ mol^{-1}.

The smectic D phase, S_D

The S_D phase exhibits an optically isotropic texture which is uniform in appearance. As the phase nucleates from the S_C phase, these isotropic areas appear as regular geometric shapes, i.e. rectangles, squares, rhombi, etc. which coalesce to provide the uniform *dark* texture.

The S_D phase is now regarded as being a three-dimensional crystal possessing a cubic lattice. Its structure is not fully understood due to the lack of compounds which exhibit this phase.

The smectic E phase, S_E

The S_E phase may be regarded as having a similar molecular short range packing as an S_B phase, but with a contracted molecular net as shown in **Fig.14**. The molecules lie orthogonal with respect to the layer planes and due to the contracted net, adopt an *orthorhombic* or *chevron* like arrangement.

Molecular rotation is rapid, however, and the close packed arrangement of molecules does not allow for free rotation. Hence only restricted rotation around the molecular axes is possible, and then only if the molecules oscillate through an angle of less than 180^{o} in a concerted *flapping* manner. The layers within the S_E phase are correlated giving rise to a three-dimensional crystal-like structure shown in **Fig.15**.

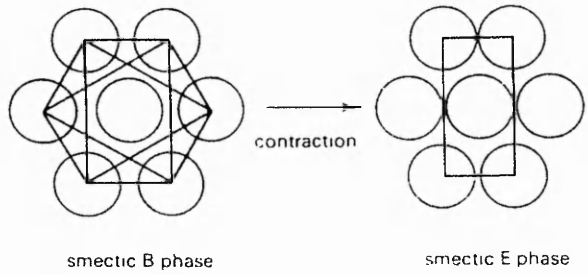

Fig.14 - Similarities between the S_B phase and the contracted net of the S_E phase

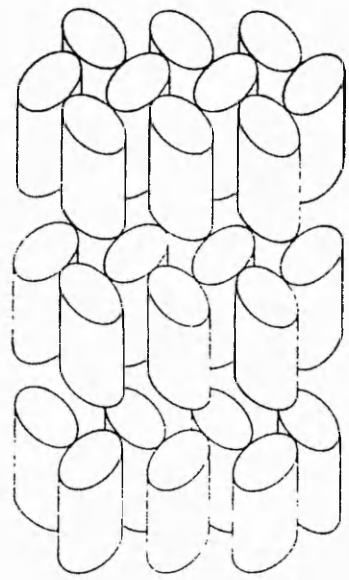

Fig.15 - The layer correlated S_E phase

The S_E phase may be observed on cooling the isotropic liquid or upon cooling the S_A or S_B phases. On cooling the isotropic liquid the natural texture of the S_E phase separates out in the form of droplets which coalesce to provide an *undulating* mosaic. The paramorphotic texture of the S_E phase can take one of three textural appearances. The focal conic texture of the S_E phase is formed on cooling the fan texture of the S_A or S_B phases. The fans become lined with concentric bands similar in appearance to the transition bars of an S_A-S_B transition. However, the banding that occurs in the S_E fan texture is not transitory but remains throughout the temperature range of the phase.

On cooling the homeotropic texture of the S_A or S_B phase, a platelet texture is observed. The platelets grow and overlap one another and generally possess a hexagonal or rhomb-like shape. The S_E phase may also adopt a mosaic texture which is generally observed on cooling the homeotropic region of an S_B phase which has formed directly on cooling the isotropic liquid.

DSC values for I-S_E, S_A-S_E or S_B-S_E transitions are first order and are generally in the range of 4-8 kJ mol^{-1}.

The smectic F phase, S_F

The molecules within the S_F phase lie tilted with respect to the layer planes, but adopt a hexagonal arrangement. X-Ray diffraction studies indicate that for TBPA (terephthalylidene-*bis*-4-n-pentylaniline) **(2)** the tilt angle midway through the temperature range for the phase is approximately 23° and generally decreases with increasing temperature.

(2)

The layers are uncorrelated as there is a shift in the position of the hexagonal nets as the layers are transcended as shown in **Fig.16**. The hexagonal symmetry is preserved throughout the sample with the bulk of the layers being free to slide over one another. They are unable, however, to rotate relative to one another.

Within the S_F phase the tilt direction of the molecular long axes is towards the side of the hexagonal net as shown in **Fig.17** (as opposed to the S_I phase were the tilt direction is towards the apex of the hexagonal net).

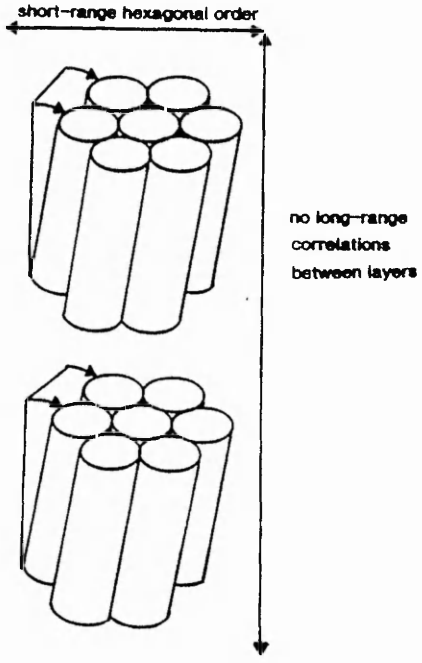

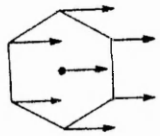

Fig.17 - Tilt direction of molecules in the S_F phase within the hexagonal net

Fig.16 - Model of the S_F phase

The optical microscopic textures of the S_F phase are very similar to those of the S_I phase often leading to difficulties in phase assignment. Very few compounds exhibit the S_F phase on direct cooling of the isotropic liquid. The two natural textures adopted are the *schlieren*-mosaic and a texture that may be of the cylindrical, spherulitic or fan type.

The paramorphotic textures of the S_F phase are varied as the phase may be obtained on cooling a variety of other textures. It is most commonly observed on cooling the S_C phase. The focal conic texture obtained in this way is very characteristic with distinctive black patches in the shape of an elongated *L* appearing across the fans. The *schlieren* areas of the S_C phase adopt a *schlieren*-mosaic texture where definitive areas of mosaic with fine lines are observed. Here some *schlieren* brushes are seen but they show no point singularities. The mosaic texture obtained on cooling from the homeotropic S_A phase is more of a true mosaic and does not show the *schlieren* characteristics.

DSC studies indicate that the S_C-S_F transition is second order or weakly first order and in the range of 1.2-2.4 kJ mol^{-1}.

The smectic I phase, S_I

The S_I phase is similar in structure to the S_F phase and mistakes in assignments of these phase types have been common in the literature. Detailed X-ray studies have shown that the difference lies in the direction of molecular tilt within the pseudo-hexagonal net, with the molecules within the S_I phase being tilted towards the apex of the net.

The natural texture of the S_I phase is that of a mosaic, although this texture is rarely seen. Paramorphotically, the S_I phase may exhibit both a broken fan texture and a *schlieren* texture. The focal conic texture for the S_I and S_F phases is virtually identical. The S_I phase, however, adopts a *schlieren* texture which is characterised by indistinct, unfocused brush areas (a photomicrograph of this texture is shown in **Plate F**, ***Appendix 1***), whereas the S_F phase exhibits a *schlieren*-mosaic texture.

DSC studies indicate that the S_C-S_I transition is second order or weakly first order (1.2-2.4 kJ mol^{-1}) and the S_F-S_I transition is second order (0.12-0.24 kJ mol^{-1}).

1.7.4 *Smectic Crystal Phases*

The three-dimensional crystal B phase and the layer-correlated crystal nature of the S_E phase have already been discussed. Certain other phases, namely those formerly designated S_G, S_J, S_H, and S_K also have inter-layer correlations extending over many hundreds of layers, and are more correctly described as *smectic crystal G*, *J*, *H*, and *K phases*, respectively.

The smectic crystal G and crystal J phases

The molecules within the smectic crystal G phase are packed in layers with their molecular long axes tilted at approximately 25-30° with respect to the layer planes.

The G phase exhibits pseudo-hexagonal close packing with well correlated layers providing a three-dimensional structure as shown in **Fig.18**. X-Ray diffraction studies indicate that the G phase exhibits monolayer stacking (**Fig.19**) and hence can be

considered to be a crystal phase, so that it is now referred to as the crystal G phase rather than as 'S_G' as in the earlier literature.

It is assumed that free molecular rotation is not possible due to the local close-packed chevron arrangement of the molecules. However, the molecules may undergo rapid reorientational motion about their long axes which is achieved via a co-operative movement of the molecules involved.

The crystal G phase is the correlated analogue of the S_F phase with the tilt direction towards the edge of the hexagonal net. Initially, the symbol S_G' was used for the crystal phase in which the tilt direction of the hexagonal net is towards the apex, but this is now assigned the letter J and described as a smectic crystal J phase. On cooling the preceding S_F or S_I phase the tilt direction (either to the edge or the apex of the hexagonal net) is maintained and hence the G phase is the correlated analogue of the S_F phase and the J phase is the correlated analogue of the S_I phase.

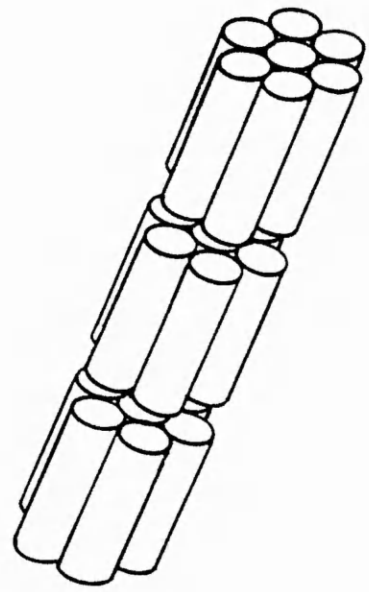

Fig.18 - The correlated structure of the crystal G phase

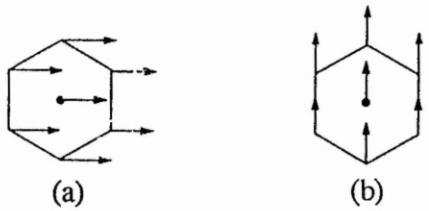

Fig.19 - Tilt directions with respect to the hexagonal net for (a) the G phase, and (b) the J phase

The natural microscopic texture of the G phase may take on different appearances. On cooling from the isotropic liquid the G phase generally nucleates via a dendritic growth pattern to coalesce to form a mosaic texture. However, on cooling from the nematic phase (also a precursor of natural textures) the G phase may separate out as large lancets or mosaic splinters, which support its crystalline character.

On cooling the S_A, S_C, or S_F phases, the paramorphotic focal conic texture of the G phase shows a characteristic chequerboard or patchwork pattern. On cooling the S_B focal conic texture a broken, arced fan texture is observed. The G phase also exhibits a mosaic texture on cooling the *schlieren* or homeotropic texture of the preceding phase.

DSC data shows transitions to the G phase are generally first order in type and have enthalpies in the region of 2.3 kJ mol^{-1}. S_F-G transitions are usually weakly first order with an enthalpy of approximately 1 kJ mol^{-1}.

The smectic crystal H and crystal K phases

The smectic crystal H and crystal K phases can be regarded as the tilted analogues of the E phase. The molecules adopt an orthorhombic arrangement, but due to the tilt the hexagonal net becomes distorted, so that the phases have the monoclinic structure shown in **Fig.20**.

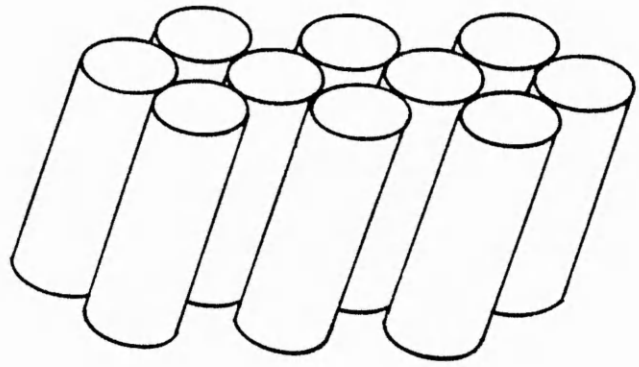

Fig.20 - Model of the layer structure of the H phase

The layers are stacked as described for the E phase to give a three-dimensional structure and hence the phases are crystalline in type. Tilt directions to both the edge and the apex of the hexagonal net are possible: in the H phase the direction of tilt is towards the edge and in the K phase (formerly designated S_H') the tilt direction is towards the apex of the hexagonal net.

The optical textures of the H and K phases are difficult to distinguish. There has been no record of an H or K phase nucleating directly from the isotropic liquid or the nematic phase. The paramorphotic focal conic textures may have either a broken or a smooth appearance. The H and K phases also exhibit a number of mosaic textures. Some of these have large cross-hatched areas whilst others display small, clear, well defined platelets. Cross-hatching may be transitory (generally for the K phase) or permanent (for the H phase).

DSC data indicates that transitions from G-H are generally first order. The enthalpy of transition, however, may vary widely but is generally in the order of 1-5 kJ mol^{-1}.

1.8 *Molecular structure and properties of liquid crystals*

In general most mesogenic compounds are elongated and lath-like in shape and therefore they are geometrically anisotropic. Compounds of this type are said to be *calamitic*. The elongated, lath-like molecular structure is normally found for molecules which give rise to nematic, smectic and cholesteric phases.

However, other molecular structures which give rise to liquid crystalline behaviour have been reviewed.[21] These deviate from the traditional calamitic compounds, and examples include:

(a) Polycatenar compounds (**Fig.21**) - these are liquid crystal compounds possessing more than two flexible chains, e.g. biforked compounds,[22] phasmidic compounds.[23]

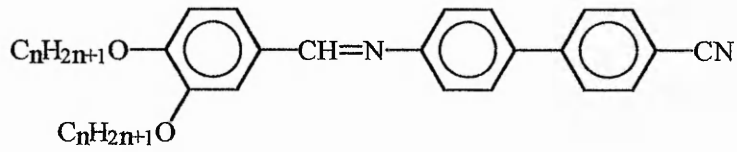

(a)

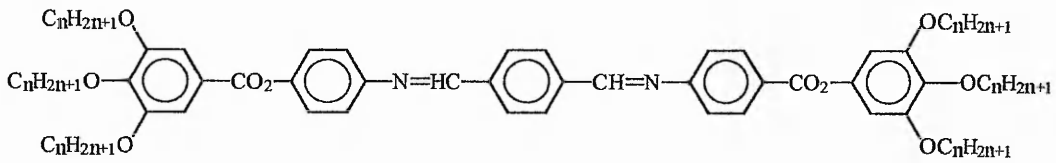

(b)

Fig.21 - Examples of (a) a biforked compound, and (b) a phasmidic compound

(b) Twin mesogens or ***Siamese Twins***[24,25] (**Fig.22**) - these consist of two mesogenic units which are linked in some way.

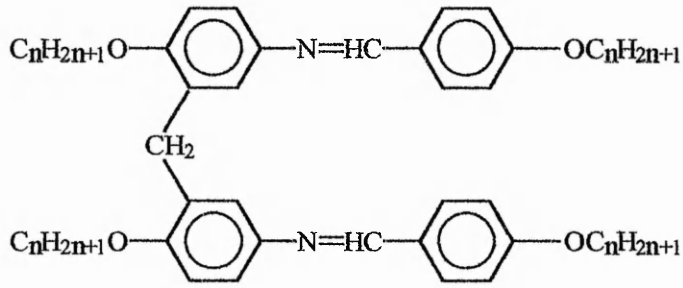

Fig.22 - A Twin mesogen

1.8.1 *Calamitic liquid crystals*

The basic structure of a liquid crystalline molecule may be represented as shown below in **Fig.23** where:

A and B are terminal groups which extend the linearity of the molecule along the long axis. A and B are attached to rigid polarisable groups which allow conjugation, e.g. phenyl.

X is a central linking group which provides linearity and rigidity (may extend conjugation).

The lateral groups, Y and Y', though not essential to liquid crystal formation, may be present either *ortho* or *meta* to the terminal groups

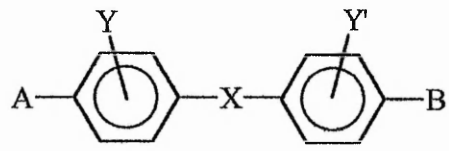

Fig. 23 - General molecular structure of a calamitic liquid crystal

Any deviations from the lath-like arrangement will result in disruptions in geometrical anisotropy and molecular packing and hence will affect the mesophase thermal stability, which is usually expressed as its clearing point, i.e. for nematics N-I, and smectics S-I or S-N.

In addition to geometrical anisotropy, in order to constitute a mesomorphic system a molecule must contain moieties with permanent dipoles and the molecule itself must be highly polarisable. Polarisability is the ability to distort an electron cloud. It increases with atomic radius and increasing bond order, e.g. the polarisability for C-C bonds follows the sequence alkane < alkene < alkyne.

The following is a brief summary of how modifications to the general structure affect liquid crystalline properties.

1.9 *Influence of terminal substituents on mesophase stability*

The terminal group A or B (**Fig.23**) extends the major axis which results in an increase in the anisotropy of molecular polarisability, $\Delta\alpha$ (which is the difference between the molecular polarisability along the molecular axis and the molecular polarisability across the molecular axis). Terminal group substitution causes an increase in the range of the nematic phase compared to hydrogen. The following is the terminal group stability order for the nematic phase:[27]

e.g. Ph > $NHCOCH_3$ > CN > OCH_3 > NO_2 > Cl > Br > $N(CH_3)_2$ > CH_3 > F > H

If the substituent is able to conjugate with the aromatic parts of the molecule then an increase in the polarisability along the molecule is achieved.

However, the effect of terminal group substitution on smectic thermal stability is less well understood. The following orders have been quoted:[27]

(a) $NHCOCH_3 > Ph > Br > Cl > F > N(CH_3)_2 > CH_3 > H > NO_2 > OCH_3 > CN$

(b) $Ph > N(CH_3)_2 > CH_3 > OCH_3 > H$.

Replacement of hydrogen by $-OCH_3$, -CN, or $-NO_2$ groups, which are capable of extending conjugation, can lead to a decrease in phase thermal stability. These groups possess large dipoles which are directed along the molecular long axes. This gives rise to repulsive forces between molecules lying parallel to each other which consequently disrupt the layer formation associated with the smectic phase. Hence, although the methoxy group possesses a dipole which lies across the molecular long axis, which in theory enhances smectic mesophase formation, the alignment of the dipole is statistically near to the major axis of the molecule due to rotation around the ring-oxygen bond. This leads to a decrease in smectic thermal stability.

1.9.1 *Homologation*

If the terminal group of the mesomorphic compound contains either an *n*-alkyl- or *n*-alkoxy-chain a regular trend in transition temperatures is observed as the chain length is extended. This can be shown by plotting transition temperatures against the number of carbon atoms in the chain. For example, for *n*-alkyl chains the plot of T_{N-I} transition temperatures would show that the odd-*n* homologues fit a smooth curve which is higher than the corresponding curve for the even-*n* homologues. For the *n*-alkoxy series the reverse is true.

These results can be explained when the preferred extended zig-zag conformation for an *n*-alkyl chain is taken into consideration as shown in **Fig.24**. For the *n*-alkyl series, the odd homologues contain more C-C bonds lying along the molecular axis than across the molecular axis. Hence there is a corresponding increase in $\Delta\alpha$ and the T_{N-I} curve lies higher for the odd members of the series.

The oxygen atom in the *n*-alkoxy series is considered to be the stereochemical equivalent of a CH_2 group in the *n*-alkyl series, hence leading to the reverse observation.

Depending on the homologous series the shapes of the T_{N-I} curves may vary, with both falling, both rising or a combination of the two with the upper curve falling and the lower curve rising.

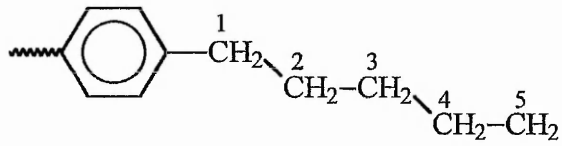

(a) alkyl

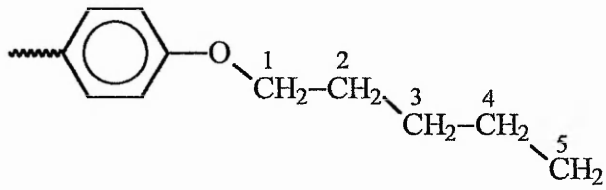

(b) alkoxy

Fig.24 - Conformations adopted by (a) alkyl and (b) alkoxy chains

An example of the odd-even effect is shown by the liquid crystal behaviour of a typical homologous series, the 4'-n-alkoxybiphenyl-4-yl carboxylic acids[28] (**Fig.25**).

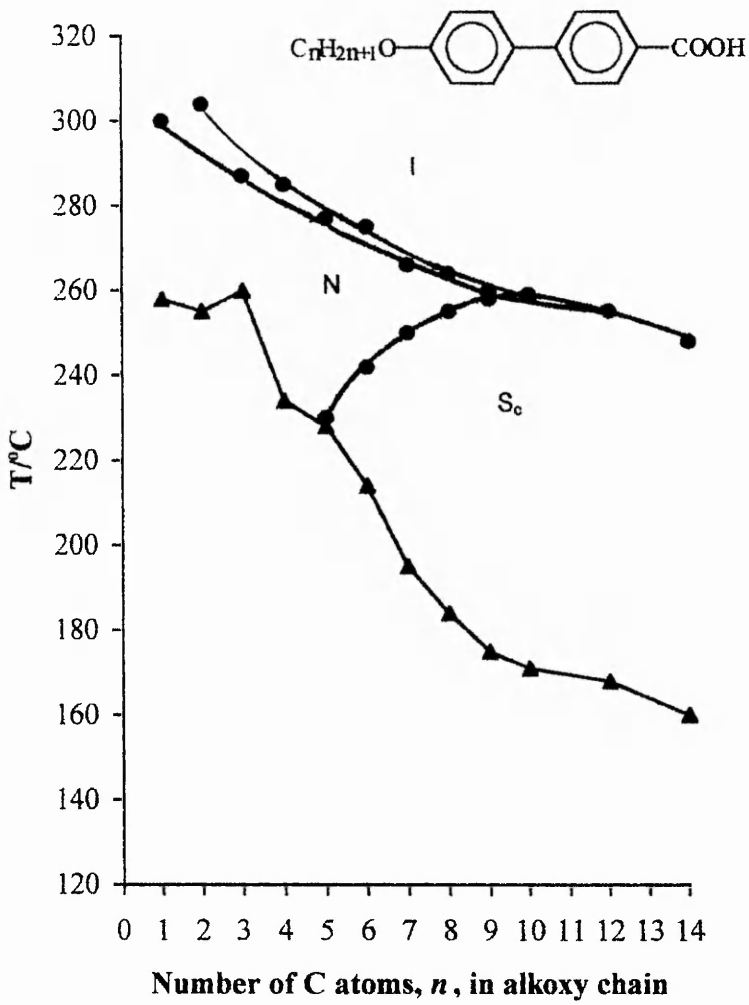

Fig.25 - Plot showing the odd-even effect for an homologous series of 4'-n-alkoxybiphenyl-4-yl carboxylic acids.

The plot of transition temperatures against *n*, the number of carbon atoms of the alkoxy group, reveals the following trends:

(a) The T_{N-I} transition temperatures fit two falling curves (even-*n* uppermost), which show a regular diminishing alternation between the odd-*n* and the even-*n* members of the series, and become coincident as the higher homologues are reached.

(b) T_{S-N} appear at $n = 5$ and the transition temperature curve rises steeply between $n = 5$-8, coinciding with the falling T_{N-I} curve at $n = 10$. Above this point the nematic properties of the compound are lost and the T_{S-I} transition temperature curve continues to fall.

The thermal stability of the nematic phase is mainly determined by the residual terminal attractions between molecules which maintain their parallel arrangement. Smectic mesophase thermal stability, however, is mainly governed by lateral molecular interactions.

With regard to the above plot therefore, certain points are of note:

(a) The lower members of the homologous series show the nematic phase only. Here the terminal forces are strongest and the nematic phase terminal stability is highest. This can be seen to decrease as the chain length increases.

(b) As the chain length increases the lateral cohesive forces also increase. This leads to the appearance of the more ordered smectic mesophase for the homologues of intermediate chain length which enable the formation of a layer-like arrangement.

(c) The higher members of the series show no nematic mesophase properties due to a weakening of terminal attractive forces.

1.9.2 Terminal alkyl chain branching

Studies of the effect of branching in alkyl chains on mesophase stability show that the effect is related to the position of the branching along the length of the chain shown in **Fig.26**.

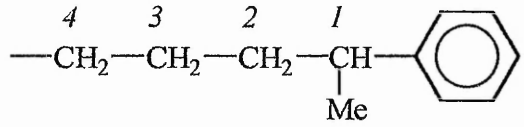

Fig.26 - Terminal alkyl chain branching

For nematogenic n-alkyl esters the following results have been observed:

(a) T_{N-I} is greatly decreased by the introduction of a 1-Me group.

(b) T_{N-I} shows a progressively smaller decrease as the Me group is moved to positions 2, 3 and 4.

Whereas for smectogenic n-alkyl esters:

(a) S_A-I is much less affected by the introduction of a 1-Me group, and this effect becomes progressively smaller as the Me group is moved towards the end of the chain.

(b) The thermal stability of higher order smectic phases either is not greatly effected (S_B), or increases (S_E) when a branched 1-Me group is introduced.

1.10 *The influence of the central linking group (X) on mesophase thermal stability*

The central linking group plays a more important role in influencing the magnitude of mesophase thermal stability than in dictating the type of mesophase formed. In order to promote thermal stability linking groups should maintain a high π-electron density throughout the system and retain the molecular lath-like shape. If the linking group can extend conjugation then this will result in an increase in the anisotropy of molecular polarisability and hence T_{N-I}.

An average central linking group efficiency for promoting T_{N-I} has been suggested by Gray,[29] as follows:

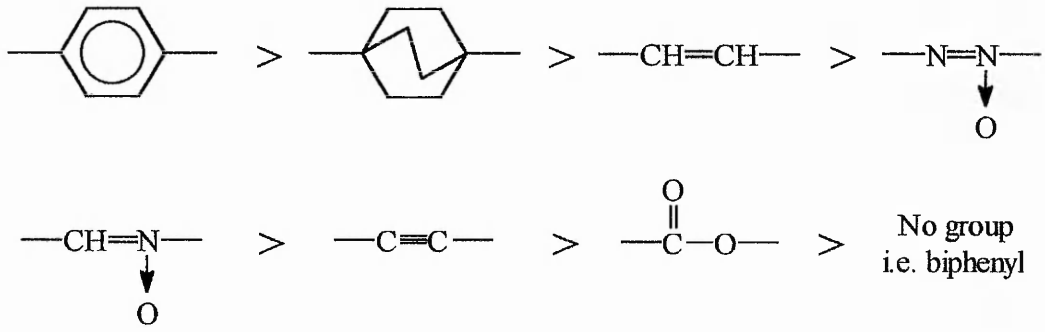

1.11 *The influence of lateral substitution on mesophase thermal stability*

Lateral substitution has the effect of decreasing the anisotropy of molecular polarisability, Δα, of the molecule. It causes an increase in the polarisability across the molecule and hence this leads to a decrease in mesophase thermal stability.

This has been shown by studies on 3'-substituted 4'-n-alkoxybiphenyl carboxylic acids **(3)**.[30] The substituent Y extends outside the perimeter defined by the rest of the molecule, interfering with its calamitic (lath-like) geometry. The size of the depression in T_{N-I} is proportional to the size of the substituent, irrespective of the permanent ring-Y dipole.

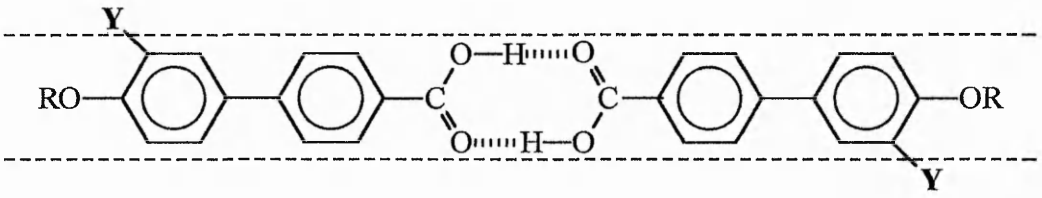

(3)

T_{N-I} order: **Y** = H > F > CH_3 ≈ Cl > Br > I >NO_2

For smectic mesophases, however, the effect of a strongly dipolar lateral substituent is to increase T_{S-N} or T_{S-I} in comparison with a less polar substituent. This suggests that for smectic mesophase thermal stability, dipolar association has a greater importance.

In some cases, the position of substitution is such that the substituent is shielded, partly or completely, by the molecular structure. This behaviour is exhibited by the 6-n-alkoxy-5-halogeno-2-naphthoic acids **(4)**.[31]

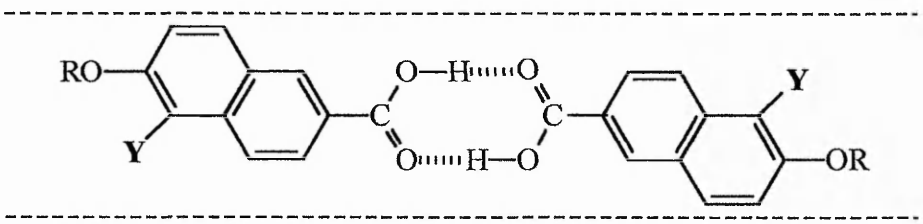

(4)

T_{N-I} order: **Y** = Cl > Br > H > I

A small substituent can easily be accommodated within the molecular perimeter. In such cases an increase in mesophase thermal stability, relative to the unsubstituted acids, occurs because the introduction of the substituent increases the molecular polarisability. If the substituent is dipolar, such as chloro-, the lateral cohesive forces are

substantially increased so that the thermal stability of the smectic phase is increased more than that of the nematic phase. Large 5-substituents, such as iodo- and nitro-, protrude outside the molecular perimeter and the breadth-increasing effect of the substituent then results in a reduction in nematic thermal stability.

Thus, in the case of the naphthoic acids **(4)**, a different order is observed as the substituent X is wholly or partially contained within the perimeter of the molecule.

1.12 *The Effect of the Introduction of Chirality into Liquid Crystal Systems*

The inclusion of a chiral centre(s) within the molecular structure of mesogens has led to the discovery of a range of new phases which have revolutionised the display industry. Liquid crystal molecules which possess to a chiral smectic C phase, S_C*, give rise to ***ferroelectric***[33] behaviour. In this case, when under stress, the dipoles of the molecules align in the same direction, with the molecules adopting a tilt angle of 22.5 ° with respect to the layer planes. When a voltage is applied the molecules will flip through 45 ° (compared to 90 ° for an analogous twisted nematic LCD) affording a very rapid switching time. This phase also exhibits bistability.

More recently sub-phases of the chiral smectic C phase have been discovered.[34] These are termed S_C*antiferro- and S_C*ferri-electric and differ from the ferroelectric phase in terms of their molecular arrangement within the layers as shown in **Fig.27**. So far, however, these sub-phases have not been found to be useful in display systems.

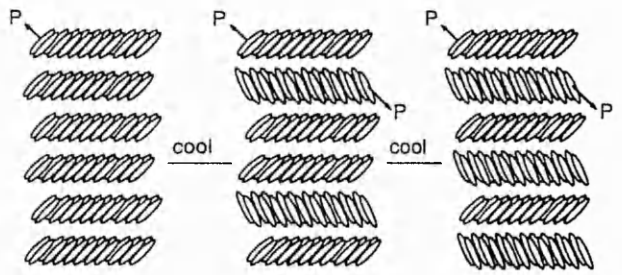

Fig.27 - Schematic representation of the ferroelectric, ferrielectric and antiferroelectric smectic C* phases in their unwound, non-helical states.

1.13 *Uses of Liquid Crystals*

The main industrial application of liquid crystals is for use in Liquid Crystalline Displays (LCD). These systems are desirable for many reasons. The devices have a low power consumption and therefore are portable and will operate off battery power. They operate at low voltages, exhibit good readability, and display compactness and flexibility of size. A liquid crystal display is also directly compatible with an integrated circuit which cuts down on the size and cost of equipment.

An LCD is a flat panel display which does not emit radiation. The display operation requires chemically and photochemically stable compounds with a wide liquid crystal range at around room temperature. As just one compound will not afford all the required parameters for a display, a mixture of compounds is used to provide the full operating requirements and to increase the liquid crystal range. Most displays utilise between 4 and 10 components, sometimes with the addition of small amounts of non-mesomorphic compounds.

LCD's are passive electro-optical displays, i.e they do not generate light but modulate it. By passing a voltage across desired segments of the screen they become visibly distinct from the background to produce a character on the display.

They have become an integral part of everyday life in digital displays and computer screens. As a result there is much commercial and academic research and development work looking at new materials and devices.

2. *Aims*

2. *Aims*

In recent years, the Liquid Crystal Group at The Nottingham Trent University has been involved in extensive investigations into the synthesis and identification of the phase types of many novel liquid crystalline compounds.[34-39,43] The work of the group has been concentrated almost exclusively on the synthesis of a wide range of mesogenic organic compounds, and a detailed study of the effect of homologation on mesophase thermal stability and phase types. The initial studies of benzenoid mesogenic systems were later extended to their heterocyclic analogues, such as derivatives of thiophene,[35,36] furan,[37] *etc.* More recent studies have included investigations of the effect of incorporation of chiral centres into such systems,[38] and the effect of lateral fluorination of the rigid organic core of mesogenic molecules on liquid crystal properties.[39]

One of the initial aims of the work detailed within this thesis was to move away from the more 'conventional' approach based purely on mesogenic organic compounds, and extend the liquid crystal research group into a new and more novel area of chemistry. The recent emergence of the first metal-containing mesogenic systems, known as ***metallomesogens***, provided an ideal way to achieve this aim.

The chemistry of metal-containing liquid crystalline compounds has been extensively reviewed,[40,41,42] and many new avenues for possible research exist. Initial studies at the University were carried out under the guidance of Dr K Moss, and concentrated on metal co-ordinated liquid crystal systems. It was hoped to extend this initial work further to incorporate the organometallic compound ferrocene.

Between the years of 1988 and 1992, a number of liquid crystalline derivatives of ferrocene were reported in the literature (reviewed in section **6.5**). However, the majority of these compounds were esters derived from either ferrocene-1,1′- **(47)** or -1,3-dicarboxylic acid **(75)**.

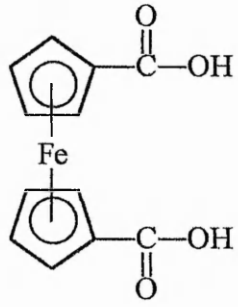

(47)

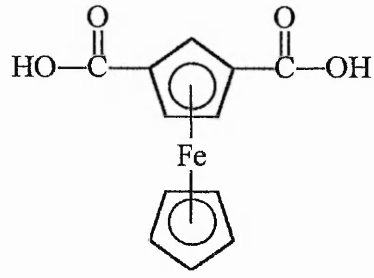

(75)

This rather limited approach to the type of linking group between the ferrocene moiety and the rigid organic core molecule seemed surprising considering the well documented chemical versatility of ferrocene. Hence, the principal aim of the investigation was to attempt the synthesis of some novel 1,1′-disubstituted ferrocene compounds incorporating linking groups which were not derived from ferrocene-1,1′–dicarboxylic acid **(47)**, and to investigate any liquid crystalline properties that these compounds might exhibit.

Two other, more conventional topics with well-defined aims were also undertaken to run in parallel with the ferrocene investigation. These involved the synthesis and study of the liquid crystal properties of homologous series of esters incorporating a biphenyl moiety. The synthetic work involved was straightforward, but a large number of compounds were prepared as each series revealed quite complex liquid crystal behaviour which required comprehensive study to provide an accurate identification of mesophase type.

The driving force for the first topic was some preliminary studies,[37] previously undertaken at The Nottingham Trent University, on members of a homologous series of 4′-n-alkoxybiphenyl-4-yl cyclohexanecarboxylates **(10)**. The transition temperature plot obtained for these compounds was of a very unusual form, exhibiting a pronounced 'hump' for the members n = 3-6. There was also uncertainty whether or not these early homologues were giving rise to a liquid crystal phase at all, as the observed texture was not recognisable as any known mesophase type but exhibited many of the characteristics of a crystalline solid separating from the isotropic liquid.

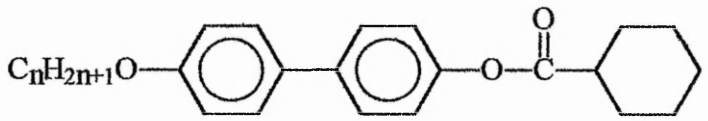

(10)

Because of the uncertainties with regard to the uncharacteristic textures and the unusual form of the transition temperature plot, the 4′-n-alkoxybiphenyl-4-yl cyclohexanecarboxylates **(10)** (n = 1-10,12,14 and 16) were resynthesised. The aim of this study was to bring the complementary techniques of thermal optical microscopy, differential scanning calorimetry and miscibility studies to bear on the identification of the phase types involved to accurately determine their nature. In order to assist, develop, and extend this study, the synthesis of the related cyclopropanecarboxylates **(7)**, (n = 1-10 and 12); cyclobutanecarboxylates **(8)**, (n = 1-10 and 12); cyclopentanecarboxyaltes **(9)**, (n = 1-10 and 12); and cyloheptanecarboxylates **(11)**, (n = 1-10,12,14 and 16) was also undertaken, and their liquid crystal behaviour investigated.

The second topic originated from the outcome of a study of the liquid crystal behaviour of the 4′-n-alkylbiphenyl-4-yl 5-n-alkylthiophene-2-carboxylates **(20)** carried out by Byron and Wilson *et al.*[43] These thiophene esters exhibit extensive smectic polymorphism and a comparison of their mesophase behaviour and thermal stability with that of the analogous benzoates, the 4′-n-alkylbiphenyl-4-yl 4-n-alkylbenzoates **(17)**, was desirable.

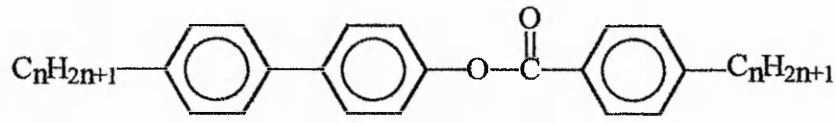

(17)

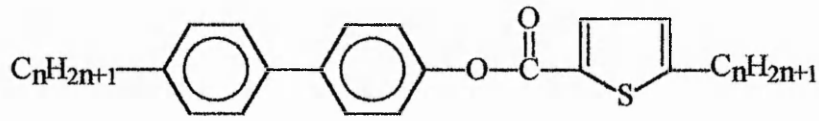

(20)

However, although a number of these benzoates had been cited in a patent granted to Steinsträsser *et al.*,[44] seemingly no attempt had been made by the authors to identify the smectic phases present. Hence, in order rectify this deficiency in the literature, the synthesis of four homologous series of 4′-n-alkylbiphenyl-4-yl 4-n-alkylbenzoates **(17)**, (m = 5,6,7 and 10), (n = 1-10) was undertaken. The mesophase behaviour of these compounds was investigated using the complementary techniques of thermal optical microscopy and differential scanning calorimetry.

2.1 *Layout of the thesis*

With these aims in mind, the research work initially concentrated upon the synthesis of some novel ferrocene derivatives. However, this investigation proved to be much more challenging than originally anticipated, and progress in this area was much slower, and with more limited outcomes than had been hoped for. Consequently, there was a shift in the emphasis of the research away from the synthesis of new metallomesogens, with the investigations into the properties of the biphenyl ester series becoming more prominent than the ferrocene work.

The layout of this thesis reflects this fact. The preparative details for the synthesis of the biphenyl esters are given in section **3.0**, and the liquid crystal behaviour of these series is discussed in sections **4.0** and **5.0**. The investigations into the synthesis of some novel 1,1′-disubstituted ferrocene derivatives are reported separately, with a brief introduction to metallomesogen chemistry and current ferrocene liquid crystal literature (section **6.0**), synthetic pathways undertaken (section **7.0**) and a discussion of the conclusions drawn from this investigation (section **8.0**).

3. *Experimental I - biphenyl derivatives*

3. *Experimental I - biphenyl derivatives*

This section gives details of the preparation of the compounds displayed in ***schemes 1*** and *2*. The structural integrity of the intermediates and products was confirmed by infra-red spectroscopy (Perkin Elmer 1600 FT-IR spectrophotometer) and nuclear magnetic resonance spectroscopy (JEOL EX 270MHz NMR spectrometer). Most commercial reagents were obtained from the Aldrich Chemical Company Ltd. and BDH (Merck UK) Chemicals Ltd. Dry solvents were obtained using the following procedures: dichloromethane (DCM) was dried over anhydrous calcium chloride; tetrahydrofuran (THF) was dried by continuously heating under reflux in the presence of sodium metal and benzophenone as indicator (a blue coloration being indicative of dry solvent); both hexane and benzene were dried over freshly extruded sodium wire.

3.1 *Experimental Discussion*

The final compounds indicated in ***Schemes 1*** and *2* were synthesised by esterification reactions involving either trifluoroacetic anhydride (TFAA) or dicyclohexylcarbodiimide (DCC) and dimethylaminopyridine (DMAP). The first of these methods proceeds via a *mixed anhydride* intermediate, and an essentially analogous intermediate may participate in the DCC esterification. The general mechanism of each reaction is discussed below:

Trifluoroacetic anhydride method

The reaction proceeds by the initial formation of the mixed anhydride **(I)** with the loss of the trifluoroacetate anion. The carbonyl carbon marked as C* might then be considered the most likely centre to undergo nucleophilic substitution by the

alcohol moiety, but it is the other carbonyl group which is attacked as the trifluoroacetate anion is such an excellent leaving group.

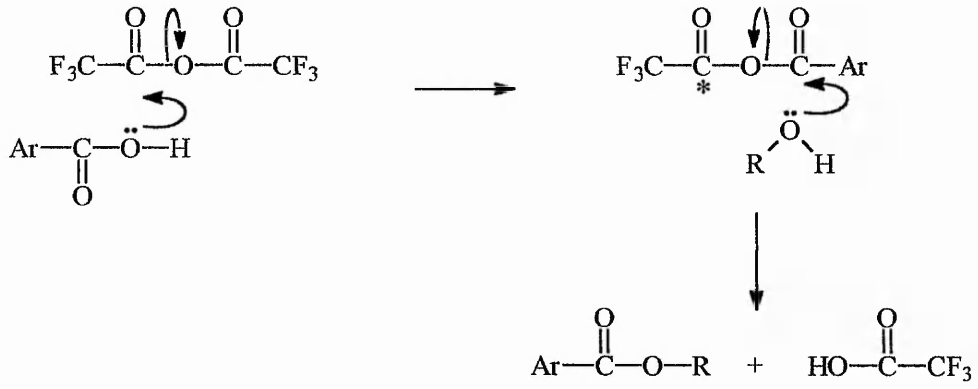

Parish and Stock[45] suggested that nucleophilic attack by the alcohol moiety occurs either **(1)** on an acylium ion intermediate derived from a protonated mixed anhydride or **(2)** directly on the protonated anhydride itself. Path **(1)** is the more favourable for sterically hindered acids.

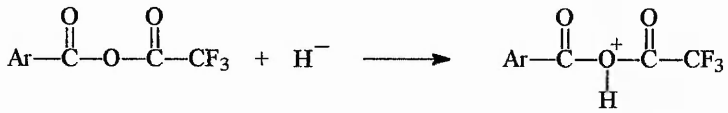

Dicyclohexylcarbodiimide and DMAP Method

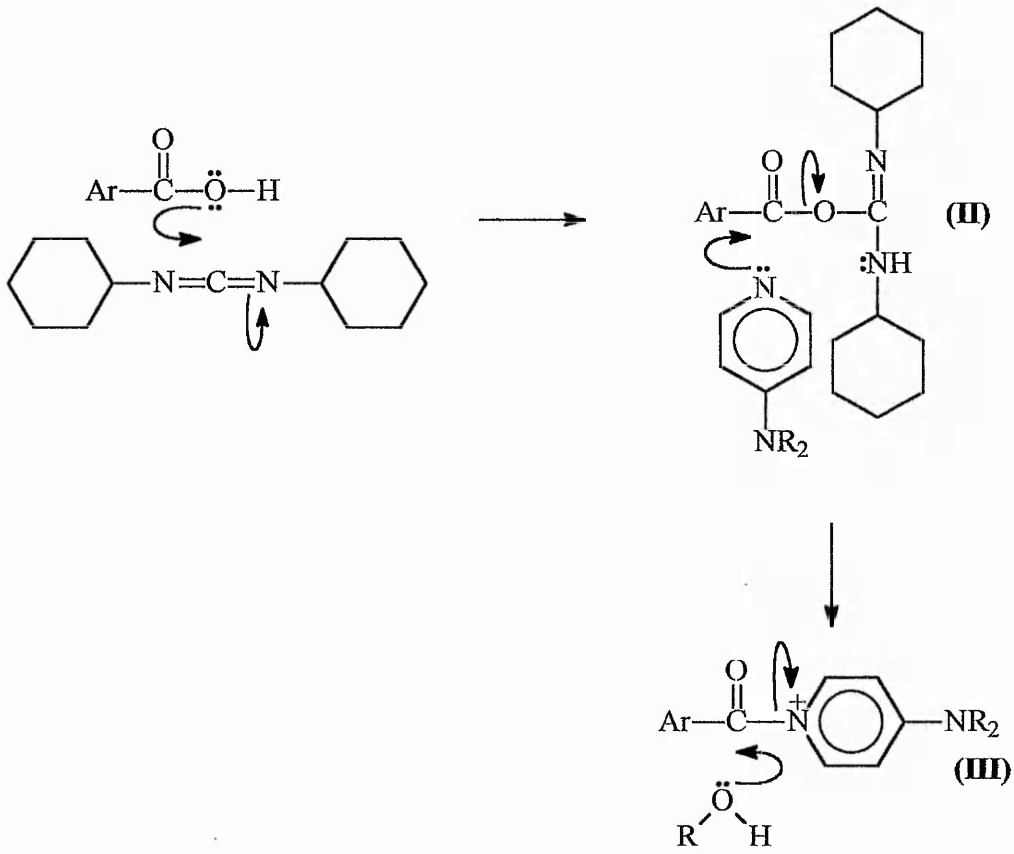

Originally proposed by Hassner and Alexanian[46], the general mechanism for esterification involving DCC with DMAP or other strong amine base, is shown above. The intermediate **(II)**, which may be regarded as electronically equivalent to a mixed anhydride, is susceptible to an internal rearrangement if left for too long, forming a stable acylurea. The introduction of DMAP in solution at the start of the reaction prevents this rearrangement by reacting rapidly with the mixed anhydride, to form the highly reactive species **(III)**. It is this intermediate which then undergoes nucleophilic attack by the alcohol. The DCC is converted into dicyclohexylurea, which is easily removed from the reaction mixture by filtration.

3.2 *Preparative Routes*

Scheme 1

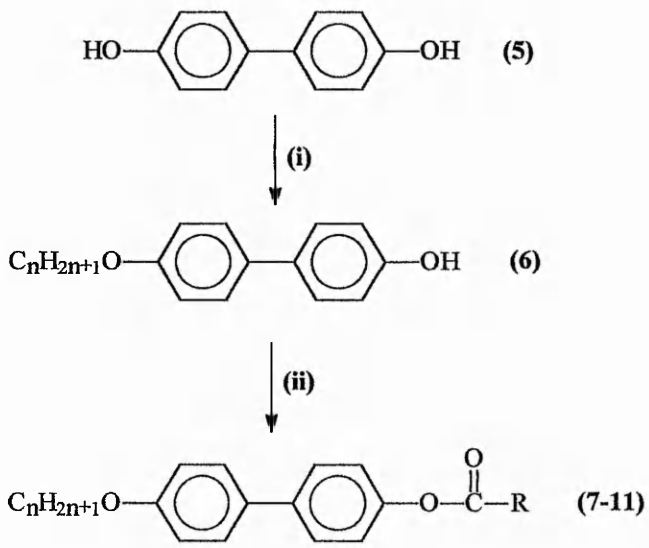

Where **R =**

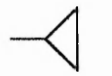

7 (n = 2-10,12)

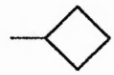

8 (n = 2-10,12)

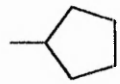

9 (n = 2-10,12)

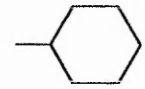

10 (n = 2-10,12 ,14, 16)

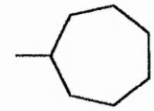

11 (n = 2-10,12 ,14, 16)

Legend

(i) $C_nH_{2n+1}Br$ / IMS / KOH **(ii)** RCOOH / TFAA / DCM

Scheme 2

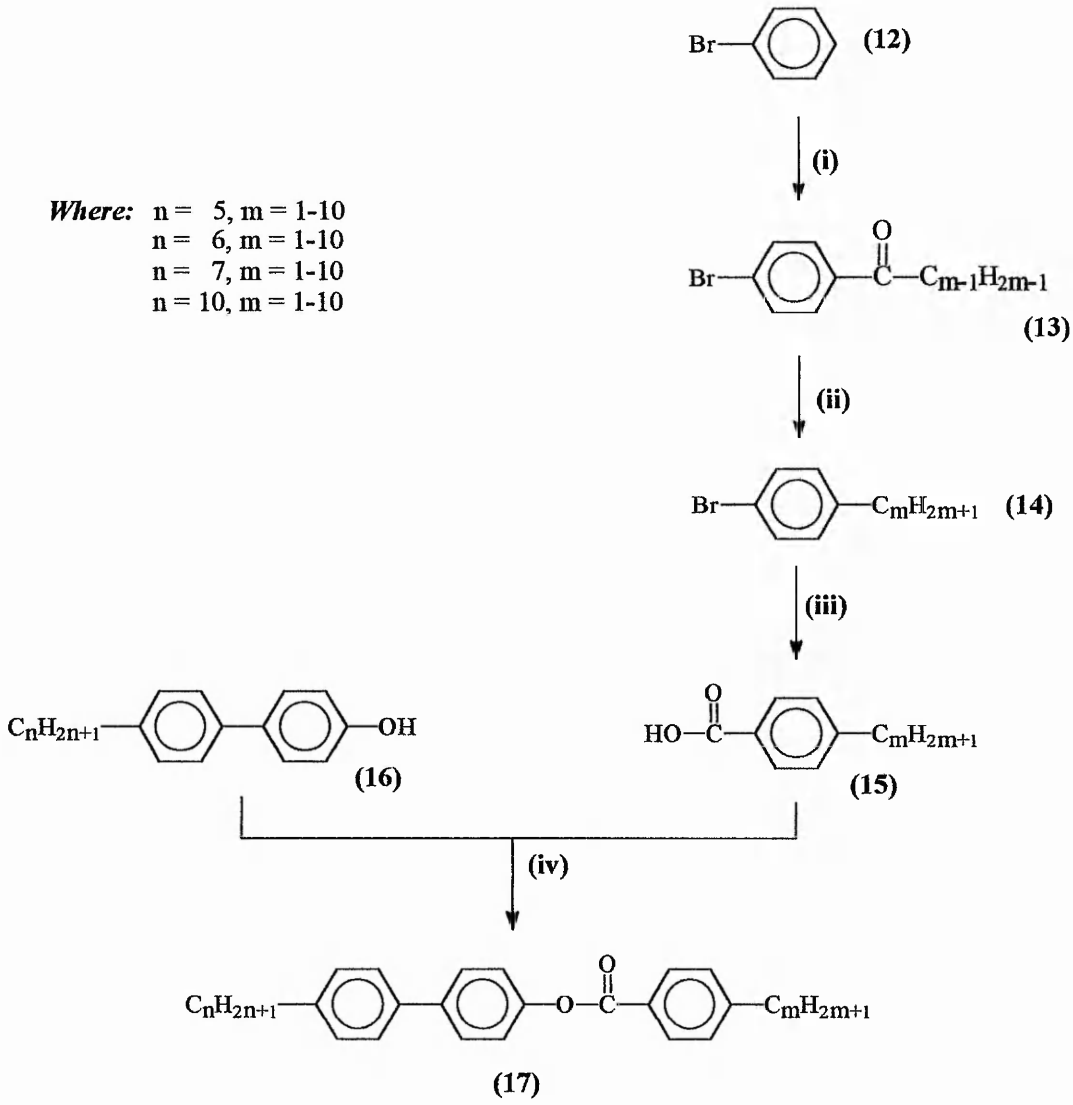

Where: n = 5, m = 1-10
n = 6, m = 1-10
n = 7, m = 1-10
n = 10, m = 1-10

Legend

(i) $C_{m-1}H_{2m-1}COCl$ / $AlCl_3$ **(ii)** $NH_2NH_2.H_2O$ / Diethylene glycol / KOH

(iii) 2.5 M BuLi / CO_2 / -78°C **(iv)** TFAA / DCM or DCC / DMAP / DCM

3.3 *Experimental methods - scheme 1*

The synthetic route for the preparation of 4′-*n*-alkoxybiphenyl-4-yl cycloalkanecarboxylates **(7-11)** is detailed in ***Scheme 1***. The reaction of commercially available 4,4′-dihydroxybiphenyl with an appropriate *n*-alkylbromide produced the corresponding mono-ether **(6)**. The esterification of these ethers was then accomplished by their reaction with the appropriate cycloalkanecarboxylic acid in the presence of trifluoroacetic anhydride to produce the desired series of compounds **(7-11)**.

3.3.1 *Preparation of 4′-n-alkoxy-4-hydroxybiphenyls* (6)

Potassium hydroxide (6.36 g, 46 mmol) in water (75 ml) was added, dropwise, during a 2h period to a mixture of 4,4′-dihydroxybiphenyl **(5)** (2.98 g, 0.16 mol), the appropriate n-alkylbromide (0.015 mol) and methylated spirit (25 ml). The reaction mixture was heated under gentle reflux throughout the addition and for a further 3h afterwards, during which time a white solid separated out of solution. The mixture was then cooled, acidified (concentrated hydrochloric acid) and the resulting white precipitate was filtered off. The desired mono-ether was purified by flash column chromatography on silica gel eluting with chloroform followed by recrystallisation from a mixture of chloroform / light petroleum (b.p. 60-80 °) to afford the desired 4′-*n*-alkoxy-4-hydroxy-biphenyl **(6)** as a white crystalline solid, 4-*n*-ethyloxy- (50%), m.p. 171-172 °C; 4′-*n*-propyloxy- (45%), m.p. 172-173 °C; 4′-*n*-butyloxy- (39%), m.p. 168-170 °C; 4′-*n*-pentyloxy- (30%), m.p. 157.5-159 °C; 4′-*n*-hexyloxy- (31%), m.p. 156-158 °C; 4′-*n*-heptyloxy- (30%), m.p. 154.5-155.5 °C; 4′-*n*-octyloxy- (41%), m.p. 152-153 °C; 4′-*n*-nonyloxy- (49%), m.p. 143-144.5 °C; 4′-*n*-decyloxy- (40%), m.p. 147-149 °C;

4′-*n*-dodecyloxy- (33%), m.p. 145-146 °C; 4′-*n*-tetradecyloxy- (44%), m.p. 138-140 °C; 4′-*n*-hexadecyloxy- (25%), m.p. 133-135 °C.

Data for the 4′-*n*-decyloxy-4-hydroxybiphenyl are given.

NMR: δ_H ($CDCl_3$) 0.90 (3H, t, CH_3), 1.32-1.82 (10H, m, CH_2), 3.98 (2H, t, OCH_2), 4.78 (1H, s, OH), 6.85-6.89 (4H, m, ArH), 7.40-7.47 (4H, m, ArH) ppm.

IR: ν_{max} (KBr), 3430 (OH broad str), 2953, 2920, 2850, 1598, 1499, 1267 cm^{-1}.

3.3.2 *Preparation of the 4′-n-alkoxybiphenyl-4-yl cycloalkanecarboxylates* (7-11)

A total of five separate series of compounds were synthesised by the esterification of cyclopropyl-, -butyl-, -pentyl-, -hexyl-, and -heptyl-carboxylic acids with the homologous series of alcohols prepared as described in **3.3.1**. As an example of a typical procedure the preparation of the 4′-*n*-nonyloxybiphenyl-4-yl cyclohexanecarboxylate is described.

Cyclohexanecarboxylic acid (0.16 g, 1.25 mmol) and the 4′-*n*-nonyloxy-4-hydroxybiphenyl **(6)** (1.25 mmol) were stirred in dry dichloromethane (DCM) (20 ml). Trifluoroacetic anhydride (0.27 g, 1.3 mmol) was added and the reaction mixture was stirred overnight. The solvent was removed under reduced pressure and the residue was purified by column chromatography on neutral alumina, eluting with chloroform, followed by several recrystallisations from petroleum ether (b.p. 60-80 °) to afford the desired 4′-*n*-nonyloxybiphenyl-4-yl cyclohexanecarboxylate, 0.21 g (40%), as a white crystalline solid, m.p.105.8 °C .

NMR: δ_H ($CDCl_3$) 0.88 (3H, t, CH3), 1.28-2.20 (23H, t, alkyl CH_2 and cyclohexyl CH_2), 2.76 (1H, m, cyclohexyl CH), 3.98 (2H, t, OCH_2), 6.93-6.96 (2H, d, ArH), 7.08-7.11 (2H, d, ArH), 7.45-7.54 (4H, m, ArH) ppm.

IR: ν_{max} (KBr), 2950, 2928, 2854, 1685 (C=O str.), 1598, 1497, 1270 cm^{-1}.

At least ten members of each homologous series of 4′-*n*-alkoxybiphenyl-4-yl cycloalkanecarboxylates **(7-11)** were synthesised. These have been designated as the following five series:

4′-*n*-alkoxybiphenyl-4-yl cyclopropanecarboxylates	**(7)**, n = 2-10, 12
4′-*n*-alkoxybiphenyl-4-yl cyclobutanecarboxylates	**(8)**, n = 2-10, 12
4′-*n*-alkoxybiphenyl-4-yl cyclopentanecarboxylates	**(9)**, n = 2-10, 12
4′-*n*-alkoxybiphenyl-4-yl cyclohexanecarboxylates	**(10)**, n = 2-10, 12, 14, 16
4′-*n*-alkoxybiphenyl-4-yl cycloheptanecarboxylates	**(11)**, n = 2-10, 12, 14, 16

A summary of the thermal data together with a detailed discussion of the phase types associated with these series is reported in section **4.0**.

3.4 *Experimental methods - scheme 2*

The preparation of some 4′-*n*-alkylbiphenyl-4-yl 4-*n*-alkylbenzoates **(17)** is detailed in ***Scheme 2***. The 4-*n*-alkylbenzoic acids **(15)** were mainly purchased from BDH (Merck UK) Chemicals Ltd., although they may be readily synthesised by the successive treatment of bromobenzene with the appropriate acid chloride to yield 1-bromo-4-*n*-alkanoylbenzene **(13)**. The reduction of this ketone was achieved by heating under reflux with an excess of hydrazine hydrate in diethylene glycol, treatment with KOH, before acidifcation to yield the desired 1-bromo-4-*n*-alkybenzene **(14)**. The 4-*n*-alkylbenzoic acids **(15)** were then obtained by the treatment of **(14)** with a commercial solution of butyl lithium, then with solid CO_2, followed by acidification with HCl. The 4-*n*-alkyl-4′-hydroxybiphenyls **(16)** were kindly donated by Dr J Butcher; the synthetic details for the preparation of these compounds are reproduced in the paper detailing the synthesis of the analogous 4′-*n*-alkylbiphenyl-4-yl 5-*n*-alkylthiophene-2-carboxylates[43] **(20)**.

The 4′-*n*-alkylbiphenyl-4-yl 4-*n*-alkylbenzoates **(17)** were synthesised by the esterification of the phenols **(16)** with the 4-*n*-alkylbenzoic acids **(15)**, either using trifluoroacetic anhydride or dicyclohexylcarbodiimide and dimethylaminopyridine to promote the reaction.

3.4.1 *Preparation of the 1-bromo-4-n-alkanoylbenzenes* (13)

The appropriate freshly distilled acid chloride (0.35 mmol) was added to a cooled suspension (<0 °C) of powdered anhydrous aluminium chloride (47 g, 0.35 mmol) in dry bromobenzene (150 ml) contained in a three-necked round bottomed flask equipped with a suitable thermometer, dropping funnel, and calcium chloride guard tube. The reaction mixture was stirred for 1h., then heated at 80 °C for a further 4 h. The reaction was then

quenched by pouring into ice and 4M-aqueous hydrochloric acid and the mixture was transferred to a separating funnel. The organic layer was isolated and the aqueous phase was extracted with chloroform (3x50 ml). The combined organic fractions were washed with water (50 ml) and steam distilled to remove the excess bromobenzene. The ketone was then extracted with chloroform, then dried over $MgSO_4$ and the solvent removed under reduced pressure. The resulting crude product was used crude in most cases, however the 1-bromo-4-n-pentanoylbenzene (82%) was distilled, b.p. 195-204 °C / 18 mmHg, to yield a pale oil which solidified on standing. Spectroscopic data are given below:

NMR: δ_H ($CDCl_3$) 1.0 (3H, t, CH_3), 1.52-2.08 (4H, m, CH_2), 2.7 (2H, t, $COCH_2$), 7.2 (2H, d, ArH), 7.65 (2H, d, ArH) ppm.

IR: ν_{max} (thin film) 2927, 1684 (C=O str), 1564, 1462,1395, 1209, 999 cm^{-1}.

3.4.2 *Preparation of the 1-bromo-4-n-alkylbenzenes* (14)

The appropriate 1-bromo-4-n-alkanoylbenzene (0.32 mol) and hydrazine hydrate (1.05 mol) were heated at 130 °C in diethylene glycol (250 ml) for 2h. The excess hydrazine hydrate was then distilled off and the mixture allowed to cool. Potassium hydroxide (53 g, 0.96 mol) was then added and the mixture heated to between 180-190 °C for a further 3h. The reaction mixture was then cooled and hydrolysed by pouring into 4M-aqueous hydrochloric acid (150 ml). The product was then extracted into ether (3x75 ml), then dried over $MgSO_4$, before the solvent was removed under reduced pressure.

The desired 1-bromo-4-n-alkylbenzene **(14)** was distilled as a colourless oil in varying yields (32-76%).

4-*n*-ethyl- b.p. 40-45 °C / 1 mmHg; 4-*n*-propyl- b.p. 60-65 °C / 0.2 mmHg; 4-*n*-butyl- b.p. 150-155 °C / 15 mmHg ; 4-*n*-pentyl- b.p. 55-60 °C / 0.1 mmHg; 4-*n*-hexyl- b.p. 87-90 °C / 0.01 mmHg; 4-*n*-heptyl- b.p. 90-95 °C / 0.01 mmHg; 4-*n*-octyl- b.p. 80-85°C / 0.5 mmHg; 4-*n*-nonyl- b.p. 120-125 °C / 0.1 mmHg; 4-*n*-decyl- b.p. 125-130 °C / 0.2 mmHg.

The following spectral data refers to the 1-bromo-4-*n*-pentylbenzene **(14)**

NMR: δ_H ($CDCl_3$) 0.9 (3H, t, CH_3), 1.25-1.6 (6H, m, CH_2), 2.5 (2H, t, CH_2), 7.0 (2H, d, ArH), 7.4 (2H, d, ArH) ppm.

IR: ν_{max} (thin film), 2953, 2925, 2852, 1518,1465,1204, 1045, 837 cm^{-1}.

3.4.3 *Preparation of the 4-n-alkylbenzoic acids* (15)

2.5M Butyllithium (6.0 ml, 15 mmol) in dry hexanes was added dropwise to a stirred solution of the appropriate 1-bromo-4-*n*-alkylbenzene (10 mmol) in dry DCM at -78 °C. The resulting mixture was stirred for 6h, then poured onto solid CO_2 and stirred overnight. The slurry was acidified and the resulting solid filtered off, washed sparingly with ether, and recrystallised from ethanol/water to yield the desired 4-*n*-alkylbenzoic acid **(15)**, as a white crystalline solid, 4-*n*-ethyl- (54%), m.p. 112-113 °C, 4-*n*-propyl- (63%) m.p. 140-142 °C; 4-*n*-butyl- (58%) m.p. 98-100 °C; 4-*n*-pentyl- (48%) m.p. 112-113 °C; 4-*n*-hexyl- (73%) m.p. 97-99 °C; 4-*n*-octyl- (55%) m.p. 96-98 °C; 4-*n*-decyl- (67%) m.p. 112-113 °C.

The following spectral data refers to the 4-*n*-pentylbenzoic acid:

NMR: δ_H ($CDCl_3$) 0.9 (3H, t, CH_3), 1.2-1.6 (6H, m, CH_2), 2.7 (2H, t, CH_2), 7.3 (2H, d, ArH), 8.0 (2H, d, ArH), 11.8 (1H, s, COOH) ppm.

IR: ν_{max} (KBr), 3700-3500, 2920, 2849, 1682 (C=Ostr), 1320, 1291 cm^{-1}.

3.4.4 *Preparation of some 4′-n-alkylbiphenyl-4-yl 4-n-alkylbenzoates* (17)

The 4′-*n*-alkylbiphenyl-4-yl 4-*n*-alkylbenzoates **(17)**, m = 5,6,7 and 10, n = 1-10, were prepared by two methods:

Method 1

Trifluoroacetic anhydride (1.6 mmol) was added to the appropriate 4-*n*-alkyl-4′-hydroxybiphenyl **(16)** (1.5 mmol) and the appropriate 4-*n*-alkylbenzoic acid **(15)** (1.5 mmol) in dry DCM (30 ml) contained in a single-necked flask fitted with a $CaCl_2$ guard tube. The reaction mixture was stirred overnight and the solvent then removed in vacuo. The resulting solid was purified by flash chromatography on silica gel using 1 : 1 chloroform : petroleum ether (b.p. 40-60 °C) as the eluent. The product was then recrystallised from ethanol yielding the desired 4′-*n*-alkylbiphenyl-4-yl 4-*n*-alkylbenzoate **(17)** as a white crystalline solid. The yields obtained were of the order of 50-60 %. The following data for 4′-*n*-decylbiphenyl-4-yl 4-*n*-decylbenzoate **(17)**, m = 10, n = 10, is representative of the series.

NMR: δ_H ($CDCl_3$) 0.86-0.91 (3H, t, CH_3), 0.95-1.00 (3H, t, CH_3), 1.27-1.77 (32H, m, CH_2), 2.62-2.72 (4H, m, $ArCH_2CH_2$), 7.24-7.34 (6H, m, phenyl and biphenyl ArH), 7.49-7.63 (4H, dd, biphenyl ArH), 8.12-8.15 (2H, d, phenyl ArH) ppm.

IR: ν_{max} (KBr), 2958,2920,2857,1730 (C=O str), 1495, 1468, 1275, 1080, 810, 720 cm^{-1}.

Elemental analysis: Found: C, 84.99, H, 9.88 per cent;

$C_{39}H_{54}O_2$ requires C, 84.47, H, 9.75 per cent.

Method 2

Dicyclohexylcarbodiimide (0.31 g, 1.5 mmol) and dimethylaminopyridine (0.02 g, 0.15 mmol) were added to the appropriate 4-*n*-alkyl-4′-hydroxybiphenyl **(16)** (1.5 mmol) and the appropriate 4-*n*-alkylbenzoic acid **(15)** (1.5 mmol) in dry DCM (30 ml) contained in a single-necked flask fitted with a $CaCl_2$ guard tube. The reaction was left to stir overnight before the suspended solid material was removed by filtration through a sintered glass funnel. The solvent was removed in vacuo, and the desired 4′-*n*-alkylbiphenyl-4-yl 4-*n*-alkylbenzoate **(17)** was purified as described in *Method 1*. The yields (75-80 %) obtained by this procedure were generally greater than those obtained by *Method 1*, although *Method 1* was used more extensively for the preparation of these compounds.

Ten members of each of the following homologous series of 4′-*n*-alkylbiphenyl-4-yl 4-*n*-alkylbenzoates **(17)**, m = 5,6,7 and 10, n = 1-10, were synthesised:

4′-*n*-pentylbiphenyl-4-yl 4-*n*-alkylbenzoates

4′-*n*-hexylbiphenyl-4-yl 4-*n*-alkylbenzoates

4′-*n*-heptylbiphenyl-4-yl 4-*n*-alkylbenzoates

4′-*n*-decylbiphenyl-4-yl 4-*n*-alkylbenzoates

A summary of the thermal data together with a detailed discussion of the phase types associated with these series is given reported in section **5.0**.

4. *Discussion of the liquid crystal behaviour of the 4′-n-alkoxybiphenyl-4-yl cycloalkanecarboxylates*

4. *Discussion of the liquid crystalline behaviour of the 4′-n-alkoxybiphenyl-4-yl cycloalkanecarboxylates* (7-11)

4.1 *Background and Introduction*

As part of his Ph.D. studies at The Nottingham Trent University, J.W Brown[37] carried out some preliminary work on members of an homologous series of 4′-n-alkoxybiphenyl-4-yl cyclohexanecarboxylates **(10)**. The transition temperature plot obtained was of a very unusual form, the main anomalous feature being the existence of a pronounced 'hump' for the points corresponding with the first transition observed on cooling the isotropic liquid for the homologues from $n = 3$ through to $n = 6$. For these early members there was uncertainty whether or not this transition was, in fact, to the crystalline solid rather than to a mesophase, as the optical textures displayed were not recognisable as those of a known mesophase type but showed many of the characteristics of crystallisation (see **Plates A** and **B**, ***Appendix 1*** for similar textures shown by other homologous series). For later members of the series, the corresponding transition was tentatively assigned as being from the isotropic liquid to the smectic crystal G phase.

Because of the uncertainties with regard to the uncharacteristic textures and the associated doubts concerning the assigned mesophase type, it was decided that the cyclohexanecarboxylates **(10)** should be resynthesised and investigated. It was intended to augment and confirm the conclusions deduced by thermal optical microscopy with additional information obtained with the aid of the complementary characterisation techniques of Differential Scanning Calorimetry (DSC) and miscibility studies (i.e. investigation of the phase-composition diagrams for binary mixtures with known liquid crystal standards). Extension of the work to the related homologous series of

cyclopropane- **(7)**, cyclobutane- **(8)**, cyclopentane- **(9)**, and cycloheptane-carboxylates **(11)** was undertaken to confirm and develop the conclusions reached for the cyclohexane analogues **(10)**. Initial optical studies of the 4′-n-alkoxybiphenyl-4-yl cycloalkane-carboxylates **(10)** proved as confusing as the preliminary investigations. The pronounced 'hump' was displayed not only for the cyclohexanecarboxylates, but also for the analogous cyclopentane **(9)** and cycloheptane **(11)** derivatives. The sketch (see below) shows the general form of the graph observed when the transition temperatures are plotted against the number of C atoms, *n*, in the alkyl group. The occurrence of such behaviour within an homologous series is very uncommon, although a similar plot with a much less pronounced 'hump' has been reported by Gray[13] for other esters, e.g. the ethyl 4′-n-alkoxybiphenyl-4-carboxylates.

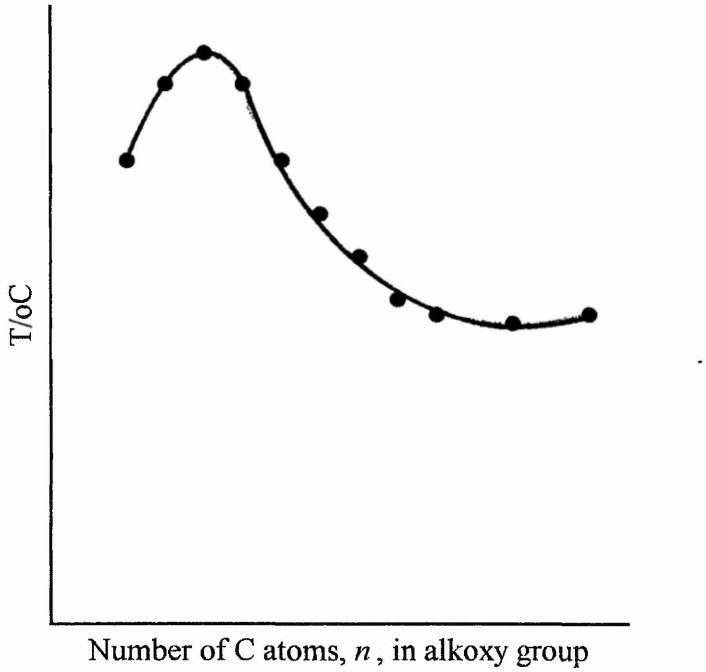

The identification of melting points and crystallisation temperatures by thermal optical microscopy proved to be exceptionally difficult for some of the compounds synthesised. The unusual textures for all members of the cyclopropane- **(7)** and cyclobutane-carboxylates **(8)** and the lower homologues of the cyclopentane- **(9)**, cyclohexane- **(10)**, and cycloheptane-carboxylates **(11)** once again posed the question: what is being seen on cooling the isotropic liquid; is it the formation of a liquid crystalline phase (and if so, which one?) or merely crystallisation? There was no certain answer from the optical evidence. **Plates A-F**, in ***Appendix 1*** show some of the typical textures observed.

However, despite the inconclusive optical studies, several supporting pieces of circumstantial evidence could be gathered to indicate that these compounds were, in fact, giving rise to a liquid crystal phase on cooling the isotropic liquid. Firstly, the cyclopentane- **(9)** , cyclohexane- **(10)**, and cycloheptane-carboxylates **(11)** all exhibited a nematic phase for the $n = 2$ homologue and both the cyclohexane **(10)** and cycloheptane **(11)** derivatives showed other textures, more readily identifiable as smectic modifications, at higher chain lengths. Logically, it would be highly unusual if these mesomorphic homologues were bracketing a region of the homologous series in which no liquid crystalline behaviour was displayed. Secondly, all of the series, with the possible exception of the cyclobutanecarboxylates **(8)** (where the effect, if present, is very small), displayed an odd-even effect for the transition temperature associated with the onset of the formation of the phase with the unusual texture. This type of behaviour would not be expected if the compounds were crystallising directly from the isotropic liquid. A much more irregular, haphazard spread of recrystallisation temperatures is normally observed. Finally, data from DSC studies indicated that the transition enthalpies

associated with the phase are of the same order of magnitude for all the homologues, and that most give rise to another transition at a lower temperature. This constitutes strong supporting evidence for the assignment of the texture observed on cooling the isotropic liquid as that of a liquid crystal, with the lower temperature transition corresponding to the onset of crystallisation rather than a crystal-crystal transition.

Careful miscibility studies with suitable standard materials have enabled the liquid crystal phase formed on cooling the isotropic liquid to be identified.

The compounds studied in the present work were members of five homologous series of 4′-n-alkoxybiphenyl-4-yl cycloalkanecarboxylates **(7-11)**. These were synthesised in moderate yields from the appropriate 4-hydroxy-4′-n-alkoxybiphenyl **(6)** and cyclo-propane-, -butane-, -pentane-, -hexane-, and -heptane-carboxylic acids according to the method detailed in section **3.3.1**. Homologues n = 2-10 and 12 were synthesised for each of the cycloalkane series **(7-11)** studied together with the homologues n = 14 and 16 for the cyclohexane- **(10)** and cycloheptane-series **(11)**.

4.2 *Summary of Thermal Data*

In the following section, Tables of transition temperatures for each of the homologous series together with the associated enthalpies of transition obtained by DSC are listed. The results are represented graphically in corresponding plots showing transition temperatures against *n*, the number of carbon atoms in the alkoxy group for each series.

Table 1, Plot 1 - The 4′-n-alkoxybiphenyl-4-yl cyclohexanecarboxylates **(10)**

Table 2, Plot 2 - The 4′-n-alkoxybiphenyl-4-yl cyclopropanecarboxylates **(7)**

Table 3, Plot 3 - The 4′-n-alkoxybiphenyl-4-yl cyclobutanecarboxylates **(8)**

Table 4, Plot 4 - The 4′-n-alkoxybiphenyl-4-yl cyclopentanecarboxylates **(9)**

Table 5, Plot 5 -The 4′-n-alkoxybiphenyl-4-yl cycloheptanecarboxylates **(11)**

The full list of the abbreviations used in the following tables and a comprehensive guide to their meanings are given at the beginning of this thesis.

Transitions seen on both heating and cooling cycles are said to be ***enantiotropic***. Transitions which are only observed on cooling are said to be ***monotropic***.

Plot 1 - *Representation of transition temperatures for the 4'-n-alkoxybiphenyl-4-yl cyclohexanecarboxylates*

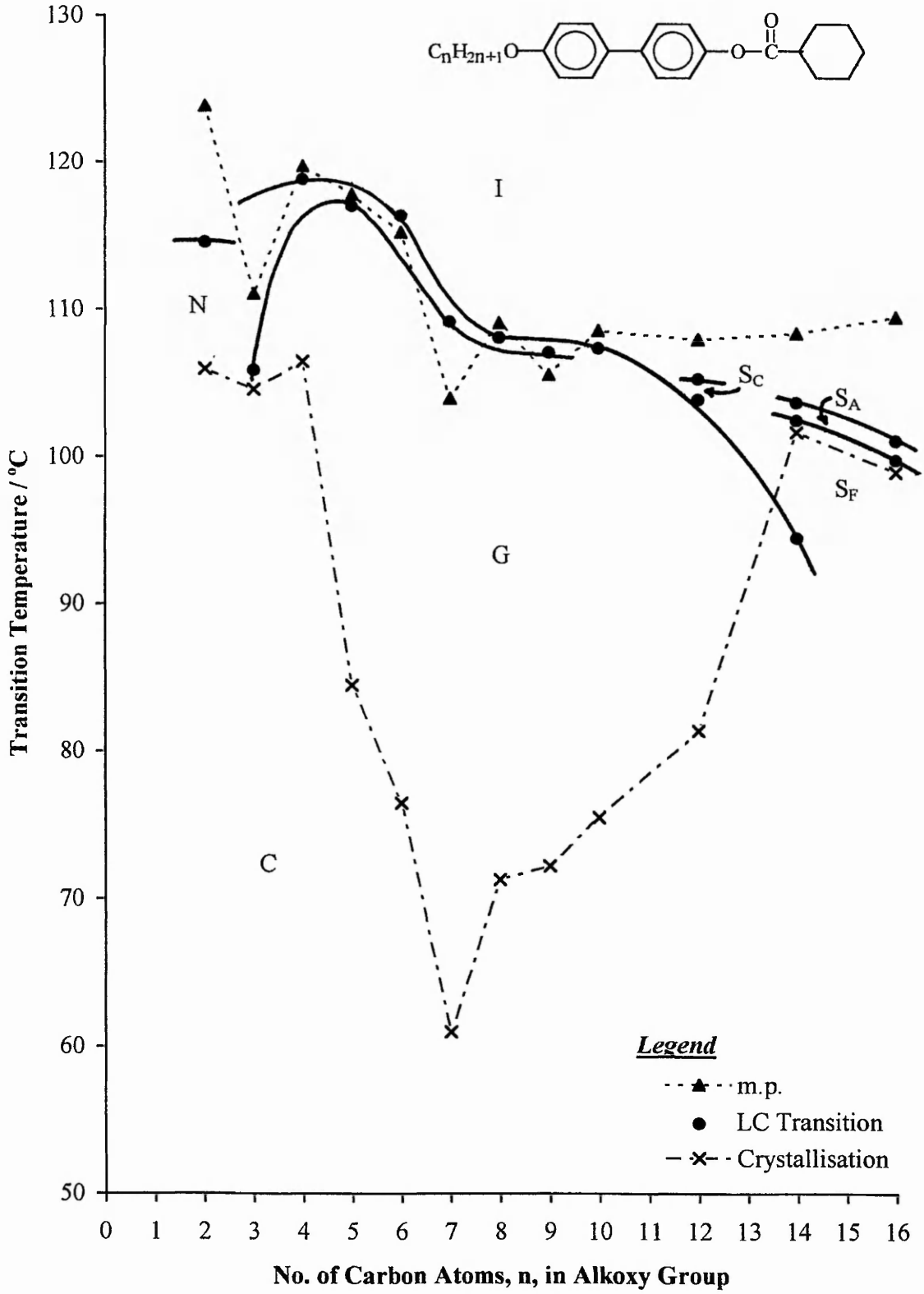

Table 1 - ***Mesophase transition temperatures and enthalpy data for the 4'-n-alkoxybiphenyl-4-yl cyclohexanecarboxylates*** **(10)**

	C-I	I-N	C-G	I-G	I-S_C	S_C-S_F	S/N-C
2	123.9†	(114.6)					106.0
	27.46‡	*0.67*					
3	111.1			(105.9)			104.6
				11.50			
4	119.8			(119.3)			106.5
				14.41			
5			117.8	117.5			84.5
				15.55			*5.26*
6			115.1	115.1			76.5
			12.45	*14.45*			*4.71*
7			104.0	109.2			61.0
			20.07	*13.70*			
8			108.4	108.1			71.3
				12.39			*14.55*
9			105.8	106.3			72.2
				13.01			*24.46*
10	108.2			(107.4)			75.5
	42.76			*12.71*			*27.04*
			S_F-G				
12	108.0		(103.2)		(104.8)	(104.5)	81.4
	47.45						*32.47*
					I-S_A	S_A-S_F	
14	108.4		(94.5)		(103.7)	(102.5)	102.5
	51.56						
16	109.5				(100.7)	(99.8)	99.8
	56.16						

( ) denotes a monotropic transition; † transition temperatures listed were determined by thermal optical microscopy, the reported values being obtained on cooling (except melting points); ‡ values in italics represent enthalpies of transition (kJ mol^{-1}) obtained by differential scanning calorimetry at a cooling rate (heating for m.p.) of 10 °C/min, where no DSC value is quoted the enthalpy of transition could not be accurately calculated.

Plot 2 - *Representation of transition temperatures for the 4'-n-alkoxybiphenyl-4-yl cyclopropanecarboxylates*

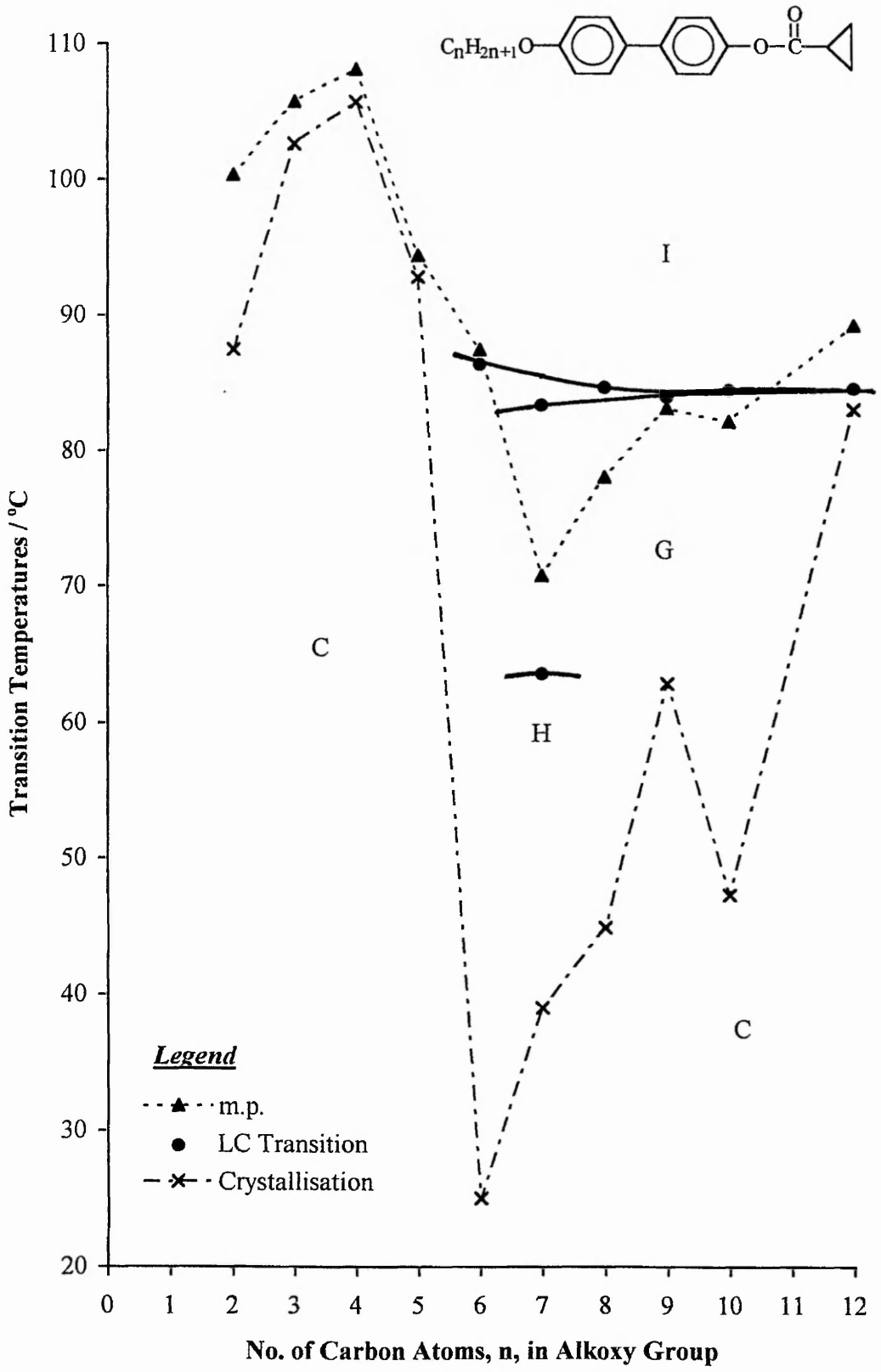

Table 2 - *Mesophase transition temperatures and enthalpy data for the 4'-n-alkoxybiphenyl-4-yl cyclopropanecarboxylates* (7)

n	C_1-C_2	C-I	I-G	G-H	H-C	I-C
2	90.7†	**100.4**				**87.5**
		18.34‡				15.46
3		**105.8**				**102.7**
		16.15				16.02
4		**108.2**				**105.8**
		15.20				*15.13*
5		**94.5**				**92.9**
		14.56				*14.19*
		C-G				**G-C**
6		**86.9**	**(86.4)**			**25.0**#
7		**70.8**	**83.4**	**(63.6)**	**39.0**	
		17.86	*10.52*	*0.90*	*7.31*	
8		**78.1**	**84.7**			**44.9**
			10.72			*17.10*
9		**83.2**	**84.0**			**62.9**
			10.52			26.62
10		**82.2**	**84.5**			**47.3**
		18.95	*11.19*			16.98
12		**89.3**	**(84.6)**			**83.1**
		44.49	*12.08*			*31.93*

( ) denotes a monotropic transition; † transition temperatures listed were determined by thermal optical microscopy, the reported values being obtained on cooling (except melting points); ‡ values in italics represent enthalpies of transition (kJ mol^{-1}) obtained by differential scanning calorimetry at a cooling rate (heating for m.p.) of 10 °C/min, where no DSC value is quoted the enthalpy of transition could not be accurately calculated; # crystallisation occured over a period of hours at room temperature (arbitrarily quoted as 25 °C).

Plot 3 - *Representation of transition temperatures for the 4'-n-alkoxybiphenyl-4-yl cyclobutanecarboxylates*

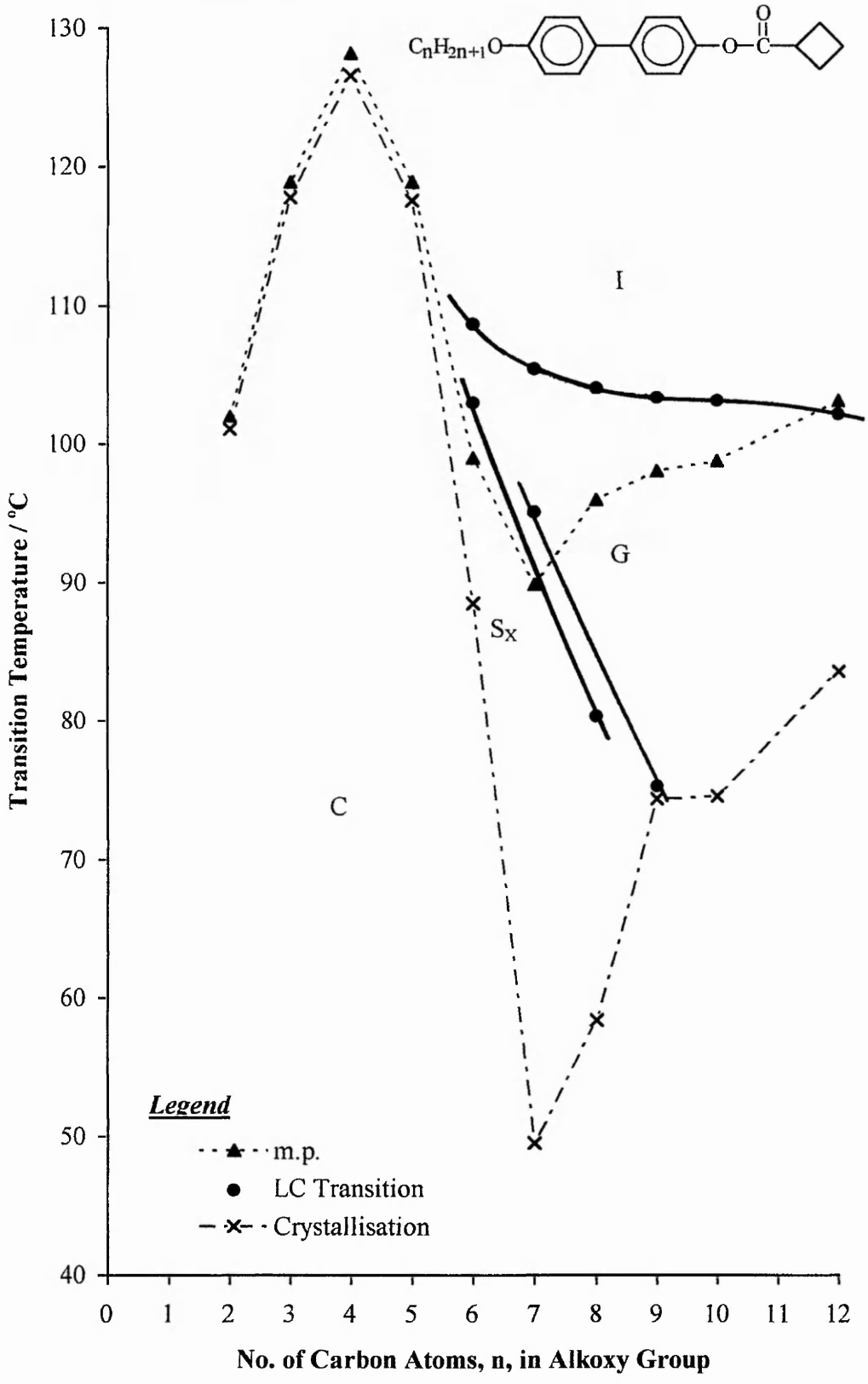

Table 3 ***Mesophase transition temperatures and enthalpy data for the 4'-n-alkoxybiphenyl-4-yl cyclobutanecarboxylates*** **(8)**

n	C_1-C_2	C-I	I-G	G-S_x	S_x-C	I-C
2	79.8†	102.0				101.1
	5.31‡	*13.62*				*13.37*
3		118.9				117.8
		19.13				*18.32*
4		128.2				126.6
		20.72				*20.42*
5		118.9				117.6
		21.26				*21.00*
		C-S_x				
6		99.0	108.7	103.0	88.5	
		1.52	*14.46*	*1.39*	*0.49*	
7		89.9	105.5	95.1	49.5	
		13.78	*13.85*	*1.36*	*10.45*	
		C-G				G-C
8		96.0	104.1	(80.4)	(58.4)	
		21.42	*13.69*	*0.92*	18.80	
9		98.1	103.4	(75.3)	(75.1)	
			14.18	*0.50*	*31.40*	
10		98.8	103.2			74.6
		28.22	*13.87*			*28.04*
12		102.6	102.2			83.6
			14.05			*34.19*

( ) denotes a monotropic transition; † transition temperatures listed were determined by thermal optical microscopy, the reported values being obtained on cooling (except melting points); ‡ values in italics represent enthalpies of transition (kJ mol^{-1}) obtained by differential scanning calorimetry at a cooling rate (heating for m.p.) of 10 °/min, where no DSC value is quoted the enthalpy of transition could not be accurately calculated.

Plot 4 - ***Representation of transition temperatures for the 4'-n-alkoxybiphenyl-4-yl cyclopentanecarboxylates***

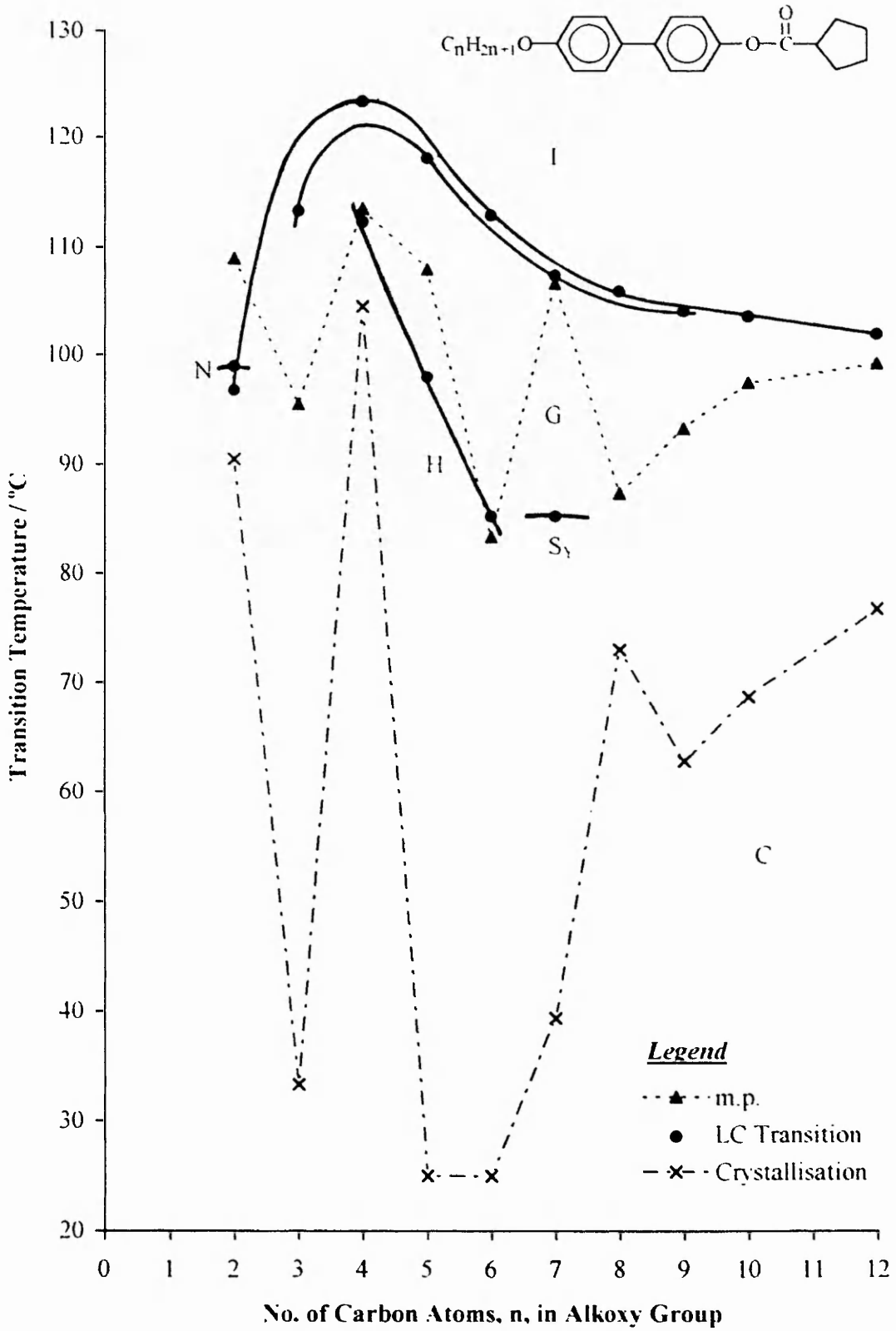

Table 4 - *Mesophase transition temperatures and enthalpy data for the 4'-n-alkoxybiphenyl-4-yl cyclopentanecarboxylates* (9)

n	C-I	I-N	N-G	G-H	G-S_V	G-C	H-C
2	109.0†	(99.0)	(96.8)			90.5	
						6.89‡	
	C-G		I-G				
3	95.5		113.3			33.3	
	11.18						
4	113.1		123.4	(112.3)			104.5
	2.87		16.12	*0.91*			*1.92*
5	107.9		118.1	(98.0)			25.0#
	2.11		*14.85*	2.32			
6	83.4		112.9	86.2-			25.0#
			15.82	84.4			
				0.98			
							S_V-C
7	107.3		107.4		85.3		39.4
			13.56		*1.02*		10.17
8	87.4		105.9			73.0	
	20.37		*12.63*			*16.17*	
9	93.3		104.1			62.8	
	27.09		*13.90*			*23.88*	
10	97.5		103.6			68.7	
	27.05		*12.71*			*26.55*	
12	99.3		102.0			76.8	
						31.13	

( ) denotes a monotropic transition; † transition temperatures listed were determined by thermal optical microscopy, the reported values being obtained on cooling (except melting points); ‡ values in italics represent enthalpies of transition (kJ mol^{-1}) obtained by differential scanning calorimetry at a cooling rate (heating for m.p.) of 10 °C/min., where no DSC value is quoted the enthalpy of transition could not be accurately calculated; # crystallisation occured over a period of hours at room temperature (arbitrarily quoted as 25 °C).

Plot 5 - *Representation of transition temperatures for the 4'-n-alkoxybiphenyl-4-yl cycloheptanecarboxylates*

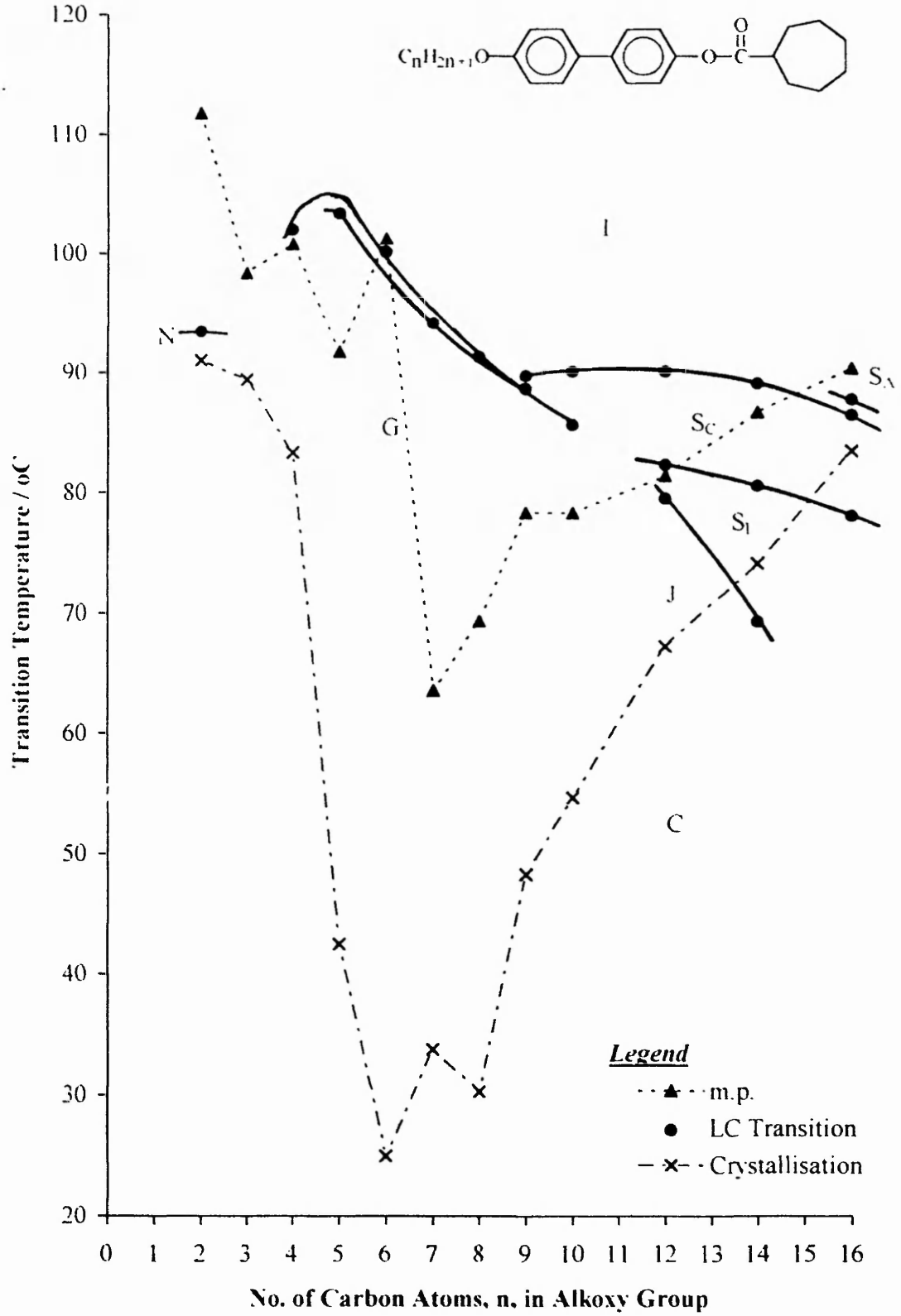

Table 5 - ***Mesophase transition temperatures and enthalpy data for the 4'-n-alkoxybiphenyl-4-yl cycloheptanecarboxylates*** **(11)**

n	C_1-C_2	C-I	I-N		I-G		I-C	N-C
2		**111.8**†	**(93.5)**					**91.1**
		25.80‡	16.67					
3	**82.1**	**98.4**					**89.5**	
	4.95	*17.55*					*16.26*	
	C-G							G-C
4	**101.6**				**102.0**			**83.4**
					12.55			
5	**91.8**				**103.4**			**42.5**
	10.36				*13.96*			*4.32*
6		**101.3**			**(100.2)**			**25.0**#
		14.62			*14.41*			*1.19*
7	**63.6**				**94.2**			**33.8**
					13.01			*0.66*
8	**69.4**				**91.4**			**30.3**
	1.44				*11.55*			
			C-S_C		I-S_C	S_C-G		
9			**78.4**		**89.5**	**(88.7)**		**48.3**
			26.37					
10	**78.4**				**90.2**	**85.7**		**54.7**
	26.13				*6.23*	*3.47*		*19.02*
				C-S_I		S_C-S_I	S_I-J	J-C
12				**82.2**	**90.2**	**82.4**	**(79.6)**	**67.3**
					6.26	*2.76*	*0.14*	*24.84*
14			**86.8**		**89.2**	**80.7**	**69.4***	**74.2**
					5.90	*2.49*		
			I-S_A		S_A-S_C			S_C-C
16		**90.5**	**(87.5)**		**(86.6)**	**(78.2)***		**83.6**
		45.85	*7.28*			*3.03*		*49.10*

( ) denotes a monotropic transition; † transition temperatures listed were determined by thermal optical microscopy, the reported values being obtained on cooling (except melting points); ‡ values in italics represent enthalpies of transition (kJ mol^{-1}) obtained by differential scanning calorimetry at a cooling rate (heating for m.p.) of 10 °C/min. § where no DSC value is quoted the enthalpy of transition could not be accurately calculated; * indicates a mesophase transition occuring below the reported temperature of the onset of slow crystallisation; # crystallisation occurs over a period of hours at room temperature (arbtrarily quoted as 25.0 °C).

4.3 *The 4'-n-alkoxybiphenyl-4-yl cyclohexanecarboxylates* (10)

These compounds were the first to be prepared and have received the most extensive study, details of which are now given. The transition temperatures for homologues n = 2-10 and 12, 14 and 16 together with the associated DSC results, are listed in **Table 1**. A graphical representation of the transition temperatures plotted against n, the number of carbon atoms in the alkoxy group, is given in **Plot 1**.

4.3.1 *Thermal Optical Microscopy*

The n = 2 homologue displays a monotropic nematic phase upon cooling the isotropic liquid. Nematic droplets are formed which rapidly coalesce to produce a characteristic threaded texture.

On cooling the homologues n = 3-6 from the isotropic liquid, a liquid crystal phase is formed. This displays a very unusual optical texture which at first sight is readily confused with crystallisation (see **Plates A** and **B**, ***Appendix 1*** for similar textures shown by other homologous series). Extended lancets are formed which grow rapidly from the isotropic liquid with dendritic growth filling in areas between lancets. As **Plot 1** shows, the transition temperatures for homologues n = 3-10 show an unusual 'hump', i.e. a sharp rise, followed by a sharp then a more gradual fall. Homologues n = 7-10 show a texture more recognisable as a liquid crystal phase, most probably a smectic crystal G phase, with dendritic growth leading to the formation of a typical highly coloured mosaic. The unusual textures exhibited by the earlier members prompted the miscibility investigations, the results of which are detailed in the next section. The transition temperatures for the homologues n = 3-10 reveal an odd-even effect and the points fit two falling curves, with those for the even members uppermost.

The $n = 12$ homologue gives rise to a short monotropic S_C phase on cooling from the isotropic liquid. A broken fan texture is observed with patches of *schlieren* texture showing point singularities with four brushes.

It is possible that this S_C phase of the $n = 12$ homologue is formed via a very short lived S_A phase as it separates out of the isotropic liquid as bâtonnets, and by the fact that the fan texture is not the naturally occurring texture of the S_C phase. On further cooling, the texture of the S_C phase changes to a *schlieren*-mosaic texture indistinct, whilst the fans take on a striped appearance with concentric banding. Although some of the *schlieren* areas appear marginally unfocused, this texture has been classified as an S_F phase rather than an S_I phase. Further cooling produces a crystal G phase with a well defined mosaic texture together with a characteristic *chequerboard* broken fan texture.

The S_C phase shown by the $n = 12$ member is absent in the homologues $n = 14$ and 16, which instead give rise to an S_A phase on cooling the isotropic liquid. Initially bâtonnets form which then quickly coalesce to give an unmistakable S_A focal conic texture. If the S_A phase is then cooled rapidly an S_F phase is observed with similar textural characteristics to those reported for the $n = 12$ homologue, although the mosaic areas are much more distinct. On slower cooling crystallisation generally occurred before the appearance of the S_F phase. On rapid cooling of the $n = 14$ homologue to 94.5 °C another phase is formed from the preceding S_F phase. This may be a G phase but the identity of the phase is not certain as crystallisation is already occurring in many areas of the sample.

4.3.2 *Miscibility Studies*

Due to the very uncharacteristic microscopic textures of the liquid crystal phase formed by the homologues n = 3-6 of the 4′-n-alkoxybiphenyl-4-yl cyclohexane-carboxylates **(10)**, miscibility studies were undertaken to establish the nature of the phase type in this series of compounds. The n = 10 homologue, 4′-n-decyloxybiphenyl-4-yl cyclohexanecarboxylate (referred to as C-10/C-6), **(10)**, n = 10, which gives a liquid crystal phase with a well defined mosaic texture, was studied by thermal optical microscopy in mixtures of varying percentage compositions with a known standard, the thioester **(18)** (referred to as 14OS5) derived from 4-n-tetradecyloxybenzoic acid and 4-n-pentylthiophenol. The compound 14OS5 exhibits well documented[47] mesophase transitions of I-S_A-S_B-G on cooling from the isotropic liquid at the temperatures (°C) given below:

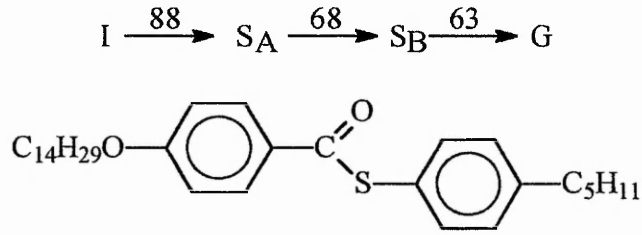

(18)

A number of other standard materials containing G phases were investigated in miscibility studies with these cycloalkanecarboxylates but with less satisfactory results.

Table 6 shows the transition temperatures for the various percentage compositions of 14OS5 and C-10/C-6 investigated, and these are displayed graphically in **Plot 6** as a binary phase-composition diagram. Studies of such binary-phase composition diagrams allows the identification of some unknown phases. A smooth uninterrupted curve for all percentage compositions indicates that the phase is common to both compounds in the mixture.

Plot 6 - ***Binary phase-composition diagram representing transition temperatures for percentage compositions of 14OS5 and C-10/C-6***

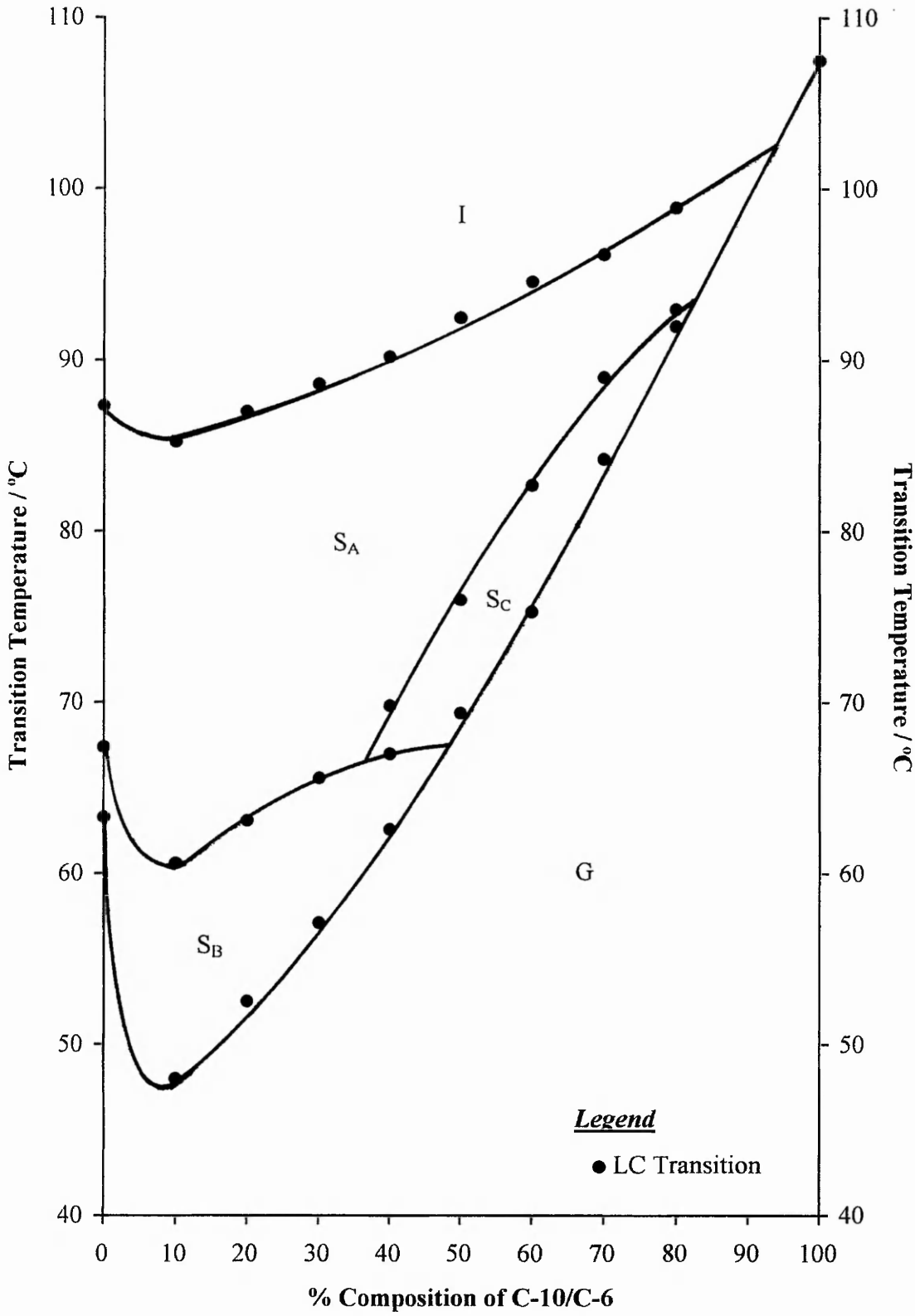

Table 6 - *Transition temperatures for mixtures of a range of percentage compositions of C-10/C-6 and 14OS5*

% Composition		Transition Temperatures / °C				
C10/C-6	140S5	I-S_A	S_A-S_C	S_A-S_B	S_C-G	S_B-G
00	100	87.3		67.4		63.3
10	90	85.2		60.6		48.0
20	80	87.0		63.1		52.2
30	70	89.3		65.6		56.3
				S_C-S_B		
40	60	90.2	69.0	67.0		62.6
50	50	92.5	77.3		71.2	
60	40	94.6	82.7		75.3	
70	30	96.2	89.0		84.2	
80	20	98.9	92.0		93.0	I-G
100	00					107.5

Plot 6 clearly shows an uninterrupted curve for the G phase which falls smoothly from 100% C-10/C-6 down to 10% C-10/C-6, from where it rises sharply to 100% thioester. Similar behaviour is also observed for the I-S_A curve, which shows that the S_A phase is present in all of the compositions studied. The curve associated with the appearance of the S_B phase reveals the same trend as those for the S_A and G phase transitions, although the S_B phase is no longer present at percentage compositions of

C-10/C-6 greater than 40%. An injected S_C phase is seen between compositions of 40-80% C-10/C-6, however this does not interrupt the continuity of the G phase across the miscibility plot.

The data obtained shows that the suspected G phase of the C-10/C-6 ester is completely miscible with the G phase of the thioester over the entire composition range. Hence, it follows from the *Miscibilty Rule*† that the mosaic texture exhibited by the pure C-10/C-6 is that of a smectic crystal G phase.

With this established, miscibility studies were undertaken on compounds in the 'humped' region of **Plot 1**, in particular 4′-n-pentyloxybiphenyl-4-yl cyclohexane-carboxylate (referred to as C-5/C-6), and 4′-n-butyloxybiphenyl-4-yl cyclohexane-carboxylate (referred to as C-4/C-6). Initially studies into the phase type of C-5/C-6 were carried out utilising the thioester (14OS5) as the standard. However, these were abandoned as the optical textures proved very difficult to distinguish (a predominantly homeotropic alignment was obtained). Hence miscibility with the newly characterised crystal G phase compound, C-10/C-6, was investigated and found to be successful.

Table 7 shows the transition temperatures for the various percentage compositions of C-5/C-6 and C-10/C-6, which are displayed graphically in **Plot 7** as a binary phase-composition diagram.

† The *Miscibility Rule* states that 'all liquid crystalline modifications which exhibit an uninterrupted series of mixed crystals in binary systems without contradiction can be marked with the same symbol' [20]

Plot 7 - *Binary phase-composition diagram representing transition temperatures for percentage compositions of C-10/C-6 and C-5/C-6*

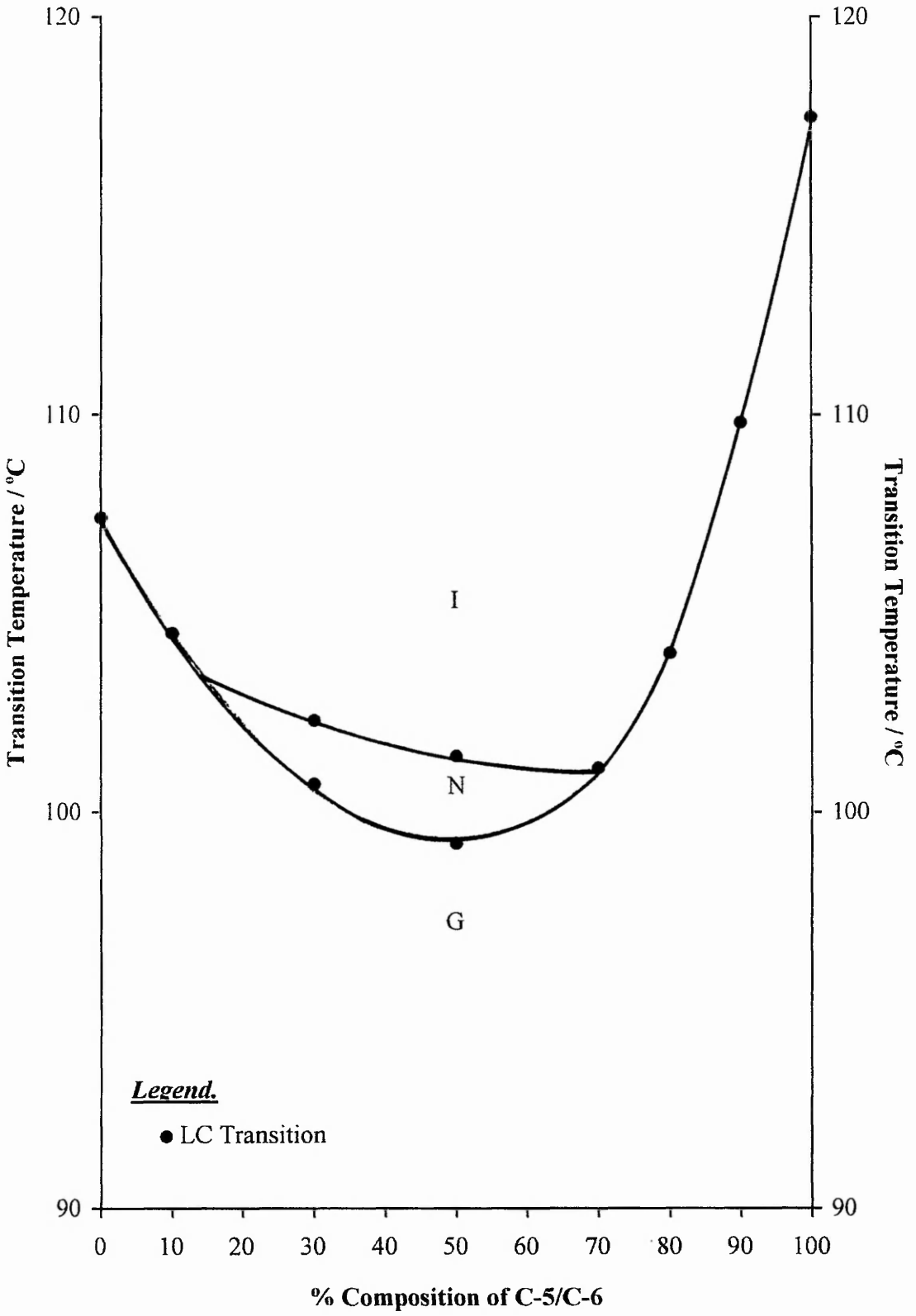

Table 7 - ***Transition temperatures for mixtures of a range of percentage compositions of C-5/C-6 and C-10/C-6***

% Composition		Transition Temperatures / °C		
C-5/C-6	C-10/C-6	I-N	N-G	I-G
00	100			107.4
10	90			104.5
30	70	102.3	100.7	
50	50	101.4	99.2	
70	30	101.1	101.1	
80	20			104.0
90	10			109.8
100	00			117.5

The miscibility diagram for C-5/C-6 utilising C-10/C-6 as the standard is relatively simple, presumably because neither compound gives rise to a complex sequence of phases in the pure state. The curve denoting the onset of the G phase falls away smoothly from 100% C-5/C-6 to a minima at a composition of 50%, then gradually rises as the percentage composition of the standard material increases.

The optical texture of the G phase is dependent upon the phase preceding it. On cooling from the nematic phase, dendrites form throughout the marbled texture and these rapidly grow to give a mosaic texture with regular, many sided areas. When the G phase is formed on direct cooling of the isotropic liquid the phase separates out as lancets, with

Plot 8 - ***Binary phase-composition diagram representing transition temperatures for percentage compositions of C-10/C-6 and C-4/C-6***

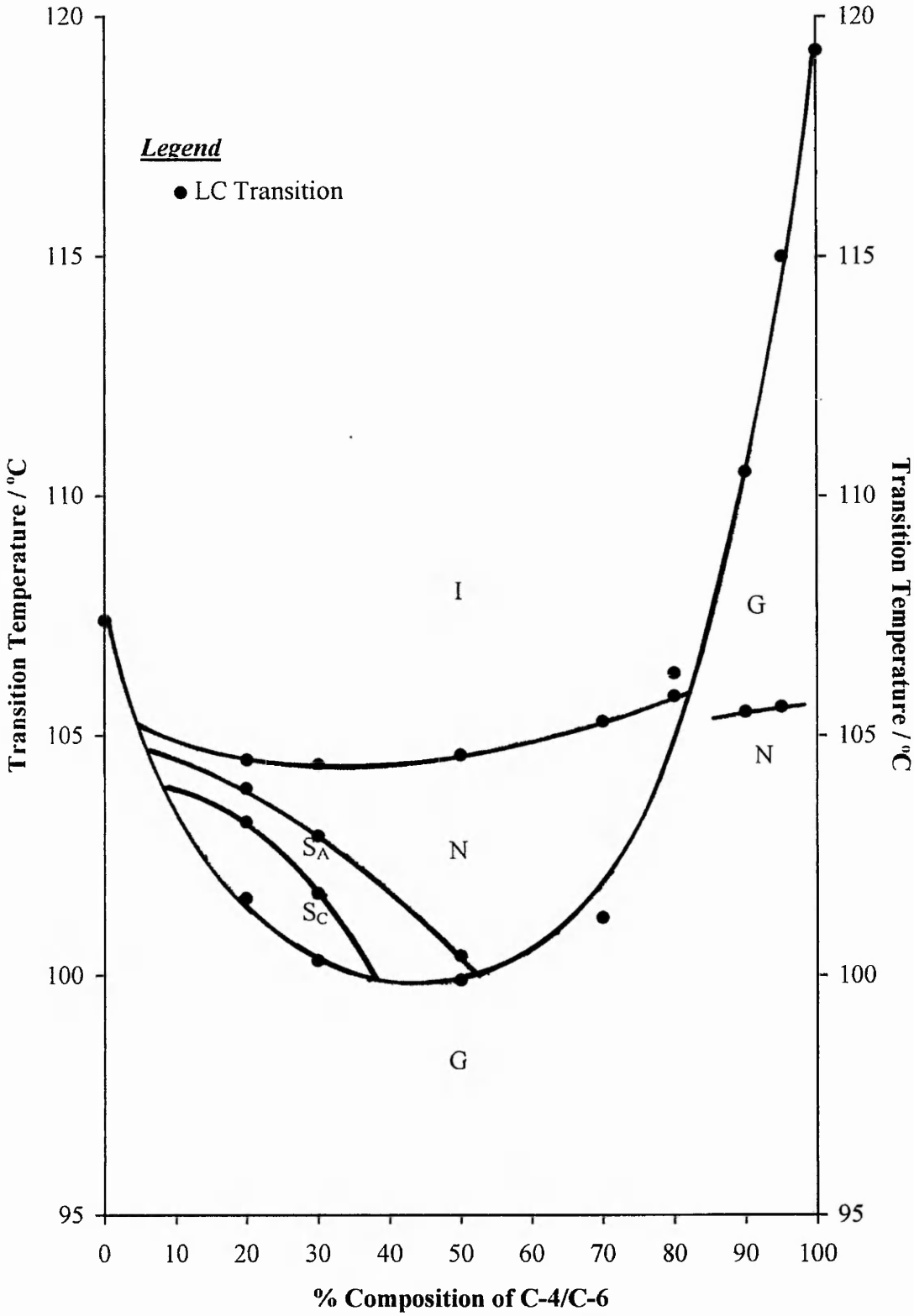

dendritic growth occurring in between to form a mosaic texture with sharper, more elongated and angular shaped areas.

The 4′-n-butyloxybiphenyl-4-yl cyclohexanecarboxylate (C-4/C-6) was also studied utilising C-10/C-6 as the standard G phase material. The transition temperatures for various percentage mixtures of C-4/C-6 and C-10/C-6 are listed in **Table 8** and represented graphically in **Plot 8** as a binary phase-composition diagram.

Table 8 - ***Transition temperatures for mixtures of a range of percentage compositions of C-4/C-6 and C-10/C-6***

% Composition		Transition Temperatures / °C					
C-4/C-6	C-10/C-6	I-N	N-S_A	S_A-S_C	I-G	N-G	S_C-G
00	100				107.4		
20	80	104.5	103.9	103.2			101.6
30	70	104.4	102.9	101.7			100.3
							S_A-G
50	50	104.6	100.4				99.9
70	30	105.3				101.2	
80	20	106.3				106.1	
						G-N	
90	10				110.5	105.5	
95	05				115.0	105.6	
100	00				119.3		

Plot 8 is a more complex miscibility diagram but clearly gives considerable support for the crystal G phase assignment to the phase obtained on cooling the isotropic liquid of the homologues n = 3-6, and dispels the alternative possibility that the texture that these compounds give rise to is merely due to crystallisation. As can be seen from the plot, injected N, S_A and S_C phases appear, but the curve associated with transitions to the G phase is similar to that for the C-5/C-6 compound and is uninterrupted throughout the entire composition range. However the most interesting observations are for very high percentage concentrations of C-4/C-6, i.e. the 90% and 95% mixtures. On cooling from the isotropic liquid small areas of the G phase begin to separate out as dendrites. These have the appearance of 'butterflies', which grow very slowly across the field of view in these mixtures. However, if cooling is continued before the G phase has fully formed a nematic texture forms more uniformly across the slide, although the G phase remains intact as the initially formed 'butterflies'. This indicates that the phase giving rise to the `butterfly' texture on cooling the mixtures of the C-4/C-6 ester must be liquid crystalline, rather than the crystalline solid, owing to the appearance of the highly disorganised nematic phase after the initial nucleation from the isotropic liquid as the 'butterflies' of the organised smectic crystal G phase.

It should be noted that the 4′-n-alkoxybiphenyl-4-yl cyclohexanecarboxylates **(10)** are nematogenic, the n = 2 homologue giving rise to a nematic phase only, and that the temperature at which the nematic phase is formed in the C-4/C-6 mixtures is consistent with that which might have been predicted from the N-I transition temperature of the n = 2 homologue.

4.3.3 *DSC Studies*

The members of the series of 4′-n-alkoxybiphenyl-4-yl cyclohexanecarboxylates **(10)** were also studied by differential scanning calorimetry (DSC). The transition temperatures obtained by DSC were in broad agreement with those obtained by thermal optical microscopy, and the enthalpies of transition are given below the relevant transition temperatures determined from the optical microscopy studies in **Table 1**.

The DSC results support the conclusions obtained by optical microscopy and miscibility studies. The information obtained is best explained by consideration of the heating and cooling cycles of two representative homologues, which are reproduced in ***Appendix 2***.

The trace **DSC 1** shows the heating and cooling cycles for the decyloxy derivative, C-10/C-6. The heating cycle clearly shows that enantiotropic mesophases are not formed by this homologue. The single peak recorded on the heating cycle is associated with the transition from the crystalline solid to the isotropic liquid. The large enthalpy value of 42.76 kJ mol^{-1} is consistent with the expected value for a melting point because at such a transition all the cohesive forces within the crystalline structure breakdown at once. In contrast, the cooling cycle shows two peaks, one associated with the I-G transition, and one with the G-C transition. The enthalpy value for the I-G transition is calculated at 12.71 kJ mol^{-1} which is consistent with values obtained for this transition for other members of this homologous series. When added to the enthalpy value, 27.04 kJ mol^{-1}, for the G-C transition the total enthalpy for the two cooling transitions approximately equates with that obtained for the melting point on the heating cycle, confirming that these are indeed the only transitions that occur in the cooling process.

The trace **DSC 2** shows the heating and cooling cycles for one member taken from the 'humped' region of the transition temperature graph (**Plot 1**), this being the pentyloxy derivative, C-5/C-6. The heating cycle shows two peaks corresponding with two transitions, although the transition enthalpy for only one of these can be calculated accurately. The C-G transition appears as a peak with a shoulder which may be an indication of a crystal-crystal transition preceding the melting point. The calculated value for the enthalpy of the G-I transition is 15.78 kJ mol^{-1}. The cooling cycle for the compound C-5/C-6, however, shows no evidence of a crystal-crystal transition, but shows two clear peaks associated with the I-G and G-C transitions. The I-G transition has a calculated enthalpy value of 15.55 kJ mol^{-1}, which compares well with the value calculated for the G-I transition. Although slightly higher than the value obtained for the C-10/C-6 homologue, this value is still within an acceptable range to be able to classify the phase transitions as being of the same type. The G-C transition has an enthalpy of 5.26 kJ mol^{-1}.

The enthalpy values for the I-G transitions of these compounds are larger than expected, although this is most likely due to the highly crystalline nature of the phase obtained on cooling the isotropic liquid.

4.3.4 *Conclusion*

From the combination of optical microscopy, and DSC and miscibility studies on this series it is concluded that homologues n = 3-10 of the 4′-n-alkoxybiphenyl-4-yl cyclohexanecarboxylates **(10)** give rise to a smectic crystal G phase on cooling from the isotropic liquid. However, the optical textures shown by the compounds n = 3-6 are not characteristic of the G phase nor readily recognisable as such, and their formation on cooling the isotropic liquid can easily be mistaken for crystallisation.

4.4 *The 4′-n-alkoxybiphenyl-4-yl cyclopropanecarboxylates* (7)

The following section details the results of similar studies carried out on the 4′-n-alkoxybiphenyl-4-yl cyclopropanecarboxylates **(7)**. The transition temperatures for homologues n = 2-10 and 12 are listed in **Table 2** and represented graphically in **Plot 2** plotted against n, the number of C atoms in the alkoxy group. **Table 2** also details the enthalpies of transition obtained by differential scanning calorimetry.

4.4.1 *Thermal optical microscopy*

The homologues n = 2-5 of this series show no mesomorphic character. However, on cooling homologues n = 6-10 and 12 from the isotropic liquid a liquid crystalline phase was obtained that displayed a similar texture to that described for the 4′-n-alkoxybiphenyl-4-yl cyclohexanecarboxylates **(10)**, with a few minor differences, e.g. on cooling the n = 7 and 8 homologues, thin, slightly curved lancets are obtained. Hence the optical evidence indicates that it is probable that the cyclopropanecarboxylates **(7)** also exhibit a smectic crystal G phase (see **Plate B**, ***Appendix 1***).

The n = 7 homologue also gives rise to another phase on further cooling. The optical characteristics of this phase strongly indicate that it is a crystal H phase. At the transition temperature to this phase, the texture of the previous (suspected) crystal G phase takes on a very distinct cross-hatched appearance which is typical of the H phase. Homologues n = 9 and 10 show another, barely perceptible texture following the G phase. This is characterised by the formation of cross-hatched regions within parts of the texture, although this feature is not as distinct as for the formation of the crystal H phase of the n = 7 homologue, nor as uniform across the sample. Consequently an optical

assignment of these changes as being due to specific liquid crystal transitions is not certain and their occurrence may be due merely to a re-ordering within the texture of the G phase on cooling.

4.4.2 *Miscibility studies*

Although the unusual optical textures of the liquid crystal phase formed by the homologues n = 6-10 and 12 are very similar to the crystal G texture observed for the 4′-n-alkoxybiphenyl-4-yl cyclohexanecarboxylates **(10)**, positive evidence for and confirmation of this was deemed necessary. A miscibility study was therefore undertaken in an attempt to establish whether or not the phase observed was indeed a crystal G phase. The $n = 9$ homologue, the nonyloxy compound, (referred to as C-9/C-3) was taken as a representative compound for this series as it lay centrally on the transition plot for the phase type in question. Mixtures of various percentage compositions were studied by thermal optical microscopy with C-10/C-6, 4'-n-decyloxybiphenyl-4-yl cyclohexane-carboxylate **(10)**, $n = 10$, the newly standardised crystal G phase material.

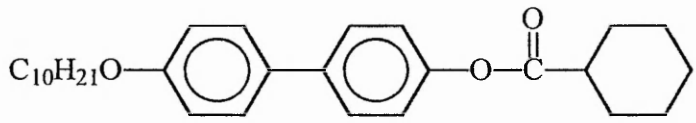

(10)
C-10/C-6

Table 9 shows the transition temperatures obtained for the various percentage compositions, and these are displayed graphically in **Plot 9** as a binary phase-composition diagram.

Plot 9 - *Binary phase-composition diagram representing transition temperatures for percentage compositions of C-10/C-6 and C-9/C-3*

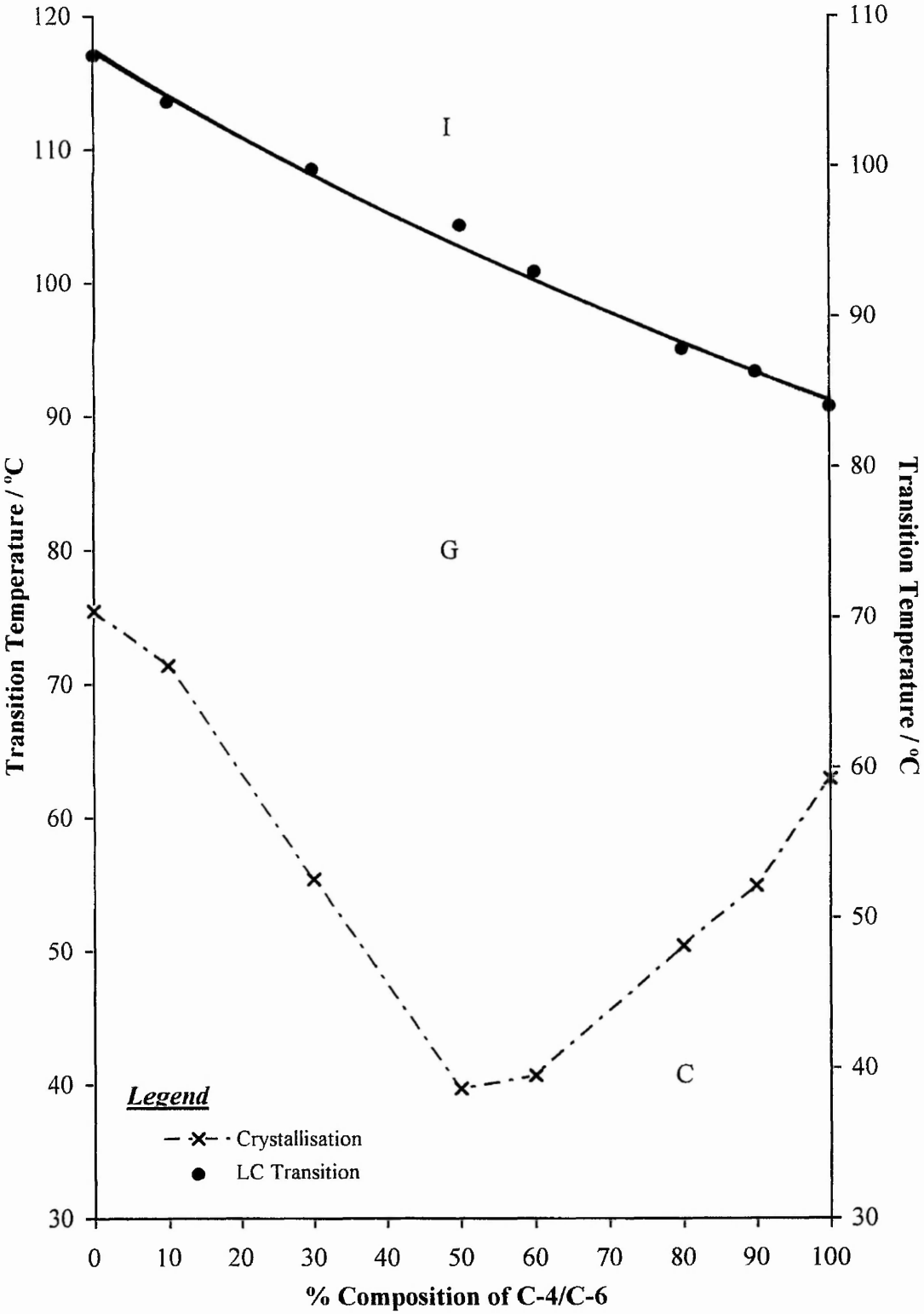

Table 9 - ***Transition temperatures for mixtures of a range of percentage compositions of C-9/C-3 and C-10/C-6***

% Composition		Transition Temperatures / °C	
C-9/C-3	**C-10/C-6**	**I-G**	**G-C**
00	100	107.4	75.5
10	90	104.3	71.4
30	70	99.8	55.4
50	50	96.1	39.7
60	40	93.0	40.7
80	20	87.8	50.4
90	10	86.3	54.9
100	00	84.0	62.9

The I-G transition temperature curve obtained is almost linear, with values falling steadily from that of the pure C-10/C-6 compound over the whole composition range to that of the cyclopropyl ester itself. Mixtures containing high percentage concentrations of the standard exhibited the dendritic growth pattern of the mosaic texture which is normally associated with the crystal G phase on cooling from the isotropic liquid (see **Plate C**, ***Appendix 1***). Mixtures with high percentage concentrations of the cyclopropane ester displayed lancets separating from the isotropic liquid, followed by rapid dendritic growth to infill the areas between lancets. No injected phases were observed.

From **Plot 9** it can be seen that the suspected G phase of C-9/C-3 is, in fact, completely miscible with the G phase of C-10/C-6 in mixtures throughout the whole

composition range. It follows from the *Miscibility Rule* that the phase type of this cyclopropane ester is smectic crystal G, and it is reasonable to assume that the neighbouring homologues, which behave similarly, also give rise to a G phase.

4.4.3 *DSC studies*

The members of the series of 4′-n-alkoxybiphenyl-4-yl cyclopropanecarboxylates **(7)** were also studied by differential scanning calorimetry (DSC). The DSC results support the conclusions obtained by optical microscopy and miscibility studies. All of the data obtained showed an excellent correlation between all members of the homologous series which give rise to a mesophase transition on both heating and cooling cycles. Hence it is likely that all of the members of this series give rise to the same liquid crystal phase, that of the crystal G phase. The information obtained is explained in the following section by consideration of the trace **DSC 3** (***Appendix 2)*** which shows the heating and cooling cycles of the heptyloxy homologue, C-7/C-3, the behaviour of which is representative of the series and which also gives rise to a crystal H phase.

The heating cycle shows two peaks, one associated with the melting point (C-G) and the other with the clearing point (I-G) of the compound. The calculated enthalpies of these transitions are 17.86 kJ mol^{-1} and 10.25 kJ mol^{-1} respectively. The cooling cycle for this homologue differs from the other mesogenic members of this series as it clearly shows the monotropic nature of the crystal H phase in this compound. The small sharp peak in between the larger I-G and H-C transitions has an associated enthalpy of transition calculated at 0.90 kJ mol^{-1} (within the expected enthalpy range for a G-H transition). The heptyloxy derivative is the only member of this series for which the occurrence of an H phase is confirmed both optically and by DSC. However, as discussed

in the thermal optical microscopy section, the nonyloxy and decyloxy derivatives both exhibit cross-hatching within some parts of the slide on cooling the G phase. The cooling traces for these compounds reveal a very minor 'dip' after the I-G phase transition shown in the trace **DSC 4** (***Appendix 2***). This may be related to the occurrence of the cross-hatching within the optical texture, but there is insufficient evidence to support and justify the existence of an independent phase type in these compounds.

4.5 *The 4'-n-alkoxybiphenyl-4-yl cyclobutanecarboxylates* (8)

These compounds were similarly investigated and the transition temperatures for homologues n = 2-10 and 12, with the associated DSC results, are listed in **Table 3**. A graphical representation of the transition temperatures plotted against n, the number of carbon atoms in the alkoxy chain, is given in **Plot 3**. It is convenient to discuss the thermal optical microscopy and DSC results for this series in a composite section.

4.5.1 *Thermal optical microscopy and DSC studies*

As with the analogous cyclopropane esters **(7)**, homologues n = 2-5 are not mesomorphic, and once again the homologues n = 6-10 and 12 show an unusual texture for the liquid crystal phase formed on cooling the isotropic liquid. There is a strong indication, based on the conclusions reached for the homologous series discussed earlier, that similar behaviour occurs in this series, namely that a smectic crystal G phase is formed on cooling the isotropic liquid. Homologues n = 6-8 display similar optical textures to those seen for the cyclopropanecarboxylates **(7)**. The n = 9 homologue shows an analogous texture, but with lancets that are more angular than those seen for the earlier

members of the series. Homologues n = 10 and 12 also show similar textural characteristics, although some of the lancets form in a radial manner, creating a texture not dissimilar to the S_B phase.

The members of the series of the 4′-n-alkoxybiphenyl-4-yl cyclobutane-carboxylates **(8)** were also studied by differential scanning calorimetry (DSC). The data obtained shows an excellent correlation between all members of the homologous series which give rise to a mesophase transition on both heating and cooling cycles. Hence, as with members of the other homologous series discussed earlier, it is likely that all the members of this series give rise to the same liquid crystal phase. The information obtained is best explained by consideration of the heating and cooling cycles of one representative homologue, reproduced in ***Appendix 2***.

The trace **DSC 5** shows the peaks recorded on the heating and cooling cycles for the decyloxy derivative, C-10/C-4. The (suspected) C-G and G-C transitions show good correlations in their associated enthalpy values, these being 28.22 kJ mol^{-1} and 28.04 kJ mol^{-1} respectively. Similar correlations can be observed for the (suspected) G-I and I-G transitions (14.04 kJ mol^{-1} and 13.87 kJ mol^{-1} respectively). In addition, the enthalpies of transition to the liquid crystal phase formed directly on cooling the isotropic liquid show a good correlation, and it seems reasonable to assume that this phase which is observed for all members of the 4'-n-alkoxybiphenyl-4-yl cyclobutanecarboxylates **(8)** is of an identical type, most likely that of the smectic crystal G phase.

Homologues n = 6-9 inclusive also give rise to a second mesophase. On cooling the G phase, the lancets develop a broken appearance whilst the infilled areas associated with the initial dendritic growth change their form to give a different mosaic texture. DSC values for this transition are of a similar order of magnitude (1.39-0.50 kJ mol^{-1}) for

the homologues n = 6-9, and hence, because they also show similar textural characteristics, it is assumed that these homologues are all of the same phase type. This has been given the symbol S_X because the phase type of this smectic modification was not established. The trace **DSC 6** (***Appendix 2***) shows the heating and cooling cycles for the heptyloxy derivative, C-7/C-4. In this compound the unidentified S_X phase is enantiotropic. This was also the case for the $n = 6$ member, whereas for the $n = 8$ and $n = 9$ members this transition is monotropic. The heating cycle trace shows a large peak for the C-S_X transition which is closely followed by the S_X-G transition. These two unresolved peaks are so closely associated that an accurate separation of their relative enthalpies is not possible and hence these have been left uncalculated for the heating cycle. The enthalpy for the G-I phase transition has been calculated as 13.82 kJ mol^{-1}. The cooling cycle, by comparison, shows sufficient resolution to enable the calculation of the enthalpy for the I-G phase transition as 13.85 kJ mol^{-1}, and that for the G-S_X phase transition as 1.36 kJ mol^{-1}. The S_X-C transition is associated with a long, flat peak indicating that the crystallisation process is slow. The enthalpy for the S_X-C phase transition is 10.45 kJ mol^{-1}.

The points for the G-S_X transition temperatures show an odd-even effect and fit two steeply falling curves, with the odd-*n* members uppermost. This behaviour is in contrast to that normally observed in alkoxy compounds for the odd-even effect of transitions from the isotropic liquid where the points for the even-*n* homologues lie on the uppermost curve. The accepted explanation for this is that the even-*n* homologues, in this case, have more bonds lying parallel to the molecular axis, which increases the anisotropy of molecular polarisability relative to the odd-*n* homologues.

4.5.2 *Miscibility studies*

Miscibility work was again undertaken to establish the phase type observed on cooling the isotropic liquid for the homologues n = 6-10 and 12. The n = 9 homologue, the nonyloxy compound (referred to as C-9/C-4), was taken as a representative compound for this series as the relevant point for this homologue lies centrally on the transition plot for this phase type. Mixtures of various percentage compositions were studied by thermal optical microscopy with the new standard material C-10/C-6, 4′-n-decyloxybiphenyl-4-yl cyclohexanecarboxylate **(10)**, n = 10, in the same manner as with the cyclopropane compounds. **Table 10** shows the transition temperatures obtained for the various percentage compositions, and these are displayed graphically in **Plot 10** as a binary phase-composition diagram.

The I-G transition temperatures follow a shallow, dipping curve, showing an overall gradual fall from the pure standard compound to the pure cyclobutane ester. Compositions containing high percentages of the C-10/C-6 standard give rise to an unmistakable G phase. Small 'butterflies' of the phase separate out from the isotropic liquid together with lancets and these grow dendritically to form the characteristic mosaic texture. Compositions of less than 50% C-10/C-6, however, give rise to the sharper, more angular texture shown by the pure 4′-n-alkoxybiphenyl-4-yl cyclobutanecarboxylates **(8)** with lancets separating from the isotropic liquid followed by the growth of the infill areas. Although the S_X phase was not visible in either the 80% or the 90% compositions of the C-9/C-4 compound, a striated appearance was observed for some of the lancets for these mixtures when the G phase was cooled. This characteristic, however, was not uniform throughout the sample under investigation.

Plot 10 - *Binary phase-composition diagram representing transition temperatures for percentage compositions of C-10/C-6 and C-9/C-4*

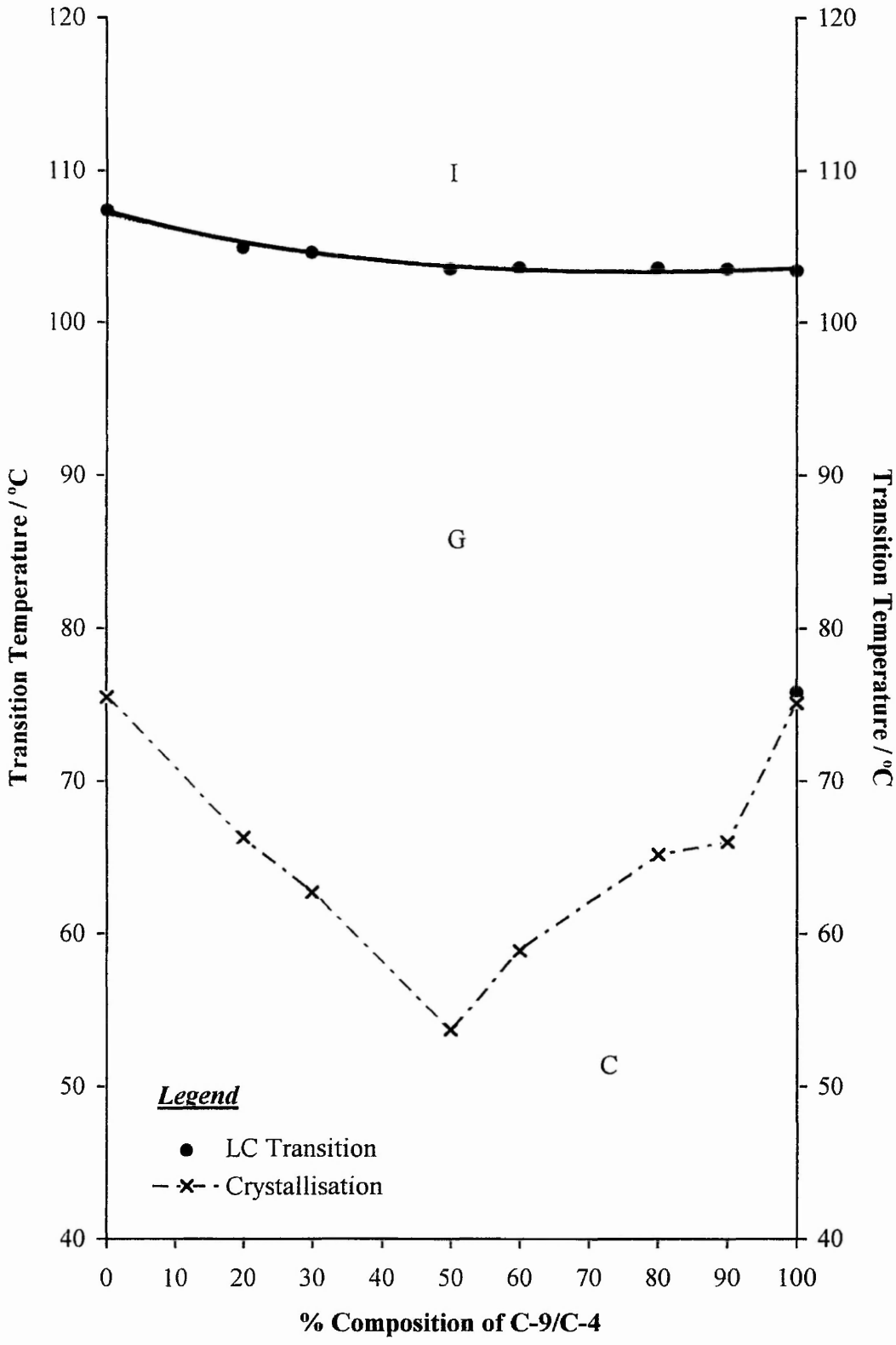

Table 10 - *Transition temperatures for mixtures of a range of percentage compositions C-9/C-4 and C-10/C-6*

% Composition		Transition Temperatures / °C		
C-9/C-4	**C-10/C-6**	**I-G**	**G-S_x**	**G-C**
00	100	107.4		75.5
20	80	104.9		66.3
30	70	104.6		62.7
50	50	103.5		53.7
60	40	103.6		58.9
80	20	103.6		65.2
90	10	103.5		66.0
				S_x-C
100	00	103.4	75.3	75.1

From **Plot 10** it can be seen that the unusual phase obtained on cooling this cyclobutane ester is, in fact, completely miscible with the G phase of C-10/C-6 throughout the whole composition range, and hence, it follows from the *Miscibility Rule* that the phase type of the $n = 9$ member of the cyclobutane esters **(8),** $n = 9$, is that of the smectic crystal G phase. Since the other members (n = 6,7,8,10,12) give rise to exactly analogous textures on cooling the isotropic liquid it is reasonable to assume that a G phase is also formed by these esters.

Miscibility studies were not considered appropriate for the identification of the phase type S_x due to the close proximity of the transition and recrystallisation temperatures of these compounds.

4.5.3 *Further studies*

The optical textures of both the 4′-n-alkoxybiphenyl-4-yl cyclopropane-carboxylates **(7)** and the 4′-n-alkoxybiphenyl-4-yl cyclobutanecarboxylates **(8)** show a more angular appearance than those of the cyclo-pentane- **(9)**, -hexane- **(10)**, and -heptane-carboxylates **(11)**. Although miscibility studies with the C-10/C-6 standard had indicated that the phase type exhibited by these compounds was indeed miscible with that of the crystal G phase, further investigations were undertaken in an attempt to lend support to this evidence.

An initial study was undertaken with the original G phase standard, 14OS5 **(18)**. Various percentage compositions were made with C-9/C-4 and these were investigated by thermal optical microscopy. Great difficulty was found in identifying the phase types shown by these mixtures, until careful study of the 30% standard : 70% cyclo-butane ester composition indicated that these compounds were not miscible. This result, however, does not mean that the previous miscibility study showing complete G phase miscibility is discredited, but rather that the C-10/C-6 standard is a much better choice for studies of compounds of this type, presumably due to the similarities in their structure. The G phase of 14OS5 **(18)** had already been shown to be completely miscible with the phase shown by C-10/C-6 which, in turn, showed complete miscibility with the analogous phases of both C-9/C-3 and C-9/C-4. Hence it can be deduced from the *Miscibility Rule* that all of these compounds exhibit a G phase.

Nevertheless, despite this result, the reason for the uncharacteristic nature of the G phase optical texture shown by so many of the compounds remained an unanswered curiosity. A possible solution that seemed very worthwhile pursuing was that we might be witnessing the formation of the crystal J phase directly from the isotropic liquid, bearing in mind that the G and J phases only differ in their molecular tilt direction within the hexagonal net. In an attempt to test this hypothesis a miscibility study was undertaken using a compound **(19)** reported by Gray and Goodby[48] to exhibit a crystal J phase as part of its phase sequence. This compound exhibited many polymorphic modifications and it was likely that this study would not prove to be as straightforward as the miscibility work previously undertaken.

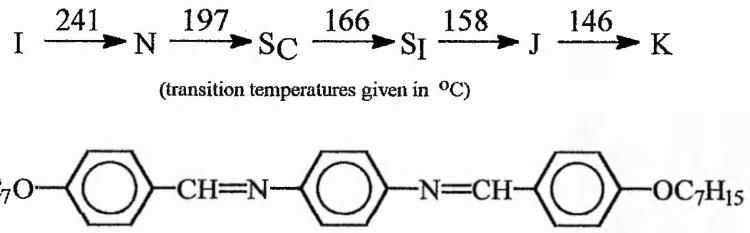

(19)

Various percentage compositions were made with C-9/C-4 and investigated by thermal optical microscopy. The optical textures, particularly the S_C and S_I phases, of these mixtures proved very difficult to distinguish and identify. Conflicting results for phase transitions on heating and cooling the samples quickly indicated that these compounds were not compatible for miscibility studies, although the crystal J to K transitions did appear to produce some of the least confusing and more readily identifiable phases of the study.

These studies, which were not taken further due to the lack of other suitable standard compounds, highlighted the difficulties in finding a suitably compatible compound on which to perform a miscibility study with the cyclobutanecarboxylates. However, the evidence acquired so far indicates that the unusual textures exhibited by the 4′-n-alkoxybiphenyl-4-yl cyclopropanecarboxylates **(7)** and the 4′-n-alkoxybiphenyl-4-yl cyclobutanecarboxylates **(8)** are those of the crystal G phase and no other.

4.6 *The 4′-n-alkoxybiphenyl-4-yl cyclopentanecarboxylates* (9)

Similar investigations of these compounds were undertaken. The transition temperatures for homologues n = 2-10 and 12, together with the associated DSC results, are listed in **Table 4**. A graphical representation of the transition temperatures plotted against n, the number of carbon atoms in the alkoxy group, is given in **Plot 4**. As with the cyclobutanecarboxylates, the results of thermal optical microscopy and the DSC studies are discussed in a composite section.

4.6.1 *Thermal optical microscopy and DSC studies*

The mesomorphic behaviour shown by the cyclopentanecarboxylates **(9)** is almost identical to that reported for their cyclohexane **(10)** counterparts. The n = 2 homologue displays a monotropic nematic phase upon cooling the isotropic liquid. Nematic droplets are observed which rapidly coalesce to produce a characteristic threaded texture.

On cooling the homologues n = 3-8 from the isotropic liquid, a liquid crystal phase is formed which displays the very unusual optical texture seen for homologues

n = 3-6 for the analogous cyclohexane compounds (**Plate A**, ***Appendix 1***). Homologues n = 9, 10 and 12 give rise to a texture which is more recognisable as a liquid crystal phase, most probably a crystal G phase, with dendritic growth leading to the formation of a typical highly coloured mosaic. The n = 12 homologue shows a slightly different texture, with the lancets forming as arcs rather than rectangular shapes.

Although the higher members of the 4′-n-alkoxybiphenyl-4-yl cyclopentane-carboxylates **(9)** do not show any other polymorphic modifications, this is not the case for the members n = 4-7. On cooling the n = 4 homologue to 112.3 °C, the texture of the suspected crystal G phase assumes a zigzag appearance. On further cooling the lancets begin to grow slowly into the areas of infix, but the cross-hatching remains. Based on these textural characteristics, this mesophase type is tentatively identified as a crystal H phase (on further cooling to 104.5 °C, another textural change occurs: the possible nature of this transition is discussed later). Homologues n = 5 and n = 6 display a similar textural appearance with cross-hatched areas and hence these too have been classified as crystal H phases (see **Plate D**, ***Appendix 1***). However, the n = 7 member of the series shows a different textural change with a slow growth of all areas to produce a more uniform but smaller mosaic, with some resemblance to the S_3 phase reported by Gray and Goodby[48] for *trans, trans*-4-n-propylbicyclohexyl-4′-carbonitrile. Consequently, this phase may not be an H phase and has been denoted S_Y.

For the homologue n = 4 there is a textural change at 104.5 °C on cooling the crystal H phase. The most likely explanation for this is that slow formation of one of several polymorphic crystalline forms begins to occur at this temperature. Support for this comes from the fact that on the first heating cycle, the DSC trace shows a very broad peak over a range which spans this temperature, but this is absent on the cooling and

subsequent heating cycles.

Unfortunately, thermal optical microscopy is unable to provide confirmation of the melting behaviour of this (and most of the other members of these homologous series). On slow, moderate, or even rapid heating a gradual change in appearance of the sample is seen, but it is impossible to determine an accurate temperature of transition until the clearing point is reached.

Alternative explanations, such as the occurrence of another unidentified mesophase, or a minor re-organisation of the H phase on cooling, are less attractive and difficult to reconcile with the DSC evidence. However, it should be noted that the DSC enthalpy results for the C-G transition of the homologues $n = 4$ and $n = 5$ are much lower than for the other members of this series (values of 2.87 kJ mol^{-1} and 2.11 kJ mol^{-1}, respectively, compared with values of >20 kJ mol^{-1} for the other homologues). This may be explained if it is considered that the large diffuse peak observed on the first heat of the DSC cycle (**DSC 7**, ***Appendix 2***) corresponds with the formation of the H phase from the crystalline solid. The smaller enthalpy value would then be associated with an H-G phase transition rather than a C-G phase transition (the enthalpy values of approximately 2 kJ mol^{-1} lie within the expected range for such a transition). The disappearance of this transition on consecutive heating cycles requires the assumption that the crystal H phase formed on cooling is of such a highly crystalline nature that the formation of a true crystalline solid occurs over a period of hours rather than minutes. A subsequent heat after such a period of time then allows for the reappearance of the diffuse peak although its shape and position upon the graph does not show a direct correlation with previous results.

For these crystal G to crystal H transitions (G-S_Y for the n = 7 homologue), DSC studies reveal a good correlation of enthalpy data for the n = 4 and 6 homologues (0.91 and 0.98 kJ mol^{-1} respectively), whereas the n = 5 member has an enthalpy value of 2.32 kJ mol^{-1} and the enthalpy of transition for the n = 7 member is 1.02 kJ mol^{-1}. Although the enthalpies of transition for the members n = 4-7 are quite similar, the unusual texture of the n = 7 homologue argues against its inclusion with the members n = 4-6 as a crystal H phase, and hence it has been denoted as S_Y on **Plot 4**.

4.6.2 *Miscibility studies*

Miscibility studies were undertaken to identify the nature of the phase observed on cooling the isotropic liquid for homologues n = 3-8. The n = 8 homologue, the octyloxy compound (referred to as C-8/C-5) was studied by thermal optical microscopy as mixtures of various percentage compositions with the standard, C-10/C-6. **Table 11** shows the transition temperatures for the mixtures studied, and these are displayed graphically in **Plot 11** as a binary phase-composition diagram.

Plot 11 shows a shallow dipping curve for the I-G transition temperatures which fall gently from the higher compositions of C-8/C-5 down to around 30% of the ester. After this point the curve rises with a slightly increased gradient up to the value recorded for the pure standard. The observed textures of the mixtures were very much the same as those reported for corresponding mixtures in the miscibility studies on the other cycloalkanecarboxylates. At higher concentrations of the standard a more usual G phase mosaic texture was observed, whereas higher concentrations of the cyclopentane ester showed lancet formation followed by dendritic growth to infill the areas in between the lancets. The plot obtained is straightforward, and clearly shows a continuous unbroken curve for the G phase over the whole composition range.

Plot 11 - ***Binary phase-composition diagram representing transition temperatures for percentage compositions of C-10/C-6 and C-8/C-5***

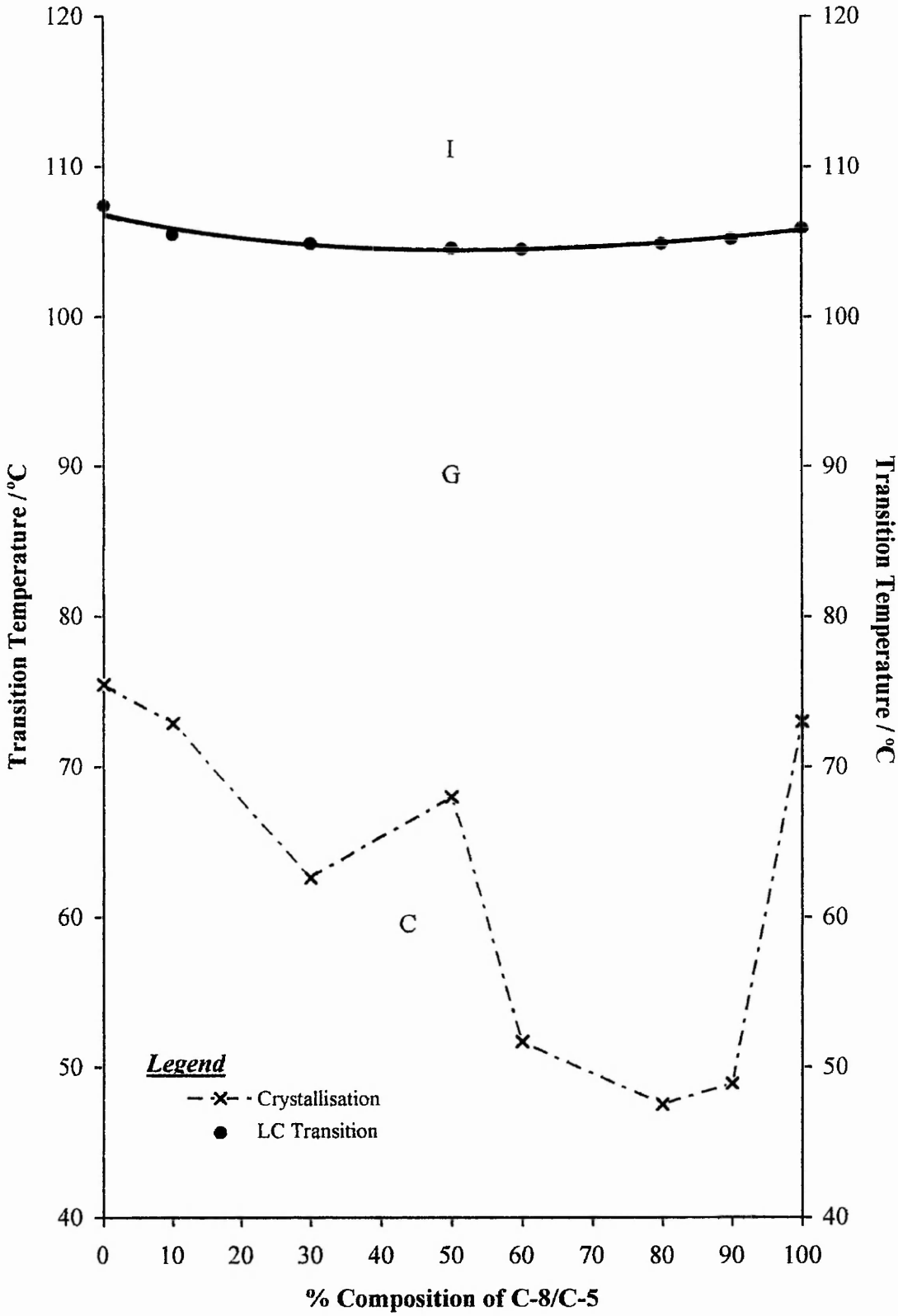

Table 11 - ***Transition temperatures for mixtures of a range of percentage compositions of C-8/C-5 and C-10/C-6***

% Composition		Transition Temperature / °C	
C-8/C-5	C-10/C-6	I-G	G-C
00	100	107.4	75.5
10	90	105.5	72.9
30	70	104.9	62.6
50	50	104.6	68.0
60	40	104.5	51.7
80	20	104.9	47.5
90	10	105.2	48.9
100	00	105.9	73.0

A further study was undertaken to establish the identity of the phase shown by the compounds in the 'humped' region of the plot. As with the previously discussed cyclohexanecarboxylates, the textures of the mesophases formed by compounds giving rise to transitions which lie in this area of the plot were the most uncharacteristic of the G phase. The $n = 4$ homologue (C-4/C-5) was studied in mixtures of varying percentage compositions with the standard ester, C-10/C-6. The resulting transition temperatures are shown in **Table 12** and represented graphically in **Plot 12** as a binary phase-composition diagram.

The miscibility plot obtained for this compound proved to be much more interesting than for that of the C-8/C-5 compound. At 80% and 90% compositions of the cyclopentane carboxylate the crystal H phase of the pure ester is still present. However,

Plot 12 - *Binary phase-composition diagram representing transition temperature for percentage compositions of C-10/C-6 and C-4/C-5*

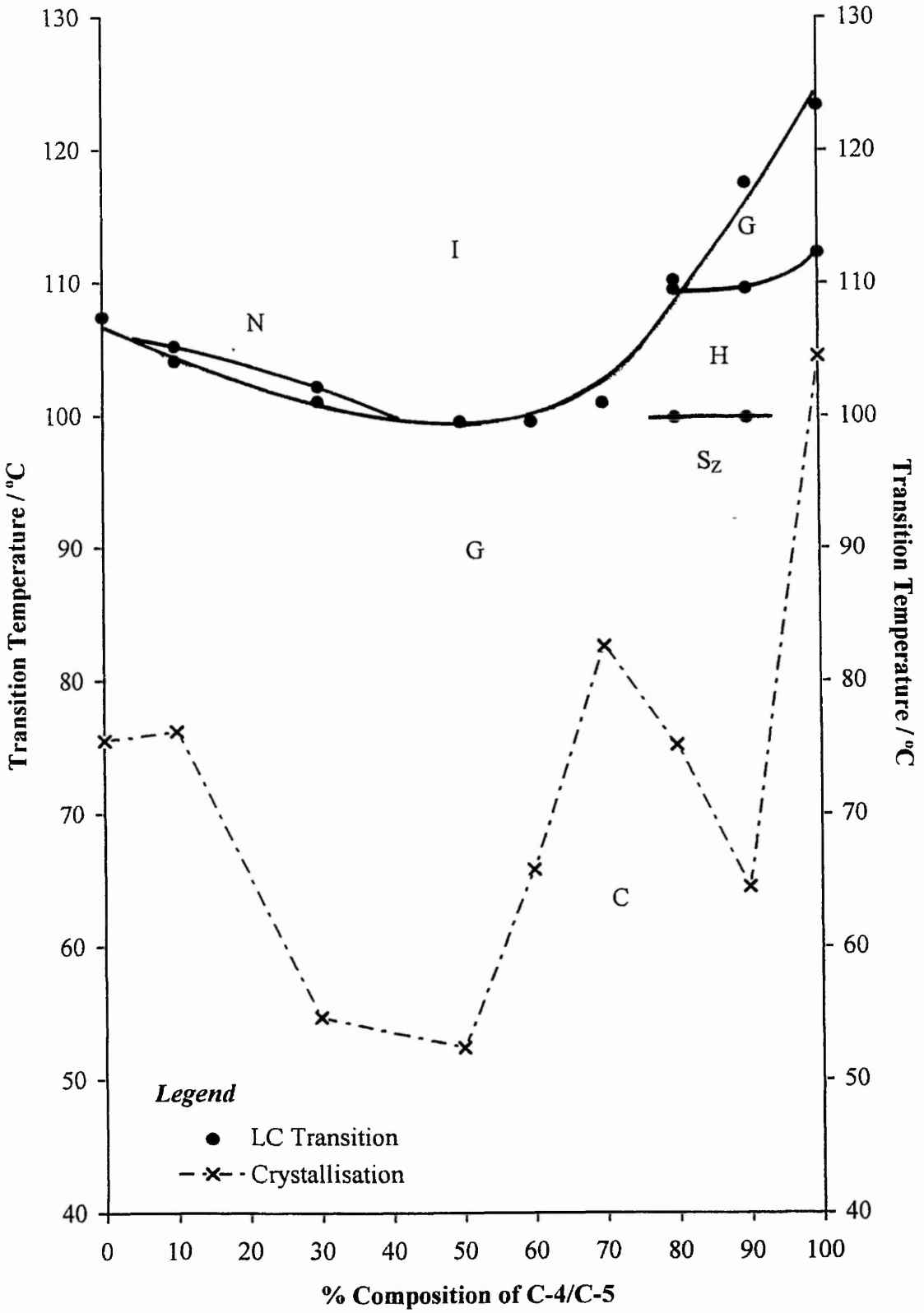

below the H phase another transition occurs to produce a texture which can be most likened to the S_3 phase discussed earlier (and first reported by Gray and Goodby[48]). This phase has been denoted as S_Z (see **Plate D**, ***Appendix 1***), as it is not possible to positively identify it as either the S_3 phase or the previously reported S_Y phase for this series of compounds.

Table 12 - ***Transition temperatures for mixtures of a range of percentage compositions of C-4/C-5 and C-10/C-6***

% Composition		Transition Temperatures / °C			
C-4/C-5	**C-10/C-6**	**I-G**	**I-N**	**N-G**	**G-C**
00	100	107.4			75.5
10	90		104.1	104.1	76.2
30	70		101.1	101.1	54.7
50	50	99.6			52.4
60	40	99.6			65.8
70	30	101.0			82.6
			G-H	**H-S_Z**	**S_Z/H-C**
80	20	110.2	110.2	99.9	75.2
90	10	117.6	109.6	99.9	64.5
100	00	123.4	(112.3)		104.5

Both of these phase types disappear when the percentage composition of the ester falls to 70%. An injected nematic phase is seen at higher percentage mixtures (70-90%) of the standard compound, C-10/C-6.

Plot 12 shows the transition temperature curve for the G phase to be continuous over the whole composition range. The curve falls steeply from higher compositions of the pure cyclopentanecarboxylate to a minimum at approximately 50-60% C-4/C-5. From this point the curve rises gently up to the point for the pure standard.

These studies show that the crystal G phase is miscible with the standard throughout the whole composition range for both the n = 4 and n = 8 members of the cyclopentanecarboxylates. Hence from the *Miscibility Rule* it follows that the 4′-n-alkoxybiphenyl-4-yl cyclopentanecarboxylates **(9)** exhibit a smectic crystal G phase which is formed directly from the isotropic liquid on cooling.

4.7 *The 4′-n-alkoxybiphenyl-4-yl cycloheptanecarboxylates* (11)

Similar investigations of these compounds were undertaken. The transition temperatures for homologues n = 2-10 and 12, 14 and 16 together with the associated DSC results, are listed in **Table 5**. A graphical representation of the transition temperatures plotted against n, the number of carbon atoms in the alkoxy group, is given in **Plot 5**.

4.7.1 *Thermal optical microscopy*

The mesomorphic behaviour observed for these compounds is almost identical to that reported for the cyclohexanecarboxylates **(10)**. The n = 2 homologue displays a

monotropic nematic phase upon cooling the isotropic liquid with the nematic droplets rapidly coalescing to produce a characteristic threaded texture.

On cooling the homologues n = 3-7 from the isotropic liquid, a liquid crystal phase is formed which displays the very unusual optical texture seen for homologues n = 3-6 for the analogous cyclohexane compounds **(10)**. The n = 6 homologue is the only derivative in this area of the plot to give rise to a monotropic transition (an observation which is confirmed by differential scanning calorimetry). The n = 8 homologue gives rise to a texture which is more clearly recognisable as a smectic liquid crystal G phase, with the initial dendritic growth leading to the formation of a typical highly coloured mosaic.

The higher homologues, n = 9,10,12,14 and 16 show a more complex phase pattern. On cooling the n = 9 and n = 10 members the isotropic liquid gives rise to an S_C phase which separates out to form a typical broken fan and a *schlieren* texture. Further cooling gives rise to an unmistakable smectic crystal G phase. A G phase is not observed in the remaining members (n = 12,14 and 16) which show quite different liquid crystal behaviour. The homologues n = 12 and n = 14 also give rise to an S_C phase on cooling the isotropic liquid (see **Plate F**, ***Appendix 1***). However, on further cooling an S_I phase is obtained which is characterised by the appearance of an unfocused *schlieren* texture. On cooling at 5 °C/min to avoid the early onset of crystallisation which occurs at slower cooling rates, this texture then gives rise to a smectic crystal J phase. This phase is characterised by the formation of large mosaic areas, with the remains of the *schlieren* areas of the previous phase appearing within them (see **Plate G**, ***Appendix 1***). The fan texture remains relatively unchanged throughout. The n = 16 homologue gives rise to a short lived S_A phase which precedes an S_C phase on cooling from the isotropic liquid. Further cooling (at a rate of 5 °C/min to avoid crystallisation) gives rise to an S_I phase

with an identical texture to that seen for the $n = 12$ and $n = 14$ derivatives.

In this series the disappearance of the crystal G phase after the $n = 10$ homologue, and its replacement by the smectic crystal J phase for the $n = 12$ and $n = 14$ members is interesting and unusual. It shows that there has been a change in the molecular ordering to form the J phase, with the tilt direction of the molecules now pointing to the apex rather than the side of the hexagonal net. This behaviour is clearly brought about by the formation of the S_I phase from the S_C phase for both the $n = 12$ and $n = 14$ homologues, as X-ray diffraction studies indicate that the molecules within the pseudo-hexagonal net of the S_I phase also lie tilted towards the apex of the net. Therefore it is the introduction of the S_I phase which dictates the tilt direction and hence gives rise to the crystal J phase rather than the crystal G phase.

4.7.2 *Miscibility studies*

Identification of the nature of the phase observed on cooling the isotropic liquid for homologues n = 3-7 was achieved by miscibility studies. The n = 6 hexyloxy compound (referred to as C-6/C-7) was studied by thermal optical microscopy as mixtures of various percentage compositions with the standard, C-10/C-6. **Table 13** shows the transition temperatures for the various percentage compositions studied, and these are displayed graphically in **Plot 13** as a binary phase-composition diagram.

Plot 13 shows a curve for the I-G transition temperatures which falls steeply from the higher compositions of C-6/C-7 to a minimum at approximately 30% of the ester. After this point the curve rises up to the value recorded for the pure standard. The observed textures of the mixtures were very much the same as those reported for corresponding mixtures in the miscibility studies on the other cycloalkanecarboxylates.

Plot 13 - ***Binary phase-composition diagram representing transition temperature for percentage compositions of C-10/C-6 and C-6/C-7***

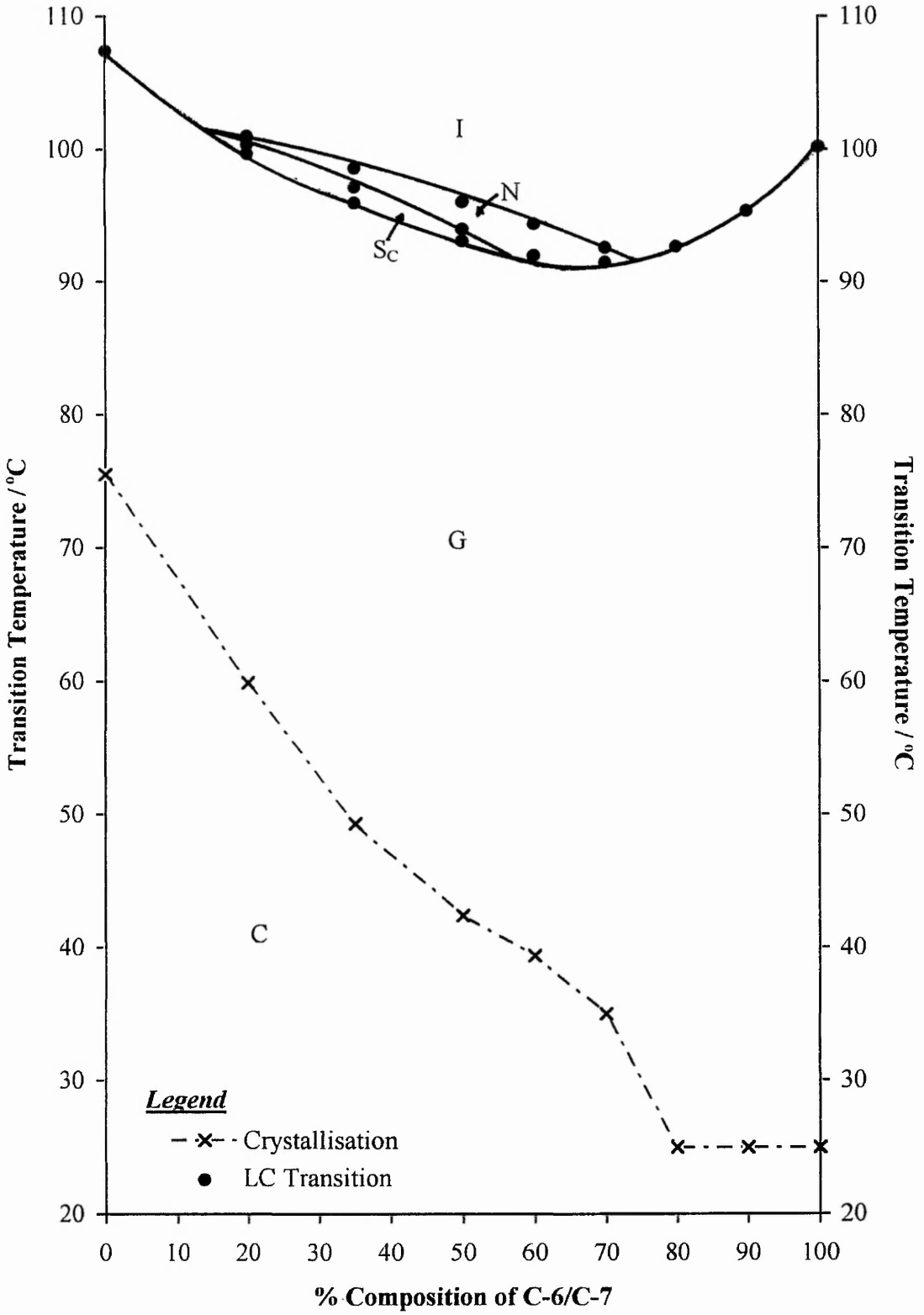

The more characteristic G phase mosaic texture was observed at higher concentrations of the standard, whereas higher concentrations of the cycloheptane ester showed lancet formation followed by dendritic growth to infill the areas in between the lancets. At percentage compositions lying more centrally on the plot an injected nematic phase and an injected S_C phase occur, but these do not interfere with the continuity of the I-G transition temperature curve which remains smooth and uniform across the plot.

These studies show that the crystal G phase is miscible with the standard throughout the whole composition range for the $n = 6$ member. Hence from the *Miscibility Rule* it follows that the 4'-n-alkoxybiphenyl-4-yl cycloheptanecarboxylates **(11)** exhibit a smectic crystal G phase on cooling from the isotropic liquid.

Table 13 - *Transition temperatures for mixtures of a range of percentage compositions of C-10/C-6 and C-6/C-7*

% Composition		Transition Temperatures / °C				
C-6/C-7	C-10/C-6	I-G	I-N	N-S_C	S_C-G	G-C
00	100	107.4				75.5
20	80		101.0	100.4	99.7	59.9
35	65		98.6	97.2	96.0	49.3
50	50		96.1	94.0	93.4	42.4
				N-G		
60	40		94.4	92.4		39.4
70	30		92.6	91.5		35.0†
80	20	92.7				r.t.†
90	10	95.4				r.t.†
100	00	100.2				r.t.*

4.7.3 *DSC studies*

The members of the series of the 4′-n-alkoxybiphenyl-4-yl cycloheptane-carboxylates **(11)** were also studied by differential scanning calorimetry (DSC). The DSC results support the conclusions obtained by optical microscopy and miscibility studies. For the members n = 3-10 there is an excellent correlation of data between the homologues which give rise to a similar mesophase transition for both heating and cooling cycles. This strongly indicates that these members (n = 3-10) give rise to the same liquid crystal phase (a crystal G phase). The DSC data of a representative member of this region, which is reproduced in ***Appendix 2***, is now discussed.

The trace **DSC 8** shows the heating and cooling cycles for the pentyloxy derivative, C-5/C-7. The heating cycle shows two peaks, one associated with the melting point (C-G) and the other with the clearing point (I-G) of the compound. The calculated enthalpies of these transitions are 10.36 kJ mol^{-1} and 13.95 kJ mol^{-1}, respectively. The cooling cycle also shows two peaks, one associated with the I-G transition, and one with the G-C transition. The enthalpy value for the I-G transition is calculated at 13.96 $kJmol^{-1}$ which is consistent with values obtained for this transition for other members of this homologous series.

The trace **DSC 9** (***Appendix 2***) shows the heating and cooling cycles for the dodecyloxy derivative, C-12/C-7 which shows smectic polymorphism (**Plot 5**). On the heating cycle two peaks corresponding with the C-S_I(S_C) and S_C-I transitions occur, although the transition enthalpy for only one of these can be calculated accurately. The C-S_I transition appears as a peak with a shoulder due to the rapid formation of the S_C phase from the S_I phase on heating this derivative. The calculated value for the enthalpy of the S_C-I transition is 6.22 kJ mol^{-1}. The cooling cycle for the compound C-12/C-7,

however, clearly shows the I-S_C, S_C-S_I and the S_I-J phase transitions prior to the (J-C) peak associated with crystallisation. The enthalpy values of these transitions have been calculated as 6.26 kJ mol^{-1}, 2.76 kJ mol^{-1} and 0.14 kJ mol^{-1} respectively.

4.8 *Concluding remarks from studies on the 4′-n-alkoxybiphenyl-4-yl cycloalkane-carboxylates* (7-11)

From the combination of thermal optical microscopy, differential scanning calorimetry and miscibility studies on these series it is concluded that the phase with a very unusual texture observed upon cooling the isotropic liquid of most homologues of the 4′-n-alkoxybiphenyl-4-yl cycloalkanecarboxylates **(7-11)** is, in fact, a smectic crystal G phase. However, the optical textures shown by the cyclopropyl- **(7)** and cyclobutyl-carboxylates **(8)** and the lower homologues of the cyclopentyl- **(9)**, cyclohexyl- **(10)**, and cycloheptyl-carboxylates **(11)** are not characteristic of the G phase nor readily recognisable as such, and their formation on cooling the isotropic liquid can easily be mistaken for crystallisation.

It is intended, in future work, to confirm the smectic crystal G assignments in representative members of these series by X-ray diffraction studies.

Both the cyclobutane- **(8)** and cyclopentane-carboxylates **(9)** show additional mesomorphic transitions for homologues in the n = 4-7 range. It has not been possible to be certain about the phase type assignments for some of the phases observed due to their highly crystalline nature and the unusual textures of the preceding G phase.

The cyclohexane- **(10)** and cycloheptane-carboxylates **(11)** both exhibit smectic polymorphism for the higher members of the homologous series. There are certain

similarities in the textures of the phases formed from the S_C phase on cooling, but, based only on the evidence of optical studies, for the cyclohexane compounds **(10)** this phase has been identified as S_F and for the cycloheptane analogues the corresponding assignment is S_I. Miscibility studies are necessary to confirm these assignments, but such studies may not be straightforward due to the close proximity of crystallisation to the phase transition temperatures in question.

In addition to the unique optical textures shown by members of the homologous series which give rise to a G phase on cooling the isotropic liquid, the cyclopentane- **(9)**, cyclohexane- **(10)**, and cycloheptane-carboxylates **(11)** reveal very unusual behaviour, namely the existence of a pronounced 'hump' for the members $n < 8$, when the G-I transition temperatures are plotted against n, the number of carbon atoms in the alkyl group (**Plot 1**,**4**, and **5**). The reason for this behaviour is almost certainly associated with the nature of the packing arrangement of the molecules in the ordered mesophase. However, why there is an optimum chain length for which the molecules pack more economically, thus requiring more energy to break down the ordered array and hence giving rise to a higher transition temperature than both earlier and later members of the homologous series is not known. Detailed X-ray studies may provide the answer.

5. *Discussion of the liquid crystal behaviour of the 4′-n-alkylbiphenyl-4-yl 4-n-alkylbenzoates*

5. *Discussion of the liquid crystal behaviour of the 4′-n-alkylbiphenyl-4-yl 4-n-alkylbenzoates* (17)

5.1 *Introduction*

The synthesis and liquid crystalline properties of certain 4′-n-alkylbiphenyl-4-yl 5-n-alkylthiophene-2-carboxylates **(20)** has recently been reported by Butcher, Byron, Matharu, and Wilson.[43] A systematic study of homologation in these compounds revealed extensive smectic polymorphism.

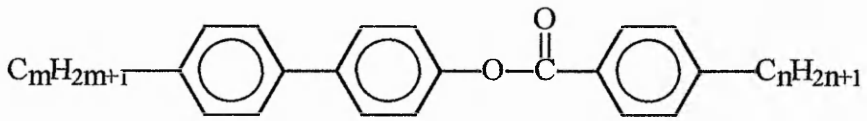

(17)

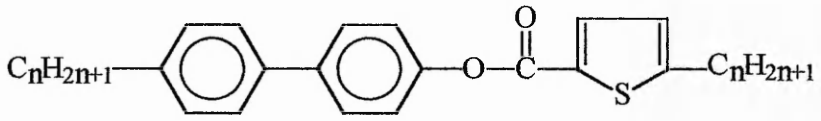

(20)

Initial optical microscopy studies were also carried out on four members of the analogous 4′-n-alkylbiphenyl-4-yl 4-n-alkylbenzoates **(17)** (m = 5-7 and 10, n = 1-10) in order to compare the thermal stability of the mesophases exhibited by these compounds with their thiophene analogues **(20)**. This limited investigation of the liquid crystalline properties of the 4′-n-alkylbiphenyl-4-yl 4-n-alkylbenzoates **(17)** indicated that these derivatives also give rise to highly smectogenic behaviour. A number of similar benzoates of the same general formula are cited in a patent granted to Steinstrasser *et al.*[44] in 1979.

However, seemingly no attempt was made to identify the smectic phases present. Indeed, the authors state "These compounds exhibit a nematic, and in some instances, *an additional smectic mesophase* within certain temperature ranges...", implying the presence of just one (unidentified) smectic mesophase for very few of the compounds studied.

Thus due to the lack of precise data regarding the 4′-n-alkylbiphenyl-4-yl 4-n-alkylbenzoates **(17)**, a wider, representative set of compounds comprising ten members of four homologous series of these esters was synthesised and their liquid crystalline behaviour investigated by thermal optical microscopy and differential scanning calorimetry. The results of this study, discussed in subsequent sections, indicate the existence of quite complex smectic polymorphism in each of the four series. A brief comparative discussion of the smectic behaviour and mesophase thermal stability of the benzoates **(17)** and their thiophene analogues **(20)** is also given.

A photographic record of some of the typical optical textures of the mesophases observed for these homologous series is given in ***Appendix 1,*** **Plates H-J**.

5.2 *Summary of thermal data*

Ten members (n = 1-10) of four homologous series of 4′-n-alkylbiphenyl-4-yl 4-n-alkylbenzoates **(17)** were synthesised in moderate yields from the appropriate 4-n-alkyl-4′-hydroxybiphenyl **(16)** and 4-n-alkylbenzoic acid **(15)**. The specific compounds studied were **(17)**, m = 5-7 and 10, n = 1-10 (methyl to decyl) and the following section lists tables of transition temperatures for each of the homologous series together with the associated enthalpies of transition obtained by DSC. The results for each series are represented graphically in corresponding plots showing transition temperatures against, n, the number of carbon atoms in the alkyl group of the substituted benzoic acid.

Table 14, Plot 14 - 4′-n-pentylbiphenyl-4-yl 4-n-alkylbenzoates

Table 15, Plot 15 - 4′-n-hexylbiphenyl-4-yl 4-n-alkylbenzoates

Table 16, Plot 16 - 4′-n-heptylbiphenyl-4-yl 4-n-alkylbenzoates

Table 17, Plot 17 - 4′-n-decylbiphenyl-4-yl 4-n-alkylbenzoates

Plot 14 - ***Representation of transition temperatures for the 4'-n-pentylbiphenyl-4-yl 4-n-alkylbenzoates***

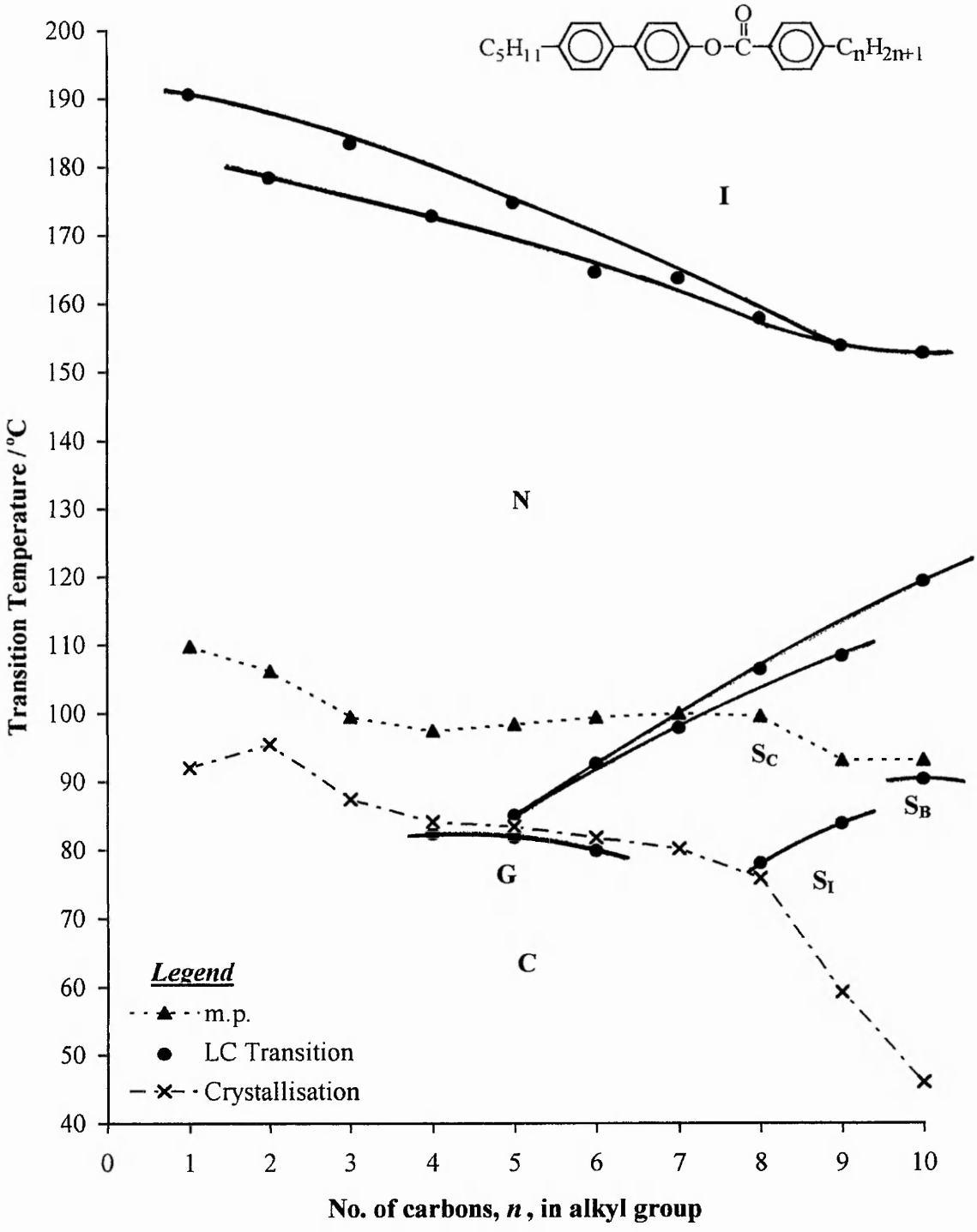

Table 14 - *Mesophase transition temperatures and enthalpy data for the 4'-n-pentylbiphenyl-4-yl 4-n-alkylbenzoates*

n	C-N	I-N	N-G		N-C
1	**109.8**†	**190.6**			**92.0**
	25.43‡	*1.02*			*22.69*
2	**106.2**	**178.5**			**95.5**
	24.41	*0.89*			*20.35*
3	**99.5**	**183.4**			**87.4**
		1.17			*31.12*
					G-C
4	**97.4**	**172.9**	**(84.1)**		**84.1**
	18.41	*0.98*			
			N-S_C	**S_C-G**	**S_C-C**
5	**98.4**	**174.8**	**(83.4)**	**(81.8)**	**83.4**
	18.41	*0.98*			
6	**99.4**	**164.6**	**(92.6)**	**(79.9)**	**81.8**
	19.91	*1.15*	*1.66*		
7	**100.0**	**163.8**	**(97.9)**		**80.2**
	20.40	*1.24*	*0.92*		
	C-S_C			**S_C-S_I**	**S_I-C**
8	**99.6**	**157.9**	**106.5**	**(78.1)**	**75.9**
	20.64	*1.21*	*0.73*		
9	**93.1**	**153.9**	**108.4**	**(83.9)**	**59.3**
	19.47	*1.18*	*0.32*	*1.84*	*12.53*
				S_C-S_B	**S_B-C**
10	**92.6**	**152.8**	**119.3**	**(91.4)**	**46.0**
	20.72	*1.51*	*0.23*	*2.72*	

( ) denotes a monotropic transition; † transition temperatures listed were determined by thermal optical microscopy, the reported values being obtained on cooling (except melting points); ‡ values in italics represent enthalpies of transition (kJ mol^{-1}) obtained by differential scanning calorimetry at a cooling rate (heating for m.p.) of 10°C/min, where no DSC value is quoted the enthalpy of transition could not be accurately calculated.

Plot 15 - *Representation of transition temperatures for the 4'-n-hexylbiphenyl-4-yl 4-n-alkylbenzoates*

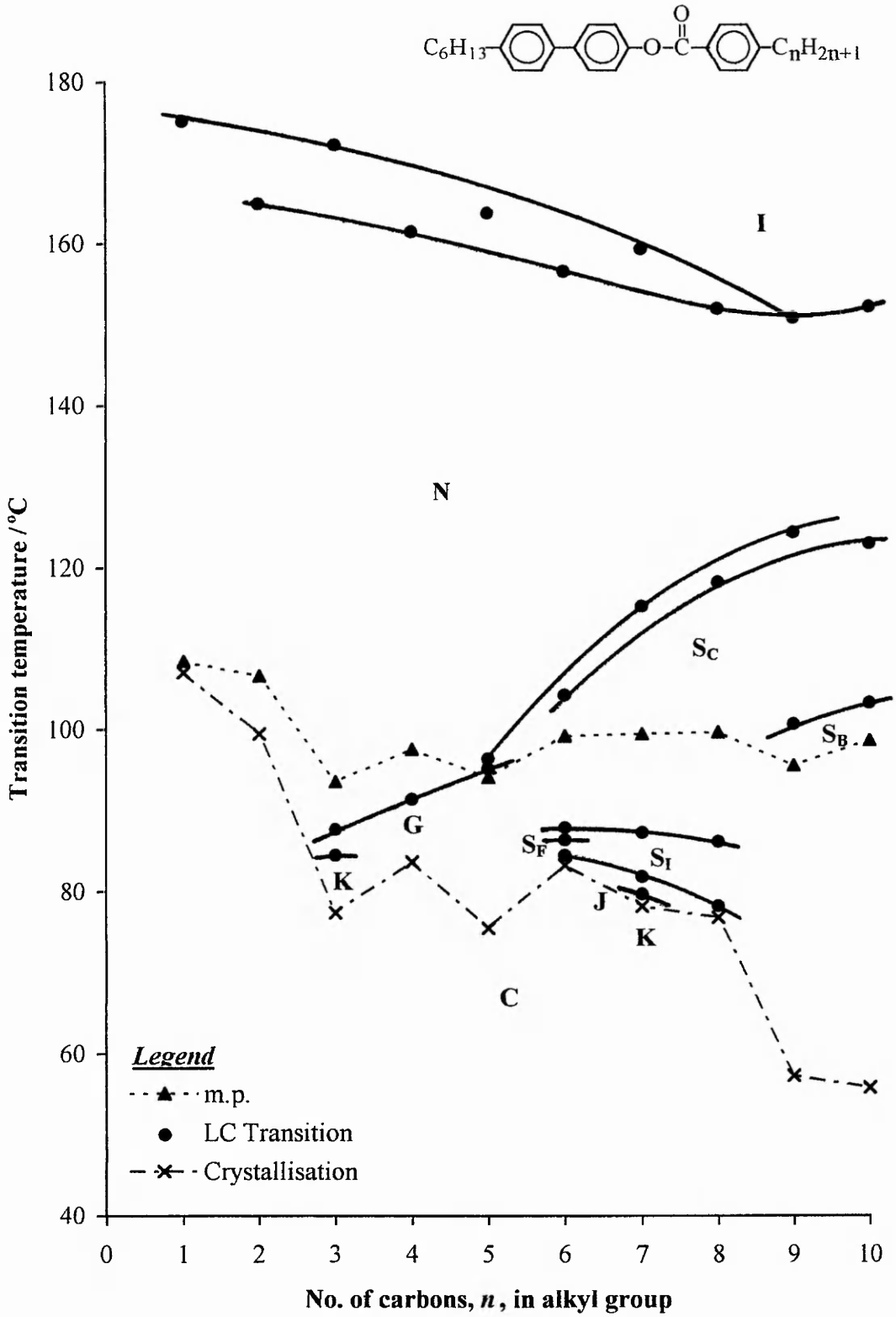

Table 15 - ***Mesophase transition temperatures and enthalpy data for the 4'-n-hexylbiphenyl-4-yl 4-n-alkylbenzoates***

n	C-N	I-N	N-S_C	N-G	G-K			N-C
1	**108.5**† *17.39*‡	**175.2** *0.47*						**107.1** *16.62*
2	**106.7** *22.52*	**165.0** *0.56*						**99.5** *21.09*
							K-C	G-C
3	**93.6**	**172.3** *0.76*		**(87.7)**	**(84.5)**		**(77.4)** *9.00*	
4	**97.6** *22.00*	**161.5** *0.83*		**(91.4)** *7.68*				**83.7**
	C-S_C			S_C-G				
5	**94.1**	**156.6** *1.01*	**95.2** *2.15*	**(86.4)** *2.93*				**75.5**
				S_C-S_I	S_I-S_F	S_F-J		J-C
6	**99.2**	**156.6** *0.97*	**104.3** *1.92*	**(87.9)**	**(87.3)**	**(84.5)**		**84.5** *12.90*
					S_I-J	J-K	K-C	
7	**99.5**	**159.4** *1.13*	**115.3** *0.93*	**(87.3)** *1.28*	**(81.9)** *0.22*	**(79.7)**	**79.7** *12.55*	
8	**99.7**	**152.0** *1.20*	**118.3** *0.87*	**(86.2)** *0.95*		**(78.2)**		**78.2**
				S_C-S_B				S_B-C
9	**95.6**	**150.9**	**124.4**	**100.7**				**57.2**
10	**98.7**	**152.2** *0.94*	**123.0** *0.24*	**103.3** *2.15*				**55.8** *4.00*

( ) denotes a monotropic transition; † transition temperatures listed were determined by thermal optical microscopy, the reported values being obtained on cooling (except melting points); ‡ values in italics represent enthalpies of transition (kJ mol^{-1}) obtained by differential scanning calorimetry at a cooling rate (heating for m.p.) of 10°C/min, where no DSC value is quoted the enthalpy of transition could not be accurately calculated.

Plot 16 - ***Representation of transition temperatures for the 4'-n-heptylbiphenyl-4-yl 4-n-alkylbenzoates***

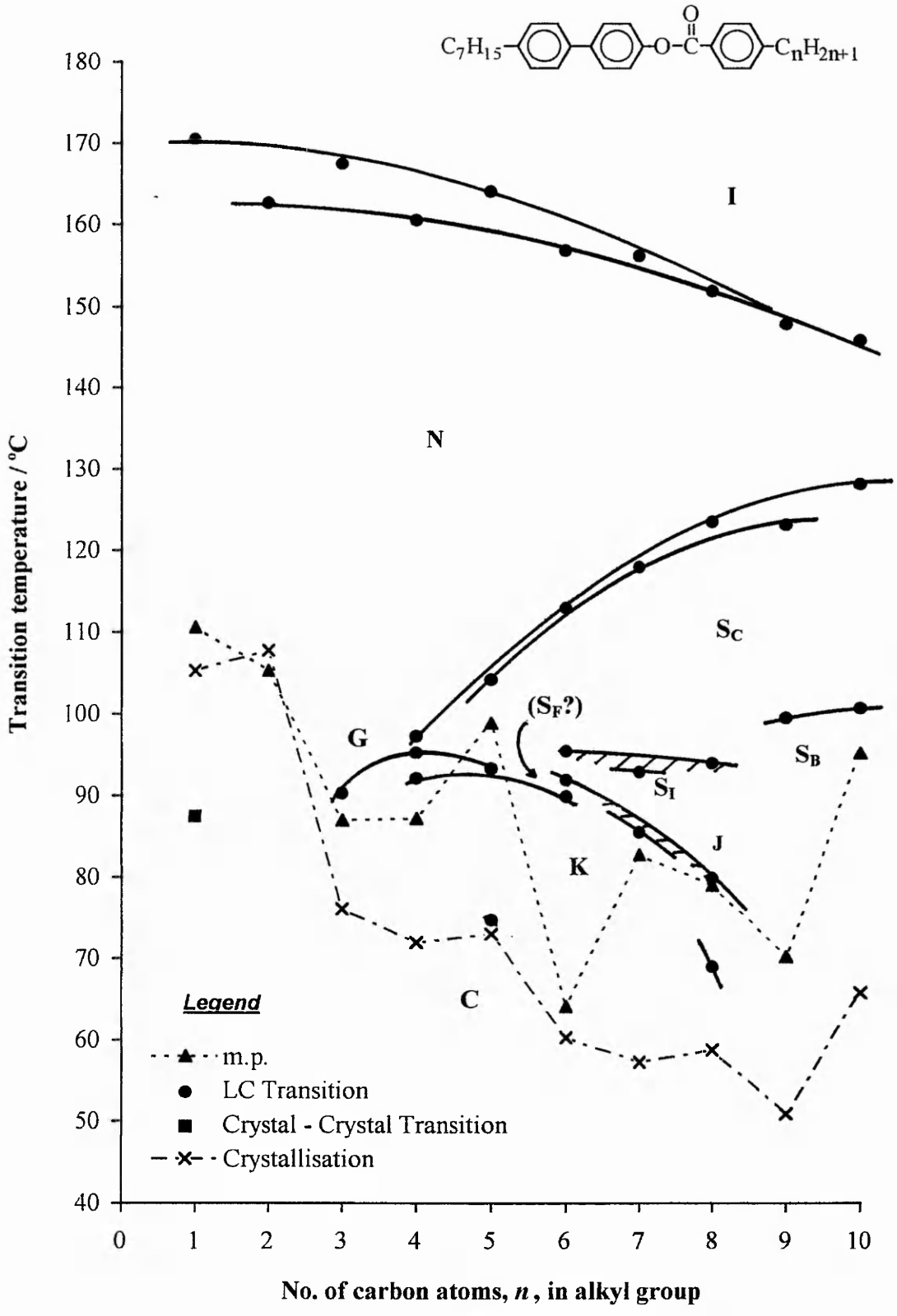

Table 16 - *Mesophase transition temperatures and enthalpy data for the 4'-n-heptylbiphenyl-4-yl 4-n-alkylbenzoates*

n	C_1-C_2	C-N	I-N	N-S_C	N-G		G-C	N-C
1	87.5	110.6†	170.5					105.3
		17.11‡	*0.79*					*16.64*
2		105.3	162.7					107.8
		24.41	*0.68*					*16.82*
3		87.0	167.5		(90.3)		76.1	
			1.04		*6.76*		*8.43*	
		C-K			S_C-G	G-K		K-C
4		87.2	160.6	97.3	95.3	92.1		72.0
		9.33	*0.94*					
		C-S_C						
5		98.9	164.1	104.2	(93.3)	(73.0)		73.0
		16.53	*0.95*	*1.31*	*2.61*			
		C-J			S_C-S_I	S_I-J	J-K	
6		64.1	156.9	113.0	95.5	91.9	89.9	60.3
							J-C	
7		82.8	156.3	118.0	92.9	85.5	57.3	
		18.39	*1.39*	*1.09*	*1.80*	*0.29*	*5.80*	
		C-S_I					J-K	
8		79.3	152.0	123.6	94.0	(79.9)	(69.0)	58.8
		14.51	*1.34*	*0.94*	*1.45*	*0.11*		*6.19*
		C-S_B			S_C-S_B			S_B-C
9		70.2	147.9	123.2	99.5			50.9
		13.67	*1.09*	*0.43*	*2.46*			
10		95.2	145.9	128.2	100.7			65.8
			1.50	*0.39*	*2.76*			*16.90*

( ) denotes a monotropic transition; † transition temperatures listed were determined by thermal optical microscopy, the reported values being obtained on cooling (except melting points); ‡ values in italics represent enthalpies of transition (kJ mol^{-1}) obtained by differential scanning calorimetry at a cooling rate (heating for m.p.) of 10°C/min, where no DSC value is quoted the enthalpy of transition could not be accurately calculated.

Plot 17 - *Representation of transition temperatures for the 4'-n-decylbiphenyl-4-yl 4'-n-alkylbenzoates*

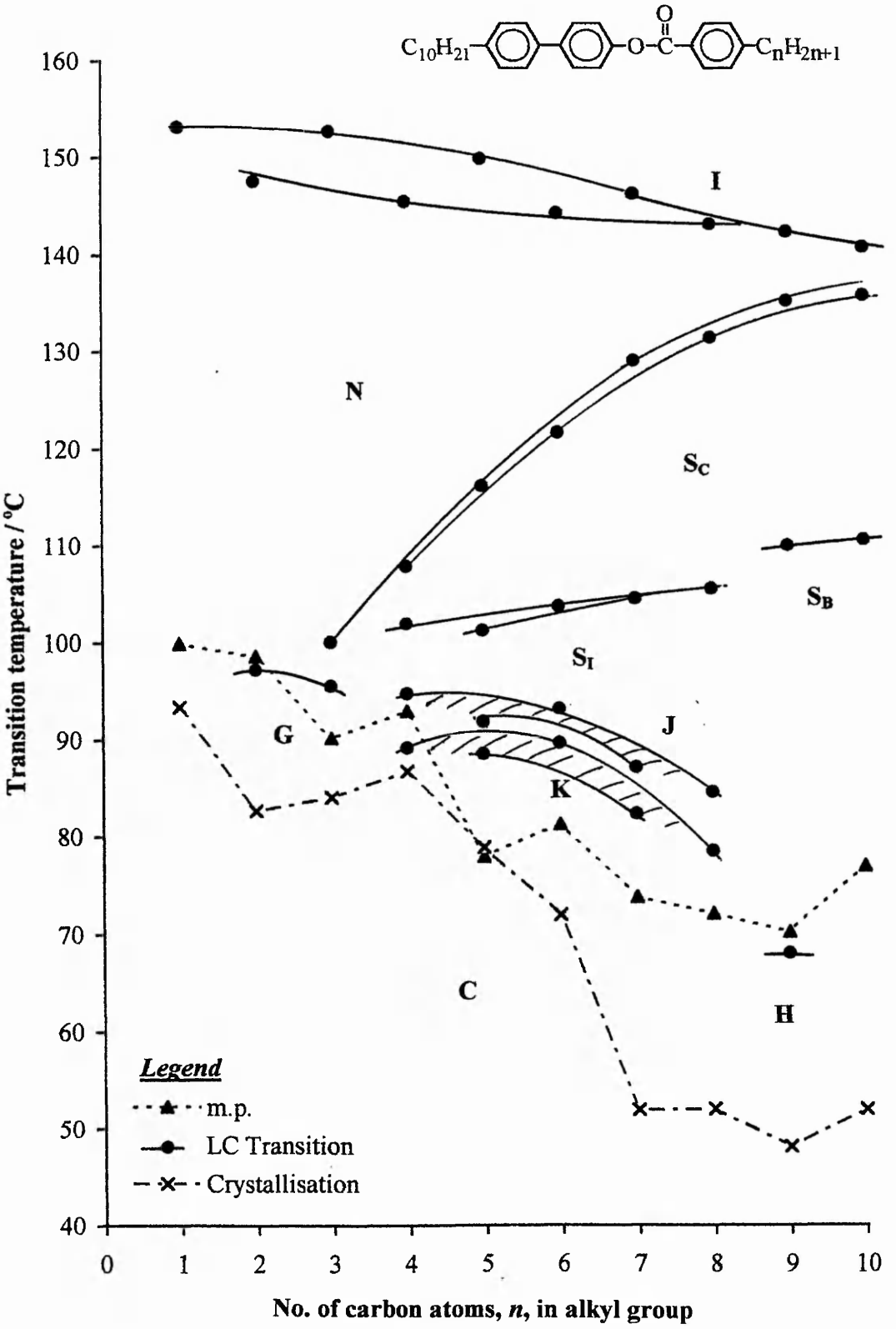

Table 17 - *Mesophase transition temperatures and enthalpy data for the 4'-n-decylbiphenyl-4-yl 4-n-alkylbenzoates*

n	C-N	I-N	N-S_C	N-G	S_I-J	J-K	N-C
1	99.9†	153.2					93.4
	36.83‡	*0.68*					*11.82*
							G-C
2	98.6	147.7		(97.2)			82.7
		0.78		*7.92*			
	C-G			S_C-G			
3	90.2	152.9	100.1	95.6			84.1
		0.89					
	C-J/K			S_C-S_I			K-C
4	93.0	145.7	108.0	102.0	94.8	(89.2)	86.8
		1.04	*1.76*	*3.83*	*0.05*		*8.71*
5	78.0	150.1	116.3	101.3	91.9	88.6	78.9
		1.60	*1.23*	*3.43*	*0.08*		
6	81.3	144.5	121.8	103.8	93.2	89.7	72.0
		1.41	*1.46*	*3.16*			*5.63*
7	73.8	146.5	129.2	104.6	87.2	82.4	51.9
		1.69	*0.96*	*2.84*	*0.05*		*4.49*
8	72.1	143.4	131.6	105.6	84.6	78.5	52.0
		2.04	*1.23*	*3.14*			*6.4*
	C-S_B			S_C-S_B	S_B-H		H-C
9	70.2	142.6	135.4	110.1	(68.0)		48.1
				3.15	*0.20*		*6.31*
							S_B-C
10	77.0	141.0	136.0	110.7			51.9
	43.08			*3.59*			

( ) denotes a monotropic transition; † transition temperatures listed were determined by thermal optical microscopy, the reported values being obtained on cooling (except melting points); ‡ values in italics represent enthalpies of transition (kJ mol^{-1}) obtained by differential scanning calorimetry at a cooling rate (heating for m.p.) of 10°C/min, where no DSC value is quoted the enthalpy of transition could not be accurately calculated.

5.3 *The 4′-n-pentylbiphenyl-4-yl 4-n-alkylbenzoates*

The 4′-n-pentylbiphenyl-4-yl 4-n-alkylbenzoates **(17)**, m = 5, provided the least complex pattern of smectic behaviour of the four homologous series investigated. The transition temperatures for the homologues n = 1-10, together with the associated DSC results, are listed in **Table 14**. A graphical representation of the transition temperatures plotted against n, the number of carbon atoms in the alkyl group of the benzoate moiety, is given in **Plot 14**. The DSC data are discussed in section **5.7**.

5.3.1 *Thermal optical microscopy*

All ten members of the 4′-n-pentylbiphenyl-4-yl 4-n-alkylbenzoates **(17)**, m = 5, n = 1-10, give rise to an enantiotropic nematic phase on cooling from the isotropic liquid. The transition temperature plot (**Plot 14**) reveals an odd-even-n effect with the points fitting two falling curves, with those of the odd-n members uppermost, which converge after the n = 8 homologue, before the curve levels off for the last two homologues. The lower members (n = 1-5) give rise to a stable nematic phase over a broad temperature range. This behaviour is also exhibited by the other homologous series which were synthesised. The appearance of this phase is characterised by the formation of nematic droplets from the isotropic liquid which rapidly coalesce to give rise to a threaded, marbled texture that exhibits Brownian motion. *Schlieren* brushes may be clearly seen (a similar texture is shown in **Plate H**, ***Appendix 1***).

The smectic character of the series comprises two distinct sections. The members n = 1-3 show no smectic mesophases. Smectic behaviour is first seen at n = 4 when, on very rapid cooling of the nematic phase, a crystal G phase can be detected at a temperature slightly lower than that at which recrystallisation occurs on slower cooling.

The higher homologues $n = 5$ -10 then give rise to a variety of smectic modifications. On cooling the nematic phase of members n = 5-10 an S_C phase is observed, the later derivatives (n = 8-10) showing enantiotropic behaviour. A study of the transition temperature plot shows that these points also show an odd-even effect fitting two rising curves which diverge slightly for the longer alkyl chain lengths. However in this instance the even-*n* members are uppermost. On cooling from the nematic phase, the onset of the S_C phase is preceded by the formation of a domain texture usually associated with the S_A phase. However, this texture did not stabilise to produce a focal conic texture typical of an S_A phase but gave rise instead to an S_C phase, characterised by shattered focal conic regions punctuated by large areas of *schlieren* texture. It is, however, feasible that the S_C phase is indeed preceded by a very short-lived S_A phase, especially in view of the shattered appearance of the focal conic fans..

As stated earlier, cooling the nematic phase of the homologue $n = 4$ gives rise to a monotropic smectic crystal G phase, and the S_C phases of $n = 5$ and 6 also give rise to a monotropic crystal G phase, concurrently with the onset of crystallisation on rapid cooling. For the member $n = 4$ the observed texture forms via the growth of dendrites across the field of view to produce a characteristic crystal G mosaic texture. The focal conic domain of members $n = 5$ and 6 exhibits the expected *chequerboard* broken fan texture of the G phase.

The homologues $n = 8$ and 9 show different smectic behaviour on cooling the S_C phase, and give rise to an S_I phase which is characterised by the indistinct, unfocusable *schlieren*-mosaic texture and associated focal conic domain. The $n = 7$ member may also give rise to an S_I phase, although with crystallisation occurring in many areas of the slide, it is not possible to ascertain with certainty whether the observed shimmering of the texture is related to the onset of the formation of a mesophase or is merely the process of crystallisation creating stress in the *schlieren* areas of the S_C phase.

Cooling the S_C phase of the $n = 10$ homologue gives rise to an S_B phase, which, as the S_C-S_B transition occurs, is characterised by the appearance of striations across the backs of the focal conic fans of the S_C phase. The overall appearance of the fan texture after completion of the transition to the S_B phase is much smoother than that of the preceding S_C phase. The schlieren areas of the S_C phase become dark homeotropic regions, characteristic of the S_B phase.

5.4 *The 4′-n-hexylbiphenyl-4-yl 4-n-alkylbenzoates*

The transition temperatures for the homologues of the 4′-n-alkylbiphenyl-4-yl 4-n-alkylbenzoates **(17)**, $m = 6$, $n = 1$-10, together with the associated DSC results, are listed in **Table 15**. A graphical representation of the transition temperatures plotted against n, the number of carbon atoms in the alkyl group of the benzoate moiety, is given in **Plot 15**. The DSC data are discussed in section **5.7**.

5.4.1 *Thermal optical microscopy*

The liquid crystalline behaviour of the 4′-n-hexylbiphenyl-4-yl 4-n-alkyl-benzoates, **(17)**, $m = 6$, $n = 1$-10, although closely similar to that of their pentyl analogues previously discussed, provides a slightly more complex mesophase pattern.

As before, all ten members of the homologous series give rise to an enantiotropic nematic mesophase, the points for the transition temperatures fitting two falling, converging curves, with the odd-n curve uppermost. Similarly, S_C and crystal G phases are present, but these appear at an earlier homologue than reported for the corresponding pentyl derivatives.

On cooling the S_C phase of the homologues n = 6-8 an S_I phase is observed, and this on further cooling gives rise to other smectic mesophase types. The n = 6 member shows the most interesting phase behaviour. At 87.3 °C an S_F phase is formed. The phase change is characterised by a sharpening of the indistinct, unfocusable *schlieren* brushes of the preceding S_I phase. A further mesophase transition is then observed at 84.5 °C, with the S_F *schlieren*-mosaic areas changing to the small mosaic texture characteristic of the crystal J phase. The appearance of the J phase is accompanied by the onset of crystallisation. The S_I-S_F-J phase sequence is highly unusual and indicates that with regard to the crystal structure, the directional alignment of the molecules within the hexagonal net *flip* from pointing to the apex, to the side, and then back to the apex as the phase pattern is traversed.

Cooling the S_I phase of the n = 7 and 8 derivatives gives the crystal J phase directly, with no evidence for the presence of the S_F phase seen for the previous n = 6 homologue.

The n = 3 and 7 members give rise to a crystal K phase characterised by the appearance of the very distinctive 'candy-striping' of the mosaic regions. As may be seen from **Plot 15** it is probable that the absence of the crystal K phase for the homologues n = 4 and 6 is due to the earlier occurrence of crystallisation for these compounds. The sample of the n = 5 member may have been slightly impure resulting in both the rather low value of the N-I transition temperature and the absence of a crystal K phase.

Cooling the S_C phase of both the n = 9 and 10 homologues gives rise to an S_B phase. At the S_C-S_B transition, striations (transition bars) appear across the backs of the focal conic fans. The appearance of the fan texture after the completion of the transition to the S_B phase is much smoother than in the preceding S_C phase. The *schlieren* areas of the S_C phase become dark regions, the homeotropic texture of the S_B phase.

5.5 *The 4′-n-heptylbiphenyl-4-yl 4-n-alkylbenzoates*

The transition temperatures of the 4′-n-heptylbiphenyl-4-yl 4-n-alkyl-benzoates **(17)**, $m = 7$, n = 1-10, together with the associated DSC results, are listed in **Table 16**. A graphical representation of the transition temperatures plotted against n, the number of carbon atoms in the alkyl group of the benzoate moiety, is given in **Plot 16**. The DSC data are discussed in section **5.7**.

5.5.1 *Thermal optical microscopy*

The liquid crystal behaviour of this homologous series shows some characteristics of both the corresponding pentyl and hexyl homologues. An enantiotropic nematic mesophase is observed on cooling the isotropic liquid for all ten members of the series. The points for the I-N transition temperatures lie on two falling curves with the odd-n members uppermost. The curves converge after the $n = 8$ homologue.

Only the members $n = 1$ and 2 do not give rise to smectic mesophases. Cooling the nematic phase of the homologues n = 4-10 gives rise to an enantiotropic S_C phase, and the points for the N-S_C transition temperatures also fit two rising curves (even-n uppermost) which diverge slightly at higher chain lengths.

The homologues n = 3-5 give rise to a crystal G phase on cooling the preceding nematic or S_C phase. However, on cooling the S_C phase of the members n = 6-8 an S_I phase is formed. At the transition a change of the *schlieren* brushes of the S_C phase to the very characteristic, non-focusable *schlieren* texture of the S_I phase occurs. Further cooling of the S_I phase of these homologues gives rise to optical textures consistent with the formation a smectic crystal J phase. When observed for the $n = 6$ homologue this phase appeared as a texture comprising small *schlieren*-mosaic areas and consequently

was at first assigned as an S_F phase. However, when compared with the more obvious smectic crystal J textures formed when the later homologues of the series were cooled from the S_I phase, the initial assignment of this texture for the $n = 6$ homologue as S_F seemed less certain. The point for the transition temperature has been included on the S_I-J plot (**Plot 16**), but with an indication that it may, in fact, be for an S_I-S_F transition. There was insufficient time to carry out conclusive miscibility studies on the $n = 6$ homologue to confirm this assignment. The curves for the S_I and crystal J phases are shown in **Plot 16** as hatched regions for the purpose of clarity. In both of these regions the points for the transition temperatures exhibit an odd-even effect with the curve for the even-*n* members uppermost.

Further cooling of the smectic crystal G phases of the homologues $n = 4$ and 5 and the crystal J phases of the homologues n = 6 and 8 gives rise to a smectic crystal K phase. **Plot 16** clearly shows the wide separation of transition temperatures to the K phase of the homologues $n = 4$ and 6 (92.1 °C and 89.9 °C respectively) compared with that of the $n = 5$ member (73.0 °C). This presumably indicates a very substantial odd-even-*n* alternation in the points for these transition temperatures. The onset of the crystal K phase is characterised by the appearance of very distinct 'candy striping' which is particularly pronounced in the large mosaic regions (a similar texture is shown in **Plate I**, ***Appendix 1***). However, the presence of the K phase could not be confirmed for the $n = 7$ homologue as when the crystal J phase of this compound is cooled further, crystallisation occurs before the 'candy striping' of the smectic crystal K phase is observed.

On cooling the S_C phase of the homologues $n = 9$ and 10, an S_B phase is obtained (**Plate J**, ***Appendix 1***). The backs of the focal conic fans reveal striations at the S_C-S_B transition temperature and the *schlieren* regions of the S_C phase become homeotropic in the S_B phase.

5.6 *The 4′-n-decylbiphenyl-4-yl 4-n-alkylbenzoates*

The transition temperatures of the 4′-n-alkylbiphenyl-4-yl 4-n-alkylbenzoates **(17)**, m = 10, n = 1-10, together with the associated DSC results, are listed in **Table 17**. A graphical representation of the transition temperatures plotted against n, the number of carbon atoms in the alkyl group of the benzoate moiety, is given in **Plot 17**. The DSC data are discussed in section **5.7**.

5.6.1 *Thermal optical microscopy*

The liquid crystal behaviour of this homologous series is closely similar to that of the analogous 4′-n-heptylbiphenyl-4-yl 4-n-alkylbenzoates discussed in section **5.5**, and the transition temperature plot (**Plot 17**) reveals only minor differences.

An enantiotropic nematic mesophase is observed on cooling the isotropic liquid for all ten members of the series, the points for the transition temperatures lying on two falling curves with the odd-n members uppermost. The curves converge at longer chain lengths.

The different smectic behaviour of the higher and lower homologues is again evident in this series. The occurrence of smectic polymorphism begins at an earlier stage than in the analogous heptyl series. Subsequently, the smectic behaviour of individual members of the series is virtually identical to that reported for the corresponding heptyl derivatives, except that the S_I and crystal J and crystal K phases have greater thermal stability, which is reflected in the earlier occurrence of these phases in this series, at the n = 4 homologue. The smectic crystal J phase is shown as a hatched region in **Plot 17** for the purpose of clarity.

As with the corresponding members of the heptyl series, on cooling the S_C phase of the homologues $n = 9$ and 10 an S_B phase is formed, characterised by the appearance of transient striations in the focal conic areas of the S_C texture at the temperature of transition. In addition, in this series further cooling of the $n = 9$ homologue gives rise to a smectic crystal H phase, the optical texture of which is characterised by the appearance of cross-hatched striations in the focal conic fans and the formation of a faint grey mosaic texture in the homeotropic region of the previous S_B phase. Optically, a corresponding smectic crystal H phase cannot be detected in the $n = 10$ homologue, although there is some evidence for its existence from the DSC trace which is discussed in section **5.7**. However, as the smectic crystal H phase could not be confirmed optically, a point indicating the presence of a crystal H phase has not been included on the transition temperature plot, **Plot 17**, for the $n = 10$ homologue.

5.7 *DSC studies*

The thermal optical microscopy studies indicate that the liquid crystalline behaviour of all four homologous series is very similar and the DSC data also clearly reflect this fact. For this reason it is not appropriate to give a comprehensive, but repetitive, account of DSC studies of each homologous series. Hence, the cooling cycles of three homologues from different series have been chosen, each one being representative of a different region of smectic behaviour on the transition temperature plots. The DSC traces referred to below are reproduced in ***Appendix 2***.

The trace **DSC 10** shows the cooling cycle for 4′-n-heptylbiphenyl-4-yl 4-n-propylbenzoate **(17)**, $m = 7$, $n = 3$. This trace is representative of the first of the three distinct areas of smectic behaviour shown by the four series of 4′-n-alkylbiphenyl-4-yl 4-n-alkylbenzoates **(17)**. On cooling the nematic phase of this compound **(17)**, $m = 7$, $n = 3$, only a smectic crystal G phase is observed before the onset of crystallisation. The associated enthalpies of transition for this homologue have been calculated as I-N, 1.04 kJ mol^{-1}; N-G, 6.76 kJ mol^{-1}; and G-C, 8.43 kJ mol^{-1}, and are consistent with values obtained for these transitions for other members of these homologous series.

The trace **DSC 11** shows the cooling cycle for one member, the 4′-n-decylbiphenyl-4-yl 4-n-hexylbenzoate **(17)**, $m = 10$, $n = 6$, taken from the region of greatest smectic polymorphism. The trace shows well defined peaks associated with the I-N (1.41 kJ mol^{-1}), N-S_C (1.46 kJ mol^{-1}) and S_C-S_I (3.16 kJ mol^{-1}) transitions, as well as providing an indication of the S_I-J and J-K phase transitions, although the associated peaks for these mesophase changes were too small for the enthalpies to be calculated accurately. The calculated values are representative of those for other homologues in these series and support the original phase assignments made by thermal optical microscopy, showing a good correspondence with the expected enthalpies for these phase transitions.

DSC 12 shows the cooling cycle for 4′-n-decylbiphenyl-4-yl 4-n-decylbenzoate **(17)**, $m = 10$, $n = 10$, which is representative of the third area of smectic behaviour observed for 4′-n-alkylbiphenyl-4-yl 4-n-alkylbenzoates **(17)**. The I-N and N-S_C transitions cannot be accurately resolved and therefore the enthalpy associated with these transitions could not be calculated. However, the S_C-S_B transition can be clearly seen and the calculated enthalpy for this transition is 3.59 kJ mol^{-1}.

The trace **DSC 12** also indicates another, much smaller transition at a lower temperature than that of the S_C-S_B transition, but before the sharp peak associated with the onset of crystallisation. When compared with **DSC 13**, the cooling trace for the previous homologue, 4′-n-decylbiphenyl-4-yl 4-n-nonylbenzoate **(17)**, m = 10, n = 9, a similar peak is also observed. However in this case, this smaller peak is associated with the S_B-H transition observed for this homologue. Although there is no supporting optical evidence to suggest that the n = 10 homologue also gives rise to a smectic crystal H phase on cooling the S_B phase, the DSC trace may well indicate that this does in fact occur. However, due to the lack of optical evidence, the formation of a crystal H phase is unconfirmed for the decyl derivative **(17)**, n = 10, m = 10.

5.8 *Comparison of the liquid crystal behaviour of the 4′-n-decylbiphenyl-4-yl 4-n-alkylbenzoates* (17) *and the corresponding 4′-n-decylbiphenyl-4-yl 5-n-alkylthiophene-2-carboxylates* (20)

The liquid crystal behaviour of the four homologous series of 4′-n-alkylbiphenyl-4-yl 4-n-alkylbenzoates **(17)** and that of their counterparts, the 4′-n-alkylbiphenyl-4-yl 5-n-alkylthiophene-2-carboxylates **(20)**, reported by Byron and Wilson *et al.*[43] is broadly very similar.

Direct correspondence between the two sets of homologous systems is possible through the respective 4′-n-decylbiphenyl-4-yl derivatives, m = 10, and the following discussion is restricted to a brief comparison of these two homologous series.

For the 4′-n-decylbiphenyl-4-yl 5-n-alkylthiophene-2-carboxylates **(20)**, m = 10, the mesophase transition temperatures are listed in **Table 18**. The corresponding transition temperature plot (reproduced from the paper by Byron and Wilson[43]) is given in **Plot 18**, together with that for the 4′-n-decylbiphenyl-4-yl 4-n-alkylbenzoates **(17)**, m = 10, for comparison.

It is clear from a cursory examination that the two plots show substantial similarities, although the benzoates have the higher nematic and smectic (S_C) thermal stability. Thus for the members, m = 10, n = 7-10 inclusive, the average nematic (143.4 °C) and smectic (S_C, 133.1 °C) mesophase thermal stability of the 4′-n-alkyl-benzoates **(17)** is greater by 36.7 °C and 30.4 °C, respectively, than the corresponding values for the average nematic (106.6 °C, assuming T_{N-I} to be the same as T_{Sc-I} for n = 10) and smectic (S_C, 102.7 °C) mesophase thermal stability of the 5-n-alkylthiophene-2-carboxylates **(20)**.

Table 18 - *Reported mesophase transition temperatures for the 4'-n-decylbiphenyl-4-yl 4'-n-alkylthiophene-2-carboxylates* (20).

n	C-N	N-I	S_C-I	S_C-N	S_I-N	G-N	S_I-S_C	S_F-S_I	J-S_F	K-J	N-C
1	102.6†	120.1									70.2
											G-C
2	72.0	109.7				(66.4)					40.0
3	83.0	110.8				(74.1)					72.2
	C-K										K-C
4	70.0	103.7			82.7			81.5	80.5	79.5	35.0
5	73.2	106.7		87.7			86.3	84.3	82.5	79.5	35.0
6	67.4	103.8		92.8			88.0	85.0	80.9	79.0	45.5
	C-J										
7	76.8	106.7		97.0			86.5	83.4	78.1	(75.6)	50.4
	C-S_F										
8	75.8	107.0		102.5			86.7	83.9	(74.0)	(66.1)	47.5
9	79.5	106.3		104.6			83.0	80.6	(67.9)	(55.1)	52.0
											J-C
10	77.0		106.5				81.9	79.9	(59.4)		45.0

( ) denotes a monotropic transition; † transition temperatures listed were determined by thermal optical microscopy, the reported values being obtained on heating (except crystallisation values). Values reproduced by kind permission of Authors.[45]

Plot 17 - *Representation of transition temperatures for the 4'-n-decylbiphenyl-4-yl 4'-n-alkylbenzoates*

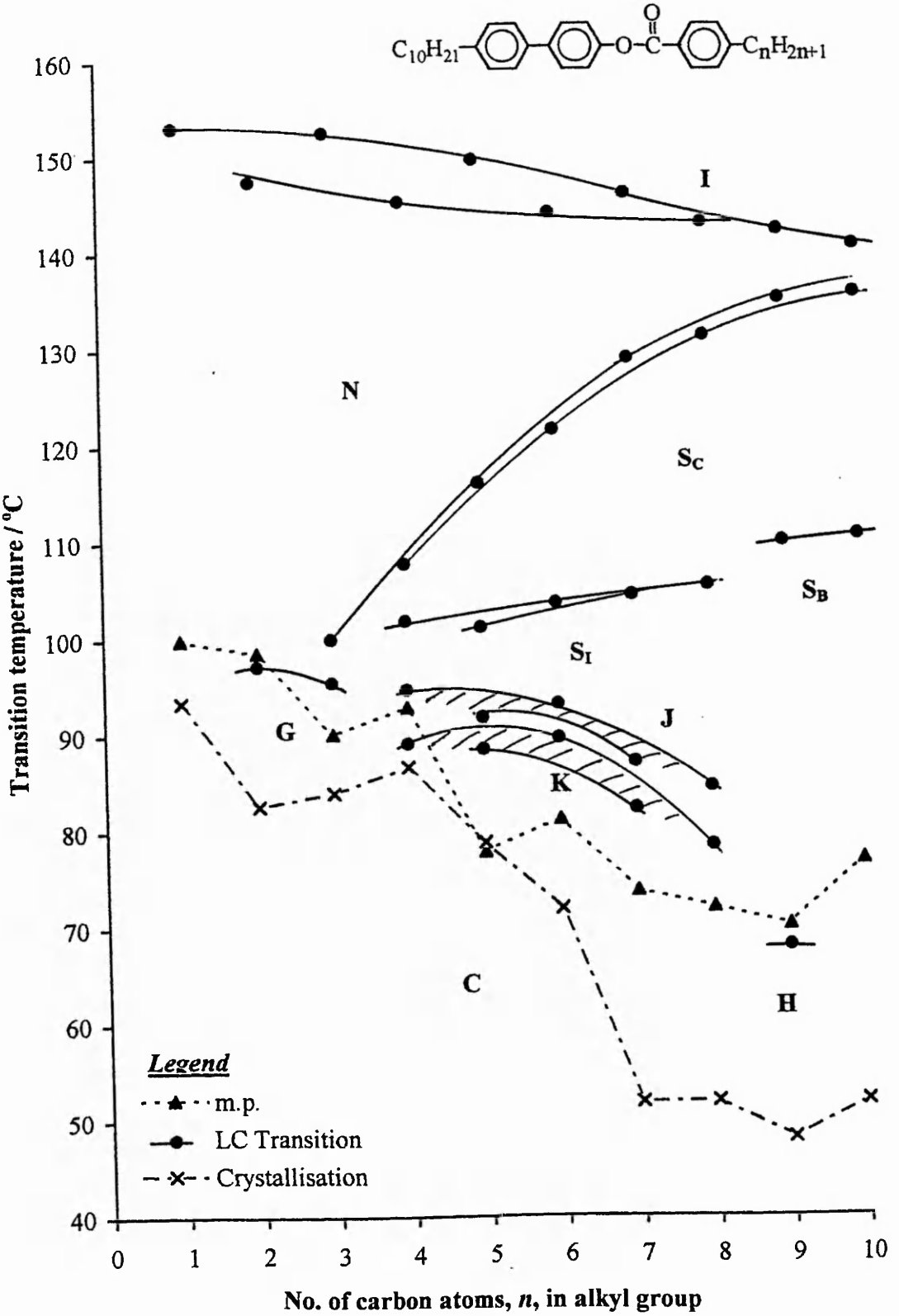

Plot 18 - ***Representation of transition temperatures for the 4'-n-decylbiphenyl-4-yl 5-n-alkylthiophene-2-carboxylates***

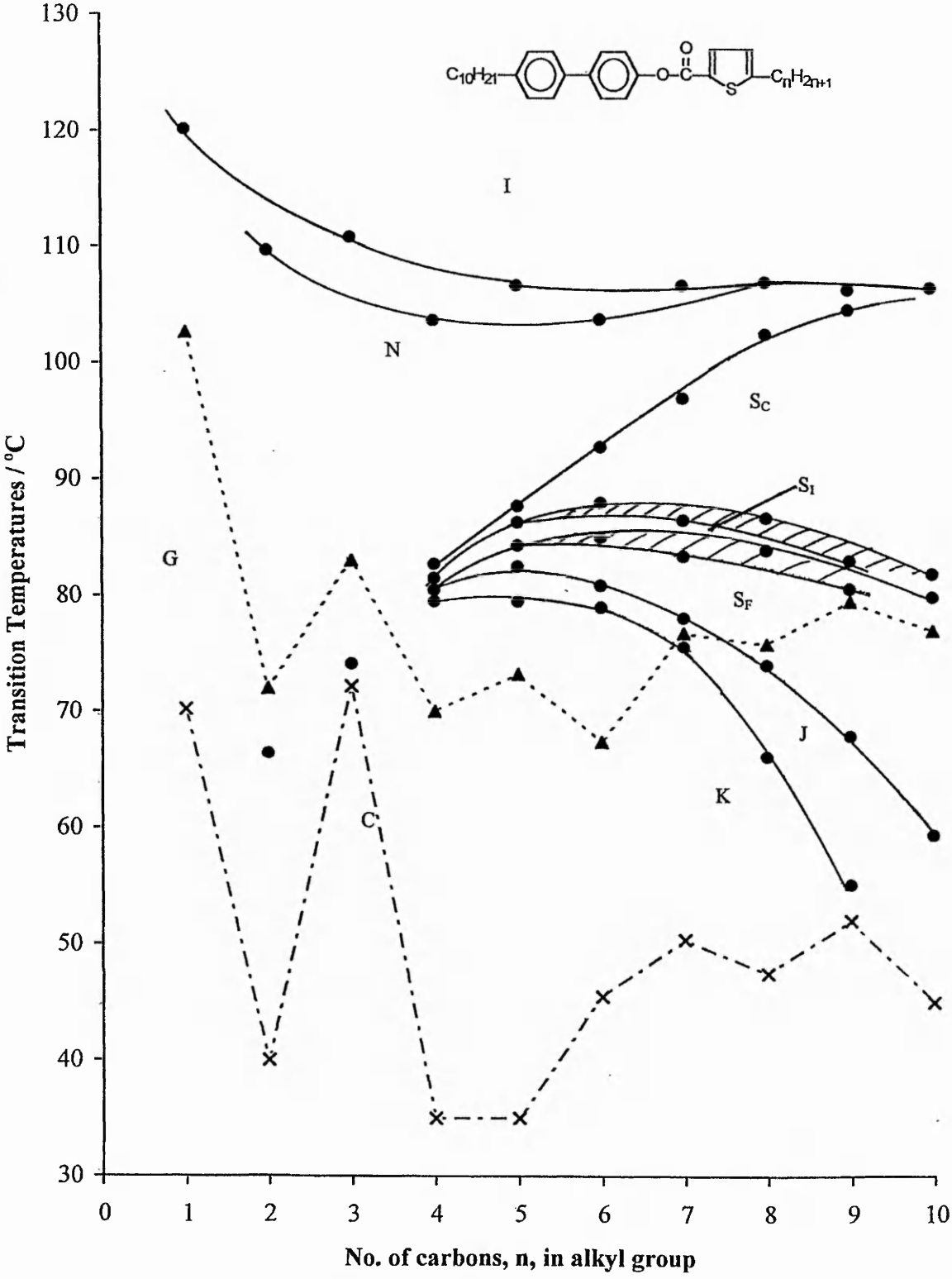

Some differences in the liquid crystal behaviour of the homologous series are apparent and these are detailed below:

(1) For the benzoates **(17)**, $m = 10$, the points for the N-I transition temperatures lie on a shallow, falling curve as n increases, whereas for the corresponding thiophene-2-carboxylates **(20)**, $m = 10$, there is an initial fall followed by a rise as n increases.

(2) The smectic behaviour of the two series **(17)** and **(20)**, $m = 10$, comprises distinctly different sections. However, the thiophene-2-carboxylates **(20)** show a sharper separation of smectic behaviour between the earlier and later members of the series (at the $n = 4$ homologue) than the analogous benzoates **(17)**, in which the initial point of the N-S_C transition temperature curve (at the $n = 3$ homologue) is seen to 'bridge' the two distinct regions of smectic character.

For the thiophene-2-carboxylates **(20)** it is clear that despite the single line drawn through the points for the N-S_C transition temperatures, an indication of an odd-even-n alternation with two curves would have been more appropriate, as with the corresponding benzoates **(17)**.

(3) The N-G transition temperatures fall from $n = 2$ to $n = 3$ in the benzoates **(17)**, $m = 10$, but rise in the corresponding thiophene-2-carboxylates **(20)**.

(4) For the thiophene-2-carboxylates **(20)**, $m = 10$, the S_C-S_I transition temperatures, which are continuous between $n = 4$ and $n = 10$, initially lie on a shallow rising curve which then falls as n increases. For the benzoates **(17)**, $m = 10$, the S_C-S_I curve rises throughout between $n = 4$ and $n = 8$, but is then replaced by S_C-S_B transitions for the $n = 9$ and $n = 10$ members of the series.

(5) For the thiophene-2-carboxylates **(20)**, $m = 10$, on cooling the S_I phase, firstly an S_F then smectic crystal J and K phases occur between $n = 4$ and $n = 10$, the points lying on curves which show a decrease in temperature as n increases. The S_I-S_F-J phase sequence is highly unusual and indicates that with regard to the crystal structure, the directional alignment of the molecules within the hexagonal net *flip* from pointing to the apex, to the side, and then back to the apex as the phase pattern is traversed. An S_F phase is only observed in the benzoate series **(17)** for $m = 6$, $n = 6$ (and possibly for $m = 7$, $n = 6$).

For the benzoates **(17)**, $m = 10$, an S_F phase is not observed and on cooling the S_I phase, smectic crystal J and then K phases are formed directly. These only occur between the members $n = 4$ and $n = 8$ of the series because of the incursion of the S_B phase for the members $n = 9$ and 10, and in this region the $n = 9$ homologue also gives rise to a smectic crystal H phase.

(6) The behaviour of the thiophene-2-carboxylates **(20)**, $m = 8$, more closely resembles that of the benzoates **(17)**, $m = 10$, in that on cooling the S_I phase, this series also fails to give rise to an S_F phase, leading to the direct formation the smectic crystal J and then K phases only.

6. *An introduction to metallomesogens*

6. *An introduction to metallomesogens*

6.1 *A brief history of metallomesogens*

The last two decades have seen the emergence of a new field within liquid crystals, with the development of mesogenic systems which incorporate metal atoms within their structure. Known as ***metallomesogens***, these compounds are providing a new area of research in which examples of both thermotropic calamitic and thermotropic discotic liquid crystals have been reported.

The first thermotropic liquid crystal containing a metal atom was reported by Vorländer[6] in 1910. He noticed that alkali metal carboxylates of the type $R(CH_2)_nCOONa$ formed classical lamella phases that were characteristic of soaps. In 1923 it was also found that the dimercurials[49] **(21)** formed smectic mesophases.

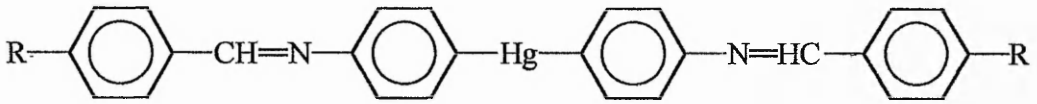

(21)

The following decades showed only a minor interest in the field of metal containing systems until the work of Giroud-Godquin and Müller-Westerhoff[50,51,52] in 1977. They described more advanced systems based on the mesogenic behaviour of some nickel and platinum dithiolenes **(22)**. Both nickel and platinum derivatives displayed nematic and S_A phases.

Many different ligands give rise to metallomesogenic compounds, without necessarily being mesogenic themselves and examples of complexed mono-, bi-, or poly-dentate ligands have all been shown to display liquid crystal character.

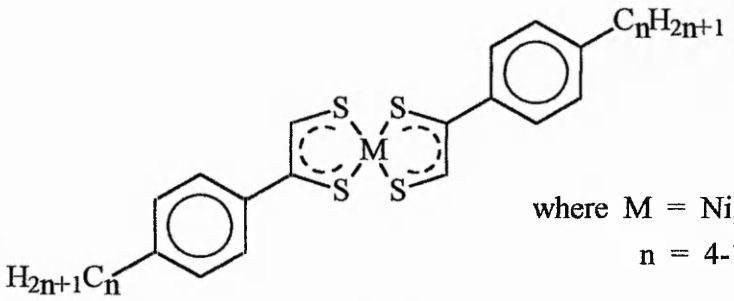

(22)

The following section does not intend to provide a comprehensive review of this rapidly growing area, but rather a brief overview of some of the properties which the incorporation of a metal atom can introduce, along with some of the considerations necessary to design a liquid crystalline system of this type. Detailed reviews on metallomesogens can be found in current literature.[40,41,42]

6.2 *Reasons for the inclusion of a metal atom*

Metallomesogens have the potential to be extremely useful for applications within the display screen industry as the inclusion of a metal centre into a liquid crystal system has major influences upon the physical properties of the molecule.[53]

Metal atoms possess high electron density which may be readily polarised with the rest of the molecule. Important physical properties such as the dielectric constant and the birefringence of a molecule are greatly influenced by polarisability, which may also govern to some degree the thermal stability of a liquid crystal phase.

Although compounds have been prepared utilising alkali metals, the systems that are of the greatest interest are those incorporating transition metals which possess partially filled d-orbitals. These unfilled orbitals provide an opportunity to introduce different physical properties within a mesogenic system that could not be obtained for a purely organic system.

Metal atoms, especially transition metals, also display some unusual magnetic properties. The possibility of producing a ferromagnetic rather than a ferroelectric display is currently being investigated.[54] However, although several liquid crystal systems containing paramagnetic compounds, e.g. copper salicylaldimine complexes **(23)** have been prepared, these show little promise for use within switching devices.

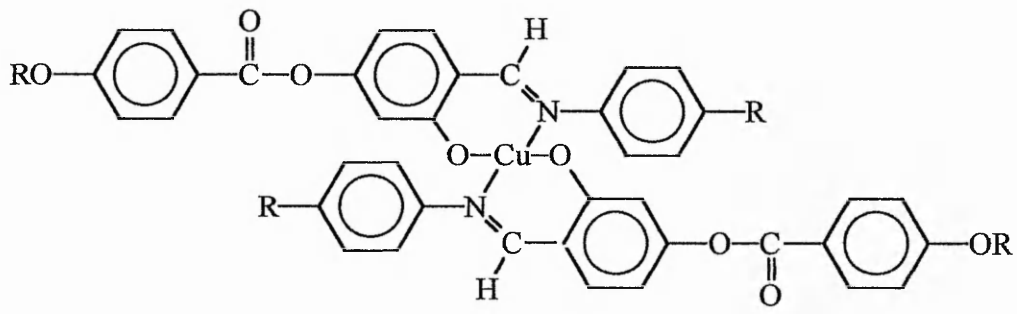

(23)

Another obvious benefit of the inclusion of a metal centre into a liquid crystal is the introduction of colour. Until now, full-colour display screens have been produced by the use of filters with colourless materials. The introduction of d- and f-block transition metals into organic systems should provide coloured mesogenic systems due to their ability to form high oxidation states. It is hoped that the inclusion of such compounds within a display system would lead to the production of a full-colour display without the need for colour filters.

6.3 Structure and metallomesogens

In organic systems, mesophase formation is dependent upon the intermediate forces within the molecule. A similar behaviour can be observed within metallomesogens as it is the structure and co-ordination of the ligand which determines the type of mesophase. Much of the space around the metal is occupied by the ligand(s), and hence the properties of the molecule are dictated by the ligand type and their arrangement in space, i.e. by the overall shape of the molecule. For example, long monodentate ligands **(24)** generally give rise to rod-like nematics and smectics, whereas flat, disc-like polydentate ligands **(25)** generally produce discotic mesophases.

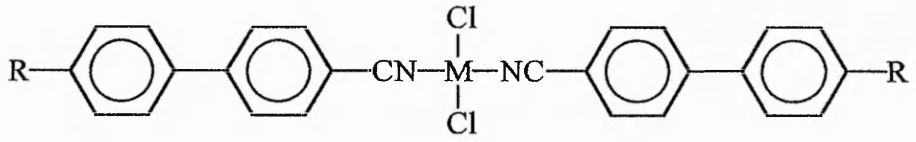

(24)

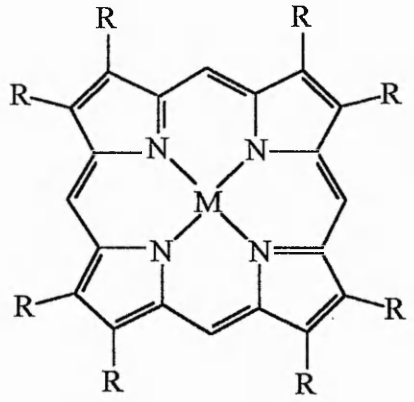

(25)

However, the general molecular structural criteria for liquid crystalline behaviour still need to be met, i.e. a rigid core and long hydrocarbon chains. The metal atom incorporated within these systems is usually found at, or near, the centre of gravity of the molecule.

Metallomesogens have the advantage of providing geometries which are not readily obtained by purely organic molecules, i.e. they can adopt square planar, e.g. **(22)**, square pyramidal, octahedral, *etc.* geometries.

6.4 *Calamitic metal containing liquid crystals*

The design of calamitic metallomesogens needs careful forethought as certain geometries created by the inclusion of a metal atom may cause a deviation or loss of the elongated lath-like shape required for liquid crystalline behaviour in compounds of this type.

This design approach can be seen in the work of Giroud-Godquin and Müller-Westerhoff,[50] who proposed that the dithiolene compound **(22)** would exhibit liquid crystalline behaviour as it appeared structurally analogous to some mesomorphic terphenyl compounds **(26)**. They postulated that the two M-S-C-C-S rings would behave as a phenyl moiety and although this hypothesis proved incorrect, the basic shape of the molecule was preserved and the compounds were indeed mesomorphic.

Most of the known calamitic liquid crystals to date have three things in common which should be considered when undertaking the synthesis of new compounds:

(a) they contain a metal atom in a d^8-d^{10} configuration

(b) they contain a mesogenic ligand (the ligand itself does not necessarily have to display liquid crystal properties, but on complexation it must be expected to exhibit mesomorphic behaviour).

(c) the ligands are effectively *trans* disposed about the metal atom.

(26)

One of the most recent areas of investigation into calamitic metallomesogens is that of ferrocene based liquid crystals. Ferrocene, with its high reactivity and extensively researched chemistry, is an ideal building block for true organometallic rather than co-ordination compounds. The following section, **(6.5)**, details some of the most recent work in the field of ferrocene liquid crystals, an area which has recently been extensively reviewed by Deschenaux and Goodby.[55]

.

6.5 *Ferrocene containing liquid crystals*

Ferrocene or *bis*(η^5-cyclopentadienyl)iron was first discovered in 1951.[56,57] It is an orange crystalline solid which is soluble in many organic solvents but not in water. On heating, ferrocene will undergo sublimation, which can be used to purify crude samples.

Ferrocene exhibits a sandwich type structure in which two cyclopentadienyl rings lie parallel to one another with an iron atom buried within the electron cloud between them. There are two possible conformations for the rings to adopt (**Fig.28**):

(a) prismatic (b) anti-prismatic

Fig.28 - Possible conformations for ferrocene

It was originally thought that the crystalline form of ferrocene exhibited the staggered anti-prismatic form, with the carbon atoms of one ring between those of the other. In solution however, the rings are free to rotate unless tied by a hydrocarbon bridge, and hence, the stereochemistry of ferrocene in the solid state is determined largely by crystal lattice forces. However, more recent studies[58] show that at temperatures below 164 K, ferrocene exhibits the eclipsed or prismatic form. Above this temperature, rotation of the cyclopentadienyl rings leads to a disordered crystal state, giving the appearance that an anti-prismatic form is more favoured.

Due to its sandwich type structure, most common ferrocene derivatives may either be mono- or di-substituted. Di-substitution may be homoannular (both substituents on one ring), denoted by the prefix 1,3- or 1,2-, or heteroannular (substituents on different rings) denoted by the prefix 1,1′-. These substitution patterns are shown below (**Fig.29**).

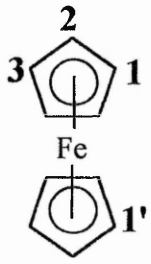

Fig.29 - Substitution patterns of ferrocene

6.5.1 *Monosubstituted ferrocene derivatives*

The first reported synthesis of a liquid crystal containing ferrocene was by Malthete and Billard[59] in 1976 who prepared a series of substituted N-(*p*-benzoyloxybenzylidene)anilines **(27)**. The ferrocene unit had been incorporated to facilitate studies in a mesomormorphic system utilising a Mössbauer marker. The compounds synthesised showed enantiotropic nematic phases.

(27)

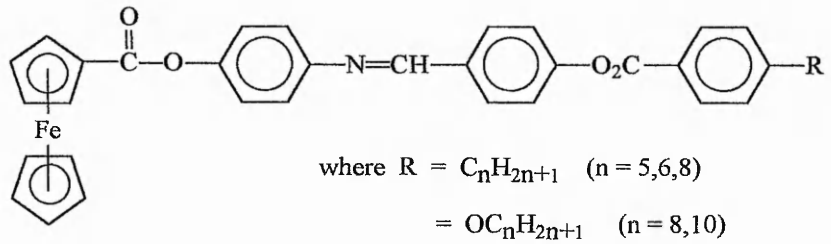

where R = C_nH_{2n+1} (n = 5,6,8)

= OC_nH_{2n+1} (n = 8,10)

(28)

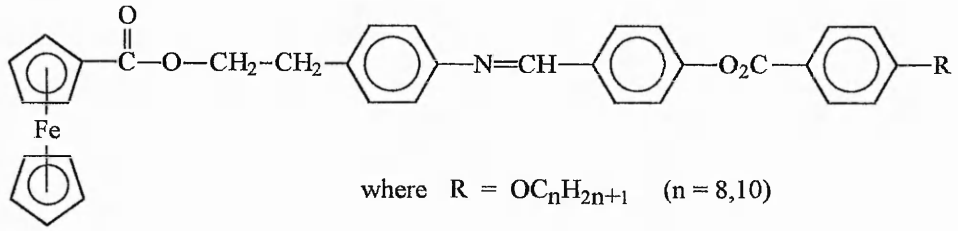

where R = OC_nH_{2n+1} (n = 8,10)

When a -CH_2CH_2- spacer was introduced between the ferrocenyl moiety and the rigid organic core the resulting compounds **(28)** gave rise only to monotropic nematic phases. These monosubstituted ferrocene derivatives are the first well documented organotransitionmetal- metallomesogens.

In 1992 Galyametdinov[60,61] reported the synthesis of the ferrocenyl derivative **(29)**, which in turn was complexed with a Cu(II) species to produce the compound **(30)**. Compound **(29)** gave rise to an enantiotropic nematic phase between 140 and 184 °C, whereas the complexed species **(30)**, although also displaying a nematic phase, showed increased melting and clearing points (C · 221 · N · 230 · I) over a depressed temperature range (only 9 °C).

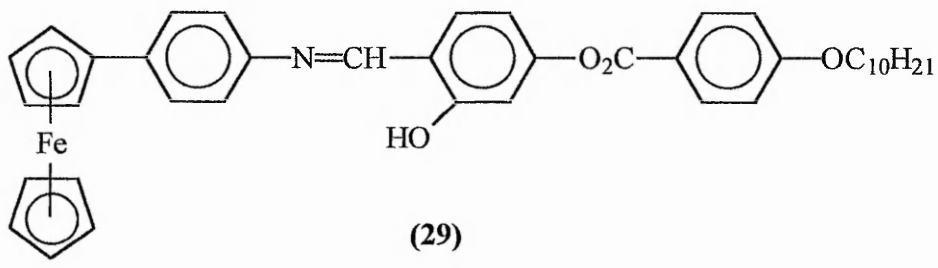

(29)

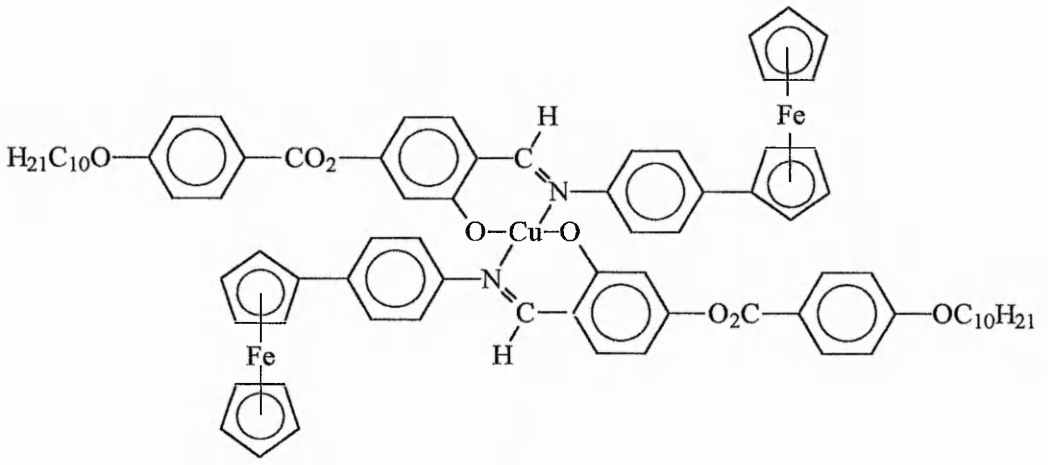

(30)

Nakamura, Hawasaki and co-workers have also prepared some interesting ferrocene mesogens. Their first publications detailed the preparation and liquid crystalline properties of ferrocene derivatives of cholesterol,[62,63] while later publications dealt with the mono-substituted derivatives **(31)**[64] and the 1,1′-disubstituted derivatives **(32)**.[65] An unidentified liquid crystal phase was reported in both cases.

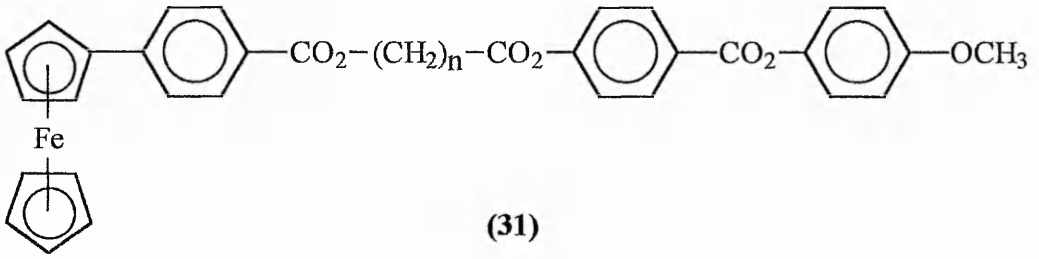

(31)

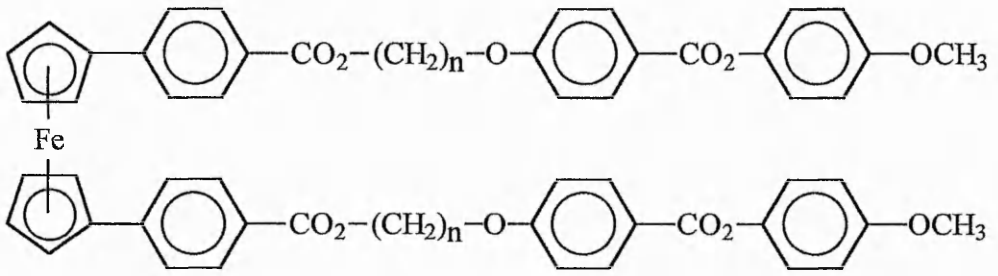

(32)

6.5.2 *Disubstituted derivatives of ferrocene-1,1'- and -1,3-dicarboxylic acid*

The first disubstituted ferrocene liquid crystals were reported in 1988 by Bhatt *et al.*,[66] who published work on a series of *bis*-(4'-n-alkoxybiphenyl-4-yl) ferrocene-1,1'-dicarboxylates **(33)**.

Three members of the homologous series gave rise to monotropic smectic phases (n = 5, 6, 11). The corresponding benzoates (n = 5, 6) also give rise to (enantiotropic) smectic phases over a similar temperature range (8-10 °C). A single analogous ferrocenemonocarboxylate (n = 6) was also synthesised but was not mesomorphic.

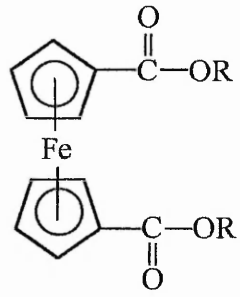

(33) R = 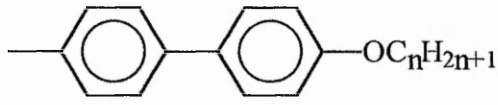

where n = 4-11

(34) R = 

where n = 3,4,6,8,10

There is some conjecture about whether the 1,1'-disubstituted compounds occupy an *S* (elongated or *trans*) or *U* (bent or *cis*) conformation. X-Ray work[67] upon the liquid crystal phases of the n = 5 derivative of the compound **(33)**, indicates that this compound

adopts the *S* geometry in both the crystalline and mesomorphic states. This arrangement provides the best theoretical packing array for the molecules. For ease of representation however, most compounds are shown in their *U* forms.

Bhatt *et al.*[68] followed up this work in 1991 with the preparation of esters derived from ferrocene-1,1′-dicarboxylic acid and 4′-cyanobiphenyl-4-yloxyalkanols **(34)**. Of the synthesised compounds the n = 3 , 4 and 8 homologues showed ordinary melting behaviour, but the n = 6 compound was reported as being "polymorphic with one portion melting at 30-32 °C and another portion melting at 98-100 °C". It is possible that the authors confused polymorphism with an unusual optical texture of a mesophase, or that the compound was simply impure. For n = 10 a similar two fraction system existed, with the second fraction exhibiting a smectic phase between 85-88 °C.

It was suggested that, although one compound displayed liquid crystalline properties, the ferrocene moiety appeared to destabilise the system. The authors pointed out that the first reported ferrocene mesogens had the ferrocene moiety at the end rather, than in the middle of the compound, and suggested that the length to width ratio of a ferrocene liquid crystal may need to be greatly increased to overcome the adversely affected symmetry and packing of the molecules.

1991 also saw some novel ferrocene liquid crystals, **(35)** and **(36)**, prepared by Singh *et al.*[69] The n = 7 homologue of compound **(35)** appeared to display a monotropic smectic phase, however, even with miscibility studies this phase could not be identified. X-Ray diffraction studies of this compound also produced results not typical of normal smectic materials. The n = 10 member of this series gave rise to a nematic phase on heating, but no phases were reported on cooling. In contrast compound **(36)** exhibited a nematic type phase between 107-128 °C that was only seen to reform on cooling after

standing 24hr. Singh and co-workers stated from this work that the ferrocene core could be an effective mesogenic component.

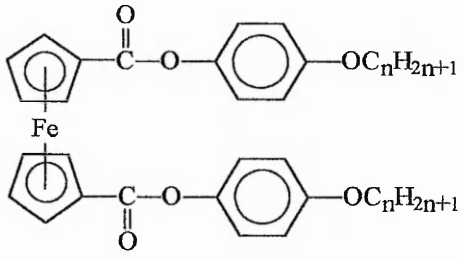

(35)

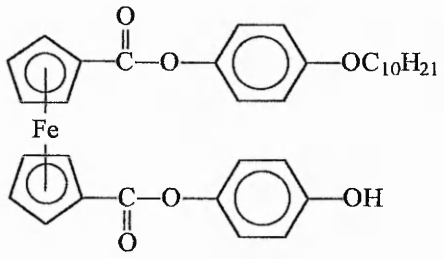

(36)

Deschenaux and Marendaz[70] also published work in this area with the synthesis of some novel 1,1′- **(37)** and 1,3-disubstituted **(38)** derivatives. Studies showed that all of the 1,3-disubstituted compounds exhibited wide nematic phases (for $n = 6$ the phase was stable over 64°C) which were enantiotropic. Conversely only one of the 1,1′-disubstituted compounds ($n = 6$) gave rise to any liquid crystalline properties with a monotropic nematic phase being observed on cooling. It was suggested that the other compounds of this type may also display nematic phases with controlled supercooling.

Deschenaux *et al.*[71] later reported an extended synthesis of the 1,3-diesters of type **(38)** for lengths n = 1-14, 16 and 18. These compounds displayed nematic phases and the higher order derivatives (n = 13, 14, 16, 18) also displayed a S_C phase.

In 1992 Reddy and Brown[72] synthesised a mesomorphic series of di-Schiff bases **(39)** derived from 4-n-alkoxyanilines and *bis*(4-n-formylphenyl) ferrocene-1,1′-dicarboxylate. The Schiff base derivatives with the shorter chain lengths (n = 4-7) exhibited predominantly monotropic nematic phases, whilst the compounds with longer chain lengths (n = 8-12) gave rise to an S_A phase (which was enantiotropic only for the n = 8 and 9 members).

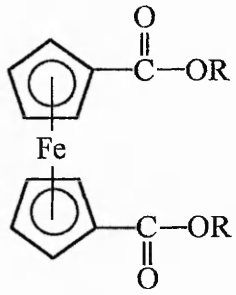

(37)

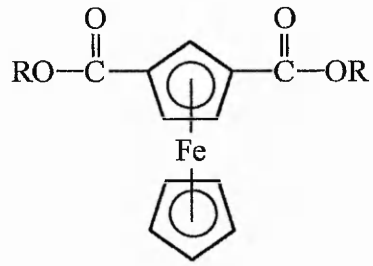

(38)

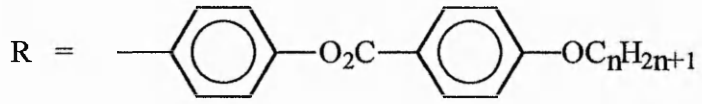

where n = 6,7,8

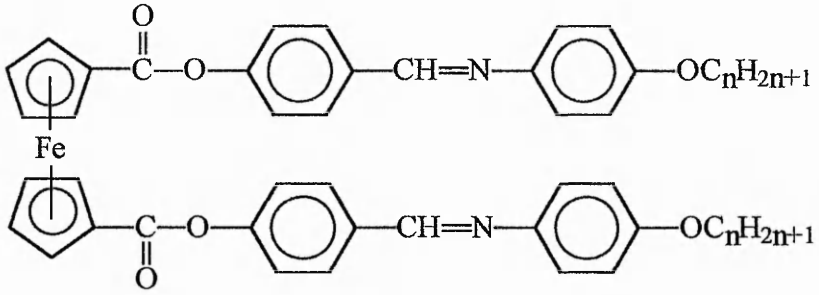

where n = 4-12

(39)

In 1993 came the publication of a major study on ferrocene liquid crystal systems by Thompson, Goodby and Toyne[73]. They reported the synthesis of many ferrocene-containing compounds of which only four unsymmetrical 1,1′-disubstituted derivatives gave rise to mesogenic behaviour, all showing nematic phases. These structures had short alkyl chains bonded to one cyclopentadienyl ring, whilst the other cyclopentadienyl ring was substituted with a long linear molecule, typical of a liquid crystalline core. When

compared with the analogous benzyl- and cyclohexyl- derivatives, it was clear that the ferrocene moiety depressed liquid crystalline behaviour due to its non-linear shape resulting in non-uniform packing.

In the same year Deschenaux *et al.*[74] reported the synthesis of some other unsymmetrically 1,1′-disubstituted ferrocene **(40)** liquid crystals of the following type:-

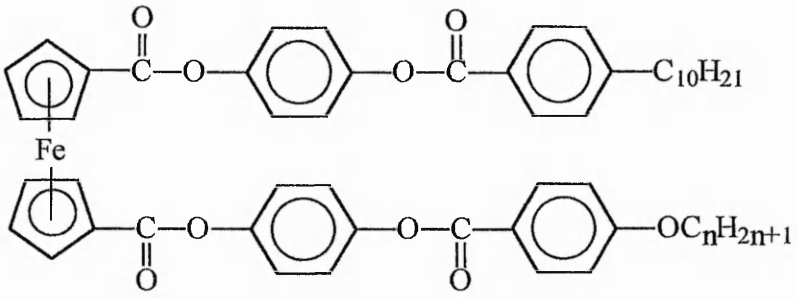

where n = 11-16

(40)

The unsymmetrical nature of these compounds had two effects on the thermal properties. Compared to the symmetrically substituted compounds there was a depression in the melting point and secondly for the first time both S_A and S_C phases were present in certain compounds of the same series.

Later in the same year Deschenaux *et al.*[75] reported the synthesis and mesomorphic properties of 1,1′-disubstituted derivatives of type **(41)** and **(42)**. This work concentrated on the effect on mesomorphic behaviour caused by the orientation of an ester moiety at the centre of the organic ligand. None of the ferrocenes of type **(41)** showed any mesomorphic behaviour on heating. On cooling however, members n = 1-6 gave rise to a monotropic nematic phase. For the rest of the series it was suggested that the nematic phase would be observed if sufficient supercooling could be achieved. Compounds of type **(42)** showed a greater variety of mesophase. Lower members

(n = 2-4) only displayed monotropic nematic phases. Later homologues displayed S_A phases. In all cases the melting points of compounds of type **(42)** were lower than the corresponding homologues of type **(41)**. The reported results indicate that the orientation of the central linking ester function is crucial to mesomorphic behaviour; this topic is discussed in more detail in section **7.3**.

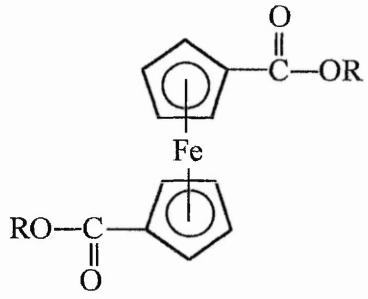

where R = 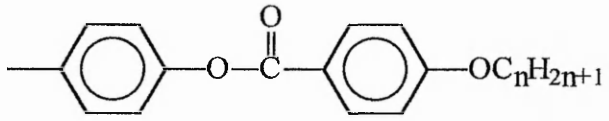

(41)

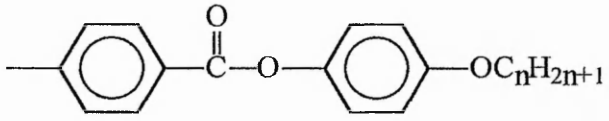

(42)

6.5.3 *Other mesomorphic 1,1'-disubstituted ferrocene derivatives*

There are only two reported mesomorphic 1,1′-disubstituted ferrocene derivatives that do not contain an ester linkage connected directly to the ferrocene moiety: Firstly there are the ferrocene analogues of the 4-n-alkoxy-4′-cyanobiphenyls **(43)** reported by Bhatt and co-workers,[76] which are similar to the compounds **(34)** they studied earlier. In these later compounds **(43)**, the 4′-cyanobiphenyl moiety is joined directly to the

cyclopentadienyl rings by a -$(CH_2)_n$-O- spacer. The removal of the ester linkage greatly improved the liquid crystalline properties and gave much lower transition temperatures: S_C phases, and in one case ($n = 8$), a monotropic S_A phase, were reported.

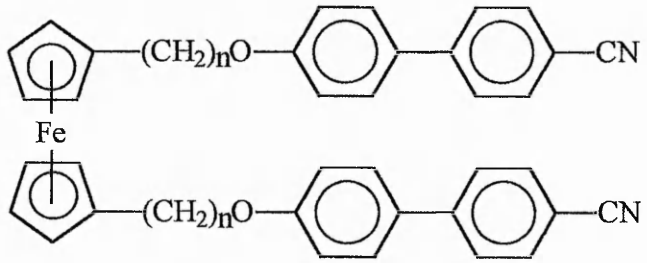

(43)

The compounds **(44)** reported by Polishuck and co-workers[77] in 1992 contain ester linkages which are not directly attached to the 1,1′-positions of ferrocene. Two of the homologues, $n = 3$ and 8, are quoted as showing a nematic phase, but the former homologue decomposes rapidly.

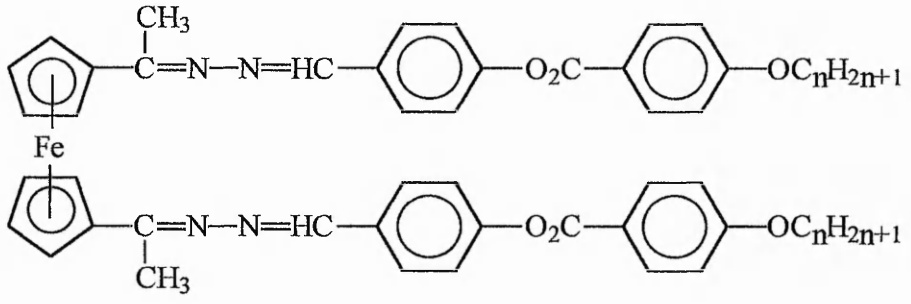

(44)

The $n = 3$ homologue is also reported as having a *cis* (or *U*) conformation, which is the alternative geometry to the *trans* or *S* conformation displayed by the *bis*-(4′-n-alkoxybiphenyl-4-yl) ferrocene-1,1′-dicarboxylates **(33)** of Bhatt *et al.*[67]

6.5.4 *Summary*

From the literature it can be seen that although the ferrocene core has a non-linear shape it can still form part of a liquid crystalline compound as long as appropriate steps are taken to control the geometry and polarisability of the overall structure. The majority of compounds prepared to date have taken some standard liquid crystalline compounds and linked them to the ferrocene moiety by an ester linkage. On the whole, the transition temperatures of these compounds are high (100-200 °C) and they show a limited range of phase types (N, S_A and S_C), generally only one phase being present for each compound. The thermal stability of these phases can be seen to be greatly reduced by the inclusion of the ferrocene moiety when compared to a phenyl system. Further work carried out on the development of ferrocene compounds without the standard ester linkage would prove interesting to see if these problems could be overcome.

7. *Experimental II - ferrocene derivatives*

7. *Experimental II - ferrocene derivatives*

This section details the synthetic methods undertaken in the preparation of some novel ferrocene compounds which it was hoped would show some mesomorphic character. ***Scheme 3*** details methods of preparation of some useful ferrocene derivatives, most notably ferrocene-1,1′-dicarboxaldehyde **(51)** which was subsequently reacted to provide the novel compounds **(67)** and **(70)** shown respectively in ***Schemes 6a*** and ***6b***. ***Scheme 4*** details methods of preparation of some 4′-*n*-alkylbiphenyl-4-carbonyl chlorides **(57)**, which were reacted with 1,1′-*bis*(hydroxymethyl)ferrocene **(50)** to provide the novel esters **(58)** and **(59)**, whilst ***Scheme 5*** shows the direct acylation of ferrocene with **(57)** to provide the ketones **(60)** and **(61)**. ***Schemes 7*** and ***8*** show the preparative routes to two compounds derived from ferrocene-1,1′-dicarboxylic acid **(47)**, detailing the synthesis of the chiral derivative **(72)** and *bis*[N-(4-*n*-butyloxyphenyl)benzaldimin-4-yl] ferrocene-1,1′-dicarboxylate **(74)**.[72]

The structural integrity of the intermediates and products was confirmed by infra-red spectroscopy (Perkin Elmer 1600 FT-IR spectrophotometer) and nuclear magnetic resonance spectroscopy (JEOL EX 270MHz NMR spectrometer). Ferrocene **(45)** was purchased solely from Lancaster Synthesis Ltd. whilst most other reagents were obtained from the Aldrich Chemical Company Ltd. and BDH (Merck UK) Chemicals Ltd. Dry solvents were attained using the following procedures: dichloromethane (DCM) was dried over anhydrous calcium chloride; tetrahydrofuran (THF) was dried by continuously heating under reflux in the presence of sodium metal and benzophenone as indicator (a blue coloration being indicative of dry solvent); both hexane and benzene were dried over freshly extruded sodium wire.

7.1 *Experimental discussion*

In order to produce many of the desired target compounds, it was necessary to prepare some derivatives of ferrocene which could be used for further substitution. ***Scheme 3*** outlines the common ferrocene intermediates which were synthesised for this purpose.

Substituted ferrocenes may be prepared by either the direct or the indirect approach. Most methods adopt the indirect pathway where ferrocene is first synthesised and subsequently substituted. The direct method involves preparation from the appropriately substituted cyclopentadiene and an iron compound. This synthesis requires the presence of a strong base (Grignard, organolithium or metallic sodium) to obtain the desired compound in an acceptable yield and is less frequently used for the preparation of the more functionally substituted ferrocenes. The reactions of ferrocene have been extensively reviewed in many publications.[78,79,80]

Although ferrocene is highly susceptible to electrophilic substitution, many media which effect this reaction are strong oxidising agents. The iron atom within the ferrocene core exists in a Fe^{2+} state and is readily oxidised even by very mild reagents. Consequently attempts to nitrate or halogenate ferrocene directly lead only to the oxidation of the iron nucleus to Fe^{3+}.

Although reversible, the molecule now bears an overall positive charge and is hence, deactivated with respect to electrophilic attack. The product of this oxidation is called the ferrocinium ion **(Fig.30)**, which forms a blue/green solution in water.

Hence, ferrocene is only available to electrophilic substitution in non-oxidising conditions, e.g. Friedel-Crafts acylation, metallation, Mannich reaction.

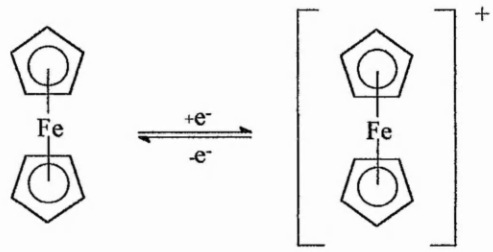

Fig.30 - The ferrocinium ion.

There are three possible pathways for the electrophilic substitution of ferrocene, shown schematically in **Fig.31**:

(i) *exo-attack* - the direct attack of the electrophile from above the ring;

(ii) *endo-attack* - the direct attack of the electrophile from below the ring; possibly a more favoured route due to the high electron density near the metal atom;

(iii) the electrophile attacks the metal atom before repositioning by an intramolecular migration to the *endo*-position, followed by elimination of H^+.

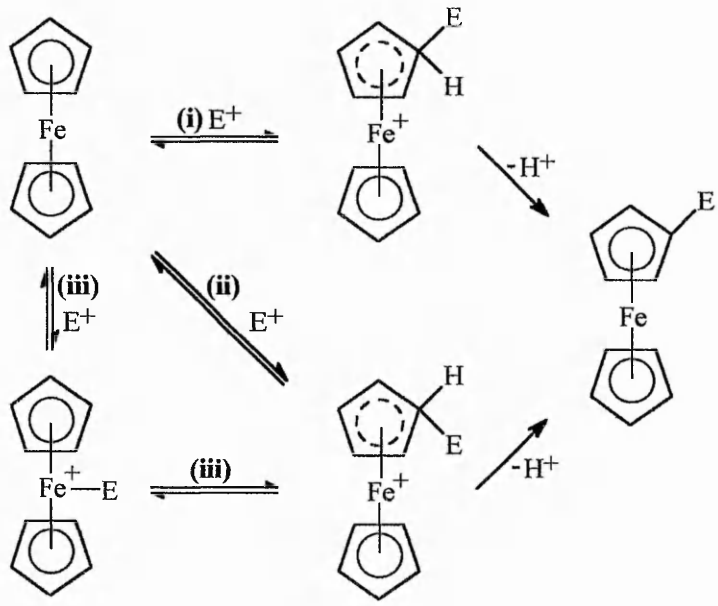

Fig.31 - Proposed mechanisms for the electrophilic substitution of ferrocene

It is not certain as to which of these routes is the most likely for the mechanism of substitution of the ferrocene core.

7.1.1 *The present work - directions and difficulties*

The introduction of ferrocene into complex organic systems proved more challenging than originally anticipated. A search of the general literature surrounding ferrocene chemistry revealed that the reported experimental methodology was often inadequate. Problems were encountered when attempting to purify many of the intermediate compounds required; a procedure of major importance in liquid crystal synthesis. Although ferrocene itself is chemically stable, many early attempts to purify its derivatives by column chromatography led to their degradation, a situation that was further compounded by the tailing or overlapping of the compounds which did prove stable to this method of separation. The only apparent literature reference to this problem is found in a 1958 publication where Rosenblum and Woodward[81] reported the photochemical sensitivity of ferrocenes on alumina

> '*many ferrocene derivatives darken at the alumina surface on exposure to diffuse sunlight...*'.

It would appear that the most probable cause of the observed degradation, in this case, was photochemical oxidation of the compounds on the column.

As the stability of any novel ferrocene compound to column chromatography could not be predicted, a new approach to the planned synthetic pathways was deemed necessary. A solution arose with the exclusion of the ferrocene moiety until the final stages of preparation of the target compounds. A number of synthetically useful ferrocene starting materials were hence prepared in advance (detailed in ***Scheme* 3**). The remaining synthetic work concentrated on the preparation of organic core ligands, which could then be linked to the ferrocene unit at a later stage of the scheme. This removed the need for many lengthy separations of mixtures of both mono- and di-substituted ferrocene intermediates. However, as a consequence of this change in strategy, the final range of novel ferrocene compounds produced was restricted.

7.1.2 *The identification of ferrocenyl hydrogens by ^1H N.M.R. spectroscopy*

In the following sections proton N.M.R. spectroscopy has been used extensively to verify the structural identity of many compounds. Ferrocene provides a sharp well defined singlet at δ_H 4.13 ppm as all of its hydrogen atoms are in equivalent environments, *a*, as shown in **Fig.32, (i)** below. These values are anomalous if ferrocene is regarded as an aromatic system, i.e. containing fully delocalised p-orbitals, as this value is surprisingly low compared with benzene which has a δ_H value of approximately 7 ppm.

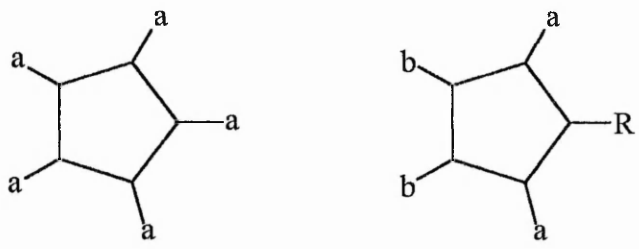

(i) **(ii)**

Fig.32 - the equivalent environments of both (i) unsubstituted and (ii) substituted cyclopentadiene

However, a more perplexing problem arises with the introduction of a substitutent atom or group, R, to either one or both of the cyclopentadiene rings, with the observed splitting patterns for the ring protons not always matching those which would have been expected. When a substituent is introduced the equivalence pattern within the cyclopentadiene ring is altered to produce the scenario shown in **(ii)**. The expected splitting pattern for this case would be one doublet (*a* is split by neighbouring *b*, integration is equivalent to two protons per ring) and one triplet (*b* is split by both neighbouring *a* and *b* protons, integration is equivalent to two protons per ring).

However, the observed splitting patterns for many of the prepared compounds do not exhibit this expected pattern, but rather show a combination of singles, doublets or

triplets. The observed patterns have been recorded in each case for the compounds prepared in the following schemes. It is not thought that this unexpected behaviour is a reflection on the purity of the compounds, but rather an averaged value due to the free rotation of the rings within solution (fluxionality). This phenomenon, although not recorded, can be observed within other literature publications involving ferrocene metallomesogens.[73]

7.2 *Preparative routes*

The following section gives details of the reaction pathways undertaken, which are represented diagrammatically as ***Schemes 3-8***, summarised below:

Scheme 3 - The preparation of some useful ferrocene intermediates **(46-53)**.

Scheme 4 - The preparation of novel esters, **(58)** and **(59)**, of 1,1′-*bis*(hydroxymethyl)ferrocene **(50)**.

Scheme 5 - The preparation of mono- **(60)** and di-substituted **(61)** acylferrocenes.

Scheme 6a - The preparation of *bis*[N-(4′-*n*-alkoxybiphenyl-4-yl)]ferrocene-1,1′-dialdimines **(67)**

6b - The preparation of *bis*[N-(4-phenyl)]ferrocene-1,1′-dialdiminyl di-4-*n*-octylbenzoate **(70)**.

Scheme 7 - The preparation of *bis*[4′-(R-1-methylheptyloxycarbonyl)biphenyl-4-yl] ferrocene-1,1′-carboxylate **(72)**.

Scheme 8 - The preparation of *bis*[N-(4-*n*-butyloxyphenyl)benzaldimin-4-yl] ferrocene-1,1′-dicarboxylate **(74)**.

A comprehensive account of the experimental methodology associated with each Scheme is given in ***Experimental methodology,*** sections **7.3-7.8**.

Scheme 3

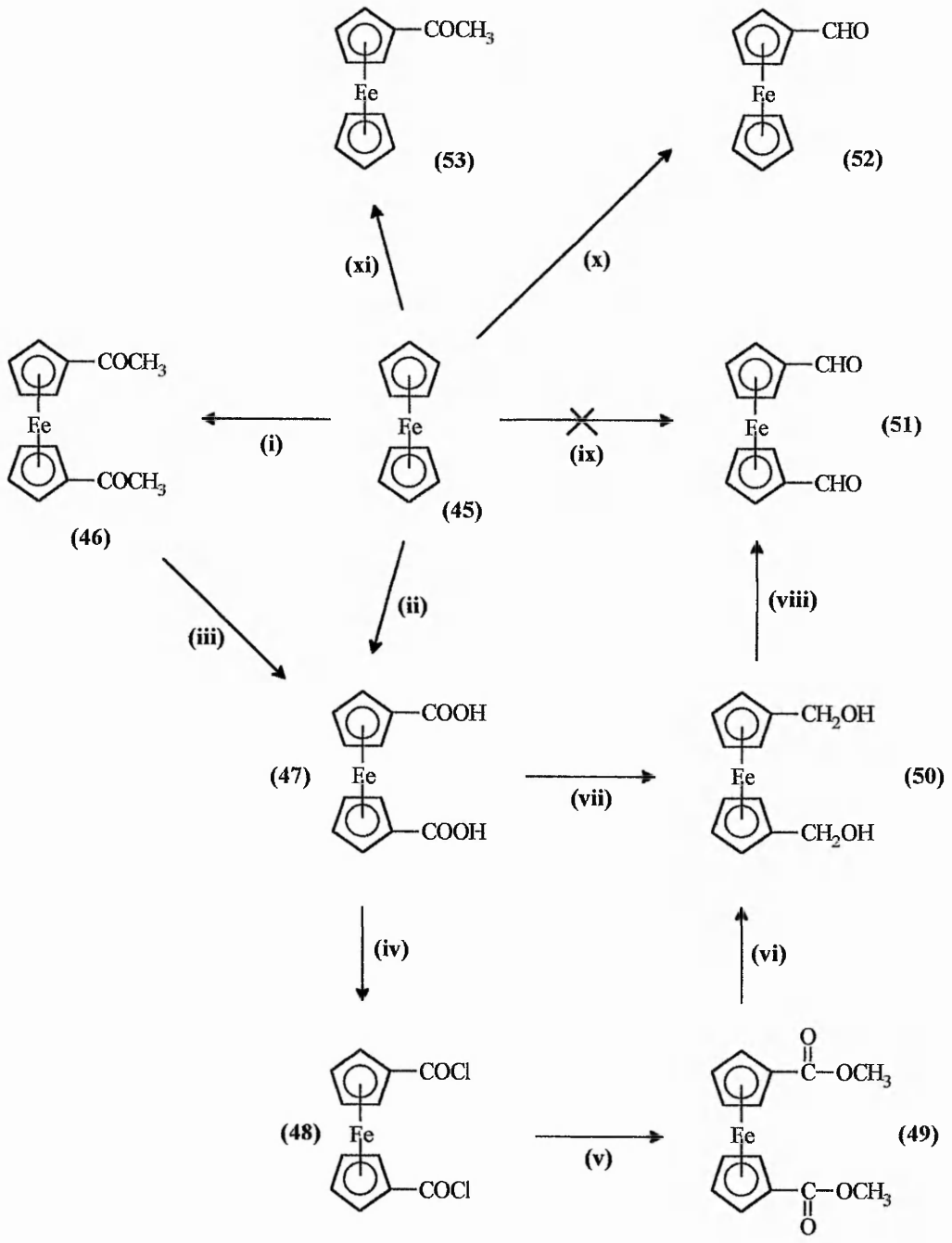

Legend

(i) CH_3COCl / $AlCl_3$ / DCM **(ii)** BuLi / TMEDA / Hexane / -78°C **(iii)** 4% aq. NaOCl

(iv) $(COCl)_2$ / Pyridine / DCM **(v)** CH_3OH / Pyridine **(vi)** $LiAlH_4$ / Ether

(vii) $LiAlH_4$ / THF **(viii)** MnO_2 / DCM **(ix)** BuLi / TMEDA / -78°C / N,N-dimethylformamide

(x) N-methyl formanilide / $POCl_3$ **(xi)** *ortho*-phosphoric acid / $(CH_3CO)_2O$.

Scheme 4

Where: $n = 7$ and 10.

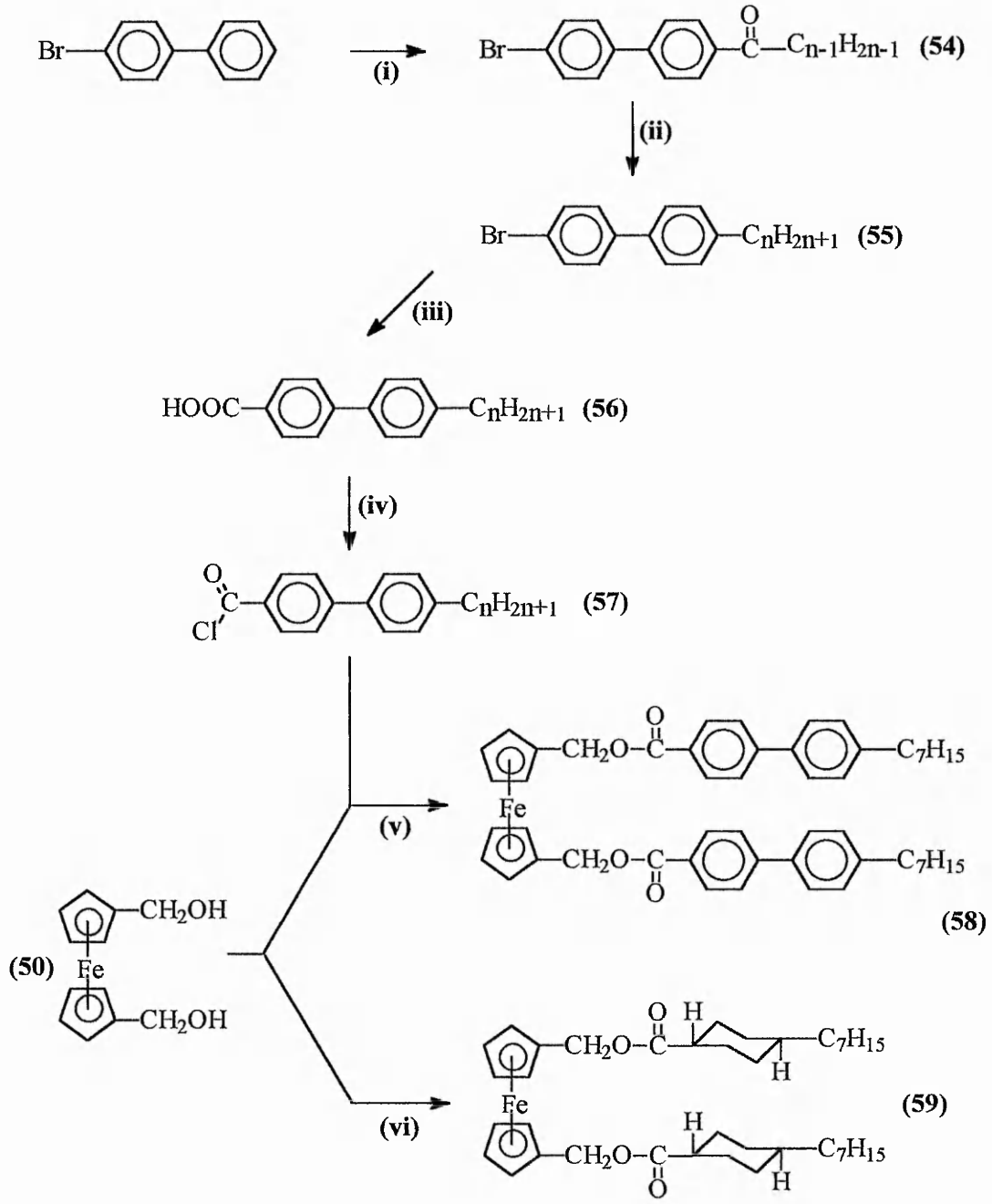

Legend

(i) $C_{n-1}H_{2n-1}COCl$ / $AlCl_3$ / DCM **(ii)** $LiAlH_4$ / $AlCl_3$ / Ether / DCM

(iii) 2.5 M BuLi / THF / CO_2 / -50°C **(iv)** $(COCl)_2$ / DCM

(v) Pyridine / DCM **(vi)** *trans*-4-n-cycloheptylcarboxylic acid / Toluene / HCl.

Scheme 5

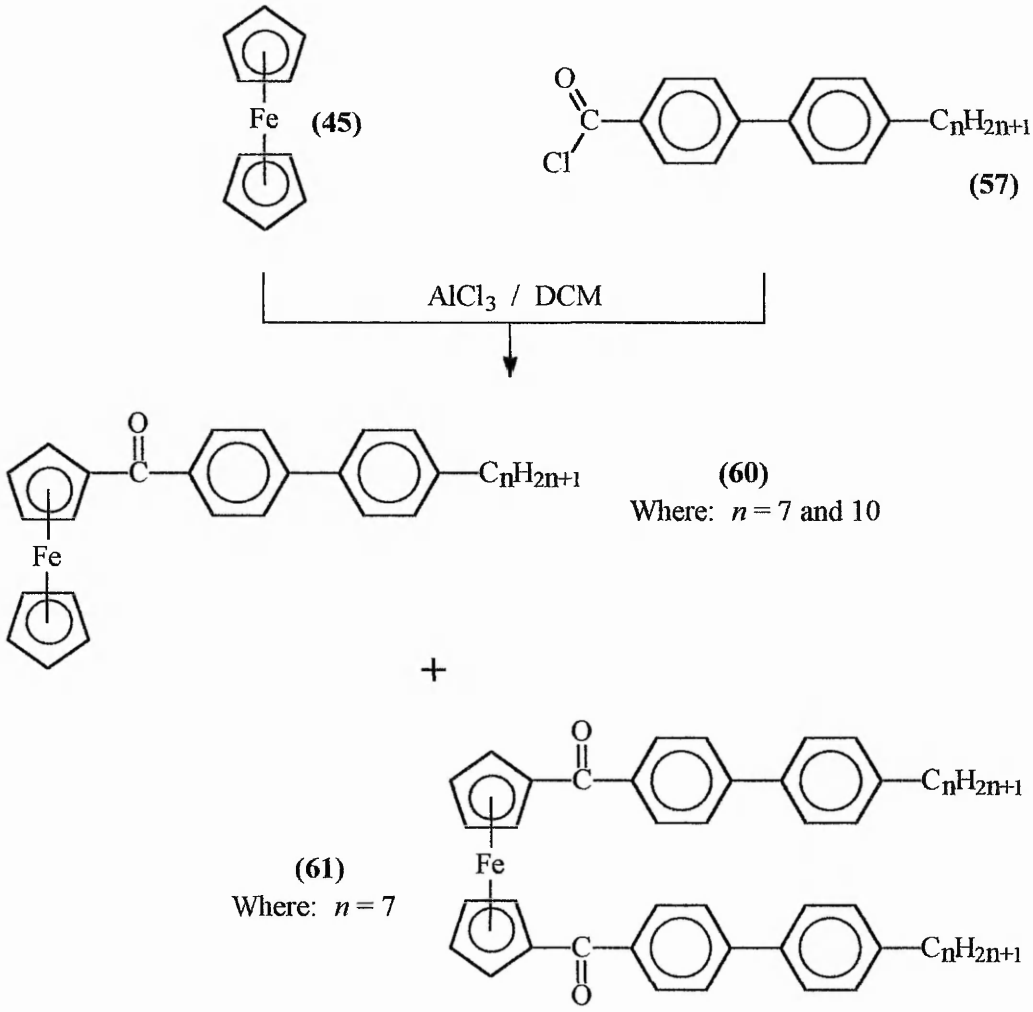
Fe
(45)
O
C
Cl
CnH2n+1
(57)
AlCl3 / DCM
O
C
CnH2n+1
Fe
(60)
Where: n = 7 and 10
+
(61)
Where: n = 7
O
C
CnH2n+1
Fe
C
O
CnH2n+1

Scheme 6a

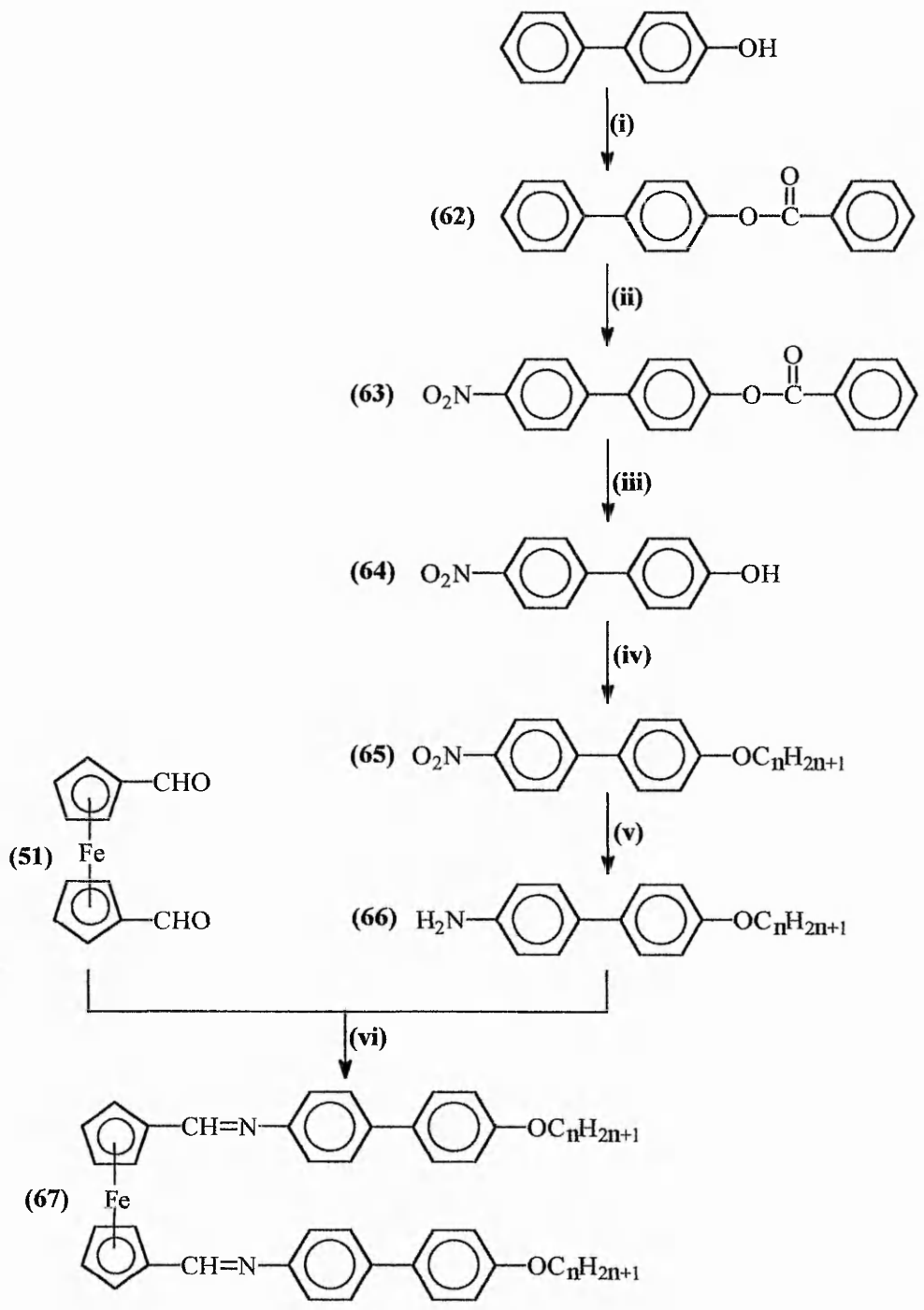

Legend

(i) Benzoyl Chloride / Pyridine / THF **(ii)** HNO_3 / GAA / 85 °C

(iii) KOH / EtOH **(iv)** $C_nH_{2n+1}Br$ / K_2CO_3 / Acetone

(v) 5% Pd/C / EtOH / 27 bar **(vi)** EtOH / GAA

Scheme 6b

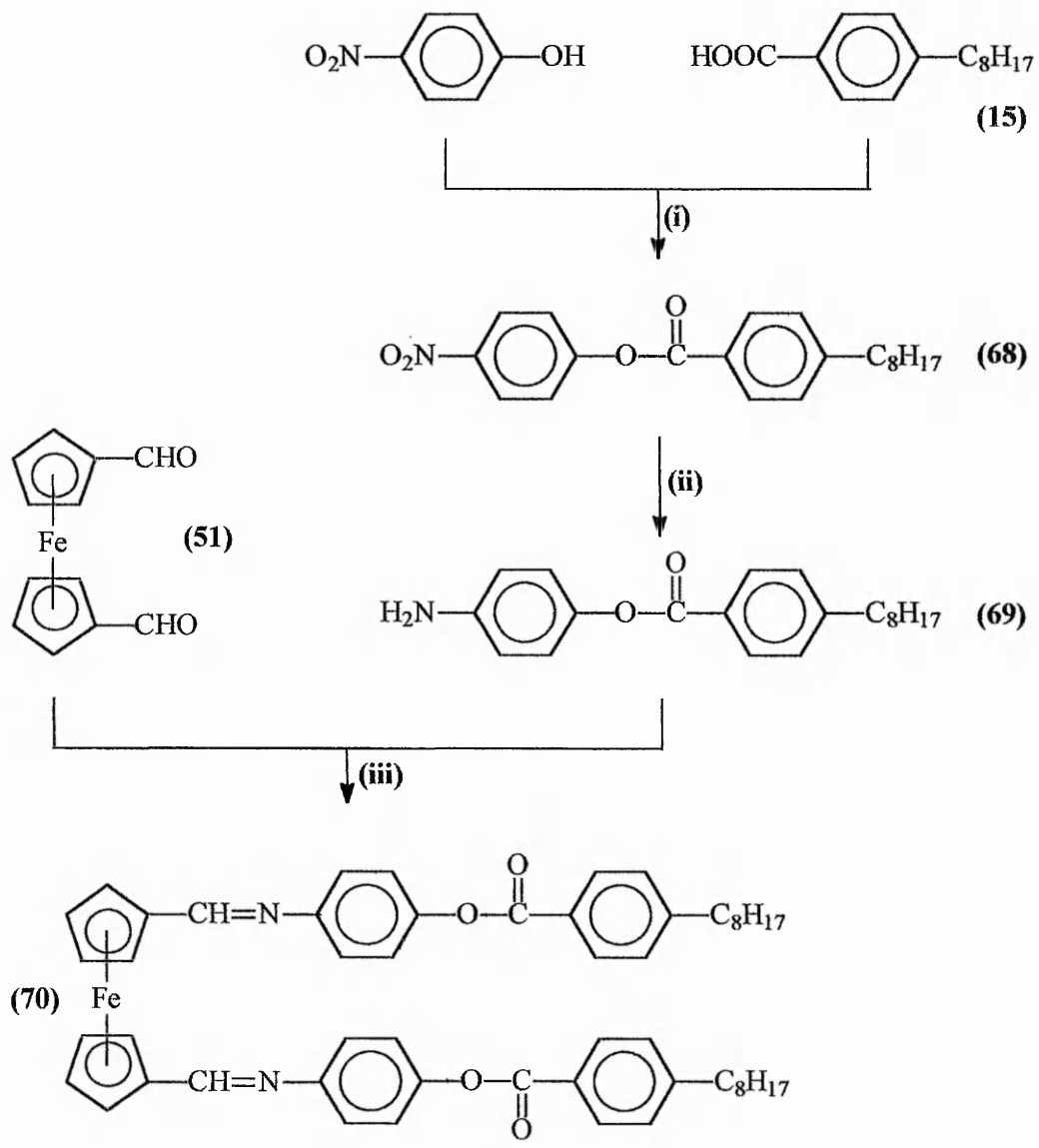

Legend

(i) DCC / DMAP / DCM **(ii)** 5% Pd/C / EtOH **(iii)** EtOH / GAA

Scheme 7

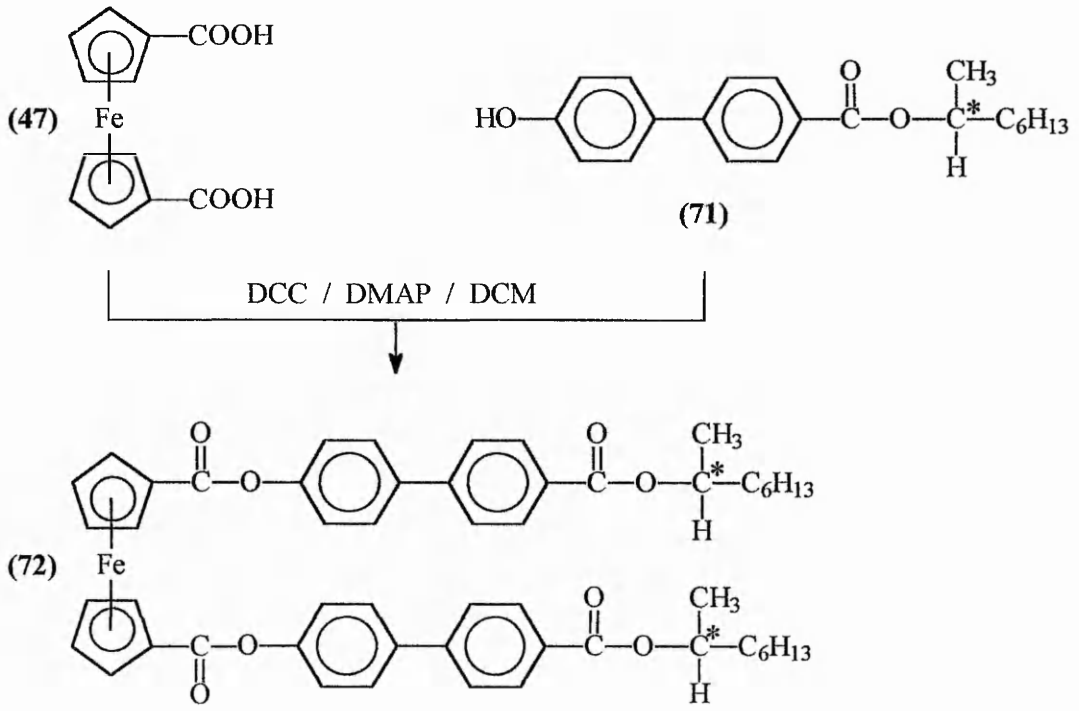

Scheme 8

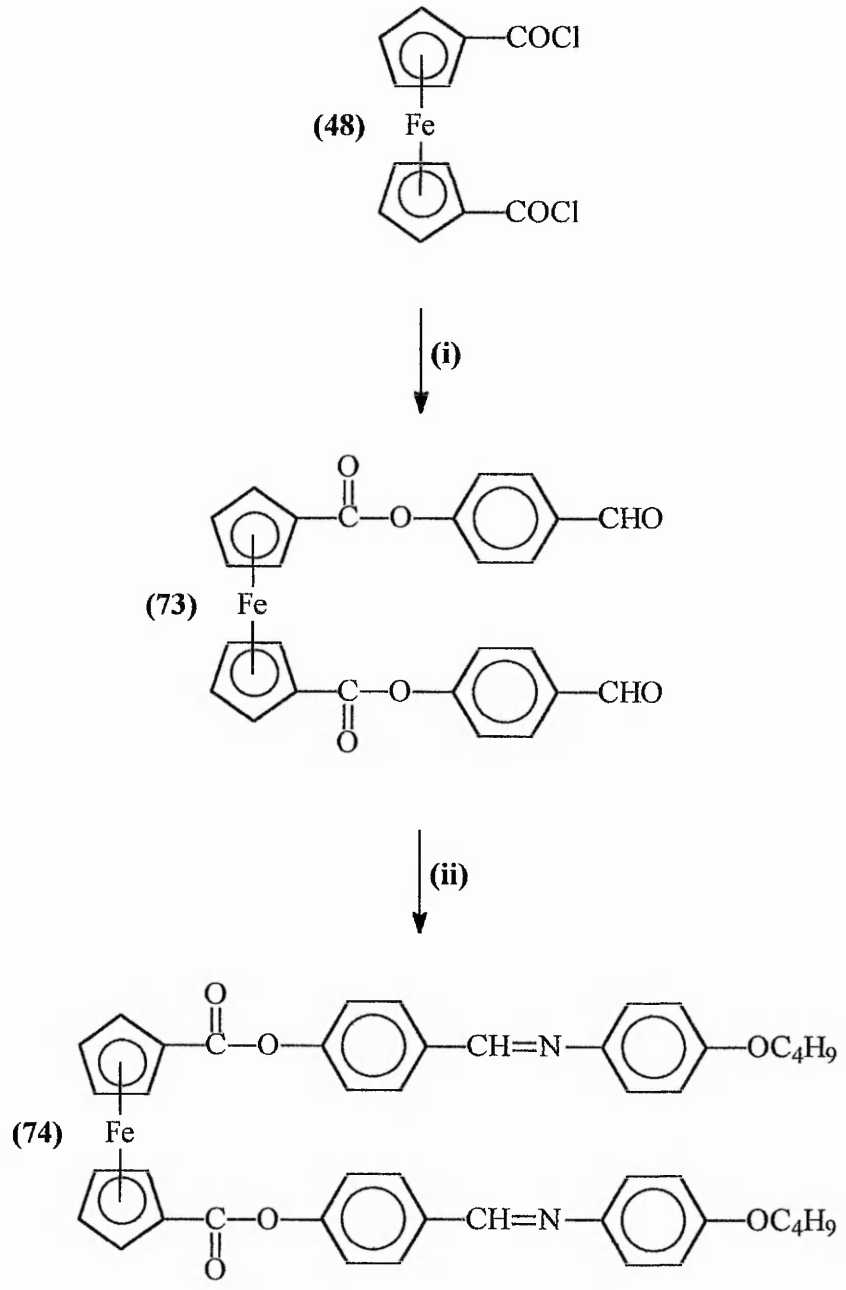

Legend

(i) *p*-hydroxybenzaldehyde / Pyridine / DCM **(ii)** 4-n-butyloxyaniline

7.3 Experimental methods - scheme 3

Scheme 3 summarises some general procedures undertaken to obtain a selection of ferrocene intermediates for further modification. Friedel-Crafts acylation of ferrocene **(45)** with acetyl chloride in the presence of aluminium chloride afforded 1,1′-diacetylferrocene **(46)** which was converted into the corresponding di-acid **(47)** via a hypohalite oxidation. Compound **(47)**, ferrocene-1,1′-dicarboxylic acid, was also prepared directly from ferrocene **(45)** via a metallation reaction using commercial butyllithium and solid carbon dioxide. The di-acid **(47)** was then reacted with oxalyl chloride in an inert nitrogen atmosphere to afford the corresponding di-acid chloride **(48)**. 1,1′-*Bis*(hydroxymethyl)ferrocene **(51)** was synthesised via two routes: (i) the esterification of ferrocene-1,1′-dicarbonyl chloride **(48)** with methanol in the presence of pyridine afforded dimethyl ferrocene-1,1′-dicarboxylate **(49)** which, when added to a stirred suspension of $LiAlH_4$, afforded the desired alcohol **(50)**, and (ii) the reduction of ferrocene-1,1′-dicarboxylic acid **(47)** using $LiAlH_4$ also yielded the required alcohol **(50)**.

The preparation of ferrocene-1,1′-dicarboxaldehyde **(51)**, the precursor to the Schiff bases **(67)**, n = 5-7 and 10, and **(70)**, n = 8, was accomplished by the treatment of **(50)** with activated MnO_2 . The attempted synthesis of **(51)** directly from ferrocene **(45)** via treatment with a commercial solution of BuLi followed by N,N-dimethylformamide proved unsuccessful as the product obtained by this method could not be purified.

Some other ferrocene intermediates were synthesised and are shown in ***Scheme 3***, although these were not used in any further syntheses due to time constraints. Treatment of ferrocene **(45)** with phosphorous oxychloride and N-methylformanilide afforded ferrocene carboxaldehyde **(52)**, whereas treatment with *ortho*-phosphoric acid and acetic anhydride yielded the mono-ketone, acetylferrocene **(53)**.

7.3.1 *Preparation of 1,1'-diacetylferrocene* (46)

Ferrocene **(45)** (10 g, 0.054 mol) in dry DCM (150 ml) was added, dropwise, to an ice-cold mixture of freshly distilled acetyl chloride (0.135 mol), powdered anhydrous aluminium chloride (18 g, 0.135 mol) and dry DCM (50 ml) contained in a three-necked round bottomed flask equipped with a suitable thermometer, dropping funnel, and calcium chloride guard tube. The temperature was maintained below 5 °C throughout the addition. After the addition was complete the reaction mixture was stirred for a further 4h. The reaction was then quenched by pouring into ice and 4M-aqueous hydrochloric acid and the mixture was transferred to a separating funnel. The organic layer was isolated and the aqueous phase was extracted with DCM (3x50 ml). The combined organic fractions were washed successively with water (50 ml) and 1% aqueous sodium hydroxide (50 ml), dried ($MgSO_4$) and the solvent removed under reduced pressure. The resulting crude product was purified by column chromatography on silica gel eluting with petroleum ether (b.p. 40-60 °C) affording the desired 1,1'-diacetylferrocene **(46)**, 11.4 g (78%) as dark red/purple crystals, m.p. 125.5-127.5 °C (lit.[82] 125-127 °C).

NMR: δ_H ppm ($CDCl_3$) 2.36 (6H, s, O=C-CH_3), 4.51 (4H, s, ferrocenyl-H), 4.77 (4H, s, ferrocenyl-H).

IR: υ_{max} cm^{-1} (KBr) 1660 (C=O str.), 1450, 1370, 1350, 1280, 1120, 840, 500.

7.3.2 *Preparation of ferrocene-1,1'-dicarboxylic acid* (47)

Ferrocene-1,1'-dicarboxylic acid **(47)** was prepared either by the direct metallation of ferrocene **(45)** or the oxidation of the diketone **(46)**. Both methods are described overleaf:

Method 1

Commercial 2.5M butyllithium (30 ml, 74 mmol) was injected into a stirred mixture of dry hexane (10 ml) and tetramethylethylenediamine (TMEDA) (11.1 ml, 74 mmol) contained in a flask fitted with a nitrogen line, a rubber septum and a dropping funnel. After 15 min. ferrocene **(45)** (5.6 g, 30 mmol) in dry hexane (250 ml) was added, dropwise , over 30 min., after which the reaction was stirred for 6h., and then poured onto solid CO_2. The mixture was allowed to warm to room temperature with stirring continued overnight before acidification with concentrated hydrochloric acid. The resulting orange precipitate was filtered off and washed with diethyl ether to remove any unreacted ferrocene. The crude ferrocene-1,1′-dicarboxylic acid **(47)** was purified by Soxhlet extraction with benzene to remove the more soluble mono-acid from the mixture of mono- and di-substituted acids, to yield ferrocene-1,1′-dicarboxylic acid **(47)**, 7.4 g (90%) as an orange powder, m.p. 250 °C (dec.) (lit.[83] >250 °C[dec.]).

NMR: δ_H ppm ($CDCl_3$) 4.4 (4H, s, ferrocenyl-H), 4.73 (4H, s, ferrocenyl-H), acidic protons not seen;

^{13}C 169.88 ppm (COOH).

IR: υ_{max} cm^{-1} (KBr) 1680 (C=O str.), 1490, 1300, 1170, 510.

The crude ferrocene-1,1′-dicarboxylic acid **(47)** was frequently used without further purification (crude yields were in the region of 98%) as it was often easier to obtain a pure 1,1′-disubstituted product at a later stage of a synthesis.

Method 2

A suspension of 1,1′-diacetylferrocene **(46)** (9 g, 33.3 mmol) and 4% aqueous sodium hypochlorite (300 ml) was stirred vigorously and maintained at 45-55 °C for 5h. Additional portions of 4% aqueous NaOCl (50 ml) were added after 1.5, 2, and 3h. After completion of the 5h. period the orange precipitate was filtered off, added to an excess of concentrated hydrochloric acid and stirred vigorously. The suspended solid was filtered off affording the desired ferrocene-1,1′-dicarboxylic acid **(47)**, 6.94 g (76%) as an orange powder, m.p. 250 °C (dec.).

NMR and IR data are quoted in *Method 1* above.

Method 2 provided a pure disubstituted product but in a much lower yield than *Method 1*, being a two stage preparation from ferrocene **(45)**. Hence *Method 1* was preferred for its speed and higher yields, although the overall product purity was not as high.

7.3.3 *Preparation of ferrocene-1,1′-dicarbonyl chloride* (48)

In an nitrogen atmosphere, oxalyl chloride (3.1 ml, 35.2 mmol) was added, dropwise, to a stirred suspension of ferrocene-1,1′-dicarboxylic acid **(47)** (2 g, 72 mmol) in dry DCM (100 ml) and pyridine (3 drops). The reaction mixture was then heated under reflux for 6h. after which the solvent was removed under reduced pressure. The residue was extracted continuously with dry hexane to afford the desired ferrocene-1,1′-dicarbonyl chloride **(48)**, 1.17 g (52%) as dark red/purple crystals, m.p. 97-98 °C (lit.[84] 98-100 °C).

NMR: δ_H ppm ($CDCl_3$) 4.76 (4H, t, ferrocenyl-H), 5.05 (4H, t, ferrocenyl-H).

IR: υ_{max} cm^{-1} (KBr) 1760 (C=O str.), 1430, 1370, 1240, 1040, 930, 770.

7.3.4 *Preparation of dimethyl ferrocene-1,1′-dicarboxylate* (49)

Ferrocene-1,1′-dicarbonyl chloride **(48)** (1 g, 3.2 mmol) was dissolved in hot methanol (100 ml) and pyridine (3 drops) was added to initiate the reaction. The mixture was stirred at room temperature for 3h. and the excess of solvent was then removed under reduced pressure. The resulting orange powder was purified by extracting the crude solid with benzene affording a clear orange solution and leaving behind a black insoluble oil. The clear solution was decanted and the solvent removed under reduced pressure to yield the pure dimethyl ferrocene-1,1′-dicarboxylate **(49)** 0.72 g (75%), as orange/yellow crystals, m.p. 111-113 °C (lit.[85] 113-114 °C).

NMR: δ_H ppm ($CDCl_3$) 3.82 (6H, s, OCH_3), 4.41 (4H, t, ferrocenyl-H), 4.83 (4H, t, ferrocenyl-H).

IR: υ_{max} cm^{-1} (KBr) 1700 (C=O str.), 1460, 1280, 1140, 750.

7.3.5 *Preparation of 1,1′-bis(hydroxymethyl)ferrocene* (50)

1,1′-*Bis*(hydroxymethyl)ferrocene **(50)** was prepared by two methods, both of which are reductions using $LiAlH_4$. *Method 1* involves the reduction of the corresponding 1,1′-disubstituted methyl ester **(49)**, whereas *Method 2* appears to be a new synthesis, unreported in the literature, involving the reduction of ferrocene-1,1′-dicarboxylic acid **(47)**. Hence, by this method 1,1′-*bis*(hydroxymethyl)ferrocene **(50)** may be prepared in just two steps from ferrocene **(45)**, and was the favoured route for the synthesis of this compound.

Method 1

In an atmosphere of nitrogen, dimethyl ferrocene-1,1′-dicarboxylate **(49)** (1 g, 3.3 mmol) in dry benzene (40 ml) was added, dropwise, to a stirred suspension of

$LiAlH_4$ (0.3 g, 7 mmol) in dry diethyl ether (40 ml) at such a rate to maintain gentle boiling of the diethyl ether. The reaction mixture was heated gently under reflux for 3h. and then the excess of $LiAlH_4$ was destroyed by the careful addition, in turn, of moist diethyl ether, ethyl acetate and water. Inorganic salts were filtered off from the resulting slurry and the filtrate was transferred to a separating funnel. The organic layer was separated and the aqueous layer was extracted with diethyl ether (3x50 ml). The ether extracts were combined with the organic phase, dried ($MgSO_4$), and the solvents removed in vacuo to yield the crude alcohol which was purified by recrystallisation from a mixture of chloroform and petroleum ether (b.p. 40-60 °C) to afford the pure 1,1′-*bis*(hydroxymethyl)ferrocene **(50)**, 0.6 g (74%), as an orange solid, m.p. 105-106 °C (lit.[85] 107-108 °C).

NMR: δ_H ppm ($CDCl_3$) 4.13 (4H, s, $C(CH_2)OH$), 4.18-4.22 (4H, d, ferrocenyl-H), 4.30-4.34 (4H, d, ferrocenyl-H), 4.38 (2H, s, OH).

IR: υ_{max} cm^{-1} (KBr) 3298 (OH str.), 2857, 1237, 1051, 984, 812.

Method 2

In an atmosphere of nitrogen a suspension of ferrocene-1,1′-dicarboxylic acid **(47)** (6.0 g, 22 mmol) in warm dry THF (220 ml) was added, dropwise, to a suspension of $LiAlH_4$ (1.7 g, 4.5 mmol) in dry ether (30 ml) at a rate sufficient to maintain gentle boiling of the solvent. The remaining procedure and work were the same as for *Method 1* described above to yield the pure 1,1′-*bis*(hydroxymethyl)ferrocene **(50)**, 3.85 g (71%), as an orange solid, m.p. 109-110 °C.

NMR and IR data are quoted in *Method 1* above.

7.3.6 *Preparation of ferrocene-1,1′-dicarboxaldehyde* (51)

The preparation of ferrocene-1,1′-dicarboxaldehyde **(51)** was achieved by the two methods described below. The preparation of the aldehyde **(51)** by *Method 2* reported by Balavoine *et al.*,[86] involving the direct lithiation of ferrocene **(45)** followed by treatment with N,N-dimethylformamide, appeared the most attractive route providing a high yield in a single step synthesis. However, the separation and purification of the 1,1′-dicarboxaldehyde by this method could not be accomplished. Hence, *Method 1* was the preferred route to ferrocene-1,1′-dicarboxaldehyde **(51)**.

Method 1

'Active' manganese dioxide (8.7 g, 0.10 mol) was added to a solution of 1,1′-*bis*(hydroxymethyl)ferrocene **(50)** (2.5 g, 10 mmol) in chloroform (100 ml). The addition was mildly exothermic. The reaction mixture was left in the dark overnight and the MnO_2 was then filtered off using a sintered glass funnel. The filtrate was evaporated to dryness in vacuo, and the resulting red solid was repeatedly recrystallised from the minimum amount of hot cyclohexane affording ferrocene-1,1′-dicarboxaldehyde **(51)**, 1.58 g (65%), as a red powder, m.p. 181-183 °C (lit.[87] 183-184 °C).

NMR: δ_H ppm ($CDCl_3$) 4.68(4H, s, ferrocenyl-H), 4.89(4H, s, ferrocenyl-H), 9.95(2H, s, CHO).

IR: υ_{max} cm^{-1} (KBr) 1683(C=O str.), 1655, 1456, 1244, 1036, 742.

Method 2

Ferrocene **(45)** (5.6 g, 30 mmol) was lithiated by the method given in section **7.3.2**, *Method 1*. After stirring for 6 h. the reaction mixture was cooled to -78 °C and freshly distilled N,N-dimethylformamide (7 ml) was added, dropwise. The resulting

slurry was stirred for a further 2 h. before hydrolysing at -78 °C. The organic phase was separated and the aqueous phase was then extracted with DCM (2x50 ml). The combined organic extracts were dried ($MgSO_4$), before removing the solvent in vacuo. The resulting solid was a mixture of unchanged ferrocene and both the mono- and di-carboxaldehyde products. Purification was attempted both by column chromatography on aluminia using diethyl ether as the eluent and by recrystallisation from cyclohexane. Both of these methods proved unsatisfactory and the desired pure dicarboxaldehyde compound could not be isolated. Consequently, this method of preparing ferrocene-1,1′-dicarboxaldehyde **(51)** was abandoned.

7.3.7 *Preparation of ferrocenecarboxaldehyde* (52)

In an atmosphere of nitrogen, freshly distilled N-methyl formanilide (11.6 g, 10.6 ml) was added, with stirring, to phosphorus oxychloride (13.16 g, 8.6 mmol) contained in a flask cooled in an ice-water bath. The rate of addition was adjusted to maintain a temperature of 8-10 °C. After stirring for 15 min. the solution was heated gently to 40 °C and ferrocene **(45)** (7.5 g, 40 mmol) was added carefully, in portions, over 30 min. The mixture was then stirred for 2h. at 45-50 °C, before being cooled to 15 °C. An ice/water mixture (25 ml) was then added and the reaction stirred for a further 2h. at room temperature. Diethyl ether (100 ml), sodium sulphite (20 g) and 40% aqueous sodium bisulphite (40 ml) were then added in order to precipitate the bisulphite derivative. The suspension was stirred for a further 4h. then left to stand overnight. The resulting precipitate was filtered off, washed with diethyl ether to remove any unchanged ferrocene, and then stirred with 10% aqueous sulphuric acid (160 ml) at 40 °C for 30 min. The suspended product was then filtered off and washed with aqueous saturated sodium

carbonate and water, and then dried affording the ferrocenecarboxaldehyde **(52)**, 4.1 g (48%), as purple crystals, m.p. 116.5-117 °C (lit.[80] 118-119 °C, lit.[88] 124.5 °C).

NMR: δ_H ppm ($CDCl_3$) 4.28 (5H, s, ferrocenyl-H), 4.61 (2H, d, ferrocenyl-H), 4.79-4.80 (2H, t, ferrocenyl-H), 9.96 (1H, s, CHO).

IR: υ_{max} cm^{-1} (KBr) 1680 (C=O str.), 1450, 1250, 1110, 830.

7.3.8 *Preparation of acetylferrocene* (53)

A stirred mixture of ferrocene **(45)** (20 g, 0.11 mol), 85% *ortho*-phosphoric acid (5 ml) and acetic anhydride (150 ml) was heated to 100 °C for 10 minutes. The resulting slurry was then poured onto ice and left overnight. Saturated aqueous sodium carbonate was added resulting in the formation of a precipitate. This was filtered off and treated with concentrated hydrochloric acid (200 ml). Insoluble material was removed by filtration through a sintered glass funnel and the purple solution was diluted by pouring into a 5 fold excess of ice-water. The precipitated solid was filtered off, washed with water and then dried to afford the acetylferrocene **(53)**, 10.3 g (41%), as orange crystals, m.p. 85.5-86.5 °C (lit.[80] 85-86 °C).

NMR: δ_H ppm ($CDCl_3$) 2.36 (3H, s, O=CCH_3), 4.21 (5H, s, ferrocenyl-H), 4.51 (2H, d, ferrocenyl-H), 4.77 (2H, s, ferrocenyl-H).

IR: υ_{max} cm^{-1} (KBr) 1650 (C=O str.), 1456, 1380, 1280, 830.

7.4 *Experimental methods - Scheme 4*

The methods used to prepare some novel ferrocene-1,1′-diesters **(58)** and **(59)** of 1,1′-*bis*(hydroxymethyl)ferrocene **(50)** are outlined in ***Scheme 4***. Compound **(59)** was prepared as part of an initial study into the incorporation of ferrocene into an existing liquid crystalline system. This investigation was later extended to encompass two ferrocene-1,1′-diesters of the type **(58)**. It was hoped that the 4′-*n*-alkylbiphenyl-4-carboxylic acids **(56)** would sufficiently extend the molecular linearity of the compound and enable some mesogenic activity to be observed.

Scheme 4 mainly concerns the preparation of the 4′-*n*-alkylbiphenyl-4-carboxylic acids **(56)** and their conversion into the corresponding acid chlorides **(57)**. 4-Bromobiphenyl was acylated with the appropriate acid chloride to yield the desired 4′-*n*-alkanoyl-4-bromobiphenyl **(54)**, which was then reduced to the corresponding 4′-*n*-alkyl-4-bromobiphenyl **(55)** by heating under reflux in the presence of $AlCl_3$ and $LiAlH_4$. Treatment of **(55)** with butyl lithium at -50 °C (the mixture solidifies below this temperature), before pouring onto CO_2 (-78 °C) and acidification, then yielded the required 4′-*n*-alkylbiphenyl-4-carboxylic acids **(56)**, $n = 7$ and 10, which could then be converted into the corresponding carbonyl chlorides **(57)** by reaction with oxalyl chloride. The ferrocene-1,1′-diester **(58)** was then prepared by stirring 1,1′-*bis*(hydroxymethyl)-ferrocene **(50)** with the appropriate acid chloride **(57)** in the presence of a few drops of pyridine.

The other ferrocene-1,1′-diester, **(59)** was prepared by heating 1,1′-*bis*(hydroxymethyl)ferrocene **(50)**, *trans*-4-*n*-heptylcyclohexyl carboxylic acid **(76)** and a few drops of concentrated HCl in toluene under reflux in a Dean and Stark apparatus.

7.4.1. *Preparation of 4'-n-alkanoyl-4-bromobiphenyls* (54)

4-Bromobiphenyl (5 g, 21.5 mmol) in dry DCM (100 ml) was added, dropwise, to an ice-cold mixture of the appropriate acid chloride (35 mmol), powdered anhydrous aluminium chloride (4.7 g, 35 mmol) and dry DCM (20 ml). The reaction was carried out according to the method detailed in section **7.3.1**. The resulting crude product was recrystallised from ethanol to afford the desired 4'-*n*-alkanoyl-4-bromobiphenyl **(54)** as straw coloured needles: *n*-heptanoyl (72%), m.p. 97-99 °C (lit.[89] 99-100 °C); *n*-decanoyl (64%), m.p. 107-109 °C.

Spectral data for the *n*-decanoyl derivative is given below:

NMR: δ_H ppm ($CDCl_3$) 0.9 (3H, t, CH_3), 1.3-1.8 (14H, m, $7CH_2$), 2.9 (2H, t, $O{=}CCH_2$), 7.5 (2H, d, ArH), 7.57-7.65 (4H, m, ArH), 8.0 (2H, d, ArH).

IR: υ_{max} cm^{-1} (KBr) 2948, 2915, 2846,1677 (C=O str.), 1603, 1466, 1082, 1002, 810.

7.4.2 *Preparation of 4'-n-alkyl-4-bromobiphenyls* (55)

A solution of anhydrous aluminium chloride (4.0 g, 30 mmol) in dry ether (20 ml) was added, dropwise, to a stirred slurry of $LiAlH_4$ (1.14 g, 30 mmol) in dry ether (20 ml) in an atmosphere of nitrogen. The appropriate ketone **(54)** (13 mmol) in dry DCM (100 ml) was added, dropwise, over a period of 1h. to the reaction mixture at such a rate to maintain a gentle boiling of the solvent. The reaction was then heated under gentle reflux and followed by TLC. On completion, the reaction mixture was cooled before pouring into 4M-aqueous HCl (200 ml). The organic phase was then separated and the aqueous phase washed with 'diethyl ether (2x50 ml). The organic extracts were then combined, washed with saturated sodium carbonate solution (2x50 ml) and dried ($MgSO_4$). The resulting solid was recrystallised from ethanol to afford the desired

4′-*n*-alkyl-4-bromobiphenyl **(55)** as a straw coloured solid on standing: *n*-heptyl (64%), m.p. 94-95 °C (lit.[89] 93-94 °C); *n*-decyl (41%), m.p. 84-86 °C.

Spectral data for the *n*-decyl derivative is given below:

NMR: δ_H ppm ($CDCl_3$) 0.9 (3H, t, CH_3), 1.2-1.7 (16H, m, $8CH_2$), 2.6 (2H, t, $ArCH_2$), 7.2-7.6 (8H, m, ArH).

IR: υ_{max} cm^{-1} (KBr) 2949, 2916, 2846, 1601, 1465, 1080, 810.

7.4.3 *Preparation of 4′-n-alkylbiphenyl-4-carboxylic acids* (56)

Commercial 2.5M butyllithium (10 ml, 25 mmol) was injected into a stirred mixture of dry hexane (10 ml) and tetramethylethylenediamine (TMEDA) (3.8 ml, 25 mmol) contained in a flask fitted with a nitrogen line, a rubber septum and a dropping funnel. The mixture was then stirred for 15 min. and cooled to -50 °C in an ice/acetone bath, before the appropriate 4′-*n*-alkyl-4-bromobiphenyl **(55)** (10 mmol) in dry THF (50 ml) was added, dropwise, over 30 min., after which the reaction was stirred for 6h., and then poured onto solid CO_2. The mixture was allowed to warm to room temperature with stirring continued overnight before acidification with concentrated hydrochloric acid. The resulting precipitate was filtered off and purified by several recrystallisations from ethanol, to yield the desired 4′-*n*-alkylbiphenyl-4-carboxylic acid **(56)** as white plates: *n*-heptyl (82%), m.p 158 °C (lit.[90] C-S 156 °C); *n*-decyl (79%), m.p. 128 °C (lit.[90] C-S 130 °C).

Spectral data for the *n*-decyl derivative is given below:

NMR: δ_H ppm ($CDCl_3$) 0.9 (3H, t, CH_3), 1.2-1.7 (16H, m, $8CH_2$), 2.6 (2H, t, $ArCH_2$), 7.2-7.6 (8H, m, ArH), COO*H* not detected.

IR: υ_{max} cm^{-1} (KBr) 2926, 2853, 2542, 1678 (C=O str.), 1606, 1427, 1297, 774.

7.4.5 *Preparation of 4'-n-alkylbiphenyl-4-carbonyl chlorides* (57)

Oxalyl chloride (4.4 ml, 50 mmol), was added in a dropwise fashion to a stirred solution of the appropriate 4'-*n*-alkylbiphenyl-4–carboxylic acid **(56)** (20 mmol) in anhydrous DCM (80 ml). The reaction was allowed to stir for a further four hours before the excess solvent and oxalyl chloride were removed in vacuo to yield a dark oil containing the crude 4'-*n*-alkylbiphenyl-4–carbonoyl chlorides **(57)**. The product was used crude, and hence spectral data may be unreliable:

Spectral data for the *n*-decyl derivative is given below:

NMR: δ_H ppm ($CDCl_3$) 0.9 (3H, t, CH_3), 1.2-1.7 (16H, m, $8CH_2$), 2.6 (2H, t, $ArCH_2$), 7.2-7.6 (8H, m, ArH).

IR: υ_{max} cm^{-1} (Thin film) 2924, 2853, 1774 (C=O str.), 1737 (C=O str.), 1601, 1466, 1176, 878.

7.4.6 *Preparation of 1,1'-ferrocenylbis(methyl 4'-n-heptylbiphenyl-4-carboxylate)*(58)

4'-*n*-Heptylbiphenyl-4-carbonyl chloride **(57)** (4.7 g, 15 mmol) was added, dropwise, to a stirred solution of 1,1'-*bis*(hydroxymethyl)ferrocene **(50)** (1.2 g, 4.9 mmol) in dry THF (200 ml) and pyridine (1 ml). The reaction mixture was stirred for a further 4 h. before quenching the excess acid chloride **(57)** by pouring onto 4M-aqueous HCl / ice (200 ml). The resulting slurry was transferred to a separating funnel and the layers separated. The aqueous phase was extracted with DCM (3x50 ml). The extracts were combined with the organic phase and washed with 4M-aqueous NaOH (3x50 ml). The organic phase was then dried ($MgSO_4$) before removal of the solvents in vacuo. The crude product was purified by column chromatography on silica gel eluting with a 1:1 ether:petroleum ether (b.p. 40-60 °C) , to afford the desired 1,1'-ferrocenyl*bis*(methyl

4′-n-heptylbiphenyl-4-carboxylate) **(58)**, which was recrystallised from ethanol and water to yield a yellow solid (59%), m.p. 153 °C.

NMR: δ_H ppm ($CDCl_3$) 0.9 (6H, t, $2CH_3$), 1.28-1.66 (20H, m, $10CH_2$), 2.6 (4H, t, $2ArCH_2$), 4.2 (4H, t, ferrocenyl-H), 4.4 (4H, t, ferrocenyl-H), 5.2 (4H, s, C-CH_2-O), 7.25 (4H, m, ArH), 7.5 (4H, d, ArH), 7.64 (4H, d, ArH), 8.1 (4H, d, ArH).

IR: υ_{max} cm^{-1} (KBr) 2952, 2925, 2852, 1704 (C=O str.), 1605, 1275, 1098, 774.

7.4.7 *Preparation of 1,1′-ferrocenylbis(methyl trans-4-n-heptylcyclohexanecarboxylate)* (59)

1,1′-*Bis*(hydroxymethyl)ferrocene **(50)** (1 g, 4 mmol), *trans*-4-*n*-heptylcyclohexyl carboxylic acid **(76)** (2.54 g, 10 mmol), 3 drops of concentrated HCl and toluene (100 ml) were placed in a 250 ml round bottomed flask which was attached to a Dean and Stark trap which in turn was attached to a reflux condenser. The reaction mixture was then heated under reflux for eighteen hours and, after cooling, transferred to a separating funnel where it was shaken with saturated sodium bicarbonate solution (3x30 ml), before extraction into ether (3x50 ml). The combined organic fractions were dried ($MgSO_4$) and the solvent was removed under reduced pressure. The residue was purified by column chromatography on silica gel eluting with 9:1 petroleum ether:ethyl acetate followed by recrystallisation from 9:1 ethanol:water to afford the desired ester (15%) as pale yellow plates, m.p. 77.8 °C.

NMR: δ_H ppm ($CDCl_3$) 0.88 (6H, t, $2CH_3$), 1.25-2.2 (44H, m, 4CH and $20CH_2$), 4.17 (4H, t, ferrocenyl-H), 4.23 (4H, t, ferrocenyl-H), 4.85 (4H, s, $2CH_2$-O).

IR: υ_{max} cm^{-1} (KBr) 2921, 2850, 2360, 1720 (C=O), 1170, 1139.

7.5 *Experimental methods - Scheme 5*

The acylation of ferrocene proceeds extremely smoothly, and is well documented.[78,79,80] Thus acylation afforded an ideal route to some novel ferrocene derivatives. ***Scheme 5*** outlines the preparation of two novel ferrocenyl ketones **(60)** and one 1,1′-disubstituted derivative **(61)**. Ferrocene was acylated with the appropriate 4′-*n*-alkylbiphenyl-4-carbonyl chloride **(57)**, $n = 7$ and 10, as detailed below.

7.5.1 *The synthesis of two 4′-n-alkylbiphenyl-4-yl ferrocenyl ketones* (60) *and 1,1′-ferrocenyl bis(4′-n-heptylbiphenyl-4-yl) diketone* (61)

Ferrocene **(45)** (0.5 g, 2.7 mmol) was acylated with the appropriate 4′-*n*-alkylbiphenyl-4-carbonyl chloride **(57)** (10 mmol), in the presence of $AlCl_3$ (1.33 g, 10 mmol) in dry DCM (20 ml) as described in section **7.3.1**. The resulting crude product was purified by column chromatography on silica gel eluting with petroleum ether (b.p. 40-60 °C) affording both the mono- and di-ketones, **(60)** and **(61)** (only the mono-ketone was obtained for the $n = 10$ derivative) as dark red-purple crystals.

mono-ketones : $n = 7$ (24%), m.p. 165 °C; $n = 10$ (32%), m.p. 163 °C

di-ketone: $n = 7$ (14%), m.p. 192 °C.

Data for 4′-*n*-heptylbiphenyl-4-yl ferrocenyl ketone **(60)**:

NMR: δ_H ppm ($CDCl_3$) 0.9 (3H, t, CH_3), 1.2-1.6 (10H, m, $5CH_2$), 2.6 (2H, t, $ArCH_2$), 4.2 (5H, s, ferrocenyl-H), 4.6 (2H, t, ferrocenyl-H), 4.9 (2H, t, ferrocenyl-H), 7.25 (2H, d, ArH), 7.6 (2H, d, ArH), 7.7 (2H, d, ArH), 8.0 (2H, d, ArH).

IR: υ_{max} cm^{-1} (KBr) 2921,2849, 1626 (C=O str.), 1601, 1446, 1292, 1168, 812, 496.

Data for 1,1′-ferrocenyl *bis*(4′-*n*-heptylbiphenyl-4-yl) diketone **(61)**:

NMR: δ_H ppm ($CDCl_3$) 0.9 (6H, t, $2CH_3$), 1.3-1.7 (20H, m, $10CH_2$), 2.7 (4H, t, $2ArCH_2$), 4.6 (4H, t, ferrocenyl-H), 4.95 (4H, t, ferrocenyl-H), 7.26 (4H, d, ArH), 7.5 (4H, d, ArH), 7.6 (4H, d, ArH), 7.8 (4H, d, ArH).

IR: υ_{max} cm^{-1} (KBr) 2923, 2851, 1628 (C=O str.), 1602, 1444, 1374, 1292, 1169, 772, 504.

7.6 *Experimental methods - Scheme 6*

In the following section, the preparation of some novel 1,1′-disubstituted ferrocene derivatives **(67)** and **(70)**, based on simple imine condensation reactions of ferrocene-1,1′-dicarboxaldehyde **(51)**. Two independent series of Schiff bases were synthesised by methods outlined in ***Schemes 6a*** and ***6b***.

Scheme 6a

This scheme is concerned with the preparation of Schiff bases derived from certain 4′-n-alkoxy-4-aminobiphenyls **(66)** by the following route. 4-Hydroxybiphenyl was first converted into the corresponding benzoate **(62)** by reaction with benzoyl chloride in the presence of pyridine, prior to nitration using fuming nitric acid. The benzoate moiety promotes the electrophilic attack of the NO_2^+ cation at the 4′-position rather than the 2′-position producing the desired 4′-nitrobiphenyl-4-yl benzoate **(63)**. The ester was then cleaved by a simple base hydrolysis in ethanol. Alkylation of the resulting 4-hydroxy-4′-nitrobiphenyl **(64)** was carried out by heating under reflux with the appropriate 1-bromoalkane in acetone solution in the presence of potassium hydroxide to yield the desired 4′-*n*-alkoxy-4-nitrobiphenyl **(65)**. Reduction by hydrogenation in the presence of palladium on carbon yielded the 4′-*n*-alkoxy-4-aminobiphenyls **(66)** which were then condensed with ferrocene-1,1′-dicarboxaldehyde **(51)** to provide the desired Schiff bases **(67)**, n = 5-7 and 10, in 95% yields.

N.B. 4-aminobiphenyl is a known cancer agent. This synthesis involves the preparation of some 4′-substituted-4-aminobiphenyls **(66)** and hence extreme caution must be taken in carrying out this work; compounds of this type must be treated as cancer suspect agents.

7.6.1 *Preparation of biphenyl-4-yl benzoate* (62)

Benzoyl chloride (18 ml, 0.155 mol) was added, dropwise, to a stirred solution of 4-hydroxybiphenyl (25 g, 0.147 mol) in dry THF (200 ml) and pyridine (1 ml). The reaction mixture was stirred for a further 4 h. before quenching the excess benzoyl chloride by pouring onto 4M-aqueous HCl / ice (200 ml). The resulting slurry was transferred to a separating funnel and the layers separated. The aqueous phase was extracted with DCM (3x50 ml). The extracts were combined with the organic phase and washed with 4M aqueous NaOH (3x50 ml). The organic phase was then dried ($MgSO_4$) before removal of the solvents in vacuo to yield a white precipitate which was recrystallised from ethanol to give the desired ester **(62)** (65%) as white crystals, m.p. 143-145 °C (lit.[91] 148 °C).

NMR: δ_H ppm ($CDCl_3$) 7.2-7.7 (12H, complex m, ArH), 8.2 (1H, d, ArH), 8.25 (1H, d, ArH).

IR: υ_{max} cm^{-1} (KBr) 1732 (C=O str.), 1598, 1486, 1451, 1280, 759, 704, 688.

7.6.2 *Preparation of 4'-nitrobiphenyl-4-yl benzoate* (63)

Fuming nitric acid (62.5 ml) was added, with stirring, over 1 h. to biphenyl-4-yl benzoate **(62)** (25 g, 91.2 mmol) in hot glacial acetic acid (275 ml) at such a rate that the temperature was maintained at 85-95 °C. As the last few ml of nitric acid were added the nitro-ester began to separate from solution. After cooling to room temperature the resulting solid was filtered off and washed with water and sparingly with cold methanol. The product was then recrystallised from acetic acid to yield the pure 4'-nitrobiphenyl-4-yl benzoate **(63)** as a yellow solid (59%), m.p. 208-210 °C (lit.[91] 209-210 °C, lit.[92] 208-212 °C).

No spectral data were obtained for this product as the m.p. indicated it was the desired isomer and T.L.C. revealed only a single spot with no impurities.

7.6.3 *Preparation of 4-hydroxy-4′-nitrobiphenyl* (64)

4′-Nitrobiphenyl-4-yl benzoate **(63)** (17 g, 53.3 mmol) was suspended in ethanol (125 ml) and heated under reflux. The ester was hydrolysed by the careful addition of KOH (12 g) in water (30 ml), which produced an immediate deep red coloration. The mixture was heated under reflux for a further 30 min. to ensure that the hydrolysis was complete. On cooling, blue crystals formed. These were filtered off, dissolved in the minimum volume of hot water and acidified to precipitate the desired 4-hydroxy-4′-nitrobiphenyl **(64)** as a yellow solid (75%), m.p. 197-198 °C (lit.[91] 200-201 °C).

NMR: δ_H ppm ($CDCl_3$) 6.94-6.98 (2H, d, ArH-OH), 7.49-7.52 (2H, d, ArH), 7.68-7.71 (2H, d, ArH), 8.22-8.25 (2H, d, ArH-NO_2), 9.33 (1H, s, ArOH).

IR: υ_{max} cm^{-1} (KBr) 1601, 1501, 1474, 1394, 1179, 1040, 825, 814.

7.6.4 *Preparation of 4-n-alkoxy-4′-nitrobiphenyls* (65)

A mixture of 4-hydroxy-4′-nitrobiphenyl **(64)** (4.41 g, 20.5 mmol), the appropriate *n*-alkylbromide (23 mmol) and acetone (100 ml) was heated gently under reflux, with stirring. To this mixture KOH (0.95 g, 0.017 mol) in water (25 ml) was added, dropwise, during a 2h period. The reaction was heated for a further 12-15h., its progress being monitored by TLC. The resulting mixture was then cooled, poured into water, and extracted with diethyl ether (4x75 ml). The combined organic extracts were then dried ($MgSO_4$) and the excess solvent was removed in vacuo to yield the product as a yellow solid. This was purified by column chromatography on silica gel eluting with 9:1

petroleum ether (b.p. 40-60 °C) : ethyl acetate, affording the desired 4-*n*-alkoxy-4′-nitrobiphenyl **(65)** as yellow crystals: *n*-pentyloxy (61%), m.p. 54-55 °C (lit. [94] 54.5 °C); *n*-hexyloxy (56%), m.p. 67-68 °C (lit.[94] 67 °C); *n*-heptyloxy (67.5%), m.p. 36-37 °C (lit.[94] 36.5 °C); *n*-decyloxy (73%), m.p. 69.5-71.5 °C.

The following data refers to the *n*-heptyloxy derivative:

NMR: δ_H ppm ($CDCl_3$) 0.9 (3H, t, CH_3), 1.3-1.5 (8H, m, $4CH_2$), 1.8 (2H, q, OCH_2CH_2), 4.0 (2H, t, $ArOCH_2$), 6.98-7.02 (2H, d, ArH-OCH_2), 7.55-7.58 (2H, d, ArH), 7.66-7.70 (2H, d, ArH), 8.24-8.28 (2H, d, ArH-NO_2).

IR: υ_{max} cm^{-1} (KBr) 2952, 2923, 2855, 1604, 1501, 1474, 1395, 1179, 1041, 825, 814.

7.6.5 *Preparation of the 4-n-alkoxy-4′-aminobiphenyls* (66)

10% Palladium on carbon (10 mol %) was added to a stirred solution of the appropriate 4-*n*-alkoxy-4′-nitrobiphenyl **(65)** (10.5 mmol), in ethyl acetate (200 ml) and ethanol (80 ml). Hydrogenation was carried out at 25 atm. and was complete after 24 h.

The Pd/C was removed by filtration through Highflo Supercel and the solvent was removed in vacuo. The crude product was subjected to flash column chromatography on silica gel using 1 : 1 petroleum ether (b.p. 40-60 °C) : diethyl ether as the eluent, and purified by recrystallisation from ethanol to yield the desired 4-*n*-alkoxy-4′-aminobiphenyl **(66)** as white plates: *n*-pentyloxy (56%), m.p. 91-92 °C; *n*-hexyloxy (93%), m.p. 94-95 °C; *n*-heptyloxy (97%), m.p. 94-96 °C; *n*-decyloxy (98%), m.p. 98-99.5 °C.

The following data refers to the *n*-heptyloxy derivative:

NMR: δ_H ppm ($CDCl_3$) 0.9 (3H, t, CH_3), 1.3-1.5 (8H, m, $4CH_2$), 1.8 (2H, q, OCH_2CH_2), 3.67 (2H, s, $ArNH_2$), 4.0 (2H, t, $ArOCH_2$), 6.72-6.76 (2H, d, ArH-NH_2), 6.90-6.94 (2H, d, ArH-OCH_2), 7.34-7.37 (2H, d, ArH), 7.42-7.45 (2H, d, ArH).

IR: υ_{max} cm^{-1} (KBr) 3448, 3382, 3280, 3170, 1606, 1501, 1474, 1394, 1179, 1040, 825, 814.

7.6.6 *Preparation of Schiff Bases* (67)

Ferrocene-1,1′-dicarboxaldehyde (0.55 g, 2.2 mmol) **(51)** in hot ethanol (75 ml) was added, dropwise, to a stirred solution of the appropriate 4-*n*-alkoxy-4′-aminobiphenyl **(66)** (4.5 mmol) in ethanol (75 ml) and glacial acetic acid (4-5 drops) while heating under reflux. A red or pink precipitate formed as the addition progressed, and after a further 1 h. of heating under reflux, this was filtered off from the *hot* mixture to avoid the separation of unchanged starting materials from the cold mixture. The precipitate was washed with portions of hot ethanol (5x50 ml) to yield the desired imine **(67)** as a pink solid in an average 95% yield. No recrystallisation was attempted.

The following data refers to the *n*-heptyloxy derivative:

NMR: δ_H ppm ($CDCl_3$) 0.9 (6H, t, $2CH_3$), 1.3-1.6 (16H, m, $8CH_2$), 1.8 (4H, q, $2OCH_2CH_2$), 4.0 (4H, t, $2ArOCH_2$), 4.54 (4H, s, ferrocenyl-H), 4.92 (4H, d, ferrocenyl-H), 6.90-6.93 (4H, d, ArH-OCH_2), 7.12-7.15 (4H, d, ArH), 7.44-7.47 (8H, 2 overlapped d, ArH), 8.35 (2H, s, Ar-CH=N).

IR: υ_{max} cm^{-1} (KBr) 2954, 2923, 2855, 1618, 1606, 1586, 1495, 1467, 1251, 824, 812.

A summary of the thermal data along with a detailed discussion of these compounds is reported in section **8.5**.

Scheme 6b

The synthetic pathway shown in ***Scheme 6b*** leads to the novel diimine **(70)** derived from ferrocene-1,1′-dicarboxaldehyde **(51)**. In contrast to the Schiff bases outlined in ***Scheme 6a***, this compound incorporates an ester linkage as a spacer between the two phenyl rings. The ligand was prepared by a simple esterification reaction between 4-nitrophenol and 4-*n*-octylbenzoic acid in the presence of dicyclohexylcarbodiimide and N,N-dimethylaminopyridine to yield the desired 4-nitrophenyl 4-*n*-octylbenzoate **(68)**. Reduction of the nitro-moiety was achieved by hydrogenation at 25 atm. with a Pd/C catalyst to yield 4-aminophenyl 4-*n*-octylbenzoate **(69)**. The condensation of this amine with ferrocene-1,1′-dicarboxaldehyde **(51)** produced the novel diimine **(70)**.

7.6.7 *Preparation of 4-nitrophenyl 4-n-octylbenzoate* (68)

Dicyclohexylcarbodiimide (4.4 g, 22 mmol) and N,N-dimethylaminopyridine (0.26 g, 2.2 mmol) were added to a stirred solution of 4-nitrophenol (3.48 g, 25 mmol) and commercial 4-*n*-octylbenzoic acid (5 g, 22 mmol) in dry DCM (30 ml) contained in a single-necked flask fitted with a $CaCl_2$ guard tube. The reaction was left to stir overnight before the suspended solid material was removed by filtration through a sintered glass funnel. The solvent was removed in vacuo, and the product obtained was purified by column chromatography on flash silica using 1:1 diethyl ether : petroleum ether (b.p. 40-60 °C) as the eluent. Recrystallisation from ethanol yielded the 4-nitrophenyl 4-*n*-octylbenzoate **(68)** as pale yellow crystals (79 %), m.p. 47.5-49 °C.

NMR: δ_H ppm ($CDCl_3$) 0.9 (3H, t, CH_3), 1.3-1.4 (10H, m, $5CH_2$), 1.6-1.7 (2H, q, $ArCH_2CH_2$), 2.7 (2H, t, $ArCH_2$), 7.30-7.42 (4H, m, ArH), 8.08-8.11 (2H, d, ArH), 8.29-8.32 (2H, d, ArH-NO_2).

IR: υ_{max} cm^{-1} (KBr) 2920, 2865, 1741 (C=O str.), 1518, 1341, 1267, 1201, 1177, 1062, 892, 863, 758, 702.

7.6.8 *Preparation of 4-aminophenyl 4-n-octylbenzoate* (69)

10% Palladium on carbon (10 mol %) was added to a stirred solution of 4-nitrophenyl 4-*n*-octylbenzoate **(68)** (5.6 g, 15.7 mmol) in ethyl acetate (200 ml) and ethanol (80 ml). Hydrogenation was carried out at 25 atm. and was complete after 2 h.

The Pd/C was removed by filtration through Highflo Supercel and the solvents were removed in vacuo. The crude product was then subjected to flash column chromatography on silica gel using 1:1 petroleum ether (b.p. 40-60 °C) : diethyl ether as the eluent, and purified by recrystallisation from ethanol to yield the desired 4-amino-phenyl 4-*n*-octylbenzoate **(69)** as white plates (40%), m.p. 67-69 °C.

NMR: δ_H ppm ($CDCl_3$) 0.9 (3H, t, CH_3), 1.3-1.4 (10H, m, $5CH_2$), 1.6-1.7 (2H, q, $ArCH_2CH_2$), 2.7 (2H, t, $ArCH_2$), 3.68 (2H, s, Ar-NH_2), 6.71-6.74 (2H, d, ArH-NH_2), 6.97-7.00 (2H, d, ArH), 7.30-7.33 (2H, d, ArH) 8.08-8.11 (2H, d, ArH).

IR: υ_{max} cm^{-1} (KBr) 3490, 3400, 1733, 1610, 1512, 1280, 1178, 750.

7.6.9 *Preparation of the Schiff base* (70) *derived from 4-aminophenyl 4-n-octylbenzoate and ferrocene-1,1'-dicarboxaldehyde*

This compound was prepared by the method described in section **7.6.6**.

NMR: δ_H ($CDCl_3$) 0.9 (6H, t, $2CH_3$), 1.3-1.4 (20H, m, $10CH_2$), 1.6-1.7 (4H, q, $2ArCH_2CH_2$), 2.7 (4H, t, $2ArCH_2$), 4.54 (4H, s, ferrocenyl-H), 4.92 (4H, d, ferrocenyl-H), 6.97-7.00 (4H, d, ArH), 7.30-7.33 (4H, d, ArH), 7.88-7.91 (4H, d, ArH), 8.08-8.11 (4H, d, ArH), 8.35 (2H, s, Ar-CH=N).

IR: υ_{max} (KBr) 2955, 2922, 2865, 1739 (C=O str.), 1618, 1606, 1495, 1267, 1199, 892.

The thermal data for this compound is summarised and discussed in section **8.5**.

*7.7 **Experimental methods - Scheme** 7*

The preparative route for a novel chiral 1,1′-disubstituted ferrocene based on the *bis*(4′-n-alkoxybiphenyl-4-yl) ferrocene-1,1′-dicarboxylates **(33)** reported by Bhatt *et al*[66] is given in ***Scheme*** *7*. The reaxtion between ferrocene-1,1′-dicarboxylic acid **(47)** and the chiral ester, R-(-)-1-methylheptyl 4′-hydroxybiphenyl-4-carboxylate **(71)** (kindly donated by Dr I McSherry), was carried out in the presence of dicyclohexylcarbodiimide and N,N-dimethylaminopyridine, affording the chiral ester *bis*-[4′-(R-1-methylheptyloxy-carbonyl)biphenyl-4-yl] ferrocene-1,1′-dicarboxylate **(72)**.

7.7.1 *The preparation of bis[4′-(R-1-methylheptyloxycarbonyl)biphenyl-4-yl] ferrocene-1,1′-dicarboxylate* (72)

Dicyclohexylcarbodiimide (0.31 g, 1.5 mmol) and N,N-dimethylaminopyridine (0.02 g, 0.15 mmol) were added a stirred suspension R-(-)-1-methyl-heptyl 4′-hydroxybiphenyl-4-carboxylate **(71)** (1.5 mmol) and ferrocene-1,1′-dicarboxylic acid **(47)** (1.5 mmol) in dry DCM (50 ml) contained in a single-necked flask fitted with a $CaCl_2$ guard tube. The reaction was left to stir overnight before the suspended solid material was removed by filtration through a sintered glass funnel. The solvent was removed in vacuo, and the desired *bis*[4′-(R-1-methylheptyloxycarbonyl)biphenyl-4-yl] ferrocene-1,1′-dicarboxylate **(72)** was obtained by column chromotography on silica gel using 1:1 ether: petroleum ether (b.p. 40-60 °C) as the eluent. The compound was purified by recrystallisation from ethanol to yield an orange solid (75%), m.p. 148 °C.

NMR: δ_H ppm ($CDCl_3$) 0.88 (6H, t, $2CH_3$), 1.28-1.75 (26H, m, $10CH_2$ + $2R_2C$-CH_3), 4.65 (4H, t, ferrocenyl-H), 4.75 (2H, s, R_3C-H), 5.1 (4H, t, ferrocenyl-H), 7.30-7.36 (4H, d, ArH), 7.60-7.63 (8H, d, ArH), 8.08-8.11 (4H, d, ArH).

IR: υ_{max} cm^{-1} (KBr) 2952, 2925, 2852, 1730 (C=Ostr.), 1704 (C=O str.), 1605, 1275, 1098, 774.

7.8 *Experimental methods - Scheme 8*

The preparative route for the synthesis of bis[N-(4-*n*-butyloxyphenyl)-benzaldimin-4-yl] ferrocene-1,1′-dicarboxylate **(74)** is shown in ***Scheme 8***. Ferrocene-1,1′- dicarbonylchloride **(48)** (see ***Scheme 3***) was reacted with 4-hydroxybenzaldehyde in the presence of triethylamine to yield *bis*(4-formylphenyl) ferrocene-1,1′-dicarboxylic acid **(73)**. Reaction of compound **(73)** with 4-*n*-butyloxyaniline and acetic acid afforded the desired imine **(74)**.

7.8.1 *Preparation of bis(4-formylphenyl) ferrocene-1,1′-dicarboxylate* (73)

An oven-dried flask was purged thoroughly with N_2 and was charged with ferrocene-1,1′-dicarbonyl chloride **(48)** (1 g, 3.2 mmol), 4-hydroxybenzaldehyde (0.78 g, 6.4 mmol), dry DCM (75 ml) and triethylamine (0.74 g, 7.36 mmol). The reaction mixture was stirred at room temperature for 16h and then heated under reflux for 5h. The contents of the flask were cooled, transferred to a separating funnel and the aqueous layer was isolated and discarded. The organic layer was washed successively with 4% hydrochloric acid, sodium hydrogen carbonate and water, dried ($MgSO_4$) and the solvent was removed in vacuo. Purification was attempted by the method of Reddy and Brown[23] via column chromatography using 1:4 diethyl ether : ethyl acetate as the mobile phase. This proved to be far too polar and elution was successfully carried out with 3:1 petroleum ether (b.p. 40-60 °C): ethyl acetate as the eluent. Further purification was achieved by dissolving the product in the minimum amount of hot ethyl acetate before adding petroleum ether (b.p. 40-60 °C) to precipitate the desired compound, *bis*(4-formylphenyl) ferrocene-1,1′-dicarboxylate **(73)**, 1.1 g (71%) as an orange powder, m.p. 118-120 °C.

^{1}H NMR δ ppm ($CDCl_3$) 4.66 (4H, s, ferrocenyl-H), 5.09 (4H, d, ferrocenyl-H), 7.35-7.38 (4H, d, ArH), 7.88-7.91 (4H, d, ArH), 9.99 (2H, s, CHO).

υ_{max} cm^{-1} (KBr) 1724, 1694, 1599, 1586, 1456, 1277, 1020, 914.

7.8.2 *Preparation of bis[N-(4-n-butyloxyphenyl)benzaldimin-4-yl] ferrocene-1,1'-dicarboxylate* (74)

4-*n*-Butyloxyaniline (0.3 g, 1.7 mol) in ethanol (40 ml) was added to *bis*(4-formylphenyl) ferrocene-1,1'-dicarboxylate **(73)** (0.4 g, 0.82 mol) and DCM (20 ml). Glacial acetic acid (4 drops) was added to the reaction mixture which was then stirred at room temperature for 15h. Insoluble material was removed via filtration and ethanol was added to the solution. The product, an orange solid, separated out and was collected by filtration. The *bis*[N-(4-*n*-butyloxyphenyl)benzaldimin-4-yl] ferrocene-1,1'-dicarboxylate **(74)**, 0.25 g (39%) was obtained as orange crystals, m.p. 180 °C.

^{1}H NMR δ ppm ($CDCl_3$) 0.98 (6H, t, $2CH_3$), 1.5 (4H, m, $2CH_2$), 1.7 (4H, q, $2ArOCH_2CH_2$), 4.0 (4H, t, $2ArOCH_2$), 4.64 (4H, s, ferrocenyl-H), 5.09 (4H, d, ferrocenyl-H), 6.91 (4H, d, ArH-OCH_2), 7.25 (4H, d, ArH), 7.29 (4H, d, ArH), 7.88-7.91 (4H, d, ArH), 8.46 (2H, s, Ar-CH=N).

υ_{max} cm^{-1} (KBr) 1727, 1715, 1509, 1467, 1284, 1168.

The thermal data for this compound is summarised and discussed in section **8.2**.

8. *Discussion of the effect of the central linking group, X, on the thermotropic behaviour of some 1,1′-bis(4′-n-alkyl(oxy)biphenyl-4-yl)ferrocenes*

8. *Discussion of the effect of the central linking group, X, on the thermotropic behaviour of some 1,1'-bis(4'-n-alkyl(oxy)biphenyl-4-yl)ferrocenes*

8.1 *Introduction*

A review of the current literature regarding ferrocene liquid crystalline systems (section **6.5**), revealed that the vast majority of compounds synthesised to date were esters derived from either ferrocene-1,1'- **(47)** or -1,3-dicarboxylic acid **(75)**.

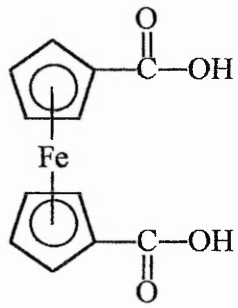

(47)

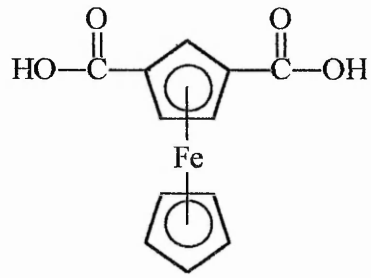

(75)

The chemical versatility of ferrocene **(45)** as a synthetic building block is well documented,[78,79,80] and hence this concentration upon systems derived purely from carboxylic acids seemed rather limited in its approach, given the possible variety of chemical linkages that could be introduced. Consequently an investigation was initiated with the aim of synthesising some novel derivatives, where the ferrocene atom is connected to an organic core by a range of different linking groups.

However, when designing a ferrocene-containing compound with the potential to form liquid crystals certain factors need to be taken into consideration. Two extensive studies on the incorporation of a ferrocene moiety into a liquid crystalline system have been published by Deschenaux *et al.*[55] and Thompson *et al.*[73] Both authors suggest

that mesogenic activity can only be sustained if the molecular length of the molecule is sufficiently extended to compensate for the increase in the molecular breadth that the molecule introduces. This would otherwise lead to a decreased anisotropy of molecular polarisability, which in turn would depress any possible mesogenic behaviour the compound may show.

Hence, to best study the effect of changing the central linking group, it was decided to concentrate on modifications to a system that had already proved to be liquid crystalline, this being the *bis*(4′-*n*-alkoxybiphenyl-4-yl) ferrocene-1,1′-dicarboxylates **(33)** reported by Bhatt *et al*[66] in 1988.

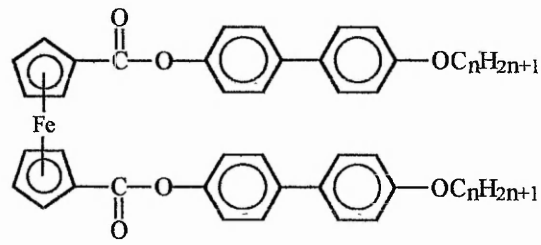

(33)

Of the eight 1,1′-diesters reported, three derivatives, the n = 5, 6 and 11 members, gave rise to monotropic smectic behaviour over a narrow temperature range (the mesophase transition temperatures for these compounds are listed in **Table 22**, p.211). This is in marked contrast to the 4′-*n*-alkoxybiphenyl-4-yl cycloalkanecarboxylates (**7-11**) discussed in section **4.0**, which gave rise to smectic behaviour for most of the derivatives synthesised.

Three different types of linking group, **X** (**Fig.33**), were investigated and the relative effectiveness of each in stabilising mesophase formation in ferrocene systems is then discussed, drawing comparisons with the original 1,1′-diesters of Bhatt *et al.*

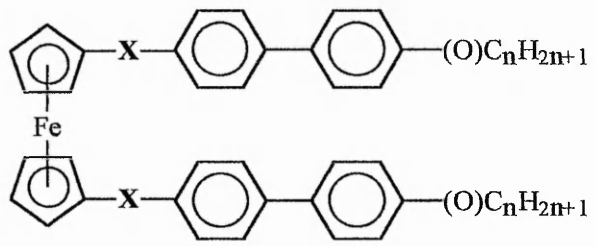

Fig.33 - The position of the central linking group, X.

These linking groups are listed below:

(i) a $-CH_2-O-\overset{O}{\overset{\|}{C}}-$ 'reversed' ester linking group

- compounds **(58)** and **(59)**;

(ii) acyl linking groups - compounds **(60)** and **(61)**;

(iii) Schiff base linking groups - compounds **(67)** and **(70)**.

The preparative routes for the novel ferrocene systems based on these linking groups are summarised in sections **7.4-7.6**, and are discussed in sections **8.3**, **8.4** and **8.5** respectively. In addition to the above systems, two other compounds derived from ferrocene-1,1′-dicarboxylic acid **(47)** were also synthesised. The first of these, discussed briefly overleaf (section **8.1**), is a repeat synthesis of a single homologue of the *bis*[N-(4-*n*-alkyloxyphenyl)benzaldimin-4-yl] ferrocene-1,1′-dicarboxylates **(74)** first reported by Reddy and Brown[72] (***Scheme 8***). The second compound **(72)** was prepared in order to study a ferrocene liquid crystal incorporating a chiral moiety (***Scheme 7***).

8.2 *Initial study of the synthesis of a ferrocene liquid crystal system: bis[N-(4-n-butyloxyphenyl)benzaldimin-4-yl] ferrocene-1,1'-dicarboxylate* (74)

Initially, in order to become familiar with ferrocene chemistry and with liquid crystalline ferrocene derivatives, it was decided to repeat the synthesis of a member of the *bis*[N-(4-*n*-alkyloxyphenyl)benzaldimin-4-yl] ferrocene-1,1'-dicarboxylates **(74)** reported by Reddy and Brown[72] in 1992. These compounds all give rise to mesogenic behaviour. The lower homologues, n = 4-7, give rise to a nematic mesophase on cooling the isotropic liquid, whereas on cooling the isotropic liquid of the homologues n = 8-12, an S_A phase is observed.

(74)

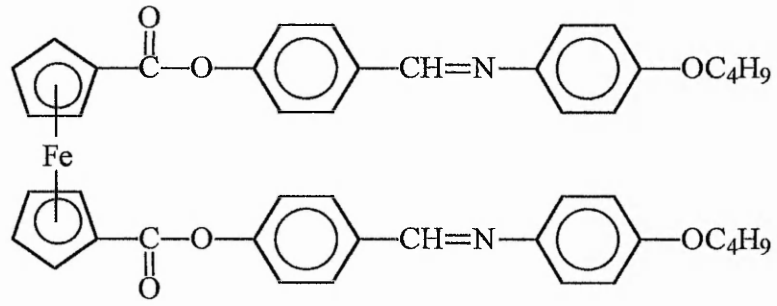

As part of the initial studies to establish suitable synthetic routes to mesogenic ferrocene-containing systems, the n = 4 derivative **(74)** of the homologous series was prepared. The synthetic route for this compound is discussed in section **7.8**, (***Scheme 8***). The mesophase transition temperatures for this derivative are listed in **Table 19**, along with the literature value quoted for this derivative.

As reported, the butyloxy derivative gives rise to a monotropic nematic phase on cooling the isotropic liquid. A slight difference in the observed and reported mesophase transition temperatures can be seen, which is most likely due to impurities within the sample. A photographic plate of this texture is shown in ***Appendix* 1, Plate K**.

Table 19 - *A comparison of the mesophase transition temperatures (°C) for bis[N-(4-n-butyloxyphenyl)benzaldimin-4-yl] ferrocene-1,1'-dicarboxylate* (74)

	C-N	N-I
Reported Values	180	191
Actual Values	186	195

With the success of this repeat synthesis, the emphasis of the study now turned to the investigation of the effect of incorporating a range of central linking groups between the ferrocene and biphenyl moieties, which is discussed in more detail in the following sections.

8.3 *Investigations into the effect of reversing the linking ester moiety*

In 1993, Deschenaux *et al.*[75] reported the synthesis of two series of 1,1′-disubstituted ferrocene derivatives, of the general formula shown by compounds **(41)** and **(42)** below, which differ only in the mode of linkage of the ester function within the rigid organic core. The liquid crystal properties of these series (discussed briefly in section **6.5.2**) were found to be strongly dependent upon the orientation of the ester moiety with **(42)** giving rise to the majority of observed mesogenic activity.

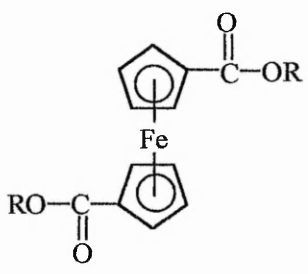

where R =

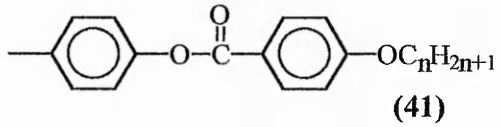

(41)

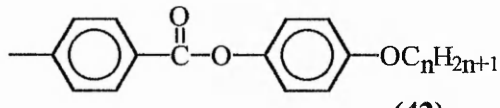

(42)

The authors suggest that the difference in liquid crystalline behaviour shown by the two series of compounds is related to a combination of electron delocalisation and rotational motion effects around the ester function. Compounds of the type **(42)** show more extensive conjugation near the centre of the molecule, as well as reduced rotation around the ester moiety, in comparison with those of type **(41)**, leading to an increase in the anisotropy of molecular polarisability and hence, compounds **(42)** give rise to the greater mesogenic character (**Fig.34**).

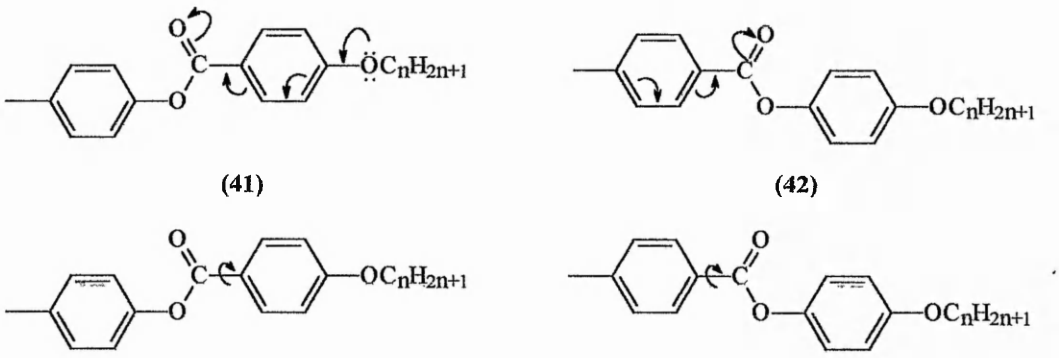

Fig.34 - ***Diagram showing comparative electron delocalisation and rotational motion for compounds*** **(41)** ***and*** **(42)**

With this in mind, it was thought to be of interest to investigate the possible effects on mesogenic behaviour caused by reversing the direction of the ester function at the ferrocene moiety itself, producing the opposite orientation of the linkage seen so frequently in the majority of compounds reported to date. However, the obvious starting material, 1,1′-*bis*(hydroxy)ferrocene is an unstable, air sensitive compound which can only be prepared and used in situ.[79] A convenient alternative was found in the disubstituted methyl alcohol, 1,1′-*bis*(hydroxymethyl)ferrocene **(50)**, which was readily synthesised from ferrocene-1,1′-dicarboxylic acid **(47)** in good yields (71%) (***Scheme* 3**).

This also provided an opportunity to study the influence of introducing a 1,1′-ferrocene-CH_2- unit into some existing liquid crystalline systems.

Two compounds incorporating the desired 'reversed orientation' of the ester linkage were prepared in moderate yields by the methods detailed in sections **7.2.7** and **7.2.6** respectively (***Scheme 4***), these being 1,1′-ferrocenyl*bis*(methyl *trans*-4-*n*-heptylcyclohexanecarboxylate) **(59)** and 1,1′-ferrocenyl*bis*(methyl 4′-*n*-heptylbiphenyl-4-carboxylate) **(58)**, respectively. Each of these compounds will now be discussed individually.

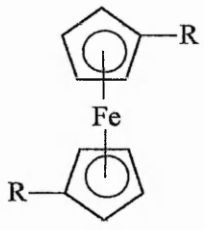

Where R =

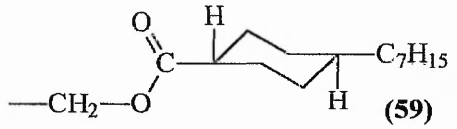

(59)

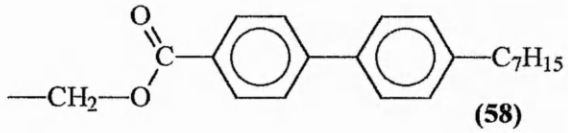

(58)

8.3.1 *1,1′-ferrocenylbis(methyl trans-4-n-heptylcyclohexanecarboxylate)* (59)

On observation of this homologue by thermal optical microscopy no mesogenic behaviour was observed either on heating to (m.p. 77.8 °C) or from the isotropic liquid. Although the *trans*-4-*n*-alkylcyclohexyl carboxylic acids are themselves liquid crystalline[13] (mesophase transition temperatures for the *n*-heptyl derivative: **C-N** 39 °C, **N-I** 101 °C) due to their ability to form dimers by hydrogen bonding, the lack of mesogenic activity of 1,1′-ferrocenyl*bis*(methyl trans-4-*n*-heptylcyclohexanecarboxylate) **(59)** was not unexpected. The structure of the acid dimer is interrupted by the incorporation of both -CH_2- spacers and the ferrocene moiety itself. The methylene

spacer groups increase the flexibility of the system leading to deviations from the rigid lath-like molecular structure that is required for a calamitic liquid crystalline system. The ferrocene core itself greatly increases the molecular breadth of the system, which again leads to a destabilisation of mesogenic behaviour. In an attempt to overcome these structural disadvantages, the biphenyl analogue **(58)** was synthesised in the expectation that the extra ring of the biphenyl system would increase both the molecular length:breadth ratio and the anisotropy of molecular polarisability sufficiently for the compound to show mesomorphic properties.

8.3.2 *1,1′-ferrocenylbis(methyl 4′-n-heptylbiphenyl-4-carboxylate)* (58)

The liquid crystalline behaviour of the 4′-*n*-alkylbiphenyl-4-carboxylic acids is documented,[90] with the *n*-heptyl derivative showing the following mesomorphic transitions:

C-S 156 °C, **S-N** 243 °C, **N-I** 262 °C.

The carboxylic acids are dimeric due to hydrogen bonding. It was hoped that the diesters would have sufficient length and rigidity to withstand the incorporation of the 1,1′-ferrocene-CH_2- unit and hence retain some liquid crystal properties.

However, thermal optical microscopy failed to reveal any mesomorphic behaviour for 1,1′-ferrocenyl*bis*(methyl 4′-*n*-heptylbiphenyl-4-carboxylate) **(58)** on heating to (m.p. 138 °C) or cooling from the isotropic liquid.

8.3.3 *Summary*

It is not possible to conclude whether the lack of mesogenic behaviour can be attributed to the 'reversed orientation' of the ester function or the introduction of the -CH_2- spacer at the ferrocene moiety, or indeed a combination of these changes. The proposed argument expounded by Deschenaux et al.,[75] with the reversal in the direction of orientation of the ester function leading to extensive conjugation away from the centre of the molecule, can also be applied to this system.

It had been hoped that the introduction of a -CH_2- moiety would be tolerated by a ferrocene-containing mesogen. Indeed such compounds have been reported within the literature,[59,68] although a destabilising effect on the mesogenic character of such systems is seen when compared with the analogous compounds in which the CH_2-spacer is absent. Although the introduction of the sp^3 hybridised carbon atom adjacent to the ferrocene moiety may lower the melting point of such systems, it introduces a degree of flexibility which affects both the molecular rigidity and polarisability of the molecule.

An accurate assessment as to whether this 'reversed orientation' of the ester linkage could be incorporated successfully into ferrocene containing liquid crystal compounds would require a more extensive study. Often, only certain members of a homologous series give rise to mesogenic behaviour and therefore this investigation needs to be extended to encompass a wider range of homologues of type **(58)**. It is clear, however, that in the systems studied the inclusion of the 1,1′-ferrocene-CH_2- unit was not conducive to liquid crystal behaviour.

8.4 *Investigations into the inclusion of an acyl linkage*

The susceptibility of the ferrocene nucleus to Friedel-Crafts acylation has been extensively documented.[78,80] Indeed, the synthesis of 1,1′-diacetylferrocene **(46)** had proved to be one of the most successful preparations undertaken with consistently good yields (76%). Although some mono-substituted product is also formed, the desired disubstituted derivative could be separated with relative ease by column chromatography. Many liquid crystalline systems containing bezenoid rings which incorporate an acyl function have been reported,[13,90] indicating that this type of linkage can be tolerated within a mesogenic system. Hence, Friedel-Crafts acylation appeared to offer an attractive route to some novel ferrocene derivatives.

In many respects ferrocene **(45)** is analogous to benzene with both compounds being electron rich and therefore highly susceptible to electrophilic attack. Ferrocene, however, reacts more rapidly than benzene, as is shown by their relative rates of reaction for Friedel-Crafts acylation.[78]

	relative reaction rate
ferrocene	3.3×10^6
benzene	1.0

The amount of electrophilic substitution in the acylation reaction is controlled by the quantity of Lewis acid added, with an excess leading to a predominately disubstituted product. It is significant to note that in the acetylation of ferrocene, the unsubstituted ring of the monoacylated derivative is more susceptible to electrophilic attack than benzene, even though it is strongly deactivated by the acyl moiety.

With these thoughts in mind, the preparation of some 1,1′-diketones was undertaken utilising the 4′-*n*-alkylbiphenyl-4-carbonyl chlorides **(57)** (see ***Schemes 4*** and ***5***).

The initial target compounds of this investigation were two 1,1′-disubstituted ferrocenes derived from 4′-*n*-alkylbiphenyl-4-carbonyl chloride **(57)**, n = 7 and 10. However, although the diacylation utilising the n = 7 homologue proceeded with relative ease (compound **(61)**, n = 7), the mono-substituted derivative **(60)**, n = 7, predominated in the final reaction mixture. This was not the expected outcome, with the literature indicating that a disubstituted product is favoured when an excess of Lewis acid is used. This unusual behaviour was even more pronounced when the acylation was attempted with the n = 10 homologue **(57)**, which failed to provide any of the desired 1,1′-disubstituted compound **(61)**, n = 10, only yielding the mono-substituted derivative **(60)**. Attempts to acylate this mono-substituted compound directly with a further amount of 4′-*n*-decylbiphenyl-4-carbonyl chloride **(57)**, n = 10 also met with no success. The failure to obtain the desired 1,1′-disubstituted product **(61)**, n = 10, may be due to steric factors, as the acid chloride involved is such a large molecule. This argument is supported by a comprehensive study on the mono- and di-acylation of ferrocene,[80] which shows that yields of disubstituted products fall greatly as the length of the alkyl chain is increased:

Acylating Agent	*% Yield*
CH_3COCl	76
$CH_3(CH_2)_6COCl$	65
$CH_3(CH_2)_8COCl$	41
$CH_3(CH_2)_{10}COCl$	44
$CH_3(CH_2)_{11}COCl$	15
$CH_3(CH_2)_{14}COCl$	12

When studied by thermal optical microscopy, neither the mono- nor the di-substituted ketones gave rise to mesogenic behaviour. The melting points for these compounds are listed in **Table 20**.

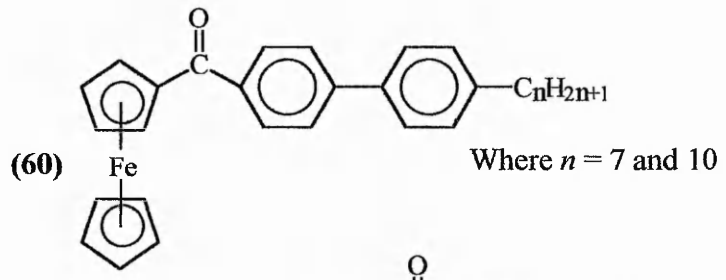

(60) Where $n = 7$ and 10

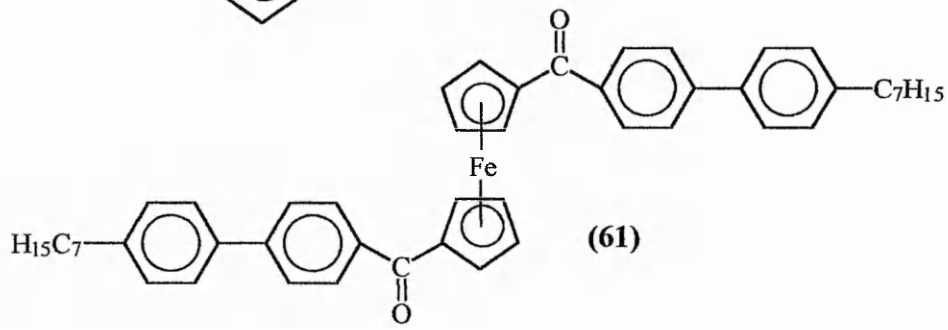

(61)

Table 20 - *Melting points / °C for*

***(a) the mono-substituted ketones*(60)**		***(b) the 1,1'-disubstituted ketone*(61)**	
$n = 7$	165	$n = 7$	192
$n = 10$	163		

It had been hoped that Friedel-Crafts acylation would provide a direct route to some novel mesomorphic ferrocene derivatives. The disubstituted compound **(61)**, $n = 7$ possesses an extended conjugation system which it was hoped would aid the formation of liquid crystals. The lack of mesogenic behaviour observed for the homologue synthesised **(61)**, $n = 7$, may arise from the bond angle of the acyl moiety causing a deviation from the lath-like geometry of the molecule, as discussed by Gray.[13] Extension to the molecule to increase the length to breadth ratio may well lead to liquid crystal properties.

The monosubstituted derivatives **(60)**, n = 7 and 10 were obtained as the predominant product in the synthesis of the desired 1,1′-diketones **(61)**. The failure of these compounds to show any mesomorphic character is most likely due to the inadequate molecular length to breadth ratio.

8.4.1 *Summary*

The possible importance of Friedel-Crafts acylation in providing novel ferrocene mesogens should not be discounted with the failure of these particular compounds to display liquid crystal behaviour. Their relative ease of preparation and separation by column chromatography indicate that further research in this area could indeed prove worthwhile.

8.5 *Investigation into the incorporation of a Schiff base linkage*

Although ferrocene containing liquid crystals incorporating a Schiff base moiety have been known for some time,[59,72] there have been no reported investigations of any 1,1′-disubstituted ferrocenes linked directly to the organic system by a Schiff base function.

Ferrocene-1,1′-dicarboxaldehyde **(51)** was chosen as a convenient starting point in the synthesis of derivatives containing this moiety, being easily prepared by the oxidation of the corresponding 1,1′-*bis*(hydroxymethyl)ferrocene **(50)** (***Scheme 3***). This route was chosen as the preferred method to the dicarboxaldehyde **(51)**, as the direct synthesis, by metallation and subsequent formylation of ferrocene, reported by Balavoine *et al.*[86] was found to be unsatisfactory (a pure product could not be separated from the complex mixture obtained). Ferrocene-1,1′-dicarboxaldehyde **(51)** has the added advantage of being relatively air stable in comparison with the alternative amine starting material, 1,1′-diaminoferrocene,[93] which could also have been used for preparing compounds of this type.

Having obtained the dicarboxaldehyde **(51)**, a suitable amine was required which would be likely to exhibit mesogenic properties when condensed to form a Schiff base derivative.

With this in mind, four members of a homologous series of 4-*n*-alkoxy-4′-aminobiphenyls **(66)** were synthesised, which it was hoped would provide a sufficiently extended organic system to give rise to mesogenic behaviour. It is interesting to note that the precursors to these compounds, the 4-*n*-alkoxy-4′-nitrobiphenyls **(65)**, are themselves liquid crystalline and had been reported by Gray *et al.*[94] as giving rise to monotropic or marginally enantiotropic nematic phases on cooling the isotropic liquid.

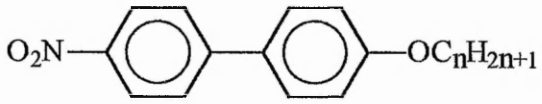

(65)

The condensation reaction between ferrocene-1,1′-dicarboxaldehyde and the 4-*n*-alkoxy-4′-aminobiphenyls proceeded smoothly with the desired imine **(67)** forming as a precipitate in the reaction mixture (***Scheme 6a***).

The *bis*[N-(4′-*n*-alkoxybiphenyl-4-yl)]ferrocene-1,1′-dialdimines **(67)** were investigated by thermal optical microscopy and differential scanning calorimetry, the transition temperatures and associated enthalpy data for the homologues synthesised are listed below in **Table 21**, together with the mesophase transition temperatures of the analogous *bis*(4′-*n*-alkoxybiphenyl-4-yl) ferrocene-1,1′-carboxylates **(33)** reported by Bhatt *et al*[66] which are given in **Table 22**.

8.5.1 *Thermal optical microscopy and DSC studies*

A direct comparison of the *bis*[N-(4′-*n*-alkoxybiphenyl-4-yl)]ferrocene-1,1′-dialdimines **(67)** can be made with the analogous *bis*(4′-*n*-alkoxybiphenyl-4-yl) ferrocene-1,1′-carboxylates **(33)** reported by Bhatt *et al.*[66] in 1988. Of the eight diester homologues synthesised, three derivatives, the n = 5, 6 and 11 members, gave rise to monotropic smectic phases over a narrow temperature range of 8-10 °C.

Heating the n = 5 and 6 members of *bis*[N-(4′-*n*-alkoxybiphenyl-4-yl)] ferrocene-1,1′-dialdimines **(67)**, led to the decomposition of the samples and these compounds were not investigated further. However on heating, the n = 7 homologue gives rise to an isotropic melt, although on cooling, no liquid crystalline behaviour was observed with recrystallisation of the isotropic liquid occurring at 196 °C.

Table 21 - ***Transition temperatures (°C) for the bis[N-(4'-n-alkoxybiphenyl-4-yl)] ferrocene-1,1'-dialdimines*** **(67)**

n	C-I	I-S_1	S_1-S_2	I-C	S_2-C
5	212(dec.)	-	-	-	-
6	210(dec.)	-	-	-	-
7	208	-	-	196	-
10	206	194	184	-	140

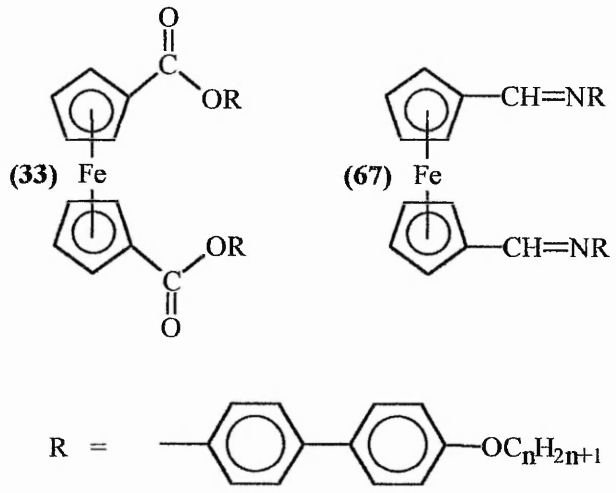

Table 22 - ***Transition temperatures (°C) of the reported[66] bis(4'-n-alkoxybiphenyl-4-yl) ferrocene-1,1'-carboxylates*** **(33)**

n	C-I	I-S_C	I-S_A	S_C/S_A-C	I-C
5	167	140	-	129	-
6	181	139	-	132	-
7	180	-	-	-	146
10	161	-	-	-	146
11	163	-	141	132	-

When studied by differential scanning calorimetry, the cooling cycle of the $n = 7$ homologue shows several unresolved peaks, shown in ***Appendix 2*, DSC 15**. These are almost certainly associated with crystal-crystal transitions, however the possibility of the formation of an unidentified, narrow range mesophase should not be discounted, although this is not confirmed by optical microscopy.

The $n = 10$ homologue provides the most interesting optical behaviour of the members investigated. On heating, the crystalline solid melts to give the isotropic liquid at 206 °C. However on cooling the isotropic liquid, an unknown phase, S_1, forms at 194 °C, which appears as regions of indistinct texture interspersed by dark, homeotropic regions. Further cooling of this phase leads to textural change at 184 °C, to another unidentified phase, S_2. This phase is characterised by the disappearance of some of the visible areas of texture in the previous S_1 phase (i.e. the regions become homeotropic). Further cooling reveals no further phase changes until crystallisation occurs at 140 °C. The phases observed were red in colour. However, despite the optical conclusions, the DSC data for this compound could lend no supporting evidence for any phase changes other than that of melting and crystallisation.

The nature of these phases, if they do exist, has not been investigated further, and therefore it is not possible to ascribe the observed textures as those of new (previously unknown) liquid crystal phases. Following discussion with Professor Duncan Bruce,[95] it was suggested that the observed textures may indicate the formation of cubic phases.[48] An alternative explanation of the unusual nature of these phase types may be the formation of a plastic crystal as reported by Verbit *et al.*[88] for the monosubstituted ferrocenecarboxaldehyde **(52)**. Indeed, Graham *et al.*[96] had originally reported that "ferrocenecarboxaldehyde exhibits a liquid crystalline state between 45 °C and 124.5 °C".

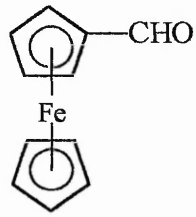

(52)

However, Verbit and co-workers reported that "at 43.5 °C, the reddish-brown birefringent crystals undergo a sharp transition involving loss of birefringence.....no further change is observed on further heating until at 123.5 °C" when the isotropic liquid was formed. This intermediate phase was reported as exhibiting high viscosity when stressed, and persisted over an 80 °C range. These findings led the authors to suggest that ferrocenecarboxaldehyde was in fact a plastic crystal, which was later supported with Mössbauer spectroscopy investigations by Wilson *et al.*[97] However, although comparisons may be drawn between the reported optical textures for ferrocenecarboxaldehyde and *bis*[N-(4′-*n*-alkoxybiphenyl-4-yl)] ferrocene-1,1′-dialdimines **(67)**, $n = 10$, the molecular structure of the diimine does not lend itself to this explanation, as compounds that exhibit plastic crystal properties have considerable rotational freedom in the crystal lattice.[27,97] It would also be expected that a plastic crystal transition would be observed by DSC and as stated previously, the $n = 10$ derivative does not show any transitions of this kind when investigated by this technique. X-Ray analysis of the diimine might provide a more definitive answer.

8.5.2 *Summary*

The -CH=N- imine linkage had been expected to show an increase in mesophase transition temperatures in comparison with the corresponding ester linkage, as reported by Gray[13] (change fron -COO- to -CH=N- normally increases T_{N-I}). In fact the C-I

transition temperatures for the Schiff bases are on average 36.75 °C higher than those observed for the corresponding diesters. However, apart from the unusual optical textures observed on cooling the $n = 10$ homologue, the incorporation of the Schiff base linkage shows an overall destablising effect, leading to the absence of mesogenic properties. The lack of liquid crystallinity may be due to increased molecular broadening, leading to a decrease in the molecular anisotropy of the molecule, due to the introduction of the imine linkage, as discussed by Gray[13] (see **Fig.35**). However, an extension of this series to incorporate higher homologues may reveal some mesogenic character.

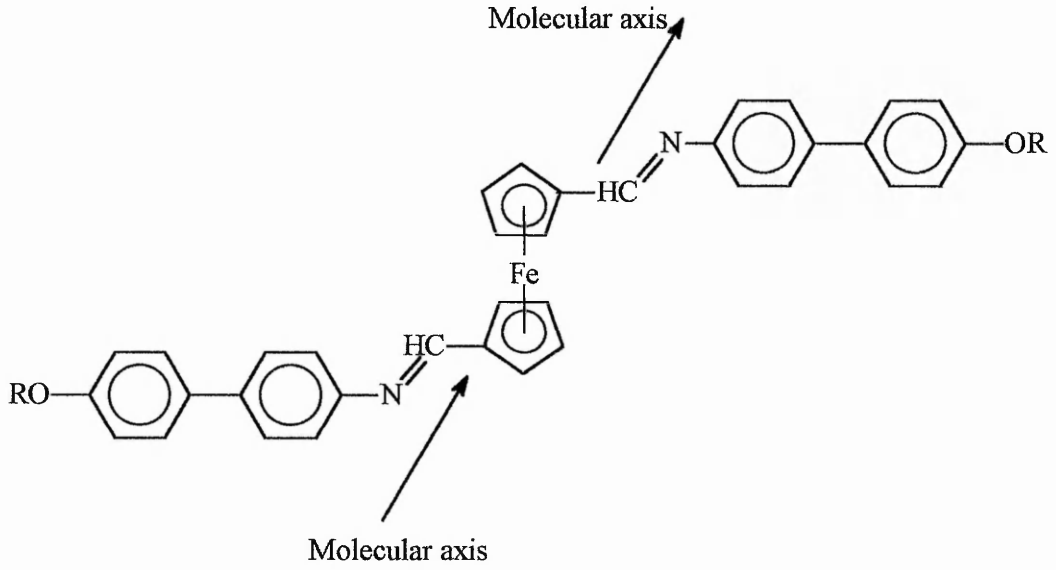

Fig. 35 - The possible deviation from the molecular axis caused by the introduction of the imine linkage

8.5.3 *A study of the effect of extending the molecular length*

With the failure of the *bis*[N-(4′-*n*-alkoxybiphenyl-4-yl)] ferrocene-1,1′-dialdimines **(67)** to give rise to a liquid crystal phase, a synthesis was undertaken to prepare a similar compound which contained a more extended molecular core. The two phenyl rings of the biphenyl moiety were separated by a central ester linkage, orientated

towards the ferrocene unit, providing the extended Schiff base analogue **(70)** of the 1,1′-diesters **(43)**, reported by Deschenaux *et al.*[75] discussed in section **8.3**. Only the n = 8 homologue of these 1,1′-diimines **(70)** was prepared (***Scheme 6b***).

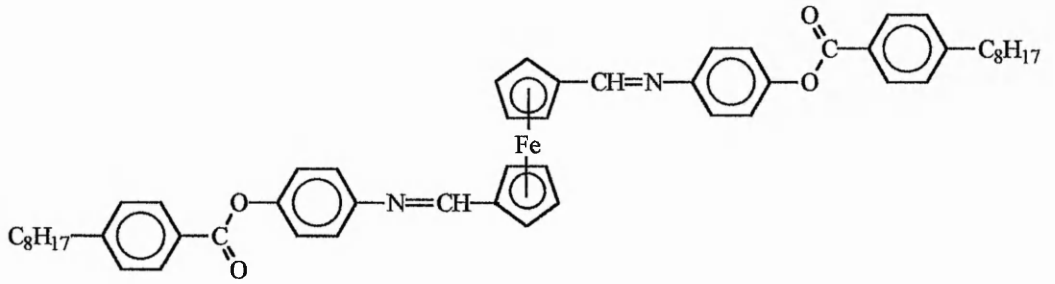

(70)

Investigation of this derivative by thermal optical microscopy failed to indicate the presence of any mesophases with the compound melting to give the isotropic liquid at 162 °C. However, DSC analysis (***Appendix 2***, **DSC15**) indicates a reversible phase change at approximately 60 °C. Rapid cooling from the isotropic melt does give rise to an unusual crystal texture, which changes rapidly to a more usual optical texture indicating that this compound may exhibit a polymorphic crystal phase. This unusual crystal texture does, however, closely resemble the columnar disordered phases,[98] and a photomicrograph of this texture is displayed in ***Appendix 1***, **Plate L**.

As with the analogous diesters reported by Deschenaux *et al.*[75] the orientation of the central ester linkage in these diimines **(70)** may indeed be crucial to the formation of a liquid crystal phase. Hence, future work could be directed at the synthesis of compounds containing the central ester linkage orientated away from the ferrocene moiety, to encourage conjugation nearer the centre of the molecule and also reduce the effects of rotation about the central ester function (see **Fig.34**, section **8.3**). This would provide an analogous series of compounds to those described by Deschenaux **(42)** in section **8.3**, and may well give rise to the increased mesogenic character observed for these diesters.

8.6 *The introduction of a chiral moiety*

In recent years there has been great interest in the field of liquid crystals containing a chiral moiety.[32,33] The incorporation of such a function into mesogenic systems has led to the discovery of many new phases[32,33] and has dramatically increased the switching times of liquid crystal displays.

It was thought of interest to attempt the synthesis of a chiral derivative of a compound similar to those reported by Bhatt *et al.*[66] The chiral ester, R-(-)-1-methyl-heptyl 4′-hydroxybiphenyl-4-carboxylate **(71)** was kindly donated by Dr I McSherry and was used to esterify ferrocene-1,1-dicarboxylic acid **(47)** using DCC and DMAP (***Scheme*** *7*).

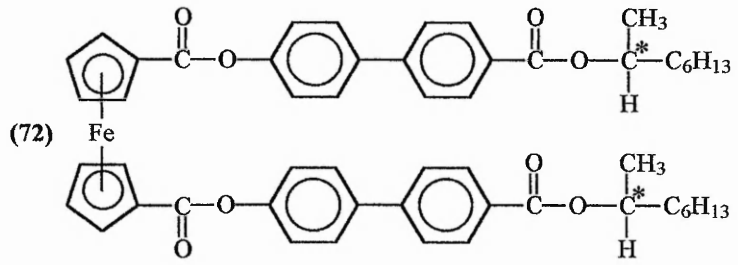

Thermal optical microscopy investigations of *bis*[4′-(R-1-methylheptyloxy-carbonyl)biphenyl-4-yl] ferrocene-1,1′-dicarboxylate **(72)** revealed no mesophases, either on heating (m.p. 148 °C) or cooling (I-C 113 °C). However, on leaving the slide overnight after such a heating and cooling cycle, a restructuring of the crystalline phase was observed, with the compound exhibiting an unusual platelet texture in many areas of the slide, reminiscent of a ***columnar phase***.[48]

The failure of this compound to exhibit any liquid crystalline behaviour was, once again, disappointing. As previously discussed, the analogous *bis*-(4′-*n*-alkoxybiphenyl-4-yl) ferrocene 1,1′-dicarboxylates **(33)** reported by Bhatt *et al.*[66] are indeed liquid crystalline. The substitution of ferrocene for a 4-*n*-alkoxybenzoate moiety also provides some standard ferroelectric liquid crystalline systems.[33] However, the compound **(72)** did show a relatively low melting point for a 1,1′-disubstituted ferrocene derivative, and the isotropic liquid could be cooled to 35 °C below the melting point, but no mesophases were detected. It is not known why this derivative did not give rise to a liquid crystal phase, but the synthesis and investigation of further homologues of this series may afford some mesogenic compounds.

8.7 *Reflections on ferrocene containing metallomesogens*

The investigations carried out so far have proved to be more limited in scope than initially hoped for. The difficulties experienced with the early attempted syntheses imposed time constraints upon this project, and so only one or two homologues of each compound type have been synthesised. It is therefore difficult to comment decisively on the lack of mesomorphic properties shown by the homologues containing the different types of linkage studied, as a review of the literature indicates that often only a few compounds within a homologous series will reveal to any liquid crystalline properties. However, with this in mind, the apparent order of (mesophase) thermal stability for the compounds investigated is:

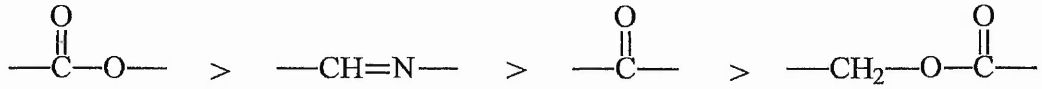

This order is based on the observed evidence that:

(a) the 1,1′-diesters derived from ferrocene-1,1′-dicarboxylic acid **(47)** promote liquid crystalline behaviour more than the other 1,1′-disubstituted linkages investigated.

(b) the 1,1′-diimines **(67)** give rise to the most interesting thermal behaviour of the compounds investigated and possess a higher $T_{C\text{-}I}$ (m.p.) than compounds containing the other linking groups studied.

(c) the 1,1′-diketones **(61)** have a higher $T_{C\text{-}I}$ (m.p.) than the esters, **(58) and (59)**, studied with 'reversed orientation' and containing a -CH_2- spacer.

Further analysis without more information would be purely speculative. However, of the compounds investigated, it is felt that the most promising direction for future study is to concentrate on the synthesis of compounds derived from ferrocene-1,1′-dicarboxaldehyde **(51)**. An extension of the linear core may give rise to mesomorphic compounds. The synthesis of a 1,3-homoannular diimine system would be of great interest as the corresponding 1,3-diesters possess more linear molecular geometry and show the most extensive liquid crystalline behaviour of any of the ferrocene systems synthesised to date.

9. *References*

9.0 *References*

1. Reinitzer, F., *Monatsh. chem.*, **9**, 421 (1888); Reproduced in *Liquid Crystals* **5(1)**, 7-18 (1989).
2. Lehmann, O., *Z. Phys. Chem.*, **4**, 462 (1889).
3. Gattermann, L. and Ritschke, A., *Ber. Deut. Chem. Ges.*, **23**,1738 (1890).
4. Vorländer, D., *Kristallinisch-flüssige Substanzen*, Enke, Stuggart (1980); *Ber. Dtsch. Chem. Ges.*, **41**, 2033 (1980).
5. Friedel, G., *Ann. Phys.*, **18**, 273 (1922).
6. Vorländer, D., *Ber. Dtsch. Chem. Ges.*, **43**, 3120-3135 (1910).
7. Bose, E., *Z. Phys.*, **8**, 513 (1907); **9**, 708 (1908); **10**, 230 (1909).
8. Ornstein, L.S. and Zernicke, F., *Z. Phys.*, **19**, 134 (1918);
9. Zocher, H., *Z. Phys.*, **28**, 790 (1927).
10. Oseen, C.W., *Trans. Faraday Soc.*, **29**, 833 (1933).
11. Frank, F.C., *Discuss. Faraday Soc.*, **25**, 19 (1958).
12. Weygand, C., 'Chemische Morphologie der Flussigkeiten und Kristallie.' *Hand und Jahrbuch der Chemischen Physik.* Bd.2, Abschn. 3c, Akadem, Verslagsgesell, Leipzig. 1941.
13. Gray, G.W., *Molecular Structure and the Properties of Liquid Crystals*, Academic Press, London and New York (1962).
14. Sackmann, H. and Demus, D., *Mol. Cryst.*, **2**, 81 (1966).
15. Scheuble, B.S., Separate print from *Kontakte* (Darmstadt) - Merck, **1**, 34-48 (1989).
16. Timmermanns, J., *Bull. Chem. Soc. Chem. belges.*, **44**, 17 (1935).

17. Chandrasekhar, S., Sadashiva, B.K. and Suresh, K.A., *Pramana*, **9**, 471 (1977).

18. Bernal, J.D. and Crowfoot, D., *Trans. Faraday Soc.*, **29**, 1032 (1933).

19. Crooker, P.P. and Seidmann, T., *Liquid Crystals*, **5**, 751 (1989).

20. Sackmann, H. and Demus, D., *Mol. Cryst. Liq. Cryst.*, **21**, 239 (1973).

21. Demus, D., *Liquid Crystals*, **5**, 75 (1974).

22. Tinh, N.H., Destrade, C. and Gasparoux, H., *Fifth European Winter Liquid Crystal Conference on Layered and Columnar Mesomorphic Systems*, Borovets, Bulgaria, Abstract A11 (1987).

23. Malthete, J., Levelut, A.M. and Nguyen, H.T., *J. Phys. Lett.*, **46**, 1 (1985).

24. Malthete, J., Billard, J. and Jacques, J., *Compt. rend. Acad. Sci.*, Paris, **C282**, 333 (1975).

25. Griffin, A.C., Campbell, G.A., and Hughes W.E., *Liquid Crystals and Ordered Fluids*, (eds. Griffin, A.C. and Johnson, J.F.) Plenum Publ. Corp., 1077 (1984).

26. Goodby, J.W., Waugh, M.A.., Stein, S.M., Chin. E., Pindak, R. and Patel, J.S., *Nature*, **337**, 449 (1989).

27. Gray, G.W. and Winsor, P.A., *Liquid Crystals and Plastic Crystals*, (eds. Gray, G.W. and Winsor, P.A.) Ellis Horwood Ltd., Chichester, Vol. 1 (1974).

28. Gray, G.W., Hartley, J.B. and Jones, B., *J. Chem. Soc.*, 1412 (1955).

29. Gray, G.W., *Advances in Liquid Crystals*, ed. Brown, G.H., **2**, 53 (1976).

30. Gray, G.W., Jones, B. and Marson, F., *J. Chem. Soc.*, 393 (1957).

31. Gray, G.W. and Jones, B., *J. Chem. Soc.*, 236 (1955).

32. Goodby, J.W., *Ferroelectric Liquid Crystals - Principles, Properties and Applications*, (eds. Taylor, G. and Shuvalov, L.,) Gordon and Breach Science Publishers S.A. (1991).

33. Goodby, J.W., Patel, J.S. and Chin, E., J. Mater. Chem., **2(2)**, 197-207 (1992).

34. Butcher, J.L., *Ph.D. Thesis*, Nottingham Polytechnic (1991).

35. Wright G., *Ph.D. Thesis*, The Nottingham Trent University (1996).

36. Sharazi S.N.R., *Ph.D. Thesis*, The Nottingham Trent University (1993).

37. Brown, J.W., *Ph.D. Thesis*, Trent Polytechnic (1986).

38. McSherry, I., *Ph.D. Thesis*, The Nottingham Trent University (1996).

39. Matharu, A.S., *Ph.D. Thesis*, Nottingham Polytechnic (1992).

40. Giroud-Godquin, A-M. and Maitlis, P.M., *Angew. Chem. Int. Ed. Engl.*, **30**, 375-402 (1991).

41. Polishchuk, A.P. and Timofeeva, T.V., *Russian Chemical Reviews*, **62(4)**, 291-322 (1993).

42. Hudson, S.A. and Maitlis, P.M., *Chem. Rev.*, **93**, 861-885 (1993).

43. Butcher, J.L., Byron, D.J., Matharu A.S. and Wilson, R.C., *Liquid Crystals*, **19(3)**, 387-396 (1995).

44. Steinsträsser, R. and del Pino, F., *Biphenyl Esters and Liquid Crystalline Mixtures Comprising Them*, U.S. Patent 4136053, (Jan. 23, 1979).

45. Parish, R.C. and Stock, L.M., *J. Org. Chem.*, **30**, 927-929 (1965).

46. Hassner, A. and Alexanian, V., *Tetrahedron Letters*, **46**, 4475-4478 (1978).

47. Neubert, M.E., Cline, R.E., Zawaski, M.J.,Wildman, P.J. and Ekachai, A., *Mol. Cryst. Liq. Cryst.*, **76**, 43 (1981).

48. Gray, G.W. and Goodby, J.W., *Smectic Liquid Crystals*, Leonard Hill, London, (1984).

49. Vorländer, D., *Z. Phys. Chem. Stoechiom. Verwandschaftsl.*, **105**, 211-254 (1923).

50. Giroud, A.-M. and Müller-Westerhoff, U.T., *Mol. Cryst. Liq. Cryst.*, **41**, 11-13 (1977).

51. Giroud, A.-M., Müller-Westerhoff, U.T, Nazzal, A. and Cox, R.J., *Mol. Cryst. Liq. Cryst.*, **56**, 249-254 (1980).

52. Giroud, A.-M., Müller-Westerhoff, U.T., Nazzal, A. and Cox, R.J., *Mol. Cryst. Liq. Cryst.*, **56**, 255 (1980);

53. Bruce, D.W., *J. Chem. Soc. Dalton Trans.* 2983-2989 (1993).

54. Bruce, D.W., *Inorganic Materials,* (Eds. Bruce, D. and O'Hare, D.), Wiley, Chichester, 405-490 (1992).

55. Deschenaux, R. and Goodby, J.W., *Ferrocenes* (eds. Togni, A. and Hayashi, T.,), VCH Weinheim, 1995.

56. Kealy, T. and Pauson, P.L., *Nature*, **168**, 1039 (1951).

57. Miller, S., Tebboth, J. and Tremaine, J., *J. Chem. Soc.*, 632 (1952).

58. *Principles of Organometallic Chemistry*, 2nd edition (ed. Powell, P.), Chapman Hall, 280 (1988).

59. Malthete, J. and Billard, J., *Mol. Cryst. Liq. Cryst.*, **34**, 117-121 (1976).

60. Galyametdinov, Yu.G., Kadkin, O.N. and Ovchinnikov, I.V., *Izv. Akad. Nauk., Ser. Khim* (Russia), **10**, 2462-2463 (1990).

61. Galyametdinov, Yu.G., Kadkin, O.N. and Ovchinnikov, I.V., *Izv. Akad. Nauk., Ser. Khim* (Russia), **2**, 402-407 (1992).

62. Nakamura, N., Hanasaki, T. and Onoi, H., *Mol. Cryst. Liq. Cryst.*, **225**, 269-277 (1993).

63. Nakamura, N., Hanasaki, T., Onoi, H. and Oida, T., *Mol. Cryst. Liq. Cryst.*, **257**, 43-48 (1994).

64. Nakamura, N., Hanasaki, T. and Ueda, M., *Mol. Cryst. Liq. Cryst.*, **237**, 329-336 (1993).

65. Nakamura, N., Hanasaki, T. and Ueda, M., *Mol. Cryst. Liq. Cryst.*, **250**, 257-267 (1994).

66. Bhatt, J., Fung, B.M., Nicholas, K.M. and Poon, C.-D., *J. Chem. Soc., Chem Commun.*, 1439 (1988).

67. Bhatt, J., Fung, B.M., Nicholas, K.M., Khan, M.A. and Wachtel, E., *Liquid Crystals*, **5(1)**, 285-290 (1989).

68. Bhatt, J., Fung, B.M. and Nicholas, K.M., *J. Organomet. Chem.*, **413**, 263-268 (1991).

69. Singh, P., Rausch, M.D. and Lenz, R.W., *Liquid Crystals*, **9(1)**, 19-26 (1991).

70. Deschenaux, R. and Marendaz, J.-L., *J. Chem. Soc., Chem Commun.*, 909 (1991).

71. Descanaux, R., Kosztics, I. and Marendaz, J.-L., *Chimie*, **47**, 206-210 (1993).

72. Reddy, K.P. and Brown, T.L., *Liquid Crystals*, **12(3)**, 369-376 (1992).

73. Thompson, N.J., Goodby, J.W. and Toyne, K.J., *Liquid Crystals*, **13(3)**, 381-402 (1993).

74. Deschenaux, R., Rama, M. and Santiago, J., *Tetrahedron Letters*, **34(20)**, 3293-3296 (1993).

75. Deschanaux, R. and Marendaz, J.-L., Santiago, J., *Helvetica Chimica Acta*, **76**, 865-876 (1993).

76. Bhatt, J., Fung, B.M. and Nicholas, K.M., *Liquid Crystals*, **12**, 263-272 (1989).

77. Polishchuk, A.P., Timofeeva, T.V., Antipin, M.Yu., Struchkov, Yu.T. and Galyametdinov, Yu.G., *Kristallografiya*, **37**, 705-711, (1990).

78. Rosenblum, M., *Chemistry of the Iron Group Metallocenes*, Interscience, New York (1965).

79. Bublitz, D.E. and Reinhart Jnr, K.L., *Organic Reactions*, Vol. 17 (eds. Adams, R., Blatt, A., Boekelheide, V., Cairns, T., Cram, D., Dauben, W. and House, H.), J. Wiley and Sons (1969).

80. Perevalova, E.G. and Nikitina, T.V., *Organometallic Reactions*, Vol. 4, (Eds.Becker, E.I. and Tsutsui, M.), Wiley (1972).

81. Rosenblum, M. and Woodward, R.B., *J. Amer. Chem. Soc.*, **30**, 5443-5449 (1958).

82. Vogel, M., Rausch, M.D. and Rosenberg, H., *J. Org. Chem.*, **22**, 1016 (1957).

83. Rausch, M.D. and Ciappenelli, D.J., *J. Organomet. Chem.*, **10**, 127-136 (1967).

84. Knobloch, F.W. and Rauscher, W.H., *J. Polymer Sci.*, **54**, 651-656 (1961).

85. Sonoda, A. and Moritani, I., *J. Organomet. Chem.*, **26**, 133-140 (1971).

86. Balavoine, G.G.A., Doisneau, G. and Fillebeen-Khan, T., *J. Organomet. Chem.*, **412**, 381-382 (1991).

87. Osgerby, J.M.. and Pauson, P.L., *J. Chem. Soc.*, 4604 (1961).

88. Verbit, L. and Halbert, T.R., *Mol. Cryst. Liq. Cryst.*, **30**, 209-212 (1975).

89. Gray, G.W., Harrison, K.J. and Nash, J.A., *Liquid Cryst. Ordered Fluids*, **2**, 617-643 (1973).

90. Demus, D., Demus, H. and Zaschke, H., *Flüssige Kristalle in Tabellen*, VEB Deutscher Verlag für Grundstoffindustrie, Leipzig (1976).

91. Jones, B. and Chapman, F., *J. Chem. Soc.*, 1829-1832 (1952).

92. Campbell, I.G.M. and Morrill, D.J., *J. Chem. Soc.*, 1662-1668 (1955).

93. Knox, G.R. and Pauson, P.L., *J. Chem. Soc.*, 4615-4618 (1961).

94. Gray, G.W., Harrison, K.J., Nash, J.A., Constant, J., Hulme, D.S., Kirton, J. and Raynes, E.P., *Liquid Cryst. Ordered Fluids*, **2**, 617-643 (1974).

95. Bruce, D.W., Personal communincation, 10th Annual British Liquid Crystal Society Conference, Southampton University, 1995.

96. Graham, P.J., Lindsay, R.V., Parshall, G.W., Peterson, M.L. and Whitman, G.M., *J. Amer. Chem.Soc.*, **79**, 3416 (1957).

97. Wilson, J.M., Harden, R. and Phillips, J., *Mol. Cryst. Liq. Cryst.*, **34**, 237-240 (1977).

98. Jeschke, U., Vogel, C., Vill, V. and Fischer, H., *J. Mater. Chem.*, **5** (12), 2073-2078 (1995).

Appendix 1

Appendix 1

Photomicrographs of the 4′-n-alkoxybiphenyl-4-yl cycloalkanecarboxylates

Plate A

An example of the unusual crystal G phase texture of the 4′-n-alkoxybiphenyl-4-yl cycloalkanecarboxylates, in this case 4′-n-heptyloxybiphenyl-4-yl cyclopentane-carboxylate, **C-7/C-5** at 104 °C.

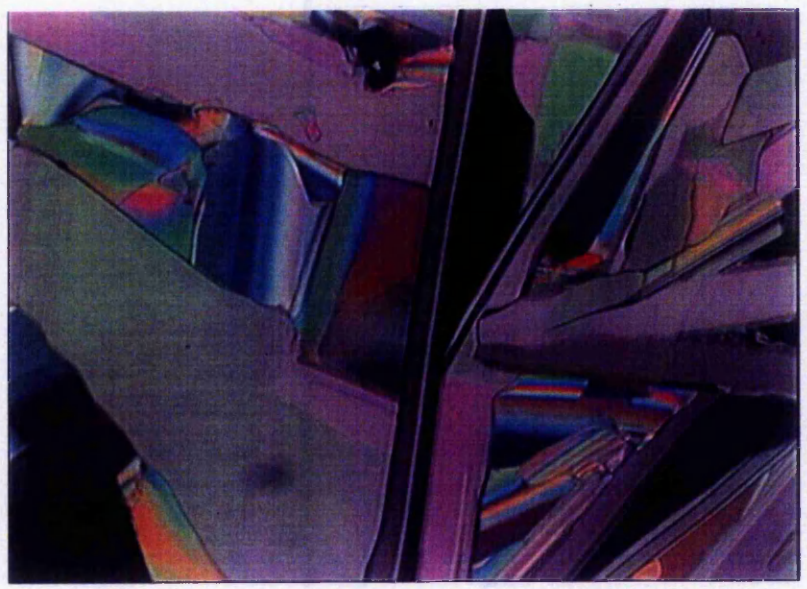

Plate B

An example of the unusual crystal G phase texture of the 4′-n-alkoxybiphenyl-4-yl cycloalkanecarboxylates, in this case 4′-n-nonylbiphenyl-4-yl cyclopropane-carboxylate, **C-9/C-3** at 84 °C.

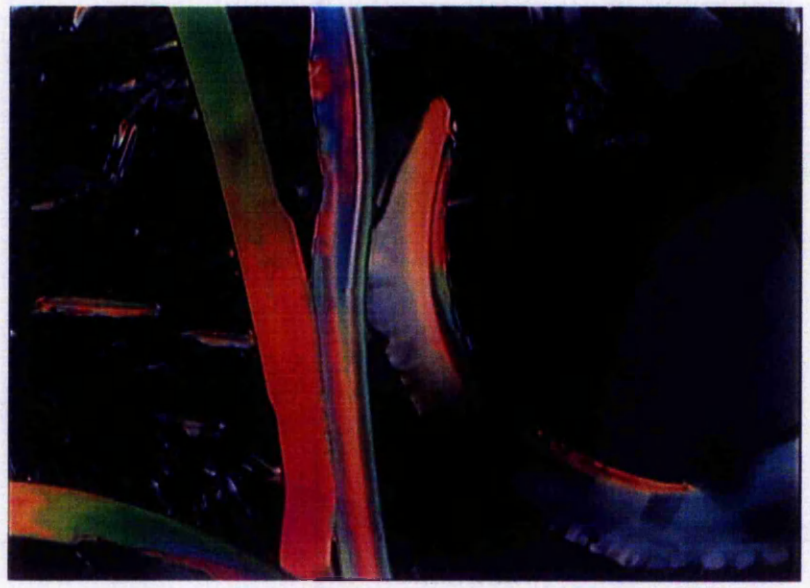

Plate C

The crystal G phase texture separating out of the isotropic liquid at 95.9 °C for a 50 : 50 mixture of 4′-n-nonyloxybiphenyl-4-yl cyclopropanecarboxylate, **C-9/C-3** and the newly standardised 4′-n-decyloxybiphenyl-4-yl cyclohexanecarboxylate, **C-10/C-6**, showing dendritic growth and the 'butterfly' shaped lancets.

Plate D

The characteristic cross-hatched texture of the smectic crystal H phase for 4′-n-pentyloxybiphenyl-4-yl cyclopentanecarboxylate, **C-5/C-5** at 98.0 °C.

Plate E

The uncharacterised texture, S_z, obtained on cooling the crystal H phase for a 80 : 20 mixture of 4′-n-butyloxybiphenyl-4-yl cyclopentanecarboxylate, **C-4/C-5** and the newly standardised 4′-n-decyloxybiphenyl-4-yl cyclohexanecarboxylate, **C-10/C-6** below 99 °C.

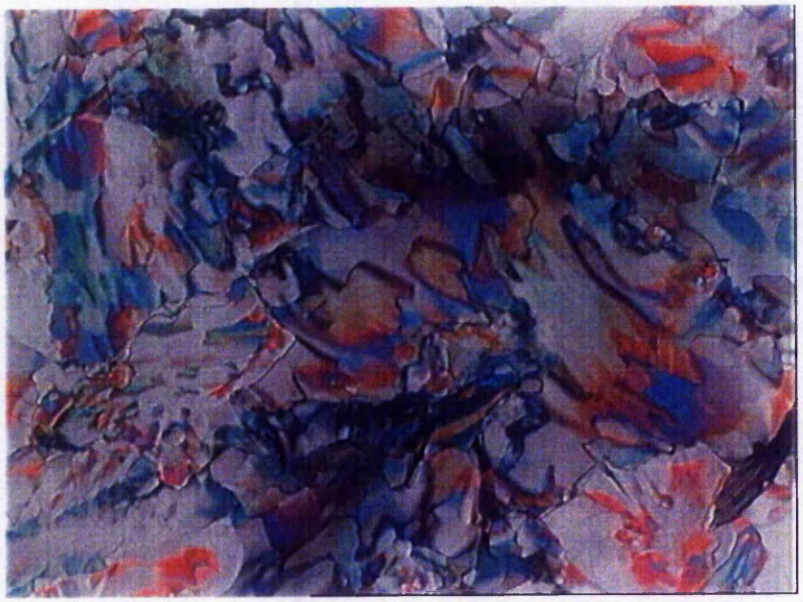

Plate F

The unfocused Schlieren texture of the S_I phase obtained on cooling the S_C phase of 4′-n-dodecyloxybiphenyl-4-yl cycloheptanecarboxylate, **C-12/C-7**, to 82.1 °C.

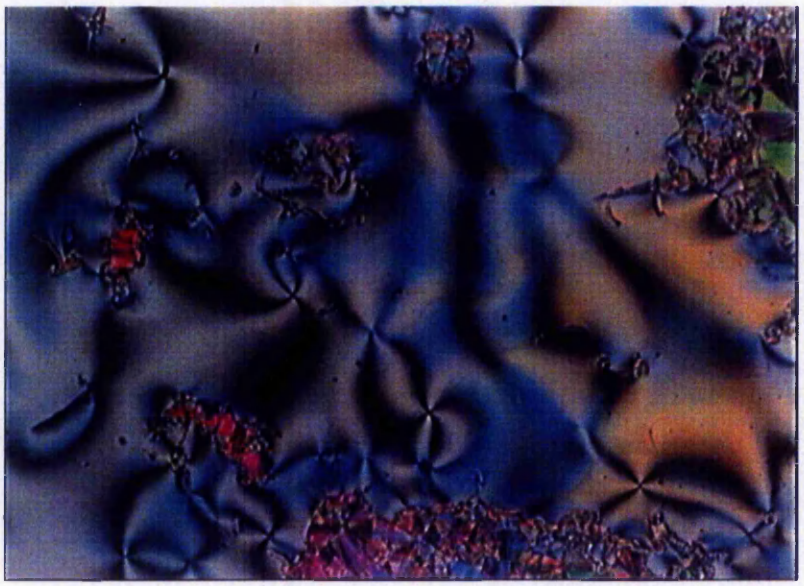

Plate G

The characteristic large mosaic plates of the cystal J phase obtained on cooling the S_I phase of 4′-n-dodecyloxybiphenyl-4-yl cycloheptanecarboxylate, **C-12/C-7**, to 78.6 °C.

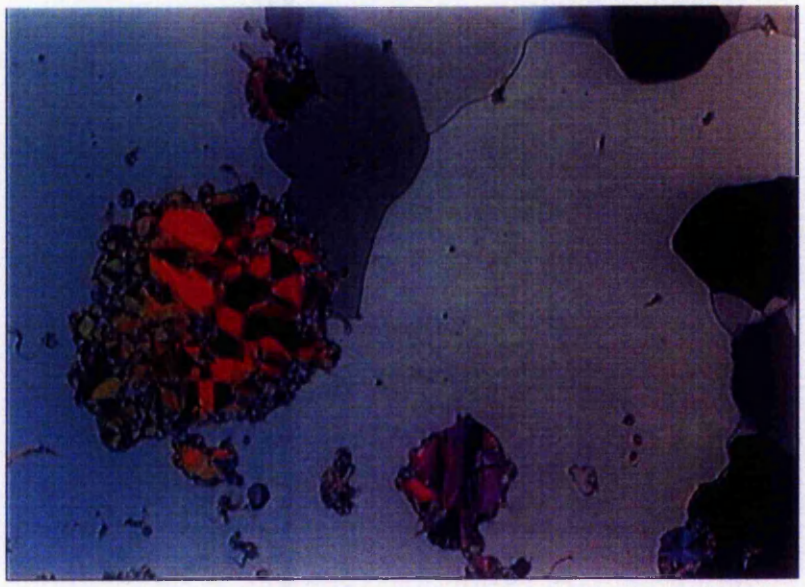

Photomicrographs of the 4′-n-alkylbiphenyl-4-yl 4-n-alkylbenzoates

Plate H

The threaded nematic texture obtained on cooling the isotropic liquid of the 4′-*n*-hexyl-biphenyl-4-yl 4-*n*-octylbenzoate, **(17)** $m = 6$, $n = 8$ to 152.0 °C, clearly showing characteristic point singularities with both 4 and 2 brushes.

Plate I

The candy striped texture of the smectic crystal K phase of 4′-*n*-decylbiphenyl-4-yl 4-*n*-pentylbenzoate, **(17)** $m = 10$, $n = 5$ at 88.5 °C.

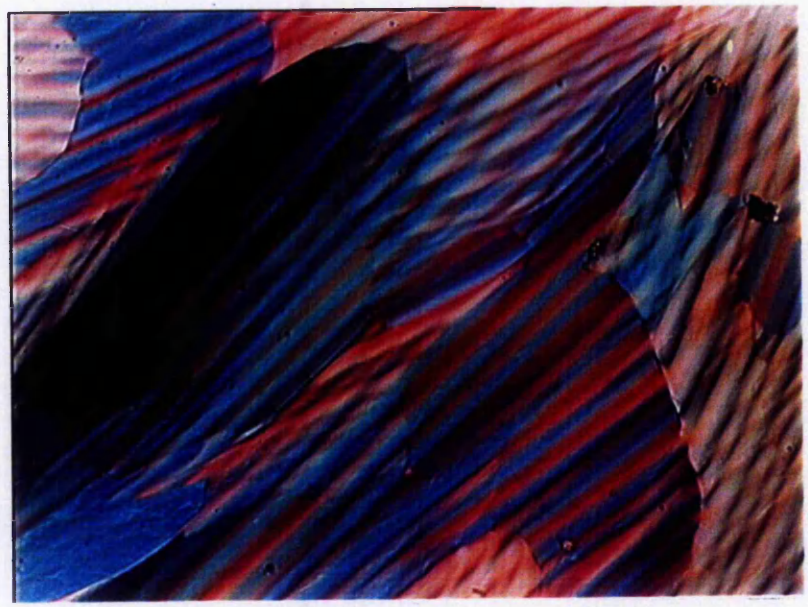

Plate J

The characteristic smooth focal conic texture of the S_B phase obtained on cooling the S_C phase of 4′-*n*-heptylbiphenyl-4-yl 4-*n*-decylbenzoate **(17)** $m = 7$, $n = 10$ to 100.1 °C.

Photomicrographs of some 1,1′-disubstituted ferrocene derivatives

Plate K

The nematic texture obtained on cooling the *bis*[N-(4-n-butyloxyphenyl)benzaldimin-4-yl] ferrocene-1,1′-dicarboxylate **(74)** to 177.1 °C. However, the solid impurities in this compound can be clearly seen.

Plate L

The unidentified texture obtained on rapid cooling of the isotropic liquid of the ferrocene-1,1′-diimine **(72)**, where the biphenyl group is interrupted by the ester linkage. This texture was only observed on cooling in this manner, and changed to the usual crystal texture in a matter of seconds.

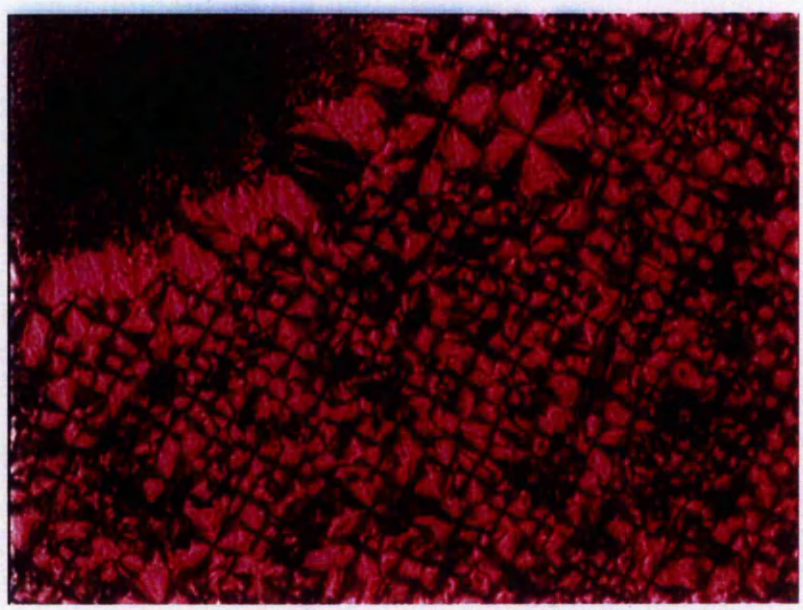

Appendix 2

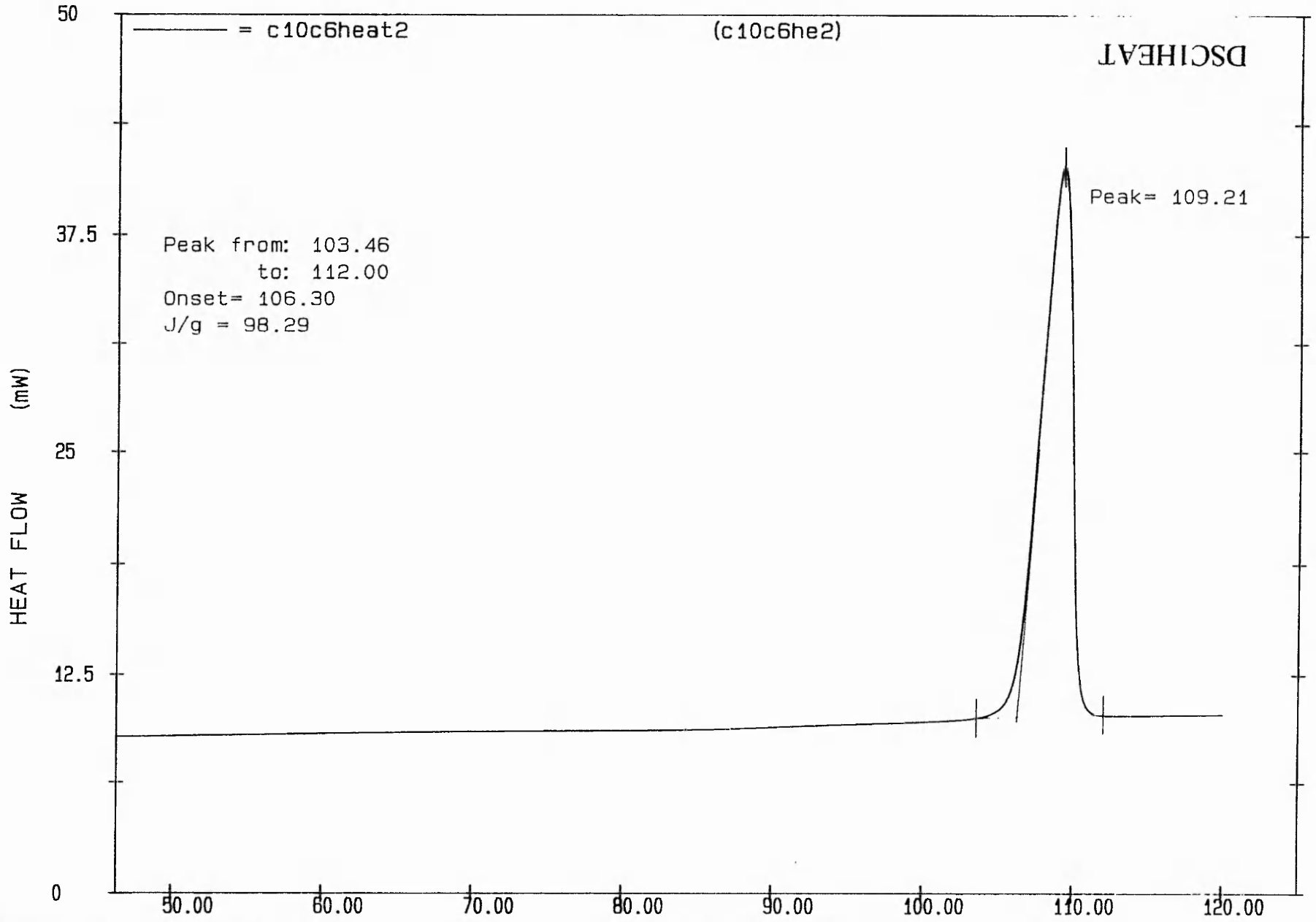

Date: Sep 23, 1994 12: 43am
Scanning Rate: 10.0 C/min
Sample Wt: 4.600 mg Path: c: \pe\ash\
File 1: C10C6HE2 ASH

PERKIN-ELMER DSC7

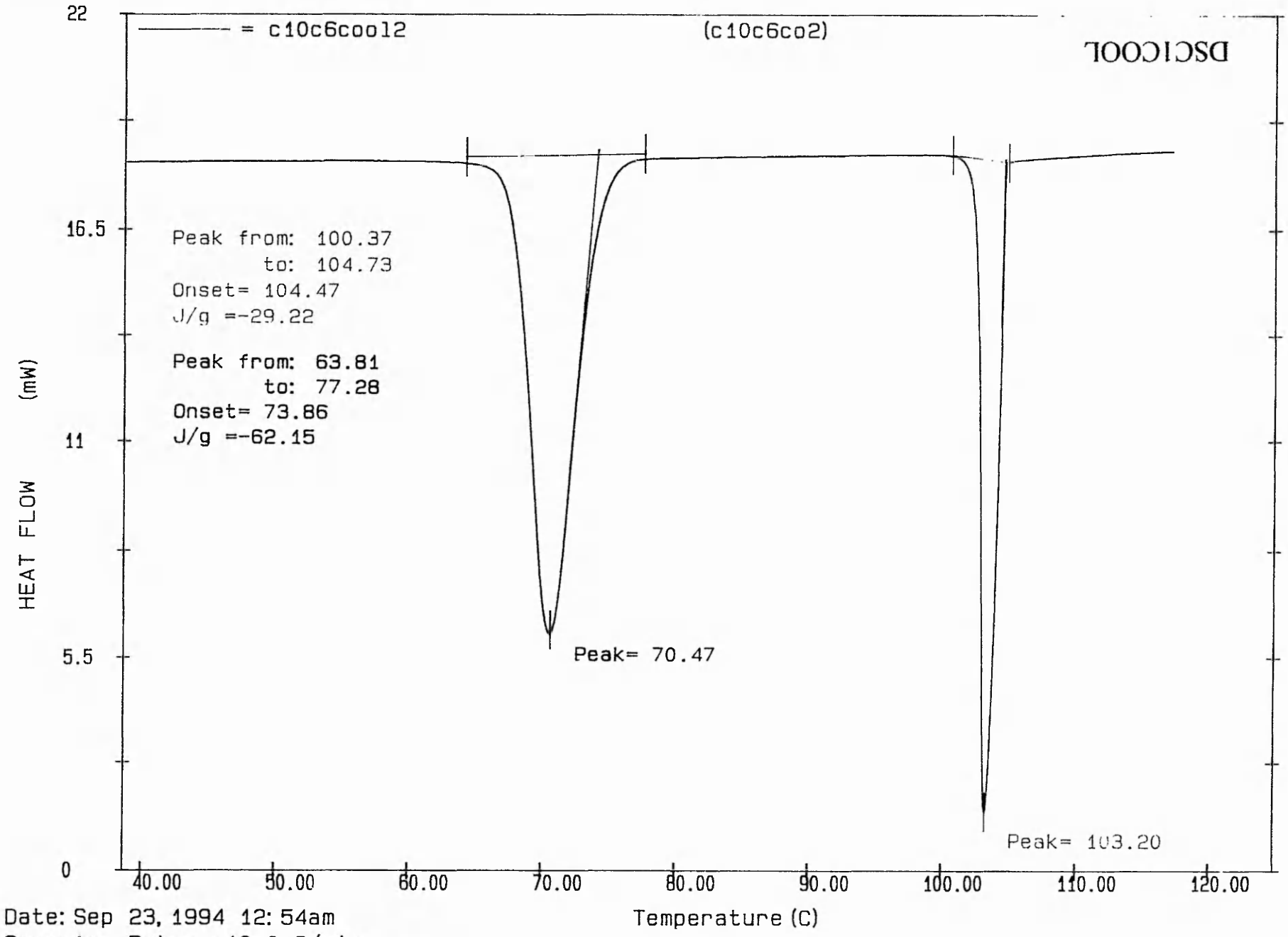

Date: Sep 23, 1994 12:54am
Scanning Rate: -10.0 C/min
Sample Wt: 4.600 mg Path: c:\pe\ash\
File 1: C10C6CO2 ASH

PERKIN-ELMER DSC7

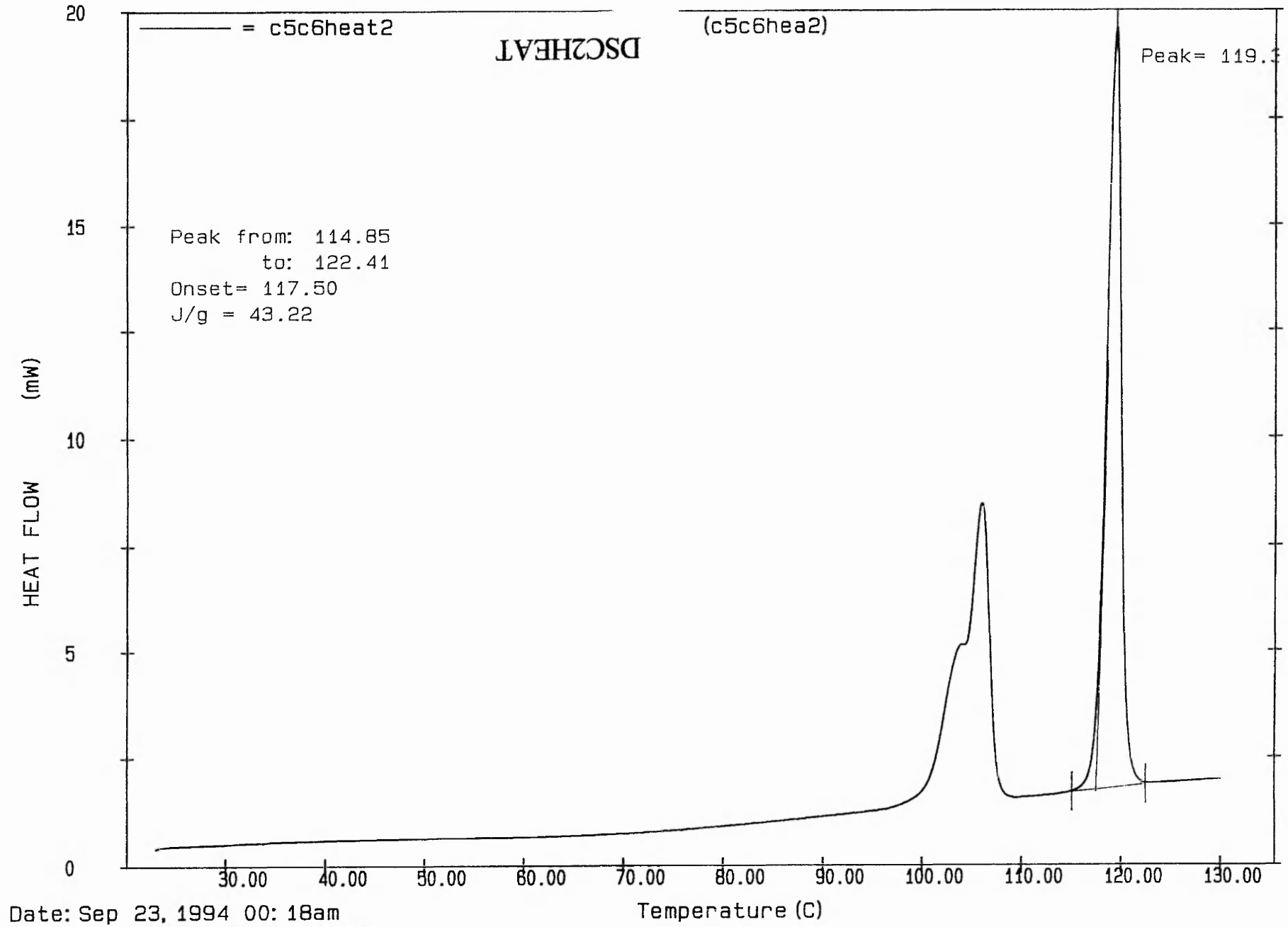

Date: Sep 23, 1994 00: 18am
Scanning Rate: 10.0 C/min
Sample Wt: 4.300 mg Path: c: \pe\ash\
File 1: C5C6HEA2 ASH

PERKIN-ELMER DSC7

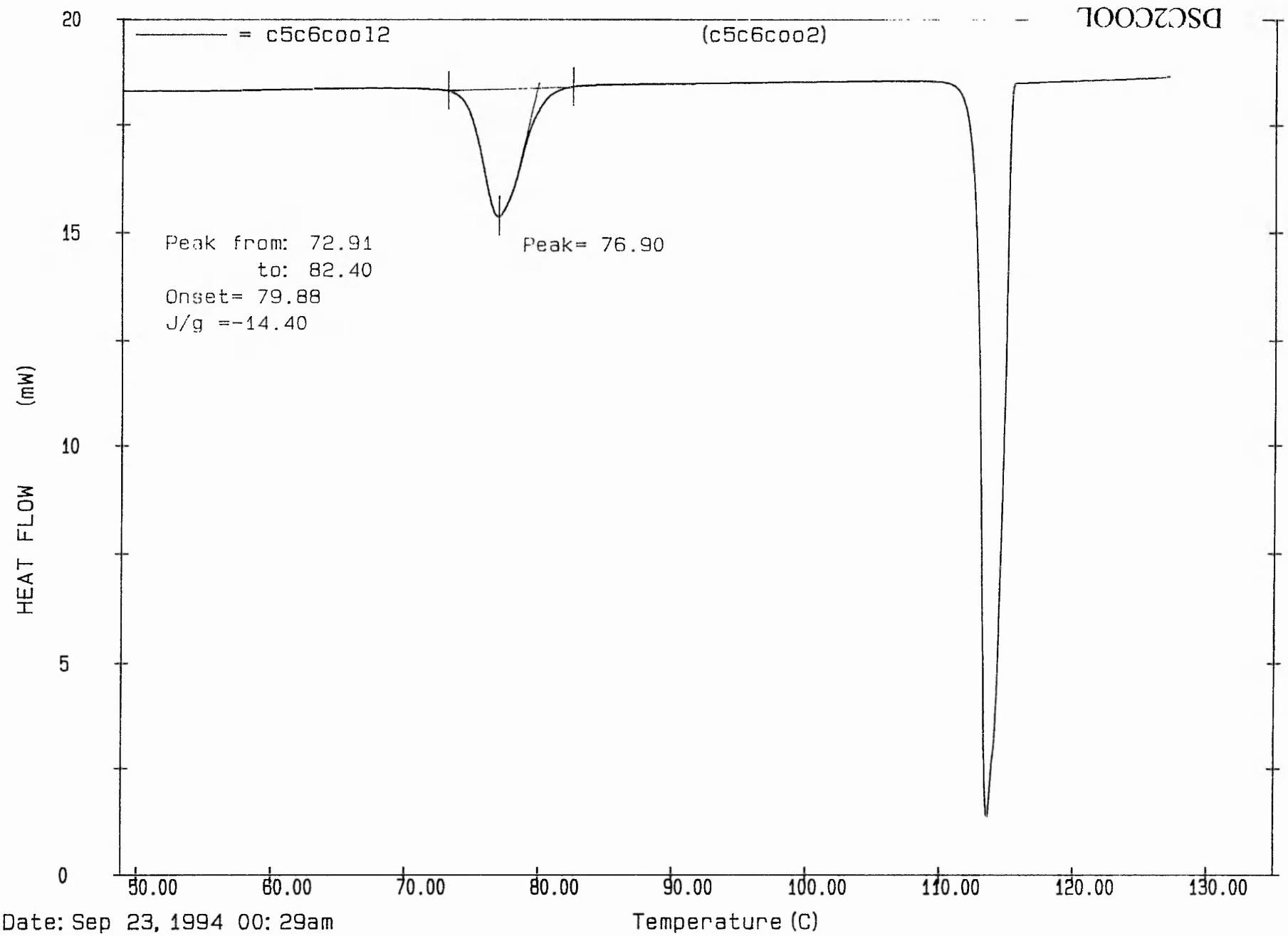

Date: Sep 23, 1994 00: 29am
Scanning Rate: -10.0 C/min
Sample Wt: 4.300 mg Path: c: \pe\ash\
File 1: C5C6C002 ASH

PERKIN--ELMER DSC7

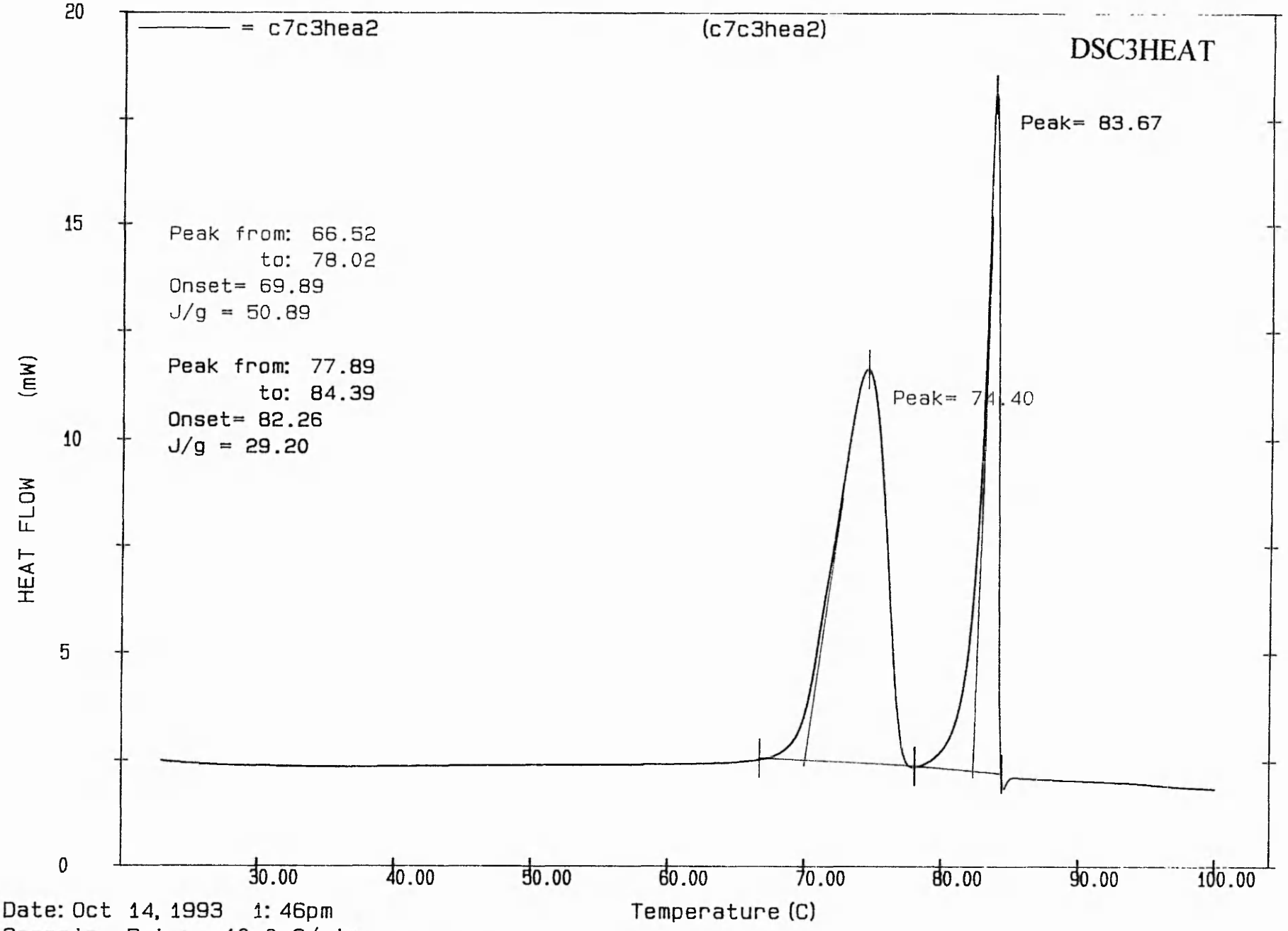

Date: Oct 14, 1993 1:46pm
Scanning Rate: 10.0 C/min
Sample Wt: 4.700 mg Path: c:\pe\ash\
File 1: C7C3HEA2 ASH

PERKIN-ELMER DSC7

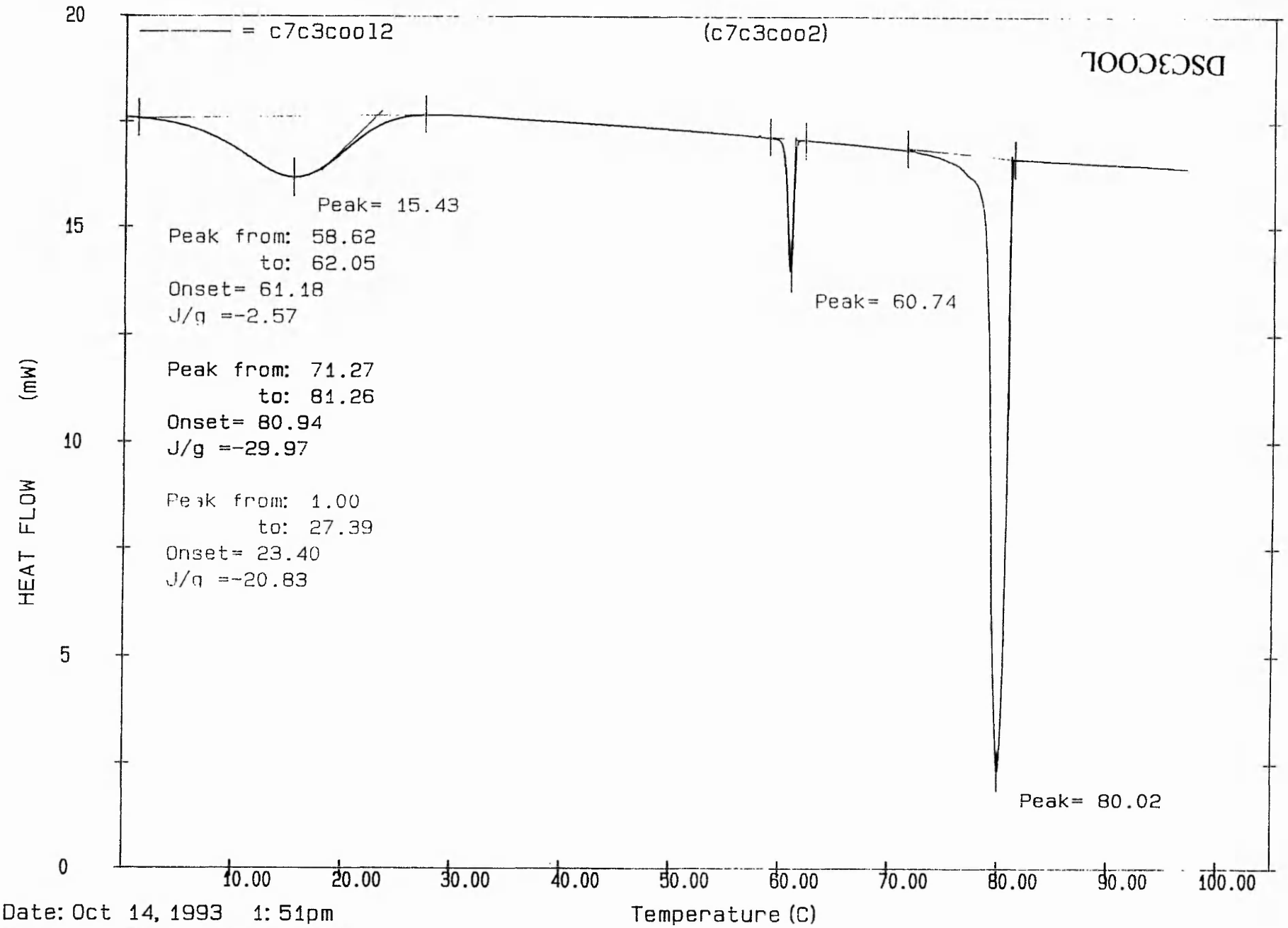

Date: Oct 14, 1993 1:51pm
Scanning Rate: -10.0 C/min
Sample Wt: 4.700 mg Path: c:\pe\ash\
File 1: C7C3C002 ASH

PERKIN-ELMER DSC7

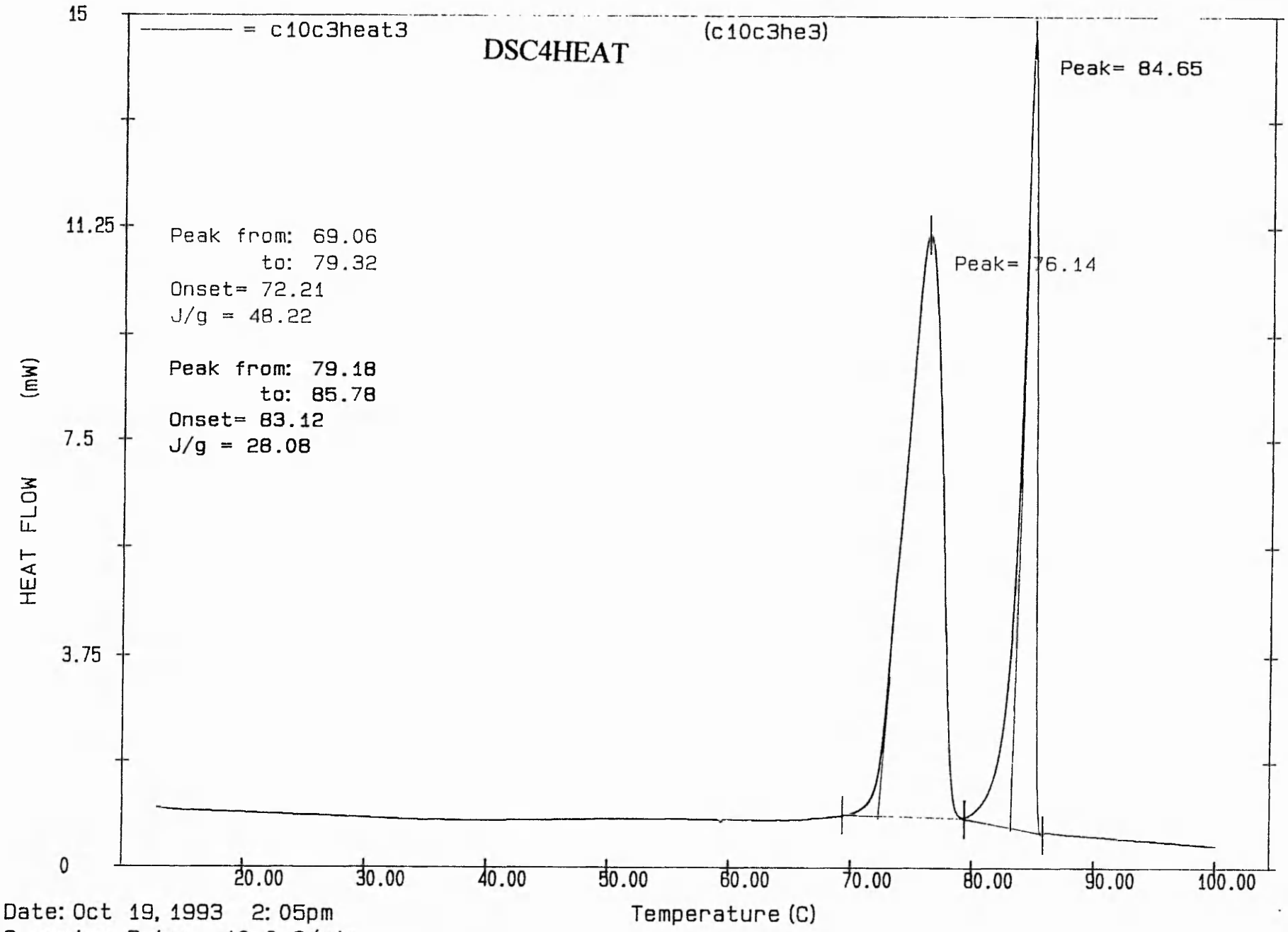

Date: Oct 19, 1993 2:05pm
Scanning Rate: 10.0 C/min
Sample Wt: 4.500 mg Path: c:\pe\ash\
File 1: C10C3HE3 ASH

PERKIN-ELMER DSC7

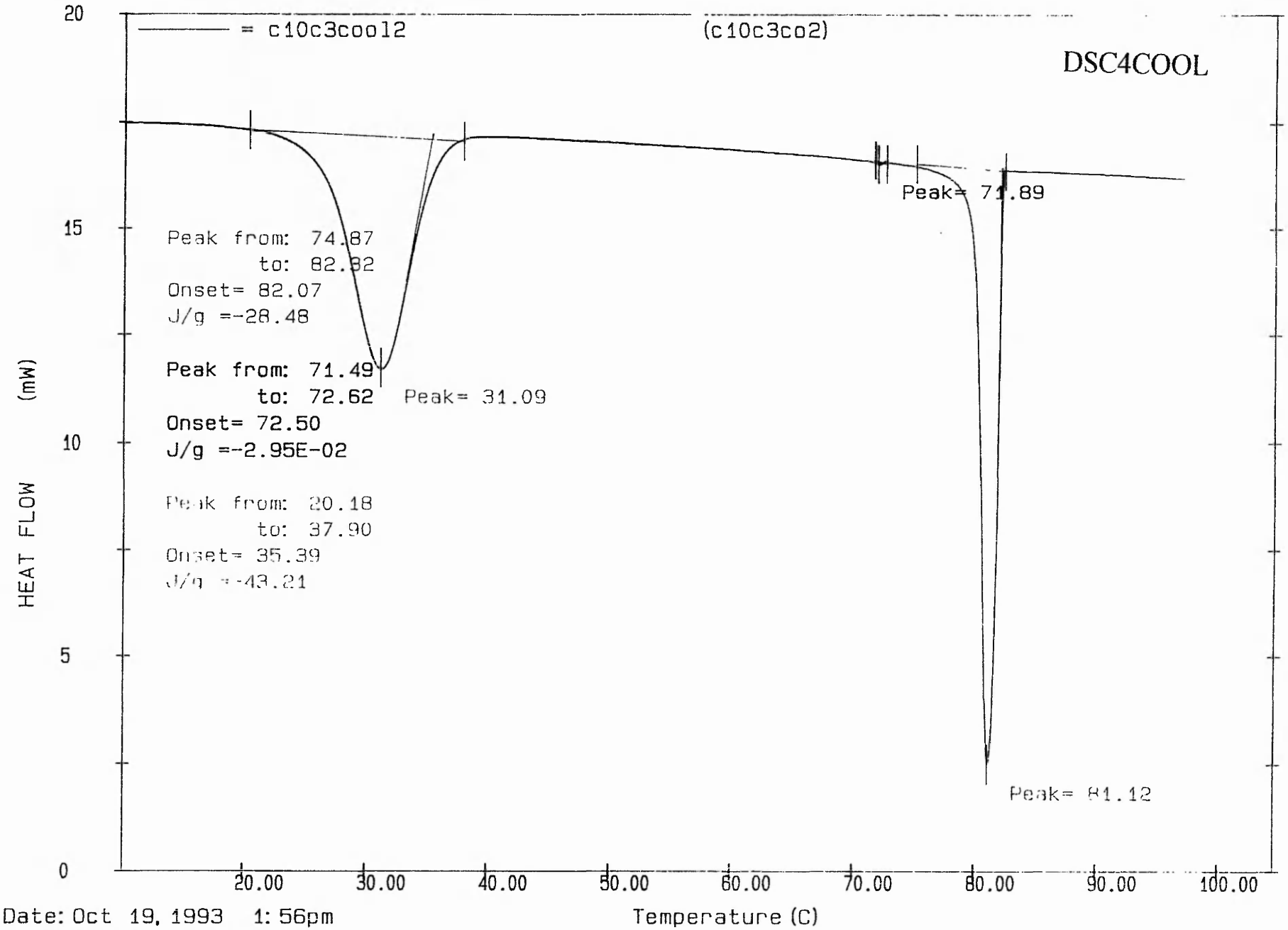

Date: Oct 19, 1993 1:56pm
Scanning Rate: -10.0 C/min
Sample Wt: 4.500 mg Path: c:\pe\ash\
File 1: C10C3CO2 ASH

PERKIN-ELMER DSC7

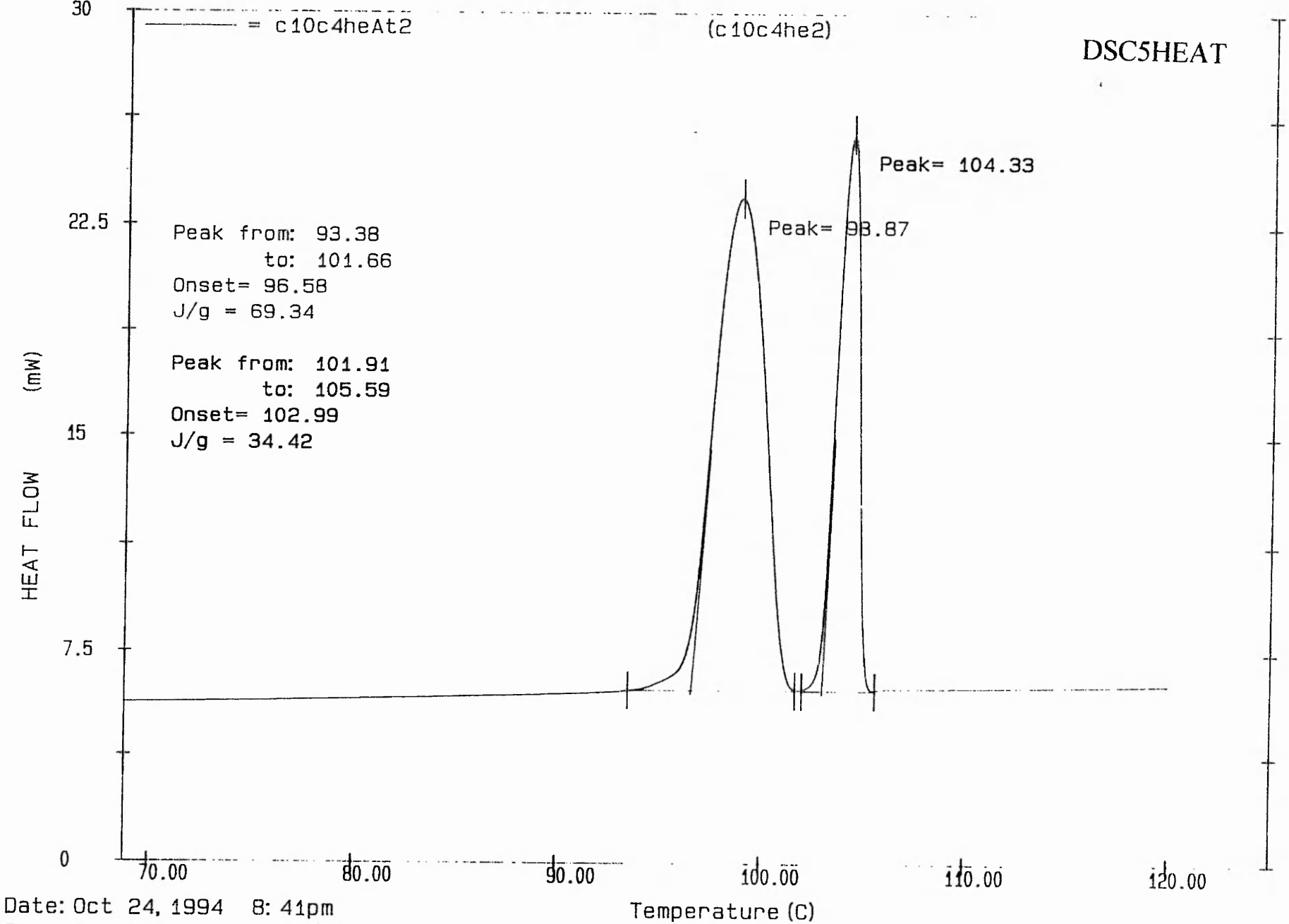

Date: Oct 24, 1994 8: 41pm
Scanning Rate: 10.0 C/min
Sample Wt: 4.300 mg Path: c: \pe\ash\
File 1: C10C4HE2 ASH

PERKIN-ELMER DSC7

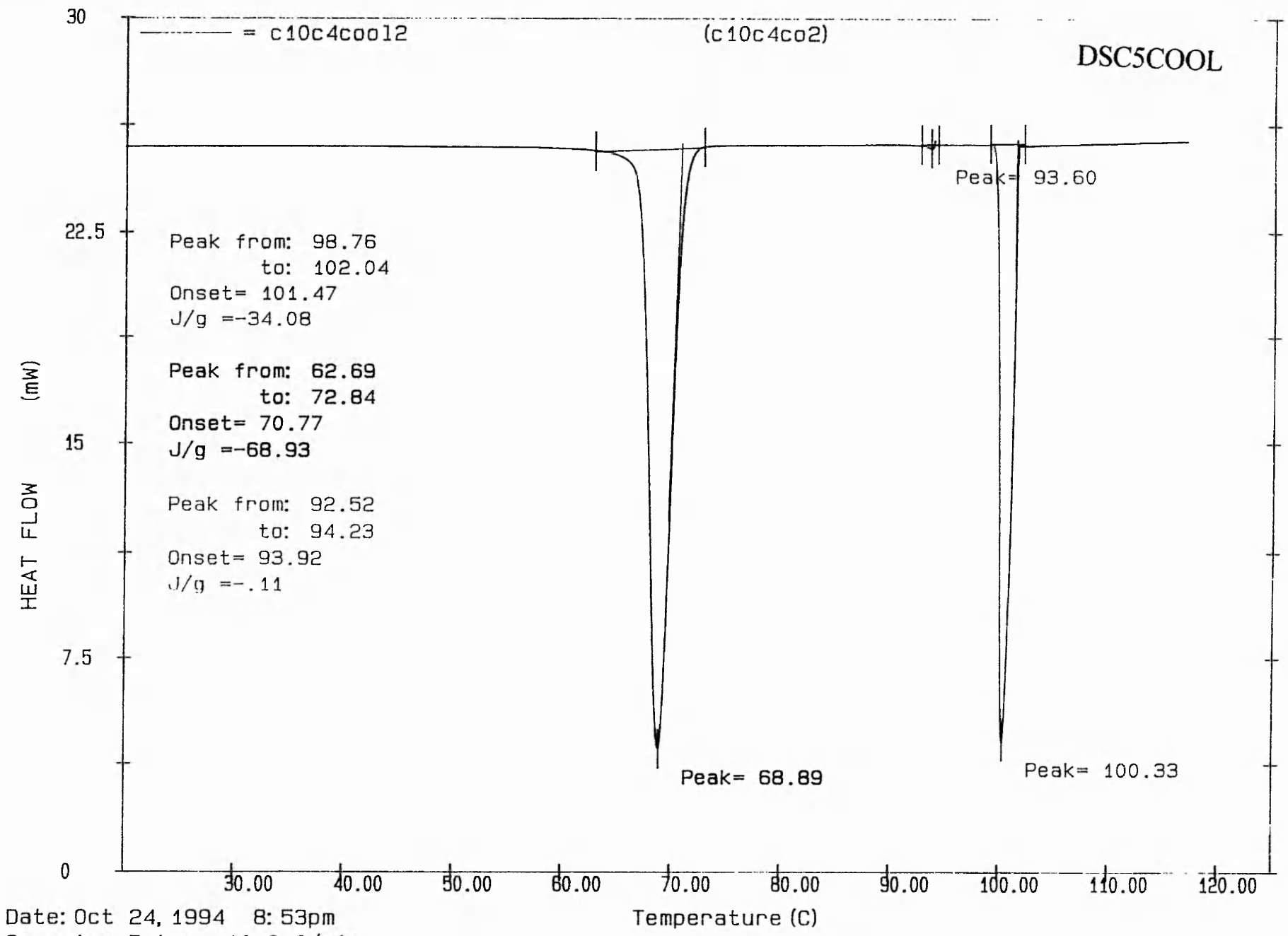

Date: Oct 24, 1994 8:53pm
Scanning Rate: -10.0 C/min
Sample Wt: 4.300 mg Path: c:\pe\ash\
File 1: C10C4CO2 ASH

PERKIN-ELMER DSC7

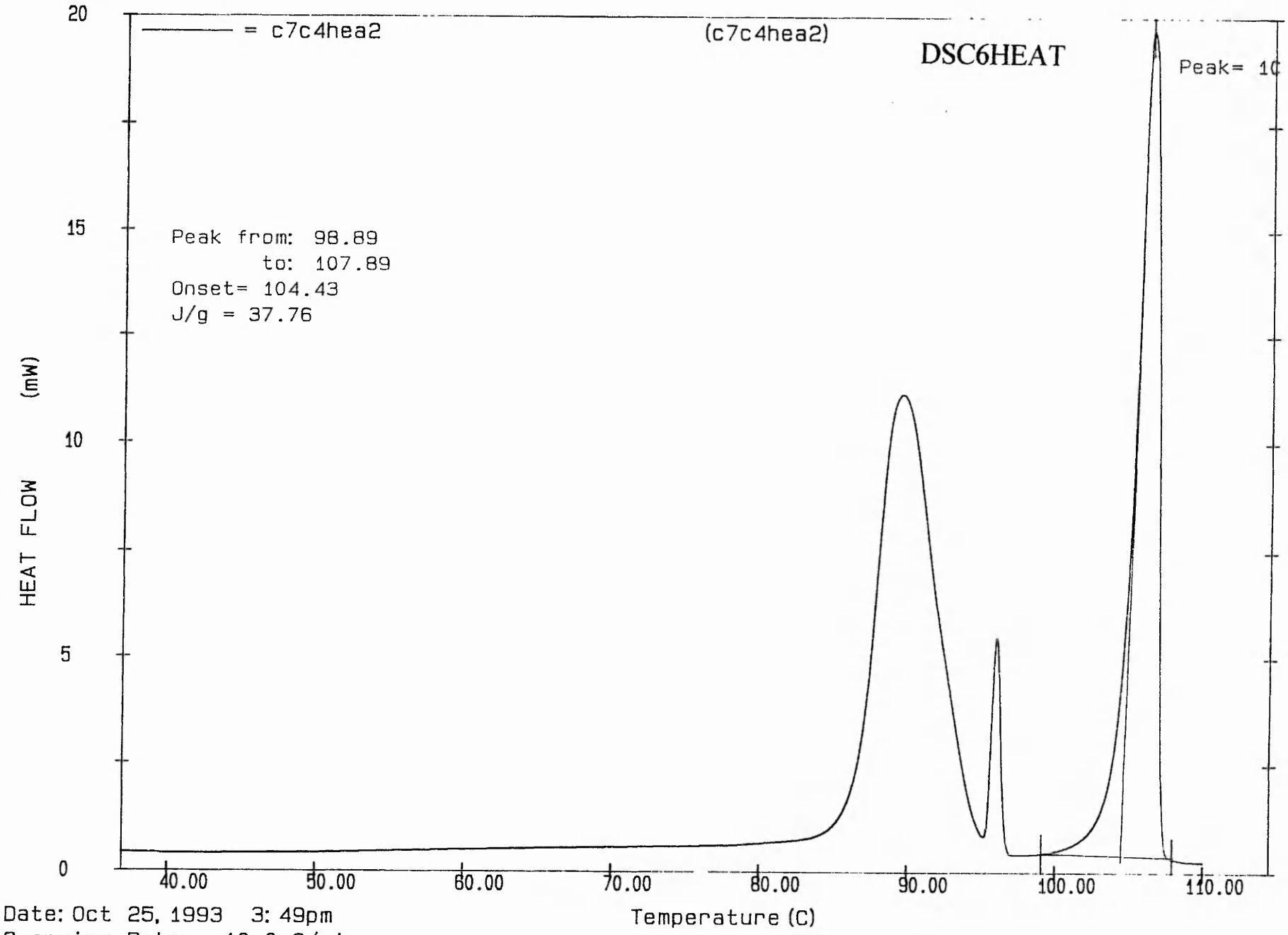

Date: Oct 25, 1993 3:49pm
Scanning Rate: 10.0 C/min
Sample Wt: 5.800 mg Path: c:\pe\ash\
File 1: C7C4HEA2 ASH

PERKIN-ELMER DSC7

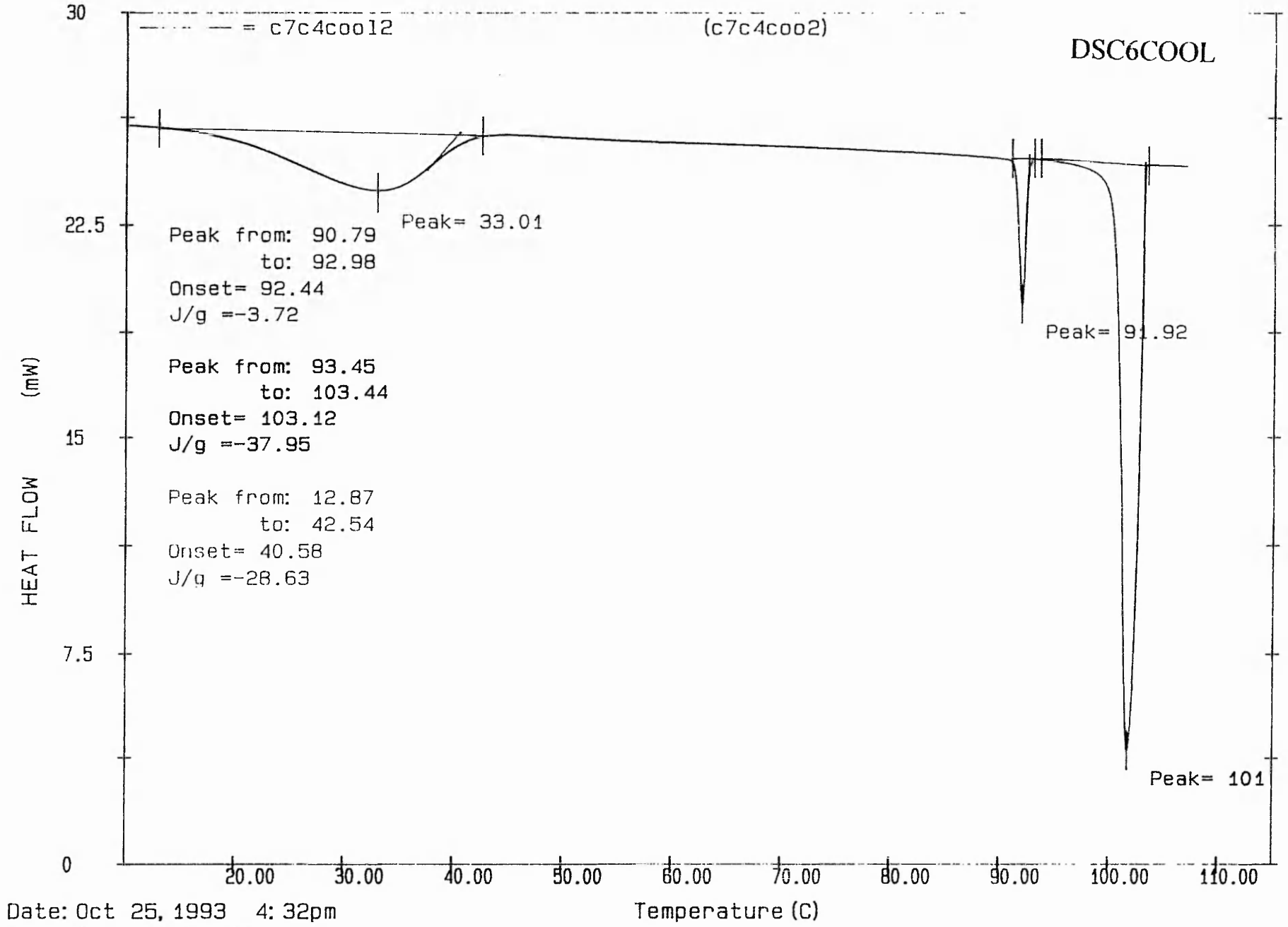

Date: Oct 25, 1993 4:32pm
Scanning Rate: -10.0 C/min
Sample Wt: 5.800 mg Path: c:\pe\ash\
File 1: C7C4C002 ASH

PERKIN-ELMER DSC7

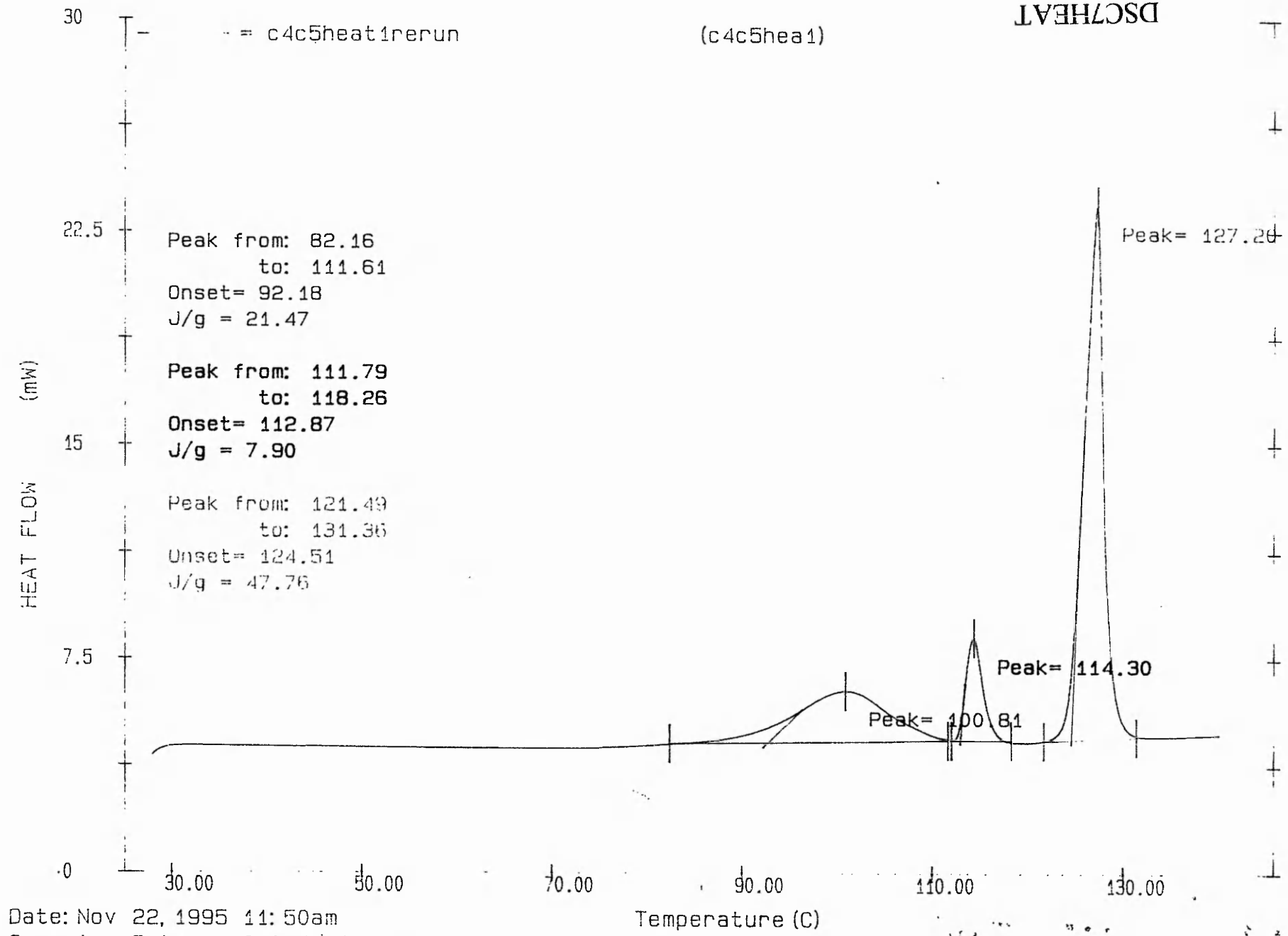

Date: Nov 22, 1995 11:50am
Scanning Rate: 10.0 C/min
Sample Wt: 5.700 mg Path: a:\
File 1: C4C5HEA1 ASH

PERKIN-ELMER DSC7

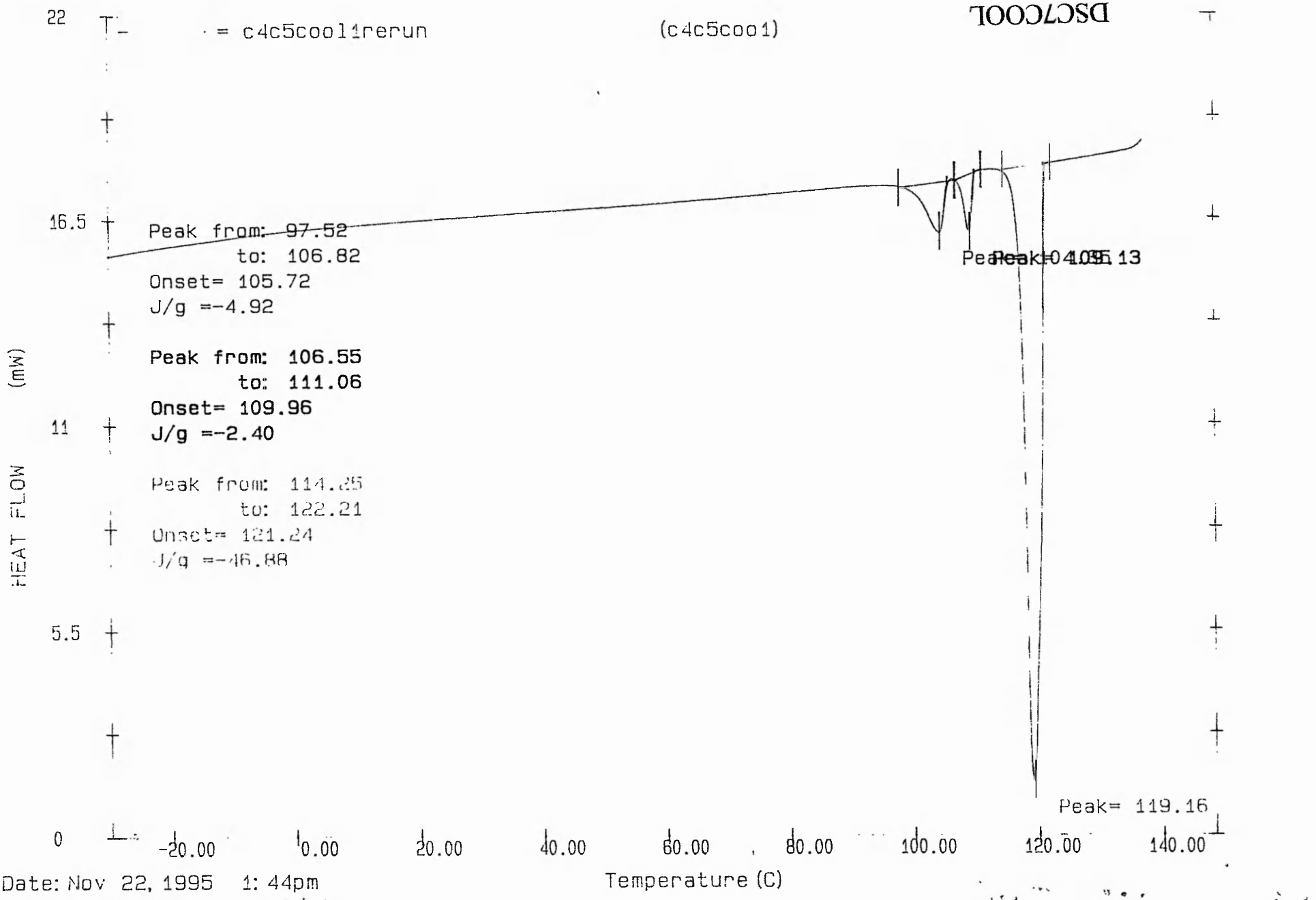

Date: Nov 22, 1995 1:44pm
Scanning Rate: -10.0 C/min
Sample Wt: 5.700 mg Path: a:\
File 1: C4C5C001 ASH

PERKIN-ELMER DSC7

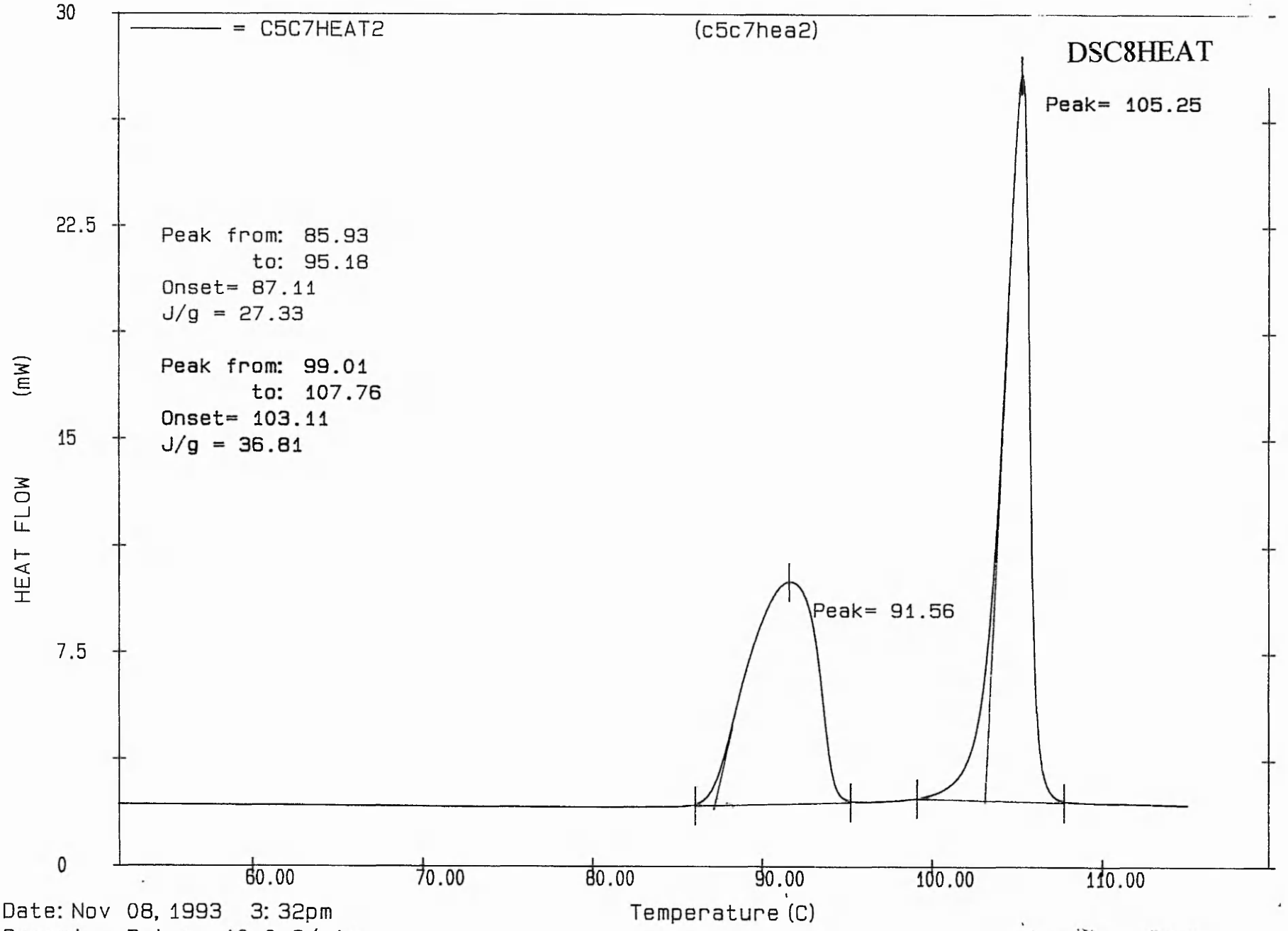

Date: Nov 08, 1993 3:32pm
Scanning Rate: 10.0 C/min
Sample Wt: 8.000 mg Path: c:\pe\ash\
File 1: C5C7HEA2 ASH

PERKIN-ELMER DSC7

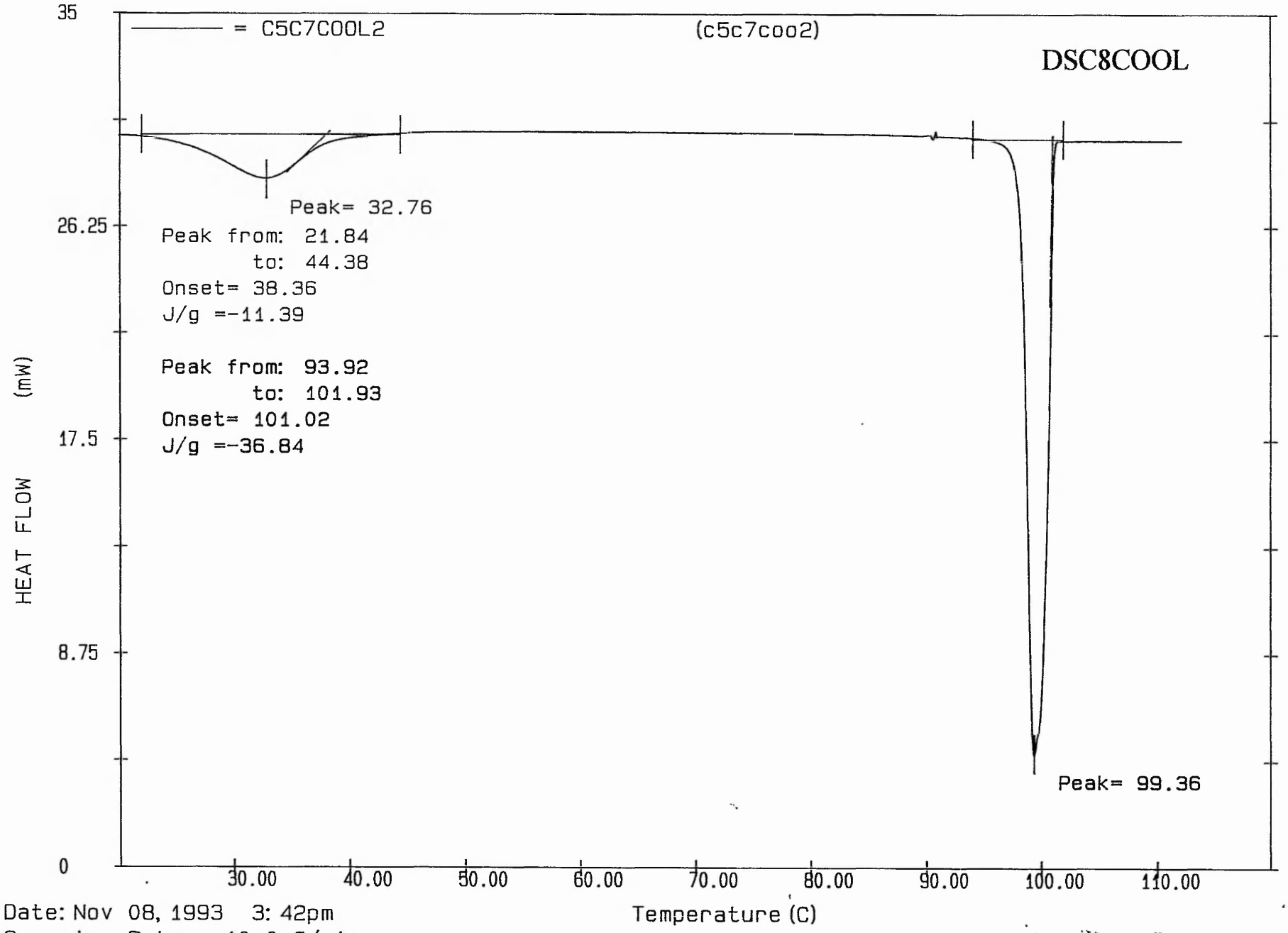

Date: Nov 08, 1993 3: 42pm
Scanning Rate: -10.0 C/min
Sample Wt: 8.000 mg Path: c: \pe\ash\
File 1: C5C7C002 ASH

PERKIN-ELMER DSC7

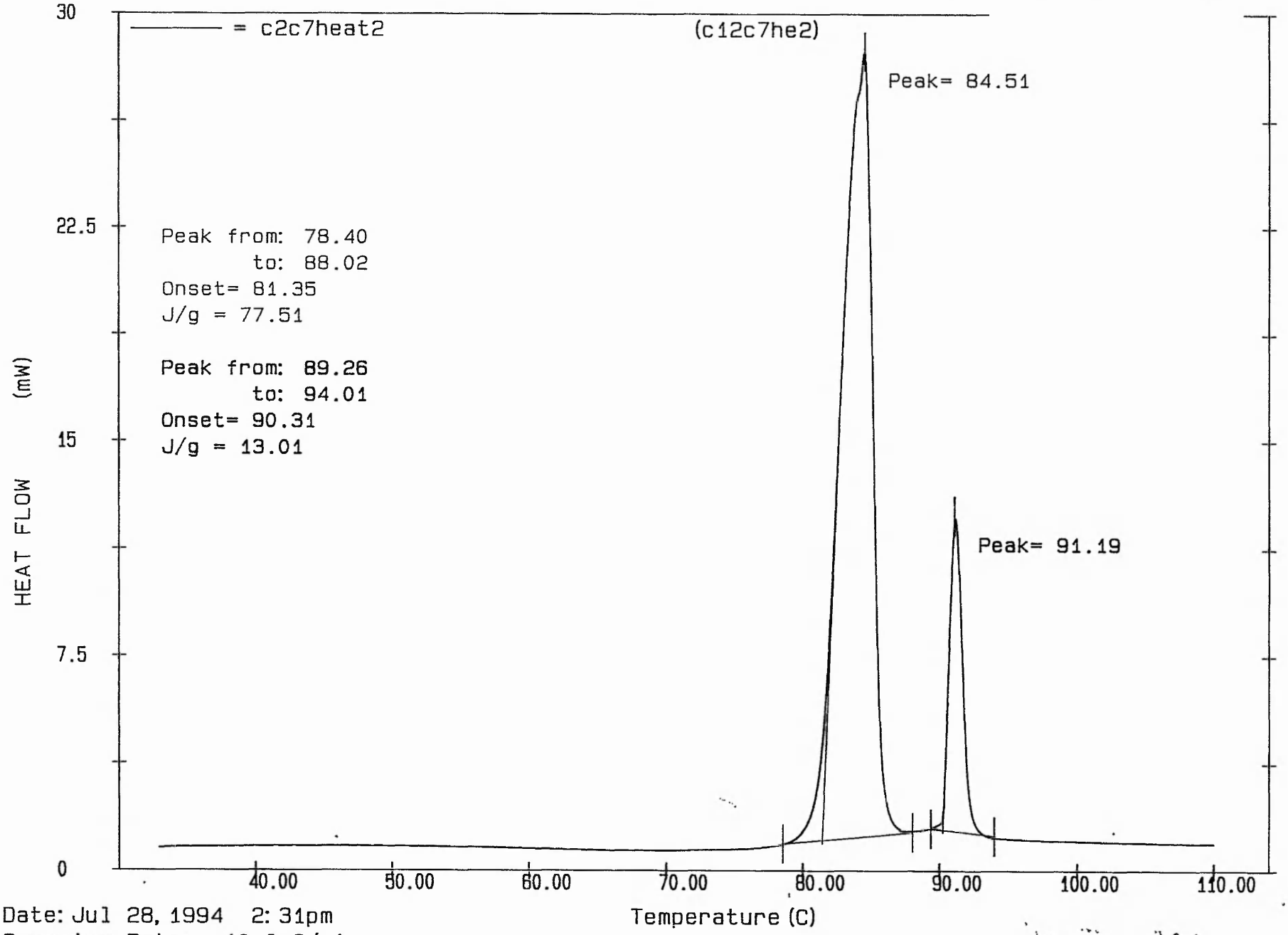

Date: Jul 28, 1994 2:31pm
Scanning Rate: 10.0 C/min
Sample Wt: 5.700 mg Path: c:\pe\ash\
File 1: C12C7HE2 ASH

PERKIN-ELMER DSC7

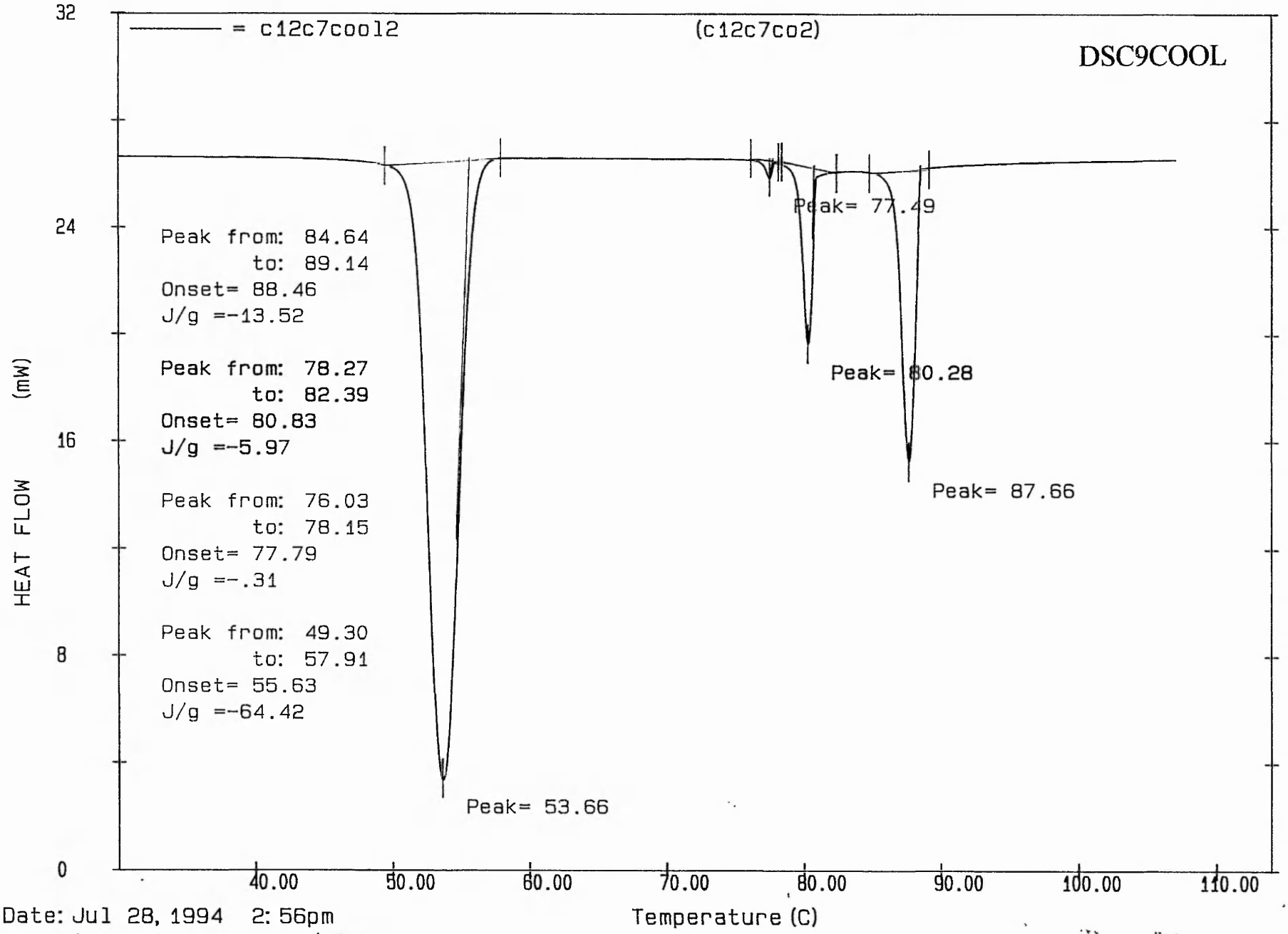

Date: Jul 28, 1994 2:56pm
Scanning Rate: -10.0 C/min
Sample Wt: 5.700 mg Path: c:\pe\ash\
File 1: C12C7C02 ASH

PERKIN-ELMER DSC7

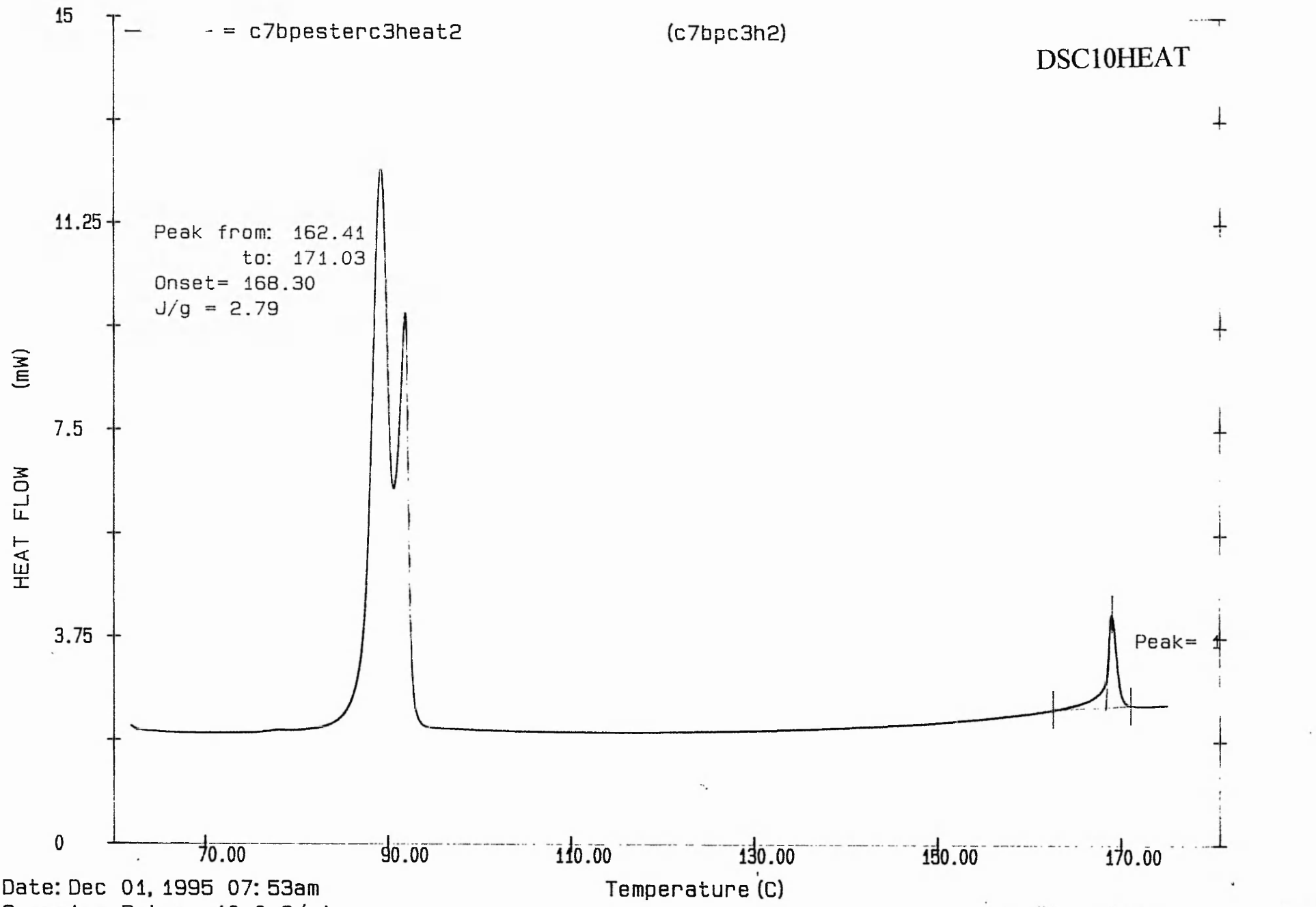
15
11.25
7.5
3.75
0
HEAT FLOW (mW)
- = c7bpesterc3heat2
(c7bpc3h2)
DSC10HEAT
Peak from: 162.41
to: 171.03
Onset= 168.30
J/g = 2.79
Peak= 1
70.00
90.00
110.00
130.00
150.00
170.00
Temperature (C)
Date: Dec 01, 1995 07:53am
Scanning Rate: 10.0 C/min
Sample Wt: 5.100 mg Path: a:\
File 1: C7BPC3H2 ASH
PERKIN-ELMER DSC7

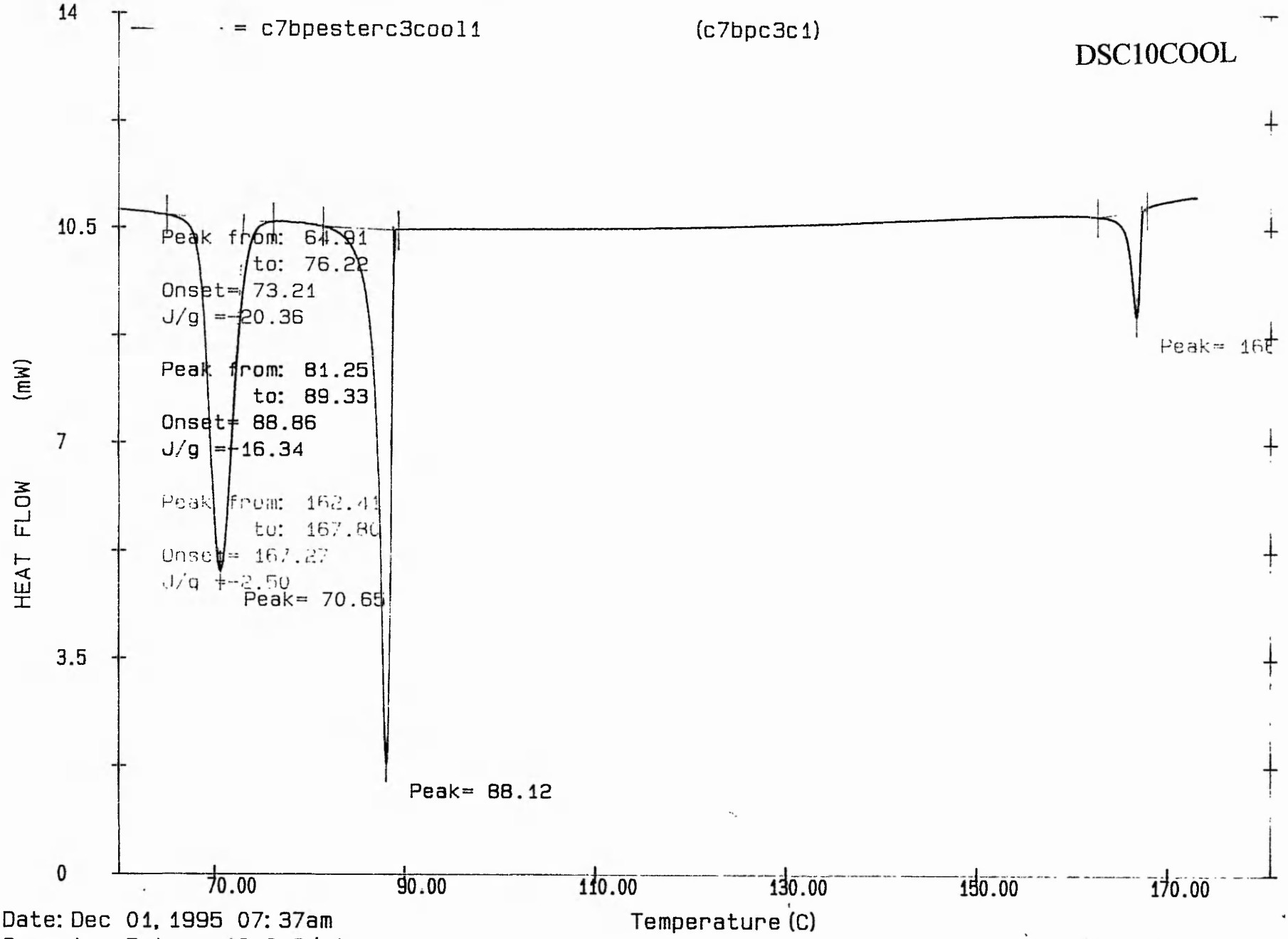

Date: Dec 01, 1995 07:37am
Scanning Rate: -10.0 C/min
Sample Wt: 5.100 mg Path: a:\
File 1: C7BPC3C1 ASH

PERKIN-ELMER DSC7

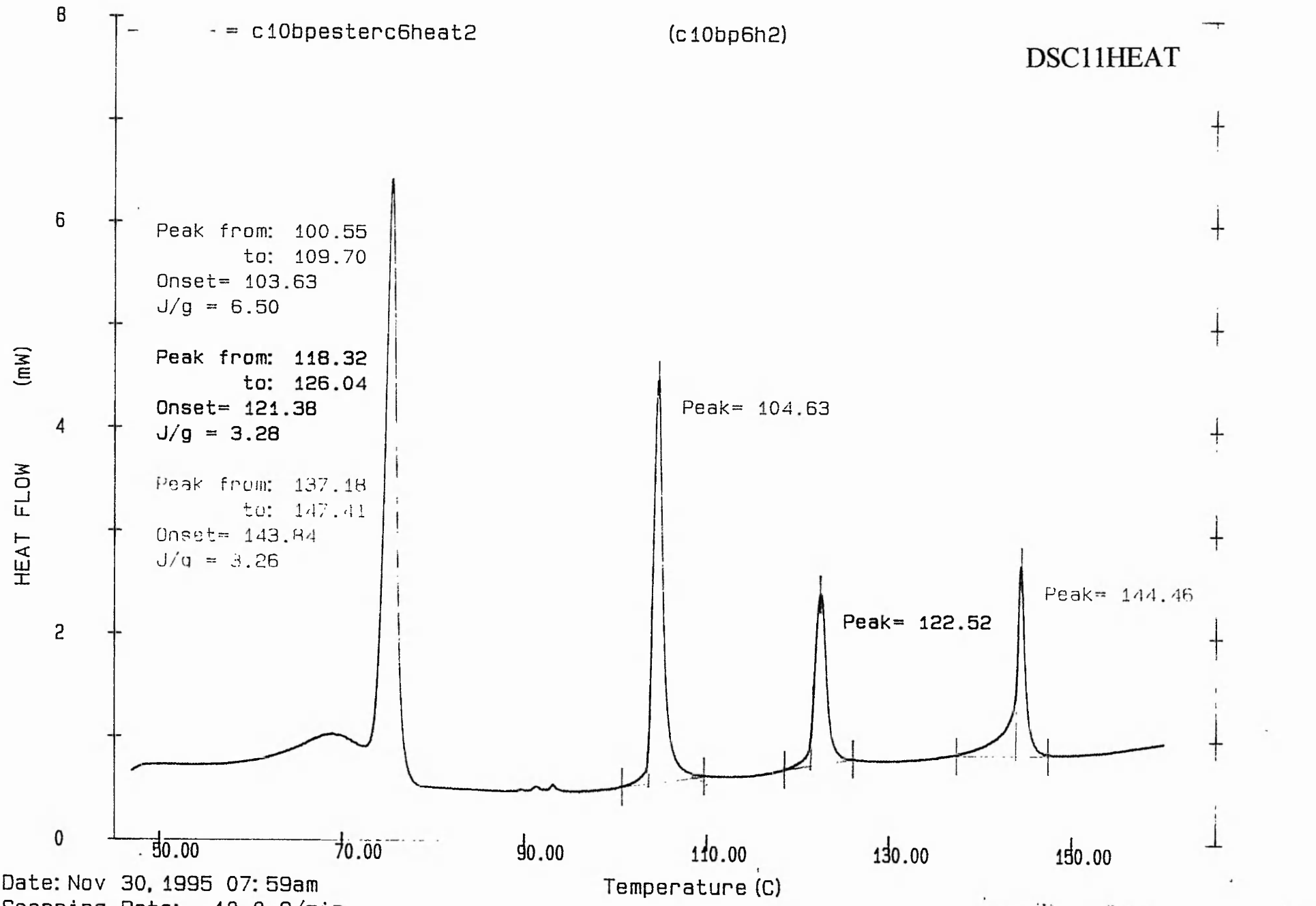

Date: Nov 30, 1995 07:59am
Scanning Rate: 10.0 C/min
Sample Wt: 4.800 mg Path: c:/pe\
File 1: C10BP6H2 ASH

PERKIN-ELMER DSC7

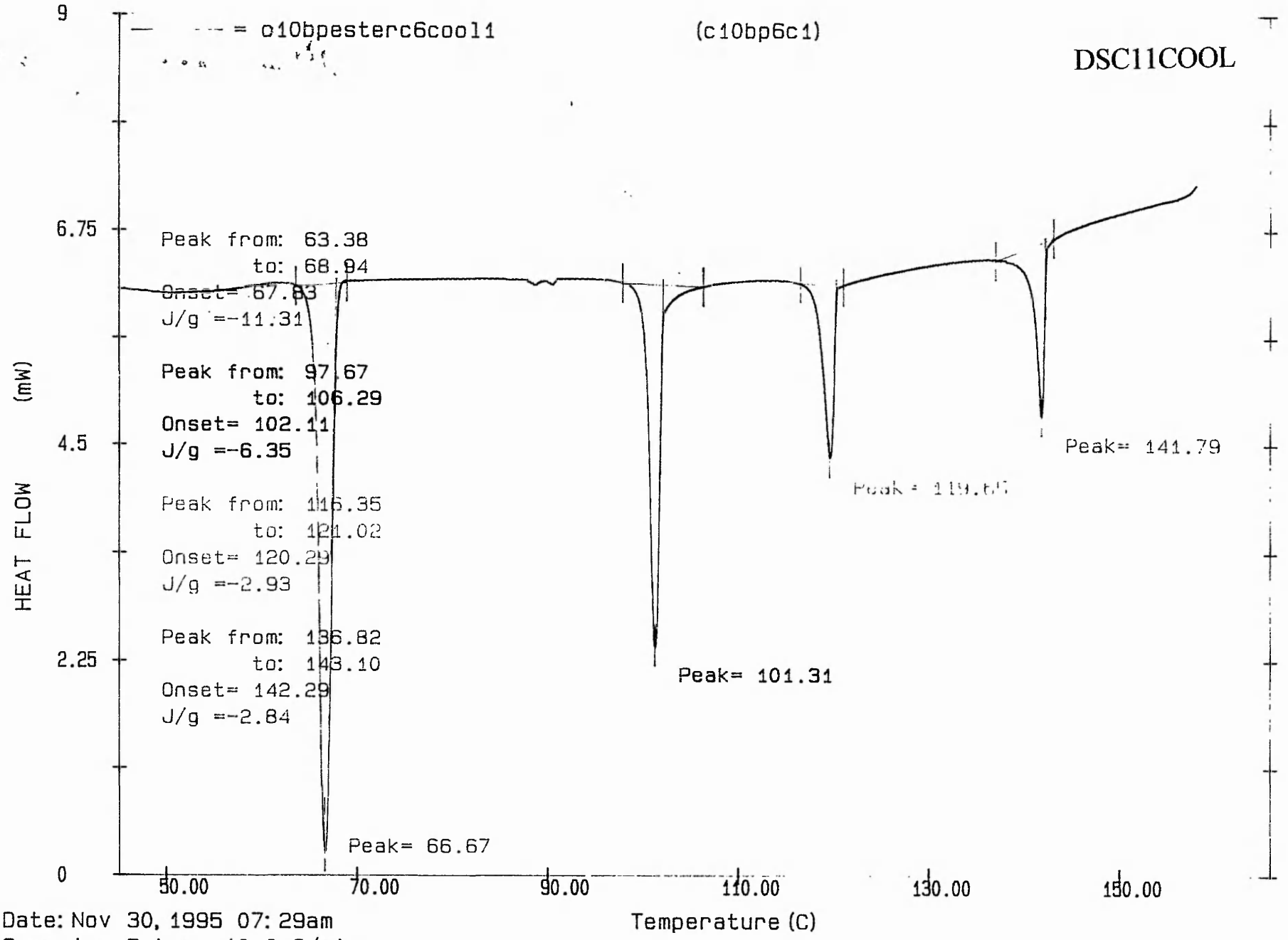

Date: Nov 30, 1995 07:29am
Scanning Rate: -10.0 C/min
Sample Wt: 4.800 mg Path: a:\
File 1: C10BP6C1 ASH

PERKIN-ELMER DSC7

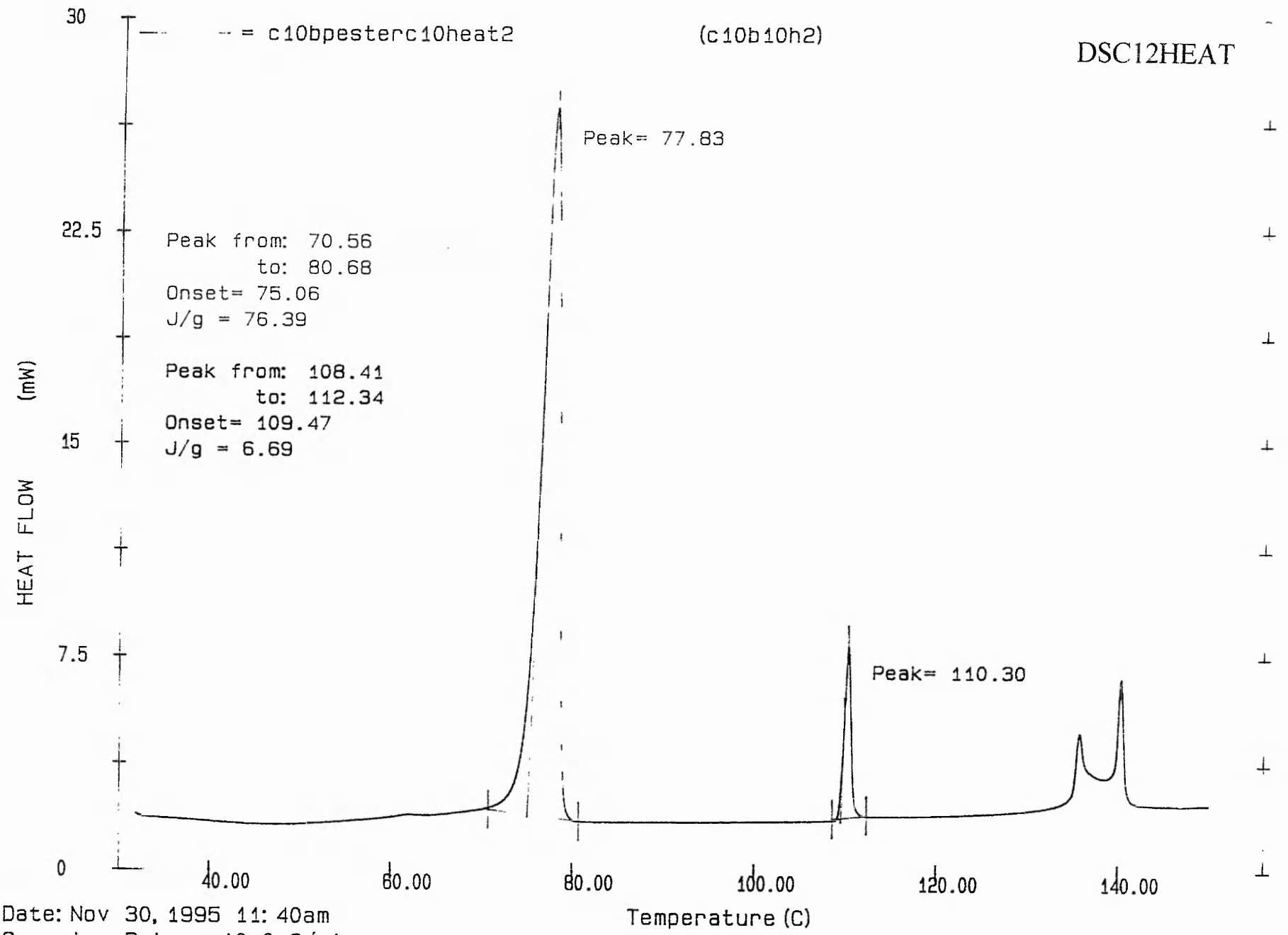

Date: Nov 30, 1995 11:40am
Scanning Rate: 10.0 C/min
Sample Wt: 4.700 mg Path: a:\
File 1: C10B10H2 ASH

PERKIN-ELMER DSC7

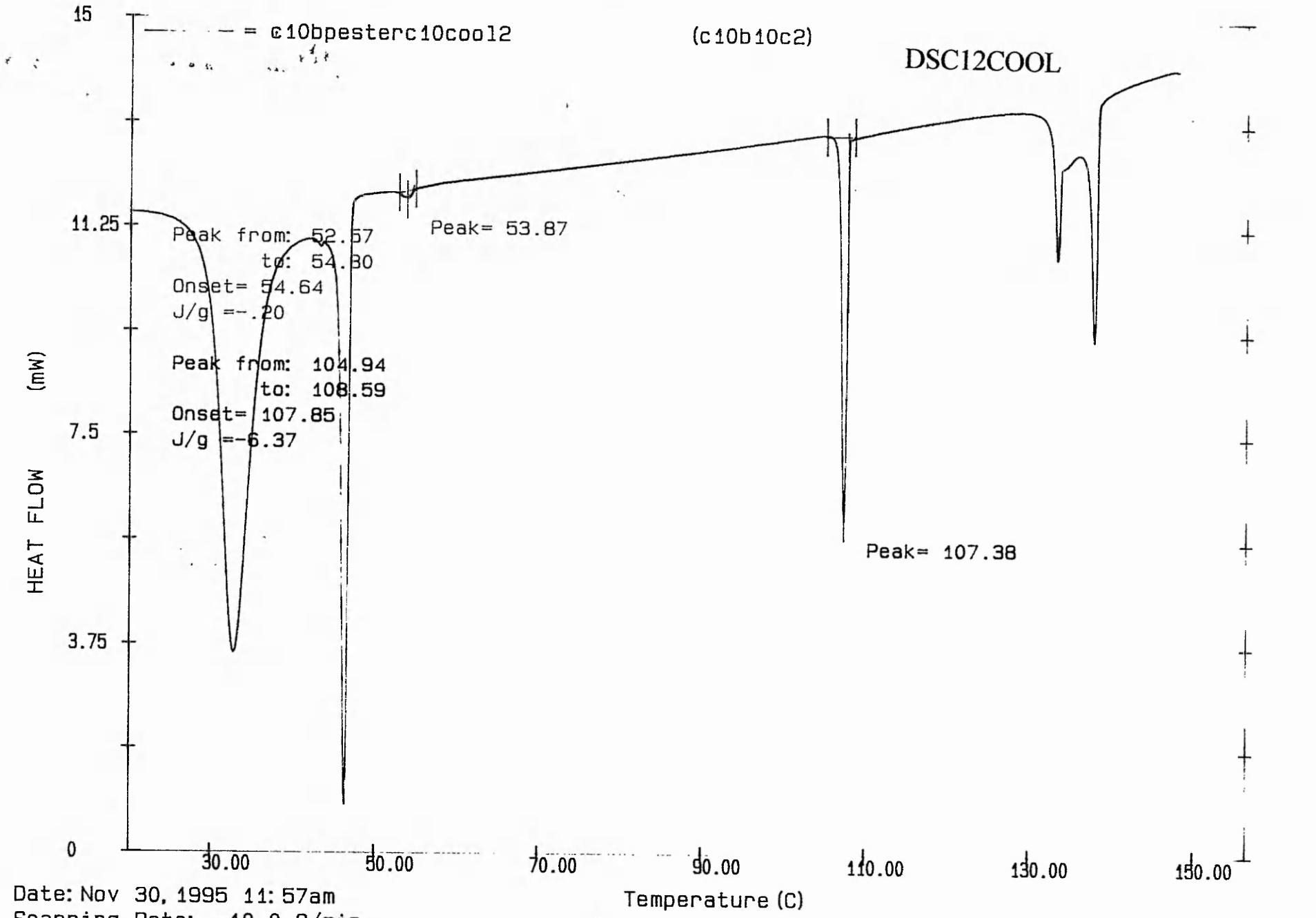

Date: Nov 30, 1995 11:57am
Scanning Rate: -10.0 C/min
Sample Wt: 4.700 mg Path: a:\
File 1: C10B10C2

PERKIN-ELMER DSC7

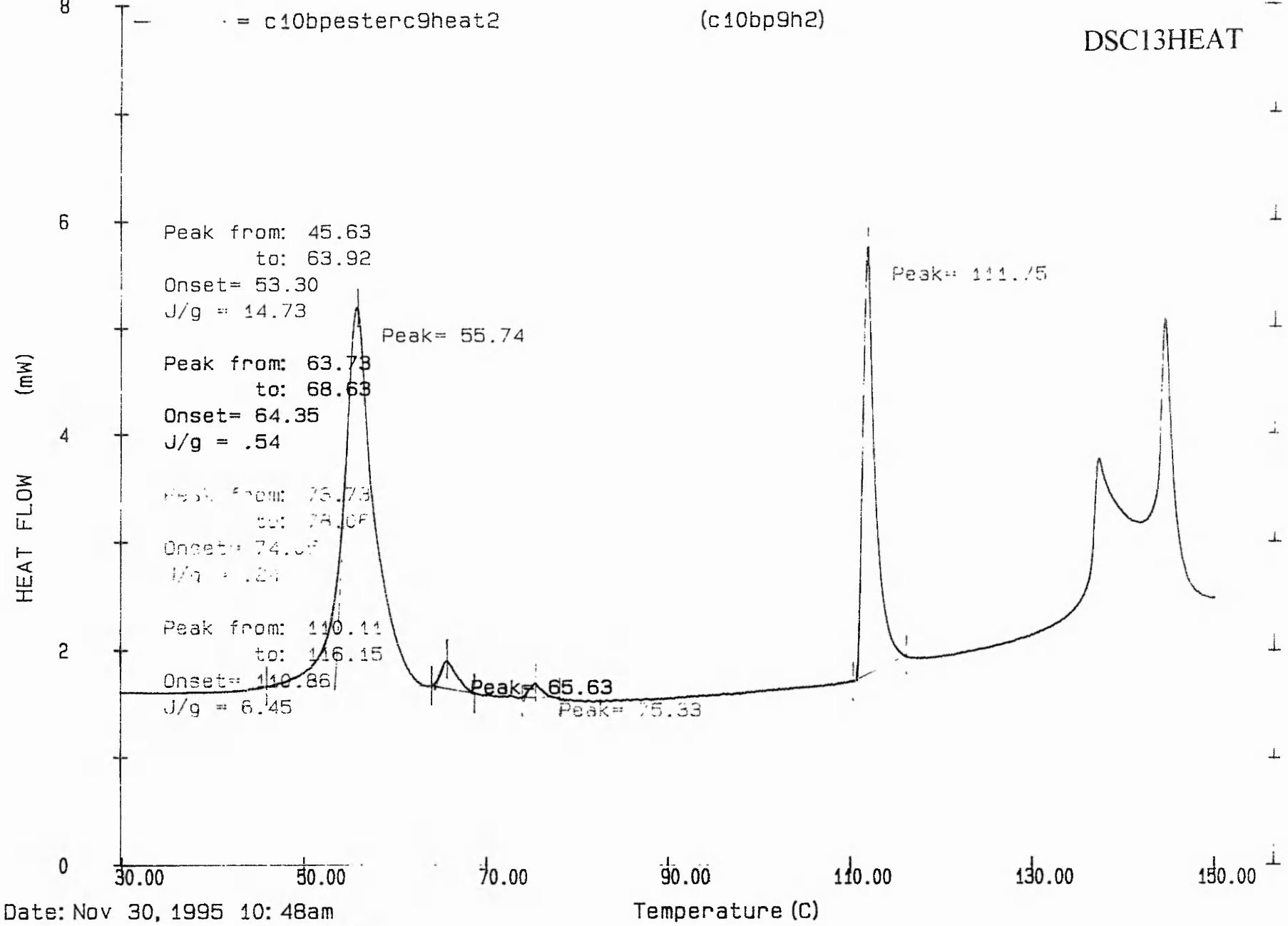

Date: Nov 30, 1995 10:48am
Scanning Rate: 10.0 C/min
Sample Wt: 5.800 mg Path: a:\
File 1: C10BP9H2 ASH

PERKIN-ELMER DSC7

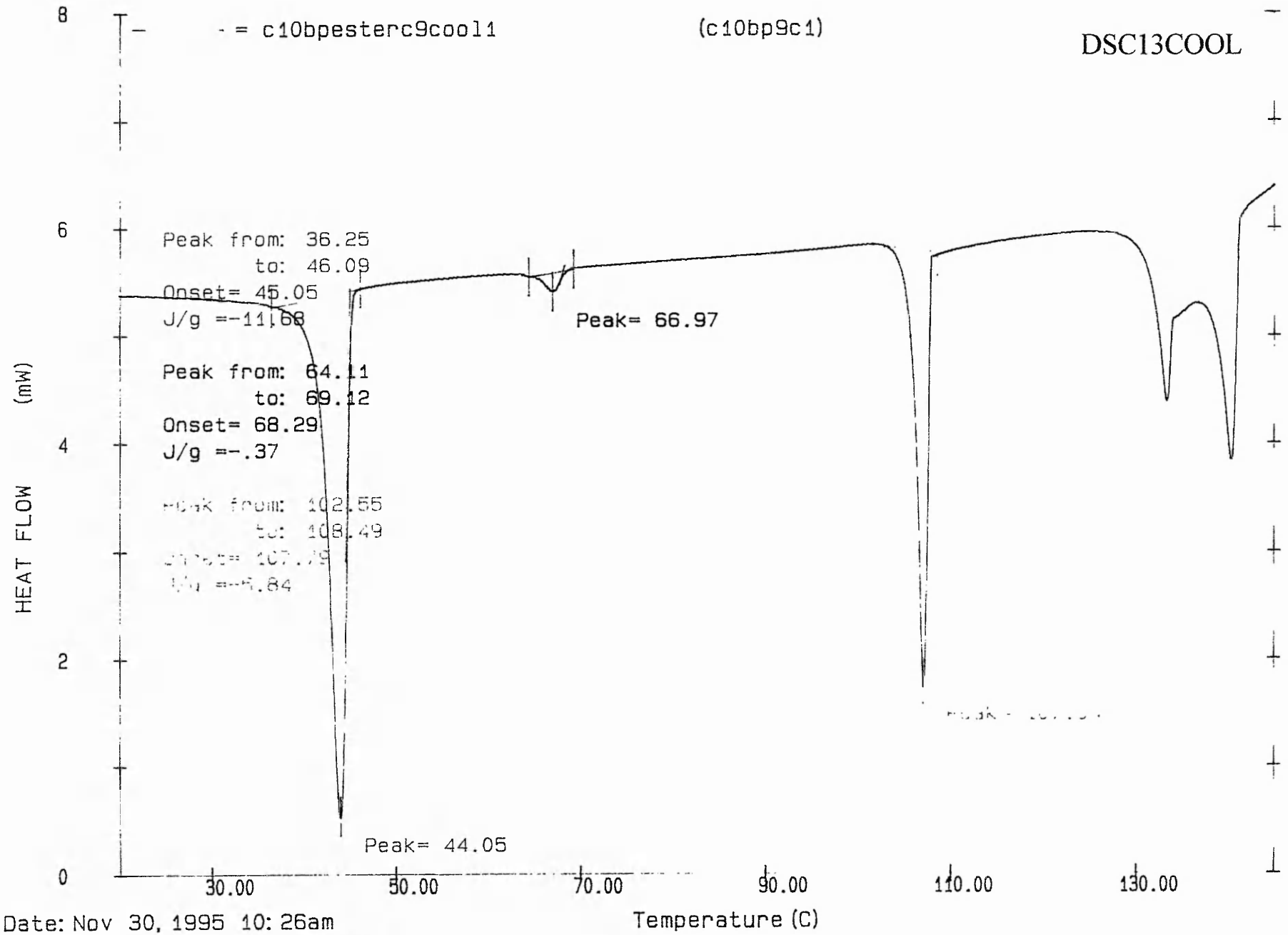

Date: Nov 30, 1995 10:26am
Scanning Rate: -10.0 C/min
Sample Wt: 5.800 mg Path: a:\
File 1: C10BP9C1 ASH

PERKIN-ELMER DSC7

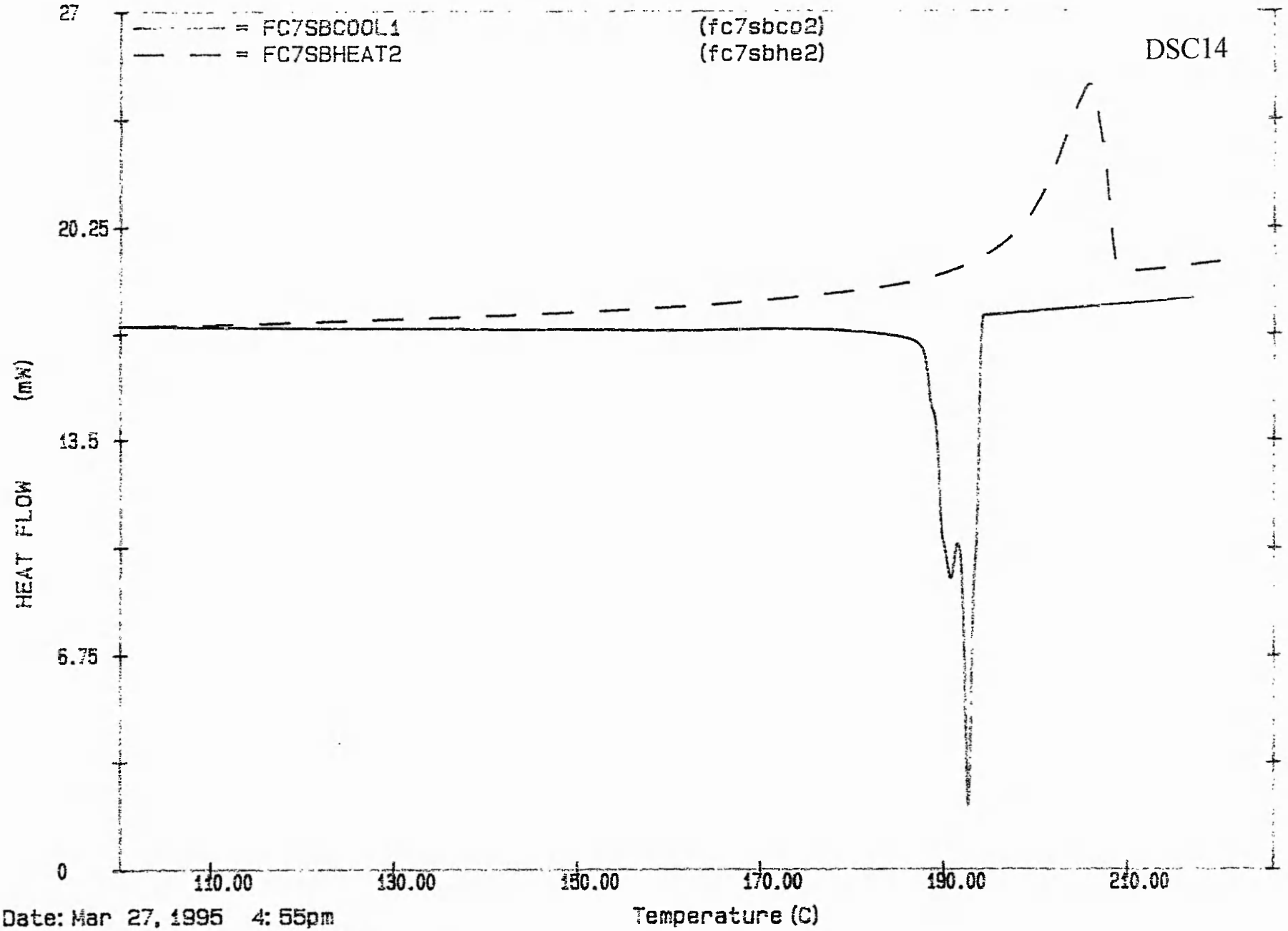

Date: Mar 27, 1995 4:55pm
Scanning Rate: -10.0 C/min
Sample Wt: 4.800 mg Path: c:\pe\ash\
File 1: FC7SBC02 ASH

PERKIN-ELMER DSC7

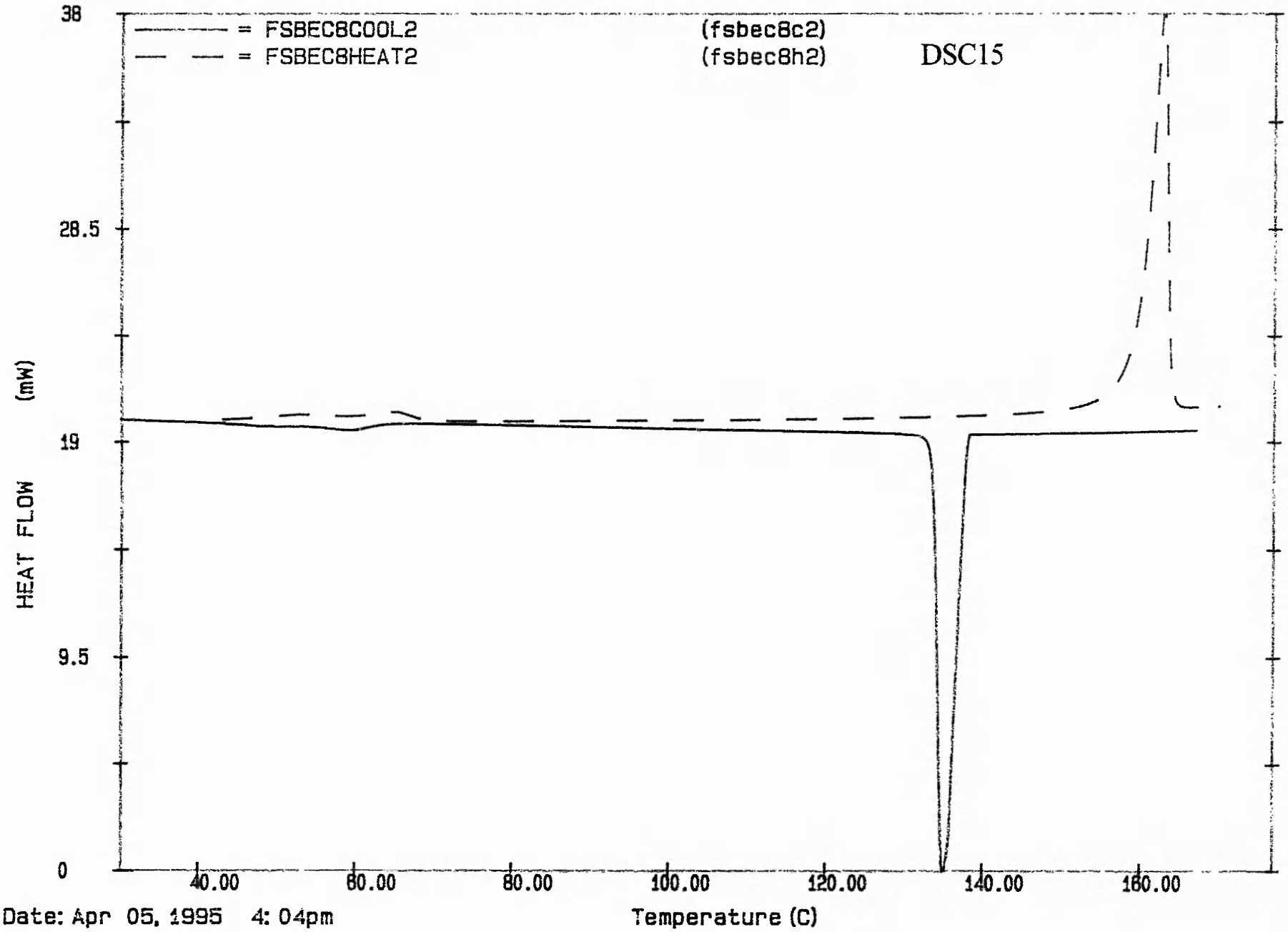

Date: Apr 05, 1995 4:04pm
Scanning Rate: -10.0 C/min
Sample Wt: 4.900 mg Path: c:\pe\ash\
File 1: FSBEC8C2 ASH

PERKIN-ELMER DSC7